SELF-FORCE-DERIVED MASS OF AN ELECTRON BUNCH

E. Saldin, DESY, Hamburg, Germany

Abstract

We study an electron bunch together with its self-fields from the viewpoint of basic dynamical quantities. This leads to a methodological discussion about the definition of energy and momentum for fully electromagnetic systems and about the relation between covariance of the energy-momentum pair and stability. We show here that, in the case of unstable systems, there is no mean to define, in a physically meaningful way, a total energy-momentum four-vector: covariance of the energy-momentum pair follows from the stability of the system and viceversa, as originally pointed out by Henry Poincaré. Another version of this paper by G. Geloni and the author can be found in [1].

INTRODUCTION

Nearly one hundred years have passed since Abraham and Lorentz calculated their famous expressions for the energy and momentum of a purely electromagnetic, spherically symmetrical distribution of charges [2], [3]. This distribution constitutes an attempt to build a classical model of the electron: according to Lorentz's initial idea, mass, energy and momentum of the electron could, indeed, be of completely elecromagnetic nature.

Nevertheless, the energy (divided by the speed of light in vacuum, as we will understand through this paper) and momentum of such an electromagnetic electron do not constitute a four-vector. In fact (as Abraham [4] pointed out already in 1904 probably, at that time, without a clear understanding of what a four-vector is), in a frame moving with velocity $\vec{v}$ with respect to the system rest frame, we have

$$E_e = \gamma U'(1 + 1/3\beta^2) \tag{1}$$

and

$$\vec{P}_e = 4/3\gamma\vec{v}U'/c^2, \tag{2}$$

where the index e indicates the electromagnetic nature of the energy E_e and momentum $\vec{P}_e$, γ is the usual Lorentz factor, β is the velocity v/c (normalized to the speed of light in vacuum c), and U' indicates the electromagnetic energy in the electron rest frame [5],

$$U' = \epsilon_0/2 \int \vec{E'}^2 dV', \tag{3}$$

where ϵ_0 is the free space permittivity. U' is purely an electrostatic quantity (in this paper the prime will always indicate quantities calculated in the rest frame; therefore $\vec{E'}$ and dV' are, respectively, the electric field and the volume element in the rest frame of the system).

It is worth to mention here that the factor $4/3$ in Eq. (2) and the term proportional to $1/3\beta^2$ in Eq. (1) depend on the choice of spherical symmetry made on the charge distribution: had we chosen, for instance, an infinitely long line distribution in the direction of $\vec{v}$, we would have found

$$E_{e2} = \gamma U'(1 + \beta^2) \tag{4}$$

and

$$\vec{P}_{e2} = 2\gamma\vec{v}U'/c^2, \tag{5}$$

while, in the case of a line charge oriented perpendicularly to the direction of $\vec{v}$,

$$E_{e3} = \gamma U' \tag{6}$$

and

$$\vec{P}_{e3} = \gamma\vec{v}U'/c^2, \tag{7}$$

which only incidentally, due to the particular choice of the distribution, behaves as a four-vector.

Henry Poincaré solved the problem of the lack of covariance shown in Eq. (1) and Eq. (2) by introducing, in the electron model, energies and momenta of non-electromagnetic nature [6]. These are actually due to non-electomagnetic interactions which keep the electron together. By doing so he strongly related the covariance of energy and momentum with the stability of the system: the electomagnetic energy-momentum pair alone is not a four-vector, but the total energy-momenum pair, accounting for the non-electromagnetic interaction, is a regular four-quantity.

In 1922, Enrico Fermi developed an original, early relativistic approach to the $4/3$ problem [7]; about forty years later a redefinition of the energy-momentum pair related to Fermi's work was proposed by Rohrlich [8], which leaves untouched the total energy-momentum vector, but splits it into electromagnetic and non-electromagnetic contribution in such a way that covariance is granted for both the electromagnetic and the non-electromagnetic part of the energy-momentum pair.

It is possible to show [9], [10] that the treatments by Poincaré and Rohrlich are not in contradiction.

Nevertheless, the approach by Rohrlich [8] was sometimes taken (see e.g. [11]) as the proof that stability and covariance are unrelated matters since, upon redefinition, the electromagnetic part alone is a four-vector.

We will show here, that such a conclusion is incorrect. The stability of the system is related to the covariance of

TECHNOLOGY CHALLENGES TOWARDS SHORT-WAVELENGTH FELS

J. Rossbach, Universität Hamburg and DESY, 22603 Hamburg, Germany

Abstract

The paper sheds some light on achievements in accelerator technology that paved the way towards short-wavelength FELs, specifically the FLASH facility at DESY. Also, a few of the technical challenges are discussed which we are facing in view of future X-ray FELs.

INTRODUCTION

Free-electron lasers (FEL) operating in the SASE mode (self-amplified spontaneous emission) at wavelengths far below the visible are now with us since several years, and more, and even more ambitious, projects are ahead of us. Although most of the basic theory is known since the early eighties, it took more than twenty years until FEL saturation was demonstrated experimentally at wavelengths below the visible. Even more, it took almost 30 years until a user facility was put in operation in the VUV regime, although it was clear from the very beginning, that such a radiation source would open up an entirely new world of possibilities for experimenters.

The major reason for this long time span was related to the unprecedented electron beam quality needed to achieve saturation within a reasonable undulator length. Considerable R&D on accelerator physics and technology was indispensable to come to a credible and reliable design of a (soft) X-ray FEL. In particular, it was not only necessary to develop technologies for producing ultra-relativistic electron bunches with high charge (typically 1 nC), small normalized emittance (typically 1 mrad mm) small energy spread (order of 100 keV after compression) and very short bunch length (10 fs range, thus achieving both the kA peak current needed for the FEL and the short radiation pulses desired by users), but it was as important to invent novel beam diagnostics tools to verify and control the beam properties at a micrometer precision level – in all three dimensions. This broad scope of tasks could only be accomplished by big accelerator centres, being able to initiate and conduct a coordinated effort of the full spectrum of accelerator scientists and engineers. This broad spectrum of expertise was traditionally cultivated at big labs dedicated to high-energy particle physics (HEP), for their permanent demand of more powerful and more sophisticated accelerators. It is thus not by accident that the first X-ray FEL programs were initiated mainly by such labs like DESY and SLAC. It will be a most awarding science management task (and, in view of the more and more project oriented funding policies, a very challenging one) to keep alive and even extend the fruitful collaboration of accelerator scientists from both HEP and FEL communities.

The present paper is not considered a review article on this extremely broad subject. It is rather a personal review, mainly referring to the almost 14 years of R&D effort conducted at DESY, Germany towards the FLASH user facility. To a large extent, this effort was based on, and conducted by, the international TESLA collaboration, with the superconducting accelerator called "TESLA Test Facility" still being the backbone hardware. In the spirit mentioned above, part of the accelerator beam time is still allocated to HEP-related accelerator R&D towards the International Linear Collider (ILC), being based on the same TESLA superconducting accelerator technology.

The list of technology issues mentioned in the following is by far not complete. It represents a personal, partly arbitrary selection of topics that are FEL specific, where considerable progress has been made, but which should keep us busy for another while.

TRANSVERSE SPACE CHARGE

In linear 1D theory [1], the power e-folding length L_g of the high-gain FEL can be expressed by

$$L_g = \frac{1}{\sqrt{3}}\left[\frac{2m}{\pi\mu_0 e^2}\frac{\gamma^3\lambda_u}{K^2 n_e}\right]^{1/3} \propto n_e^{-\frac{1}{3}} \qquad (1),$$

where λ_u is the undulator period, K the undulator parameter, γ the electron energy in units of its rest energy, and n_e is the electron density in the lab frame. In order to achieve a sufficiently short power gain length L_g, there is little alternative to calling for very high charge density. Taking into account that particles with large betatron amplitudes fall out of FEL resonance, large n_e must be realized in a combination of small radial beam emittance ε_r and large peak current $\hat{I}$. Such an electron beam is subject to considerable space charge forces, even though such forces are largely suppressed at ultrarelativistic energies. The impact on transverse electron focusing can be estimated from the focal length f generated by the linear defocusing forces on a beam drifting along the accelerator over a distance z ($f > z$ assumed):

$$f \approx \frac{ec}{r_e}\frac{\overline{\beta}\varepsilon_{norm}}{z}\frac{\gamma^2}{\hat{I}} \qquad (2)$$

With typical numbers for the normalized emittance $\varepsilon_{norm} = \beta\gamma\varepsilon_r \approx 1$ mrad mm, the average beta function $\overline{\beta} \approx 10$ m, the peak current $\hat{I} \approx 1$ kA, and the beam energy $\gamma \approx 200$, we get a focal length as small as $f \approx 10$ m already after a few meters of passage length z.

VOLC: VOLUME FREE ELECTRON LASER SIMULATION CODE

S. Sytova*, Research Institute for Nuclear Problems, Belarusian State University

Abstract

First lasing of Volume Free Electron Laser (VFEL) in mm wavelength range was obtained recently [1]. Multi-wave volume distributed feedback (VDFB) where electromagnetic waves and electron beam spread angularly one to other in a spatially-periodic structure (resonator) is the VFEL distinctive feature [2]. Mathematical model and numerical methods for VFEL nonlinear stage simulation were proposed [3] and implemented in computer code VOLC that allows to simulate different geometries of two- and three-wave VFEL in amplifier and oscillator regimes. Electron beam is modelled by averaging over initial phases of electrons. VOLC dimensionality is 2D (one spatial coordinate and one phase space coordinate) plus time. A description of VOLC possibilities and representative numerical results are presented.

INTRODUCTION

Principles and theoretical foundations of VFEL operation based on VDFB [4] put the beginning of experimental developing of new type of electronic generators. Creation of VFEL solves the problem of current threshold reduction, frequency tuning in a wide range, miniaturization of resonators. All these problems present some difficulties for widely used schemes of free electron lasers (FEL), backward wave tubes (BWT), travelling wave tube (TWT) and other electronic devices. As a rule, these high efficient devices have optimally specified parameters (electron beam, waveguides, resonators and undulators periods etc.). Changing of one of these parameters to tune frequency leads to abrupt reduction of efficiency of the system. VFEL design features allow to move and rotate diffracting gratings, change the distance between gratings and the gap between gratings and electron beam as well as orientation of grating grooves with respect to electron beam velocity. These aspects provide possibility to tune conditions of diffraction. VFEL threshold current for an electron beam passing through a spatially-periodic structure in degeneration points decreases essentially in comparison with single-wave systems [4]. This is valid for all wavelength ranges regardless the spontaneous radiation mechanism and as a consequence this means the possibility to reduce significantly system sizes.

In VFEL operation the linear stage investigated analytically [5]-[7] quickly changes into the nonlinear one where the most part of the electron beam kinetic energy is transformed into electromagnetic radiation. Nonlinear regime of VFEL operation can be investigated only using methods of mathematical modelling. Experiments on VFEL go on [8]–[9] and need optimal geometry determination and result processing.

MATHEMATICAL FORMULATION OF VFEL PHYSICAL MODEL

The scheme of VFEL resonator of the experimental installation [1] formed by two diffraction gratings with different periods and two smooth side walls the same as the scheme of the volume resonator (so-called "grid" volume resonator) built from the metallic threads inside a rectangular waveguide of the installation [8]–[9] can be considered as the following scheme of VFEL. Here an electron beam with electron velocity u passes through a spatially periodic structure. Under diffraction conditions some strong coupled waves can be excited in the system. If simultaneously electrons of the beam are under synchronism condition, they emit electromagnetic radiation in directions depending on diffraction conditions in oscillator regime. In [10]–[12] different two-wave and three-wave schemes of VFEL were considered in amplifier and oscillator regimes. System of equations for all cases of VFEL is obtained from Maxwell equations in the slowly-varying envelope approximation. For two-wave VFEL it has the following form:

$$\frac{\partial E}{\partial t}+\gamma_0 c\frac{\partial E}{\partial z}+0.5i\omega lE-0.5i\omega\chi_\tau E_\tau=$$

$$=2\pi j\Phi\int_0^{2\pi}\frac{2\pi-p}{8\pi^2}(\exp(-i\Theta(t,z,p)+$$

$$+\exp(-i\Theta(t,z,-p)))dp,$$

$$\frac{\partial E_\tau}{\partial t}+\gamma_1 c\frac{\partial E_\tau}{\partial z}+0.5i\omega\chi_{-\tau}E-0.5i\omega l_1E_\tau=0. \quad (1)$$

Here $E(t,z)$ and $E_\tau(t,z)$ are amplitudes of transmitted and diffracted waves with wave vectors $\mathbf{k}$ and $\mathbf{k}_\tau$ respectively. $l_0=\left(k^2c^2-\omega^2\varepsilon_0\right)/\omega^2$ and $l_1=\left(k_\tau^2c^2-\omega^2\varepsilon_0\right)/\omega^2$ are system parameters. $l=l_0+\delta$. δ is a detuning from synchronism condition. γ_0, γ_1 are VDFB cosines. $\beta=\gamma_0/\gamma_1$ is an asymmetry factor. $\Phi=\sqrt{l_0+\chi_0-1/(u/c\gamma)^2}$. γ is the Lorenz factor. χ_0, $\chi_{\pm\tau}$ are Fourier components of the dielectric susceptibility of the target.

System (1) must be supplemented with proper initial and boundary conditions which can contain conditions for external reflectors. Equations for the phase dynamics of elec-

* sytova@inp.minsk.by

MEASUREMENT AND ANALYSIS OF CSR EFFECTS AT FLASH

Bolko Beutner, Winfried Decking, Torsten Limberg, and Michael Röhrs
DESY, Hamburg, Germany

Abstract

The vacuum-ultra-violet free electron laser in Hamburg (FLASH) is a linac driven FEL. High peak currents are produced using magnetic bunch compression chicanes. Such peak currents are required for the SASE process in the undulators. In these magnetic chicanes, the energy distribution along an electron bunch is changed by effects of Coherent Synchrotron Radiation (CSR). Energy changes in dispersive bunch compressor chicanes lead to transverse displacements. These CSR induced displacements are measured using a transverse deflecting RF-structure. Recent experiments and simulations concerning the charge dependence of such transverse displacements are presented and analysed.

INTRODUCTION

Electron bunches in magnetic bunch compressor chicanes are subject to CSR self-forces. CSR induced energy changes along the bunch give rise to different trajectories for different longitudinal slices. Measurements of such effects were done at FLASH in 2006 [1][6]. We present results of CSR induced centroid shift measurements, in the first chicane, as a function of bunch charge.

For an undisturbed measurement of CSR effects, space charge fields are reduced by over-compressing the bunch. The longitudinal energy correlation (chirp) introduced in the accelerating module upstream of the first bunch compressor chicane is chosen to reach minimum bunch length and a peak current of about 1.2 kA toward the end of the second magnet in the chicane. Due to over-compression, the bunch will exit the chicane with a length comparable to its incoming length of about 2 mm RMS, corresponding to about 50 A peak current (see Fig. 1). The integrated effect of space-charge from the exit of the chicane to the observation point ≈ 60 m downstream is then small compared to the CSR effects.

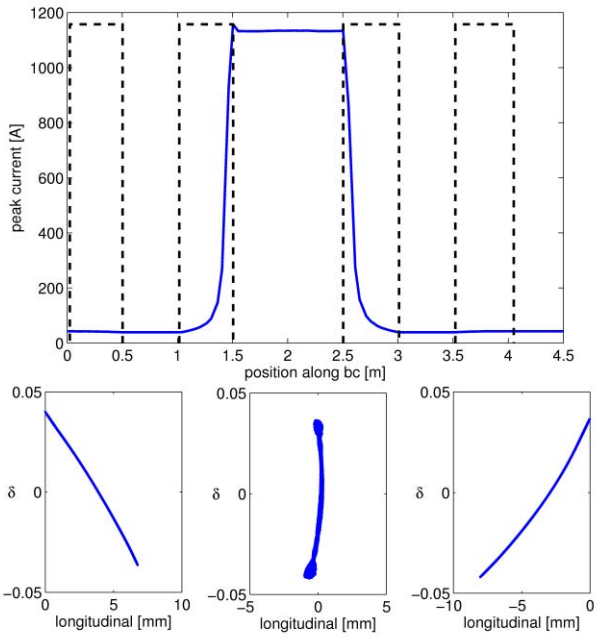

Figure 1: Top: Beam current along the bunch compressor chicane in over-compression mode. Dipoles are indicated as dashed boxes. Bottom: longitudinal phase space at the entrance, the middle, and the end of the bunch compressor.

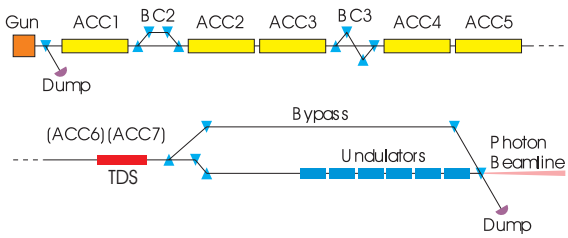

Figure 2: Sketch of FLASH. The blue triangles indicate dipole magnets, the yellow boxes symbolise TESLA accelerator modules.

MEASUREMENTS

A layout of FLASH is given in Fig. 2. We vary the phase offset of acceleration module ACC1 and keep the beam on crest in the modules ACC2/3 and ACC4/5. The expected CSR effects are created in BC2. Downstream, the transverse deflecting RF-structure (TDS) is used to analyse the longitudinal-horizontal beam profile. The experimental setup is as in [1][6].

Starting from a stable SASE working point, we achieved good transmission of the beam in the over-compression range ($\varphi_{ACC1} = 23^\circ - 26^\circ$), while keeping the beam energy constant by adjusting the RF-amplitude.

To optimise the resolution of the measurements, a special beam optics between BC2, the transverse deflecting cavity and the screen is used.

To ensure a proper optics set-up, the emittance and Twiss parameters of the beam were measured in the diagnostic section downstream the first bunch compressor [7]. The measured Twiss parameters are used to determine correc-

IMPROVEMENTS OF THE TRACKING CODE ASTRA FOR DARK CURRENT STUDIES AT FLASH

L. Fröhlich*, University of Hamburg and DESY, Hamburg, Germany,
S. Meykopff, DESY, Hamburg, Germany

Abstract

At the Free Electron Laser in Hamburg (FLASH), the activation of components due to dark current emitted by the gun has become a serious problem. To improve the understanding of dark current transport in the linac, we have used extensive tracking simulations. To reduce the required amount of computing time, we have used a novel parallelized version of the Astra tracking code. We present the main parallelization scheme and investigations on the scalability of the code. We also introduce a new library for the description of complex three-dimensional aperture models. Finally, a brief overview of the simulation results and an evaluation of possible remedies of the activation problem are given.

INTRODUCTION

The FLASH linac accelerates electron bunches from a photoinjector to beam energies of up to 700 MeV [1]. The bunch length is reduced in two magnetic chicanes, BC2 and BC3, at energies of 127 MeV and 380 MeV. In front of the undulator, a four-stage collimation system consisting of two transverse and two energy collimators removes particles deviating excessively from the designated reference orbit and momentum (Fig. 1).

Because it is operated at a high electric field amplitude of 40–44 MV/m, the normal conducting RF gun is a major source of dark current. Measurements with a Faraday cup have shown an average current of 200–300 µA exiting the structure during the RF pulse. A substantial part of it is picked up by the first superconducting acceleration module ACC1 and transported through the linac, leading to increased losses and activation of components along the machine. This has become a problem especially near the first dipole magnets of bunch compressor BC2, where the narrow vacuum chamber intercepts a major fraction of the incoming dark current. Equivalent dose rates above 16 mSv/h due to activated material have been measured in this place, requiring an increased radiation protection effort [2].

To investigate possible remedies for this problem, the transport of dark current through the linac has been studied with particle tracking simulations. The space charge tracking code *Astra* [3] was the natural choice for this task because a good model of the FLASH injector was already available for it [4]. Originally covering only the initial 14 m of the machine, this model has been extended to include the complete beamline of about 250 m length. The scope of these simulations required substantial changes to the code in order to reduce execution times as well as the development of a new aperture modelling language capable of describing the complex geometries found in the accelerator.

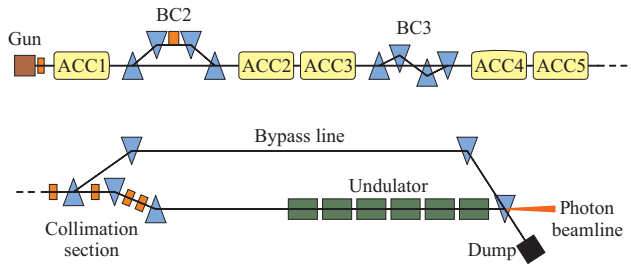

Figure 1: Schematic of the FLASH linac. The five acceleration modules ACC1-5 are shown in yellow, dipole magnets in blue, and collimators in orange color.

In this paper, we provide only a rough outline of simulation setup and results; details are found in [5]. Instead, we focus on the computational aspects of the work.

SIMULATION SETUP

The main simulation is divided into three steps:

1. Beam tracking: A bunch of 10^5 macroparticles is extracted from the cathode by photoemission and tracked to the dump. The step is iterated several times to match the beta function to the design optics.
2. Dark current tracking: 10^6 macroparticles are extracted from the cathode by field emission according to the Fowler-Nordheim model [6] and tracked to the dump. The phase space is saved in intervals of 8 cm, resulting in about 100 GB of data.
3. Aperture check: The saved phase space data are compared against a three-dimensional aperture model of the machine with a separate tool.

While space charge effects have to be included in the tracking of the beam in step 1, they are negligible in step 2 due to the low charge density of the dark current. The number of macroparticles required in step 2 is determined by the desired precision of the results. With a million macroparticles, relative dark current losses down to the level of 10^{-5} – 10^{-4} can be simulated.

We found the conventional single-processor version of *Astra* to be ill-suited for a work load of this magnitude; a single run would take several days to complete on the

* lars.froehlich@desy.de

LONGITUDINAL WAKE FIELD FOR AN ELECTRON BEAM ACCELERATED THROUGH A ULTRA-HIGH FIELD GRADIENT

G. Geloni, E. Saldin, E. Schneidmiller and M. Yurkov
Deutsches Elektronen-Synchrotron (DESY), Hamburg, Germany

Abstract

The impact of longitudinal wake fields on an electron beam accelerated through a ultra-high field gradient is discussed, based on solution of Maxwell's equations for the longitudinal field. We consider an acceleration distance much smaller than the overtaking length, as for laser-plasma devices. We give expressions for impedance and wake function that may be evaluated numerically. A limiting expression is found for a large distance of the electron beam from the accelerator compared with the overtaking length. We derive analytical solutions for a Gaussian transverse and longitudinal bunch shape. We apply our analytical asymptote by studying the feasibility of a Table-Top VUV FEL (TT-VUV-FEL) based on laser-plasma driver. Numerical estimations indicate a serious threat to the operation of this device. **A detailed report with relevant references is given in [1]**.

INTRODUCTION

In this paper we study longitudinal wake fields produced within electron beams accelerated with high-gradient fields. We assume that the acceleration distance d_a is much smaller than the the overtaking length. This is the distance travelled by the electrons as a light signal from the tail of the bunch overtakes the head of the bunch. Given a bunch of rms length σ_z, the overtaking length is $2\gamma^2\sigma_z$, and corresponds to the radiation formation length $2\gamma^2\lambda\!\!\!^{-}$ calculated at $\lambda\!\!\!^{-} = \sigma_z$, $\lambda\!\!\!^{-} = \lambda/(2\pi)$ being the reduced radiation wavelength. When $d_a \ll 2\gamma^2\sigma_z$, electrons can be assumed to be accelerated at position z_A down the beamline. This is the case for laser-plasma devices, since acceleration in the GeV range takes place within a few millimeter, but not for conventional accelerators. The assumption $d_a \ll 2\gamma^2\sigma_z$ simplifies wake calculations. When this condition is verified, the wake generated along the part of the trajectory following the acceleration point z_A is independent of any detail of the accelerator. Thus our study is valid independently of the particle accelerator technology chosen, provided that $d_a \ll 2\gamma^2\sigma_z$. One may also have contributions to the wake generated before z_A. These depend on the physical nature of the accelerator, can be separately calculated, and will be neglected here because they do not affect the bunch in the case of a laser-plasma accelerator. We base our study on solution of Maxwell's equations for the longitudinal field. Our consideration is valid in free-space. This approach gives accurate results if the typical dimension of the vacuum pipe a is larger than $\gamma\lambda\!\!\!^{-} = \gamma\sigma_z$, that is the typical transverse size related with the longitudinal electric field. Paraxial approximation can be applied to describe electromagnetic sources up to the observation point, while sources after the observation point in the beam propagation direction can be neglected. We make use of the paraxial approximation to calculate the Fourier transform of the longitudinal field produced by fixed electromagnetic sources (current and charge densities) at a certain observation plane down the beamline. This constitutes the basis of our treatment, because it allows to calculate the longitudinal impedance and the wake function. Impedance and wake function yield an analytical expression in the asymptotic limit of a large distance of the electron beam from the accelerator compared with the overtaking length, i.e. in the far-field zone for all wavelengths of interest (up to $\lambda\!\!\!^{-} \sim \sigma_z$). This asymptotic limit allows simple estimations of the impact of the longitudinal wake on the electron beam energy change. We apply our theory by studying the feasibility of TT-VUV-FELs based on parameters described in [2], and finding a serious threat.

FIELD IN SPACE-FREQUENCY

Let z_A be the exit of the accelerator. After z_A, the nominal Lorentz factor of electrons is γ. Acceleration happens on a scale $d_a \ll 2\gamma^2\lambda\!\!\!^{-}$. Significant emission is present for wavelengths longer than the longitudinal bunch length σ_z, up to transverse beam sizes $\sigma_\perp \lesssim \gamma\sigma_z$. For typical ultra-relativistic beams, condition $d_a \ll 2\gamma^2\lambda\!\!\!^{-}$ can be read as $d_a \ll 2\gamma^2\sigma_z$. We picture the fast acceleration process as a sudden "switch-on" of both harmonics of the electromagnetic sources and of the field. When the switching distance (the acceleration distance) $d_a \ll 2\gamma^2\sigma_z$, the description of the wake generated after the switching point (the acceleration point) z_A, is independent of the nature of the switcher. As long as sources are rapidly switched-on, it does not matter whether we are considering a fast longitudinal acceleration or other switching mechanisms. We first calculate $\bar{E}_z(z_o, \vec{r}_{\perp o}, \omega)$, that is the longitudinal electric field at frequency ω from given electromagnetic sources in vacuum. It is detected at longitudinal position $z_o > z_A$ and transverse position $\vec{r}_{\perp o}$. We define the Fourier transform of a function $f(t)$ as $\bar{f}(\omega) = \int_{-\infty}^{\infty} dt\, f(t) \exp[i\omega t]$, and we follow analogous conven-

THEORY OF NONLINEAR HARMONIC GENERATION IN FELS WITH HELICAL WIGGLERS

G. Geloni, E. Saldin, E. Schneidmiller and M. Yurkov
Deutsches Elektronen-Synchrotron (DESY), Hamburg, Germany

Abstract

Nonlinear Harmonic Generation (NHG) is of importance for both short wavelength FELs, in relation with the achievement of shorter wavelengths with a fixed electron-beam energy, and high-average power FEL resonators, in relation with destructive effects of higher harmonics radiation on mirrors. We present a treatment of NHG from helical wigglers with particular emphasis on the second harmonic. Our study is based on an analytical solution of Maxwell's equations, derived with the help of a Green's function method. We demonstrate that NHG from helical wigglers vanishes on axis. Our conclusion is in contrast with literature, that includes a kinematical mistake in the description of the electron motion. **A detailed report with relevant references is given in [1]**.

INTRODUCTION

NHG is of undisputed relevance in the field of FELs. It is generated by bunching of the electron beam at higher harmonics, driven by interaction with the fundamental. In general, NHG can be treated in terms of an electrodynamical problem where Maxwell's equations are solved with given macroscopic sources in the space-frequency domain. These sources are obtained through the solution of self-consistent equations for electrons and fields. Further on, solution of Maxwell's equations characterizes harmonic radiation in the space-frequency domain. The dependence of sources in the space-frequency domain on transverse and longitudinal coordinates is complicated because is the result of the above-mentioned self-consistent process. However, here we deal with an FEL setup where an ultrarelativistic electron beam is sent, in free space, through an undulator with many periods. Then, paraxial and resonance approximation can be applied. In particular, for a fixed transverse position, the longitudinal dependence is always slow on the scale of an undulator period. NHG has been dealt with in the case of a planar wiggler, both theoretically and experimentally. Odd harmonics have maximal power on axis[1] and are linearly polarized. Even harmonics have been shown to have vanishing on-axis power and to exhibit both horizontal and vertical polarization components. Here we present the first theory of NHG from helical wigglers, based on a solution of Maxwell's equations in the space-frequency domain, obtained with a Green's function technique.

NHG IN HELICAL WIGGLERS

Analysis of the harmonic generation mechanism

We use paraxial Maxwell's equations in the space-frequency domain to describe radiation from ultra-relativistic electrons. Let us call the transverse electric field in the space-frequency domain $\vec{E}_\perp(z,\vec{r}_\perp,\omega)$, where $\vec{r}_\perp = x\vec{e}_x + y\vec{e}_y$ and z identify a point in space. From the paraxial approximation follows that the electric field envelope $\vec{\tilde{E}}_\perp = \vec{E}_\perp \exp[-i\omega z/c]$ does not vary much along z on the scale of the reduced wavelength $\lambda\!\!\!^{-} = \lambda/(2\pi)$. Maxwell's equation in paraxial approximation reads: $\mathcal{D}\left[\vec{\tilde{E}}_\perp(z,\vec{r}_\perp,\omega)\right] = \vec{f}(z,\vec{r}_\perp,\omega)$, where $\mathcal{D} \equiv {\nabla_\perp}^2 + (2i\omega/c)\partial/\partial z$, ${\nabla_\perp}^2$ being the Laplacian operator over transverse cartesian coordinates. The source-term vector $\vec{f}(z,\vec{r}_\perp)$ is specified by the trajectory of the source electrons, and can be written in terms of the Fourier transform of the transverse current density, $\vec{j}_\perp(z,\vec{r}_\perp,\omega)$, and of the charge density, $\bar{\rho}(z,\vec{r}_\perp,\omega)$, as $\vec{f} = -4\pi[(i\omega/c^2)\vec{j}_\perp - \vec{\nabla}_\perp\bar{\rho}]\exp[-i\omega z/c]$. In this paper we will treat $\vec{j}_\perp$ and $\bar{\rho}$ as macroscopic quantities, without investigating individual electron contributions. $\vec{j}_\perp$ and $\bar{\rho}$ are regarded as given data, that can be obtained from any FEL code. Codes actually provide the charge density of the modulated electron beam in the time domain $\rho(z,\vec{r}_\perp,t)$. A post-processor can be used in order to perform the Fourier transform of ρ that can always be presented as $\bar{\rho} = -\widetilde{\rho}(z,\vec{r}_\perp - \vec{r}'_{o\perp}(z),\omega)\exp[i\omega s_o(z)/v_o]$, where the minus sign on the right hand side is introduced for notational convenience only. Quantities $\vec{r}'_{o\perp}(z)$, $s_o(z)$ and v_o pertain a reference electron with nominal Lorentz factor γ_o that is injected on axis with no deflection and is guided by the helical undulator field. Such electron follows a helical trajectory $\vec{r}'_{o\perp}(z) = r'_{ox}\vec{e}_x + r'_{oy}\vec{e}_y$. We assume that $r'_{ox}(z) = K/(\gamma_o k_w)[\cos(k_w z) - 1]$ and $r'_{oy}(z) = K/(\gamma_o k_w)\sin(k_w z)$, where $K = \lambda_w e H_w/(2\pi m_e c^2)$ is the undulator parameter, $\lambda_w = 2\pi/k_w$ being the undulator period, $(-e)$ the negative electron charge, H_w the maximal modulus of the undulator magnetic field on-axis, and m_e the rest mass of the electron. The correspondent velocity is described by $\vec{v}_{o\perp}(z) = v_{ox}\vec{e}_x + v_{oy}\vec{e}_y$. Finally, $s_o(z)$ is the curvi-

[1] Here we assume that the bunching wavefront is perpendicular to the (longitudinal) FEL axis.

UNDULATOR RADIATION IN A WAVEGUIDE

G. Geloni, E. Saldin, E. Schneidmiller and M. Yurkov
Deutsches Elektronen-Synchrotron (DESY), Hamburg, Germany

Abstract

We propose an analytical characterization of undulator radiation near resonance, when the presence of the vacuum-pipe affects radiation properties, as for the far-infrared undulator beamline at FLASH, that is designed to deliver pulses in the THz range. Such line can be used for pump-probe experiments where THz pulses are naturally synchronized to the VUV pulse from the FEL, as well as the development of novel electron-beam diagnostics techniques. Since the THz radiation diffraction-size exceeds the vacuum-chamber dimensions, characterization of infrared radiation must be performed accounting for the presence of a waveguide. We developed a theory of undulator radiation in a waveguide based on paraxial and resonance approximation. We solved the field equation with a tensor Green's function technique, and extracted figures of merit describing the influence of the vacuum-pipe on the radiation pulse as a function of the problem parameters. Our theory, that makes consistent use of dimensionless analysis, allows treatment and physical understanding of many asymptotes of the parameter space, together with their region of applicability. **A more detailed report of our study is given in [1]**.

INTRODUCTION AND THEORY

The accelerator complex at FLASH produces ultrashort bunches approaching sub-100 fs duration. FLASH will soon operate together with a FIR electromagnetic undulator providing coherent FIR radiation intrinsically synchronized with the VUV pulses. The wavelength range ($\lambda = 60 \div 200$ μm) will overlap with a large part of the THz-gap. This will allow pump-probe experiments combining FIR and VUV radiation, and non-destructive electron beam diagnostics. Vacuum chamber effects are expected to play an important role at longer wavelengths. Optimization of the radiation transport system calls for a precise characterization of THz pulses along the photon beamline. In the present work we focus on the characterization of undulator radiation from a filament beam (as for the FIR line at FLASH) in presence of a waveguide. One should solve the field equations in paraxial approximation with proper boundary conditions, e.g. $\mathcal{D}[\vec{\vec{E}}_\perp(z,\vec{r}_\perp)] = \vec{f}(z,\vec{r}_\perp)$, where $(\vec{n}\times\vec{\vec{E}}_\perp)_{|_S} = 0$ and $(\vec{\nabla}_\perp\cdot\vec{\vec{E}}_\perp)_{|_S} = 0$. Here S is the internal surface of the pipe, $\mathcal{D} \equiv (\nabla_\perp{}^2 + 2i\omega/c\cdot\partial/\partial z)$, $\nabla_\perp{}^2$ being the Laplacian operator over transverse cartesian coordinates and $\vec{f} = 4\pi e/c\cdot\exp\{i\int_0^z d\bar{z}\omega/[2\gamma_z^2(\bar{z})c]\}[i\omega/c^2\cdot\vec{v}_\perp(z) - \vec{\nabla}_\perp]\delta(\vec{r}_\perp - \vec{r}'_\perp(z))$. Solution must accounting for the tensorial nature of the Green's function. In the UR case, the resonance approximation can be exploited too. We thus consider planar undulator with a large number of undulator periods and a frequency range of interest close to the fundamental harmonic, where the free-space field exhibits horizontal polarization (for undulator field in the vertical direction) and azimuthal symmetry. An explicit expression for the field is calculated as a superposition of TE and TM modes. We introduce normalized units: $\hat{\vec{\vec{E}}}_\perp = [-c^2/(A_{JJ}\omega e\theta_s)]\vec{\vec{E}}_\perp$, $\hat{C} = 2\pi N_w\Delta\omega/\omega_r$, $\hat{z} = z/L_w$, $\hat{r} = r/\sqrt{L_w\lambda\!\!\!^{-}}$, $\Omega = R^2/L_w\lambda\!\!\!^{-}$, $\hat{C}_k^\mu\mu_{1k}^2/(2\Omega)$ and $\hat{C}_k^\nu = \nu_{1k}^2/(2\Omega)$. Here $\Omega = R^2/(\lambda\!\!\!^{-}L_w)$ is the main parameter of our theory, comparing the pipe area with the radiation diffraction area, while μ_{mk} and ν_{mk} are, respectively, solutions of $J'_m(\mu_{mk}) = 0$ and $J_m(\nu_{mk}) = 0$. We obtain for $\hat{E}_{x,y}(\hat{r},\phi,\hat{z})$:

$$\hat{E}_x = i\sum_{k=1}^{\infty}\left\{\mathcal{A}_k^\mu(\hat{z})\left[J_o\left(\frac{\mu_{1k}\hat{r}}{\sqrt{\Omega}}\right) + J_2\left(\frac{\mu_{1k}\hat{r}}{\sqrt{\Omega}}\right)\cos(2\phi)\right] + \mathcal{A}_k^\nu(\hat{z})\left[J_o\left(\frac{\nu_{1k}\hat{r}}{\sqrt{\Omega}}\right) - J_2\left(\frac{\nu_{1k}\hat{r}}{\sqrt{\Omega}}\right)\cos(2\phi)\right]\right\} \quad (1)$$

and

$$\hat{E}_y = i\sum_{k=1}^{\infty}\left\{\mathcal{A}_k^\mu(\hat{z})J_2\left(\frac{\mu_{1k}\hat{r}}{\sqrt{\Omega}}\right) - \mathcal{A}_k^\nu(\hat{z})J_2\left(\frac{\nu_{1k}\hat{r}}{\sqrt{\Omega}}\right)\right\}\sin(2\phi), \quad (2)$$

where we set $\mathcal{A}_k^\mu(\hat{z}) = \hat{C}_k^\mu\exp[-i\hat{C}_k^\mu\hat{z}]/[(\mu_{1k}^2-1)J_1^2(\mu_{1k})]\,\mathrm{sinc}[1/2(\hat{C}_k^\mu + \hat{C})]$ and, moreover, $\mathcal{A}_k^\nu(\hat{z}) = \hat{C}_k^\nu\exp[-i\hat{C}_k^\nu\hat{z}]/[\nu_{1k}^2J_0^2(\nu_{1k})]\mathrm{sinc}[1/2(\hat{C}_k^\nu + \hat{C})]$. The sinc(·) functions in the expressions for $\mathcal{A}_k^{\mu,\nu}$ is consequence of instantaneous switching of the undulator field. However, our theory applies with a finite accuracy related to the use of the resonance approximation. We thus introduce a spatial frequency filter in the field by redefining

$$\mathcal{A}_k^\mu(\hat{z}) = \frac{\hat{C}_k^\mu\exp[-i\hat{C}_k^\mu\hat{z}]}{(\mu_{1k}^2-1)J_1^2(\mu_{1k})}\mathcal{F}\left\{S(\hat{z}'),\left(\hat{C}_k^\mu + \hat{C}\right)\right\} \quad (3)$$

and

THREE-DIMENSIONAL ANALYSIS OF THE SURFACE MODE SUPPORTED BY A REFLECTION GRATING *

Vinit Kumar†, RRCAT, Indore, M.P. 452013, India
Kwang-Je Kim, ANL, Argonne, IL 60439, USA

Abstract

In a Smith-Purcell Free-Electron Laser (SP-FEL), the electron beam interacts with the surface mode supported by a metallic reflection grating to produce coherent radiation. All the previous analyses of SP-FEL had considered the localization of the surface mode only in the direction perpendicular to the grating surface and assumed translational invariance along the direction of grooves of the grating. In this paper, we include the localization of the surface mode along the direction of grooves as well and study the three-dimensional structure of the surface mode in order to include diffraction effects in the analysis of SP-FELs. Full three-dimensional Maxwell-Lorentz equations are derived for the self-consistent nonlinear analysis of SP-FELs.

INTRODUCTION

Smith-Purcell Free-Electron Laser (SP-FEL) is seen as an attractive option for a compact coherent terahertz source using low energy electron beam. In an SP-FEL, coherent electromagnetic radiation is generated due to the interaction of an electron beam with the surface electromagnetic mode supported by a reflection grating. Several authors have recently studied this interaction using analytical as well as numerical techniques [1-4]. In all the previous analyses, the three-dimensional effects have been either ignored or included only approximately. This is because these analyses consider the interaction of the electron beam with the two-dimensional surface mode, where the electromagnetic field has no variation along the direction of grooves of the reflection grating. The two-dimensional surface mode is therefore not localized in the direction of grooves, although it is localized in the direction perpendicular to the grating surface. We call such surface modes as nonlocalized surface modes in this paper. The diffraction of surface mode along the direction of grooves, which affects the overlap with the electron beam and hence the build-up of power is therefore not included in these analyses. It is important to include three-dimensional effects in the analysis to accurately study the performance of the system and also to accurately calculate the start current, which is the threshold electron beam current for coherent growth of power. In this paper, we study the three-dimensional surface mode, which is localized in both the transverse directions that are perpendicular to the direction of propagation. We also discuss the coupled Maxwell-Lorentz equation to describe the interaction of the electron beam with the three-dimensional surface mode.

In the next section, we discuss the dispersion relation of an off-axis nonlocalized surface mode supported by a reflection grating. The construction of three-dimensional localized surface mode using a combination of off-axis nonlocalized modes is discussed in the following section. Maxwel-Lorentz equation for the interaction of the electron beam with the three-dimensional surface mode is discussed after that and finally, we present some conclusions in the last section.

DISPERSION RELATION OF A SURFACE MODE PROPAGATING OFF-AXIS

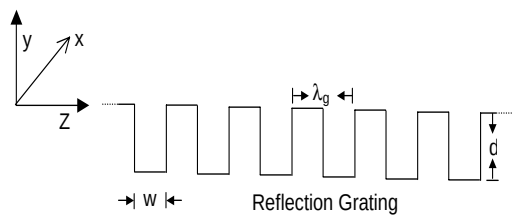

Figure 1: Schematic of a rectangular reflection grating. The top surface of the grating is in the plane y = 0.

Figure 1 shows the schematic of a rectangular metallic reflection grating having period λ_g, groove depth d, and groove width w. We want to study the self-consistent electromagnetic field supported by this structure. All the previous analyses of this problem assumed the system to have translational invariance in the x-direction and hence these are two-dimensional analyses. Here, we assume an exp($ik_x x$) type variation in EM field along the x-direction. In order to find out the dispersion relation of the surface mode, we follow our earlier approach [3, 5], where the surface mode appears in terms of singularities of the reflection matrix $\underline{\mathcal{R}}$. The EM field in the region $y > 0$ is composed of the incident and reflected wave having the following Floquet-Bloch expansion for the H-polarization:

$$H_x^I = \sum_{n=-\infty}^{+\infty} A_n^I \exp\left(ik_n z + ik_x x - ip_n y - i\omega t\right), \quad (1)$$

$$H_x^R = \sum_{n=-\infty}^{+\infty} A_n^R \exp\left(ik_n z + ik_x x + ip_n y - i\omega t\right). \quad (2)$$

* Work supported by the U.S. Department of Energy, Office of Science, Office of Basic Energy Sciences, under Contract No. DE-AC02-06CH11357.

† vinit@cat.ernet.in

COMPARISION BETWEEN KINETIC AND FLUID DESCRIPTION OF PLASMA-LOADED FREE-ELECTRON LASER

B. Maraghechi* , S. Babaei, Department of Physics, Amirkabir University of Technology, P.O. Box 15875-4413, Tehran, Iran

Abstract

In the kinetic treatment of the plasma-loaded FEL single particle equation of motion for both beam and plasma electrons in the radiation fields are used. Therefore, interaction terms between the wiggler and the space-charge wave, in the transverse velocity of electrons, which are important elements in the fluid model, are neglected. A dispersion relation of a plasma-loaded FEL with kinetic theory is used that takes into account the velocity spread of both beam and plasma electrons. In the present analysis a dispersion relation is obtained, by the fluid theory, with the interaction terms between the wiggler and the space-charge wave in the transverse velocity of electrons taken into account. Since these interaction terms are inherently missing in the kinetic theory the two dispersion relation are compared to find out about the importance of these terms. It was found that although the absence of these terms has considerable effects on the growth rate, the general kinetic dispersion relation may be used to study the temperature effects of a warm beam/plasma on the instability of a free-electron laser with a plasma background.

INTRODUCTION

The effects of background plasma on the interaction of electrons with the radiation have been of considerable interest in devices for the generation of coherent electromagnetic radiation. There are several investigations on the plasma loaded FEL[1-11]. A kinetic dispersion relation (DR) of a plasma loaded FEL is derived in Ref. 1 that takes into account the velocity spread of both beam and plasma electrons

In all of the above fluid methods[1-9] and in the kinetic treatments,[1,12,13] of the plasma- loaded FEL, single particle equation of motion for beam or plasma electrons in the radiation fields are considered. Therefore, interaction terms between the wiggler and the space-charge wave, in the transverse velocity of electrons, which are important elements in the fluid model, are neglected.

In the present work, the kinetic theory of Ref. 1 and its DR of a plasma-loaded FEL is considered. Since in this kinetic model single particle treatment of electrons in the radiation field is inherent in the theory a fluid model is used to find a DR that takes into account the interaction terms between the wiggler and the space-charge wave in the transverse velocity of electrons. The fluid DR is compared with the kinetic DR to find the importance of these interaction terms. It is found that the absence of these interaction terms in the kinetic treatment has considerable effects on the growth rate. However, characteristic behaviour of the kinetic DR is found to be satisfactory and, consequently, the general kinetic DR may be used to study the temperature effects of a warm beam/plasma on the instability of a plasma–loaded FEL.

KINETIC DESCRIPTION

Consider a relativistic electron beam propagating in the z direction through background plasma and a helical wiggler magnetic field. A general DR for a plasma-loaded FEL, using kinetic theory, is derived in Ref. 1 as

$$c^2k^2D^L(k,\omega)D^T(k-k_0,\omega)D^T(k+k_0,\omega)$$
$$=\frac{1}{2}a_w^2[D^T(k-k_0,\omega)+D^T(k+k_0,\omega)]\times$$
$$\times\{[\chi^{(1)}(k,\omega)]^2-c^2k^2D^L(k,\omega)[\alpha_3\omega_b^2+\chi^{(2)}(k,\omega)]\}. \qquad (1)$$

In order to compare the kinetic DR with that of the fluid model a relatively weak wiggler is assumed. In this case, the resonant space-charge wave $D^L(k,\omega)\approx 0$ couples to the resonant right circular wave $D^T(k-k_0,\omega)\approx 0$, which leaves the left circular wave nonresonant, i.e., $D^T(k+k_0,\omega)\neq 0$. Moreover, terms containing a_w^2 are also neglected in the coupled equations and the cold beam and plasma is assumed to obtain the following DR

$$(\omega^2-c^2k_r^2-\frac{\omega_b^2}{\hat{\gamma}_b}-\omega_p^2)(1-\frac{\omega_b^2}{\hat{\gamma}_b\gamma_z^2[\omega-kV_{\|}]^2}-\frac{\omega_p^2}{\omega^2})$$
$$=\frac{1}{2}a_w^2\frac{\omega_b^4}{\hat{\gamma}_b^4}\frac{(\omega\beta_{\|}-ck)^2}{(\omega-kV_{\|})^4}, \qquad (2)$$

where, $k_r=k-k_0$ is the radiation wave number and all other quantities are defined in Sec. III and in Ref. 1. Kinetic model DR (2) has been solved numerically to find the imaginary part of the frequency. Figure 1 shows the variation of growth rate with radiation wave number for $B_w=1$ kG, $\hat{\gamma}_b=4$, and $\hat{n}_b=1\times10^{13}$ cm^{-3}. Curves 1, 2, 3, 4, and 5 corresponding to the density of background plasma at 0.8, 1.25, 1.75, 2, and 2.3, respectively (in units of 10^{13} cm^{-3}).

FLUID DESCRIPTION

We now consider the fluid theory description of a relativistic and cold electron beam that passes through a background plasma and a static helical wiggler magnetic

* Electronic mail: behrouz@aut.ac.ir

CONSERVATION LAWS IN QUASILINEAR THEORY OF RAMAN FREE-ELECTRON LASER

B. Maraghechi, Department of Physics, Amirkabir University of Technology, Tehran, Iran
A. Chakhmachi, Plasma Physics and Nuclear Fusion Research School,
Nuclear Science and Technology Research Institute, AEOI, Tehran, Iran
and Department of Physics, Amirkabir University of Technology, Tehran, Iran

Abstract

A quasilinear theory of the free-electron laser, in Raman regime, is presented to establish that conservation laws on number, energy, and momentum are upheld. A high density electron beam is assumed so that the space-charge potential is no longer negligible. A sufficiently broad band spectrum of waves is assumed so that saturation will be due to the quasilinear spread of the beam electrons. Otherwise, for the single mode excitation, saturation will be due to the electron trapping in the space-charge potential. It is shown that the quasilinear slow variation of the background distribution function is in the form of the diffusion equation in momentum space. An expression for the time evolution of the spectral energy density is derived. Conservation laws to the quasilinear order (second order) are derived and are proved to be satisfied. Results of the present investigation may be used to study the quasilinear saturation of a free-electron laser in the presence of the space-charge wave.

INTRODUCTION

Saturation and nonlinear evolution of free-electron lasers (FEL) are of considerable importance both experimentally and theoretically. The main reason is that saturation determines the efficiency of the device.

For sufficiently broad spectrum of unstable waves, saturation is due to quasilinear energy spread of the beam electrons. This problem has been studied only in the Compton regime, where the electrostatic potential of the space-charge wave is negligible due to low density of the electron beam [1-5]. On the other hand, when there is only a single exited mode, saturation of the amplification is considered to be caused by electrons trapped in the electrostatic field of the space-charge wave in the Raman regime or the pondermotive wave in the Compton regime [6-8].

The purpose of the present investigation is to derive conservation laws in the quasilinear analysis of an FEL in the presence of the space-charge field of electrons. The method of analysis and notations are similar to Ref. 1. The quasilinear slow variation of the background distribution function is in the form of the diffusion equation in momentum space. An expression for the time evolution of the spectral energy density is derived. Conservation laws, to the quasilinear order (second order), for particle, energy and momentum are derived and are proved to be satisfied.

PHYSICAL MODEL

We consider a collisionless, relativistic, electron beam with uniform cross section propagating in the z direction. The electron beam propagates through a constant amplitude helical wiggler magnetic field specified by

$$\mathbf{B}_0 = -B_w cos(k_0 z)\widehat{\mathbf{e}_x} - B_w sin(k_0 z)\widehat{\mathbf{e}_y}, \qquad (1)$$

The transverse electromagnetic and longitudinal electrostatic perturbed fields $\delta\mathbf{E}$ and $\delta\mathbf{B}$ are defined as

$$\delta\mathbf{E} = -\frac{1}{c}\frac{\partial}{\partial t}\delta\mathbf{A} - \nabla\delta\varphi, \qquad \delta\mathbf{B} = \nabla\times\delta\mathbf{A}. \qquad (2)$$

The relativistic, nonlinear Vlasov equation for the electron beam distribution function $f_b(z,\mathbf{p},t)$ is given by

$$[\frac{\partial}{\partial t}+v_z\frac{\partial}{\partial z}-e(\delta\,\mathbf{E}+\frac{\mathbf{v}\times(\mathbf{B}_0+\delta\mathbf{B})}{c}).\frac{\partial}{\partial\mathbf{p}}]f_b(z,\mathbf{p},t)=0. \qquad (3)$$

In the present analysis, we investigate the class of exact solution to Eq. (3) of the form

$$f_b(z,\mathbf{p},t) = n_0\delta(P_x)\delta(P_y)G(z,p_z,t), \qquad (4)$$

where $n_0 = const$, and P_x and P_y are the canonical momenta transverse to the beam propagation direction. Substituting the distribution function (4) into Eq. (3) and integrating the resting equation over p_x and p_y, gives

$$[\frac{\partial}{\partial t}+v_z\frac{\partial}{\partial z}-\frac{\partial}{\partial z}H(z,p_z,t)\frac{\partial}{\partial p_z}]G(z,p_z,t)=0. \qquad (5)$$

In this equation, $H(z,p_z,t)$ is defined by

$$H(z,p_z,t) = \gamma_T mc^2 - e\delta\varphi(z,t)$$

$$= [m^2c^4 + c^2p_z^2 + e^2(A_x^0+\delta A_x)^2 + e^2(A_y^0+\delta A_y)^2]^{(1/2)}$$

$$-e\delta\varphi(z,t), \qquad (6)$$

which is the particle energy for $P_x = 0 = P_y$, and $\gamma_T mc^2$ is the kinetic energy. In the absence of perturbed fields, the energy is given by

$$\gamma mc^2 = (m^2c^4 + c^2p_z^2 + e^2B_w^2/k_0^2)^{1/2}. \qquad (7)$$

LIMIT FOR HARMONIC CONVERSION IN A SINGLE CASCADE OF COHERENT HARMONIC GENERATION

E. Allaria, G. De Ninno, Sincrotrone Trieste, Trieste, Italy

Abstract

Harmonic generation is a reliable method for producing coherent high-brightness photon pulses from relativistic electron bunches. The standard process leading to Coherent Harmonic Generation is initiated by a powerful seed laser. As a consequence, reaching short wavelengths generally requires a high order frequency conversion. For that reason some of the projects which are presently under development for coherent VUV and soft-Xray emission are based on a series of two or more consecutive "cascades". In these setups, the radiation produced into one stage is used as a seed in a following cascade. The required number of cascades depends on the maximum harmonic conversion which can be obtained in single stages. In this paper we study the mechanism underlying CHG, i.e. the bunching creation into the modulator, and we investigate the physical limits of the single-stage CHG.. The identification of the limiting parameters may allow the implementation of new methods for enhancing the conversion efficiency. One of these methods, which rely on a simple modification of the standard CHG scheme, has been recently proposed [3] and shown to be able to significantly improve the system performance. Results are confirmed by 3D numerical simulations using the FERMI electron beam parameters as initial conditions.

INTRODUCTION

It is well known that the electron bunching, which is needed for effective High Gain Harmonic Generation (HGHG), rapidly decreases with the harmonic number, unless a strong energy modulation is produced in the modulator. However, the exponential light amplification that follows the first quadratic growth is strongly sensitive to the total energy spread,i.e., the quadratic combination of initial incoherent energy spread and of the coherent modulation.

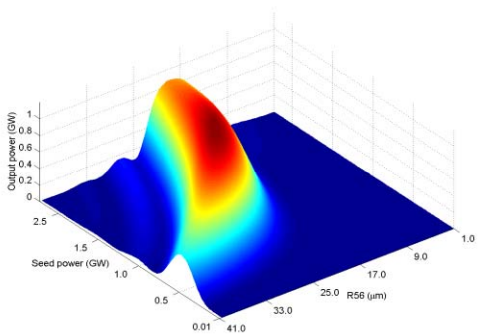

Figure 1: Example of Optimized output power for the HGHG FEL setup as a function of seed power and R56.

As a consequence, the optimization of a HGHG scheme relies on a compromise between the production of a sufficiently high bunching in the modulator (allowing a significant quadratic growth) and the need of keeping the total energy spread below the FEL parameter ρ. An example of the dependence of the produced FEL output power on the seed power and dispersive section strength (R56) is shown in Fig.1.

In this paper we study the possibility of optimizing the CHG setup once the electron-beam and the radiator parameters are given. For the presented work, electron beam parameters have been chosen to be those of the FERMI@Elettra project [1], see Table 1.

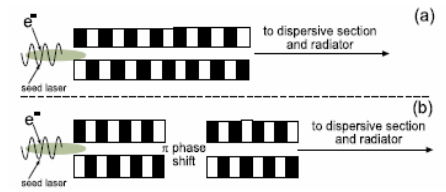

Figure 2: a) Schematic layout for the modulator in a standard HGHG setup. b) Proposed modified layout considering a phase shifter in between two modulator subsections.

The optimization is based on a modification of the standard modulator scheme, involving both the ondulator configuration and the power of the seed laser (Fig.2). The study has been done by perfomring numerical simulations with well established 3D FEL codes ginger and genesis.

Table 1: FERMI electron-beam parameters

Parameter	*Value*	*Units*
Electron Beam Energy	1.2	GeV
Peak current	1	kA
Uncorrelated energy spread	200	keV
Norm. Transverse Emittance	1.5	mm-mrad

CASCADE LIMIT IN A STANDARD CHG SCHEME

According to theoretical predictions [2], the induced energy spread needed for efficient CHG increases with the harmonic number.

Figs.3 and .4 show that, while the optimum value of energy spread increases when reducing the emitted wavelength, the optimum bunching is approximately constant (order of 4% in our case). This result can be explained considering that in HGHG bunching is necessary to induce the quadratic emission occurring in the first part of the process, AND SIMPLY HAS TO BE LARGER THAN SHOT NOISE. However, the main contribution to the final output power comes from the

1D LINEAR INTENSITY SPIKING EVOLUTION IN A SINGLE SHOT OF A SASE FEL

C. Maroli, L. Serafini, INFN-Sezione di Milano,Via Celoria 16, 20133 Milano, Italy
V. Petrillo, Dipartimento di Fisica dell'Università di Milano-INFN Sezione diMilano,
Via Celoria 16, 20133 Milano, Italy

Abstract

It is shown that the simple system of equations used by Bonifacio et al. in 1994, leads to signals characterized by the usual spiky behaviour of the FEL radiation intensity, as well as to "coherent" signals in which the spiking is reduced to a small amplitude random fluctuation on a smooth and nearly constant average value. The two types of signals are obtained with different classes of initial conditions. In particular, coherent signals correspond to initial shot-noise configurations whose closely spaced spikes have widths much smaller than the cooperation length.

INTRODUCTION

The intensity spiking in the radiation of a high-gain free-electron laser starting from noise consists of a sequence of random spikes with wide top-to-bottom variations in the signal received at the end of the undulator [1-4]. The random nature of the spiking is a direct consequence of the random character of the small electromagnetic fields created on the electron beam as it enters the undulator field and the main aspects of the spiking are described accurately by the linear form of the one-dimensional FEL equations.

Starting from the Maxwell-Lorentz 1D equations, the disturbances in the radiation field $\delta A(z,t)$ and bunching factor $\delta b(z,t)$ are given by the following simple linear system in the limit of small radiation fields and when the radiation wave length λ is much smaller than the cooperation length $L_C = \lambda/4\pi\rho$ (ρ is the FEL parameter):

$$\left(\frac{\partial}{\partial t} + c(1-\beta_0)\frac{\partial}{\partial z}\right)\delta A(z,t) = \delta b(z,t),$$
$$\frac{\partial^2}{\partial t^2}\delta b(z,t) = \frac{i}{T_G^3}\delta A(z,t) \qquad (1)$$

These equations are written in the frame moving with the undisturbed beam velocity $c\beta_0$, $T_G = \lambda_w/4\pi c\rho$ is the gain time and λ_w the undulator period. The reason why we reconsider this very simple system of equations is that it may lead to final situations in which there is no spiking and the signal found at the end of 10-20 gain times T_G consists of one single and smooth bump, even when the length L_b of the beam is much longer than the cooperation length L_C.

ONE SINGLE SPIKE

We consider the particular solution of (1)

$$\delta A(\bar{z},\bar{t}) = \int_{-\infty}^{+\infty} dh\, \delta A_0(h) e^{i(h\bar{z}-\omega(h)\bar{t})}$$

where $\omega(h)$ is the root of the dispersion relation $\omega^3 - h\omega^2 - 1 = 0$ with positive imaginary part. The integral in the preceding equation is solved numerically for the case of a Gaussian spike at t=0 and different values of the parameter $\alpha = L_0/L_C$, where L_0 is the FWHM value of the initial Gaussian spike.

Fig.1 shows that the time evolution of the spike depends on the value of its width at t=0 as compared with L_C. In particular, when $L_0 \approx L_C$, the spike increases exponentially while its width increases only slightly. Instead, when $L_0 << L_C$, the width of the spike increases by several orders of magnitude starting from the very small value at t=0.

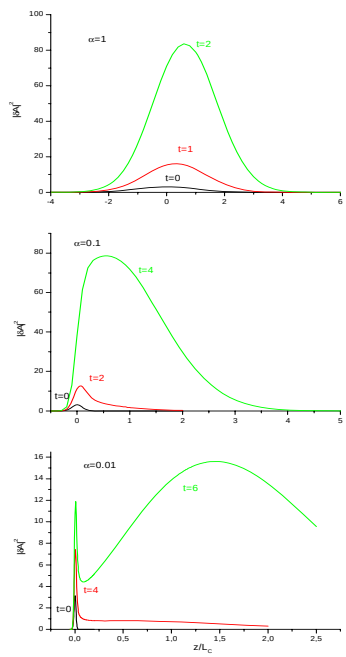

Fig.1(color) – Values of $|\delta A|^2$ *vs* z/L_C. Top figure $\alpha = 1$, curves (a, black),(b, red),(c, green) for $t/T_G = 0, 1, 2$, respectively; middle figure $\alpha = 0.1$, (a),(b),(c) for $t/T_G = 0, 2, 4$; bottom figure $\alpha = 0.01$, (a),(b),(c) for $t/T_G = 0, 4, 6$.

OPTIMIZED DESIGNS FOR CAEP IR FREE-ELECTRON LASER

Xiaojian Shu#, Yuhuan Dou, Institute of Applied Physics and Computational Mathematics, P. O. Box 8009, Beijing 100088, P. R. China

Abstract

The characteristics of CAEP IR free-electron laser are estimated and the optimized designs of the resonator parameters such as the radius of output hole, the size of mirror and the length of the resonator are carried out using our 3D FEL oscillator code. With the appropriate parameters, the saturated power, output power, gain and the construction of optical modes are calculated.

INTRODUCTION

Infrared free-electron lasers (FELs) have broken important ground in optical science for many attractive features such as most notably wavelength tunability, control of spectral and temporal pulse width. In order to bring along the development of correlative technologies such as superconducting technology, linear accelerator technology and optical cavity technology, an infrared FEL device is built at the China Academy of Engineer Physics (CAEP) which driven by superconducting linear accelerator. The radiation wavelength of the device will be in the range from 3 to 8μm.

In this paper, The characteristics of CAEP IR free electron laser devices will be estimated and the optimized design of the resonator parameters such as radius of output hole, the size of mirror, the resonator length will be carried out by using our 3D FEL oscillator code (OSIFEL)[5-7]. The design is achieved by considering two factors as optical cavity character and the transverse optical modes. Based on the appropriate parameters, the saturated power, output power, the resonator gain, the construction of optical modes are calculated.

THE ESTIMATE OF THE OPTICAL CHARACTERISTICS

Table 1: CAEP IR FEL Parameters

Electron beam	
Energy (MeV)	37
Peak current (A)	30
Micro bunch (ps FWHM)	2.5
Energy spread (%)	1
Emittance (π mm mrad)	20
Wiggler	
Period (cm)	3.2
Peak field strength (kG)	3.2
Number of periods	44
Optical	
Wavelength (μm)	4.4
Cavity length (m)	2.769
Mirror curvature (m)	1.499

#shu_xiaojian@iapcm.ac.cn

The electron-beam and wiggler parameters used are listed in Table 1. The energy spread and emittance are specified as FWHM and RMS. Using the parameters of the optical cavity, we can attain that the Rayleigh length is 40cm, the optical waist radius is 0.7mm, and the radius of the optical beam on the cavity mirror is 2.6mm.

THE NUMERICAL SIMULATIONS

To attain optimized the radius of the mirror of the optical cavity and the coupling hole, the numerical simulations are performed using the 3-D OSIFEL code. In the simulations, the distribution functions of transverse position and velocity, energy of the electron are assumed as Gaussian. The corresponding initial values of the sample electrons are given by Monte Carlo method and the initial phases are loaded according to the 'quiet start' scheme to eliminate the numerical noise.

Selection of the Radius of Coupling Hole

The influences of the hole-coupling on the gain, power, output and the mode construction are simulated and studied, as shown in Table 2, where r is the radius of the coupling hole, G_{net} the net gain, P_{in} the saturated intracavity power, P_{out} the output power, η_{loss} the total loss of the resonator, f_{00} the ratio of the fundamental mode, η_{out} the coupling efficiency, which is defined as the ratio of the useful loss to the total loss. It can be seen that the total loss of resonator and coupling efficiency decrease as a reduction in the size of hole, however, the ratio of the fundamental mode increases. If the size of hole is increase, the interaction of the optical radiation with the electrons will become weaker so the net gain of resonator is decreased. According to Table 2, we may select the optimum size of radius r as 0.3 to 0.4mm.

Table 2 Characteristics of resonator as a function of the radius of the coupling hole

r /mm	G_{net} /%	P_{in} /MW	P_{out} /MW	η_{out} /%	η_{loss} /%	f_{00} /%
0.30	23.4	131	3.58	52.7	5.40	98.0
0. 35	20.0	110	3.61	53.0	6.60	97.1
0. 40	15.5	67	3.41	54.6	10.1	94.2
0. 50	10.3	41	2.82	56.0	14.0	90.0

Effects of the Mirror Size

There are mainly two aspects from the influence of the cavity mirror size. One is the influence on the characteristics of the resonator, the other is the influence on the structure of transverse optical modes. That is, when the radius of cavity mirror becomes large, the net gain and the saturated intracavity power will increase; however, the proportion of fundamental mode will decrease because the loss of the high order modes is small. So the optimum

FEL WITH OROTRON TYPE FEEDBACK*

N.S. Ginzburg#, A.M. Malkin, N.Yu. Peskov, R.M.Rozental, A.S. Sergeev, IAP RAS, Nizhny Novgorod, Russia
K. Kamada, R. Ando, Kanazawa University, Kanazawa, Japan.

Abstract

In this paper we discuss a novel scheme of the free-electron laser in which the electromagnetic wave excited by the electron beam is coupled to the mode of a two-mirror quasioptical resonator by means of corrugation one of the mirrors. The described scheme allows to combine selective properties of quasioptical resonator with relativistic frequency up-conversion of a free electron laser.

INTRODUCTION

In microwave electronics orotron [1] is widely used as a source of radiation in millimeter and submillimeter wavebands. In this device an electron beam is coupled to a mode of quasi-optical resonator by means of the periodical grating one of the resonator mirrors. In our paper we discuss a relativistic modification of such a device which can be useful for providing spatial coherence radiation from large size electron beam

In orotron (Fig.1a) a rectilinear electron beam moving along the periodical grating on the mirror of a quasioptical cavity to be in Cherenkov synchronism to a spatial harmonic of the resonator mode. A novel FEL scheme (Fig. 1b) is suggested in which the slow wave structure of orotron is replaced by shallow Bragg corrugation which provides the coupling of the transverse (with respect to direction of beam propagation) mode of a quasi-optical resonator with longitudinally propagating wave. The latter can be excited by the relativistic electron beam wiggling in undulator field in condition of Dopper frequency up-shift. It should be noted that such a scheme is similar to FEL based on coupling between the quasi cutoff and the propagating mode in cylindrical waveguides which was described in [2,3] (above interaction mechanism will be tested on a 8 mm FEL based on high current accelerator 0.7 MeV/2 kA/200ns at Kanazawa University, Japan). In considered case we replace the waveguide by open quasi-optical resonator and suggest that FEL will be driven by large size sheet electron beam. As in [2] the transverse propagating (cut-off) mode provides the feedback in the system thus leading to self-excitation, while the longitudinal propagating wave is responsible for energy extraction in the steady-state regime of operation. But additionally as will be shown in this paper in considered geometry the cut-off mode provides spatial coherence radiation from sheet electron beam.

*Work supported by RFBR under Grant 06-02-17129-a and the Dynasty foundation.
#ginzburg@appl.sci-nnov.ru

THE ELECTRODYNAMIC MODEL

We consider a resonator consisting of two metallic mirrors . One of the mirrors is corrugated with a period *d*. This corrugation provides coupling between the modes possessing longitudinal (in *z* direction, see Fig.1b) wavenumbers differing by factor $\bar{h} = 2\pi / d$. In the simplest case of the sinusoidal corrugation

$$b(z) = b_0 \cos(\bar{h} z),$$

where $b(z)$ is the deviation of the mirror surface, $2b_0$ is tthe corrugation depth. In the case of more complicated corrugation (for example, meander type corrugation) b_0 is equal to the amplitude of the first space harmonic We assume corrugation to be shallow in the wavelength scale, so that $\bar{h} b_0 << 1$.

We use coupling between the propagating in *z* direction wave and the *q*-th mode of the quasioptical resonator (in the system with the closed waveguide [2] this mode corresponds to the quasi cut-off mode). Above coupling requires that the wavenumber of the longitudinal propagating wave $h = \omega / c$ and the wavenumber of the transverse propagating mode quasioptical resonator ($q\pi / L_y$) should be equal to the translation vector of the Bragg structure:

$$h \approx \frac{q\pi}{L_y} \approx \bar{h},$$

where ω is the operation frequency, *c* is the velocity of light, L_y is the distance between the mirrors (in *y* direction).

Note that due to the symmetry of the considered system not only the forward + *z* direction propagating wave is coupled to the transverse mode, but also a

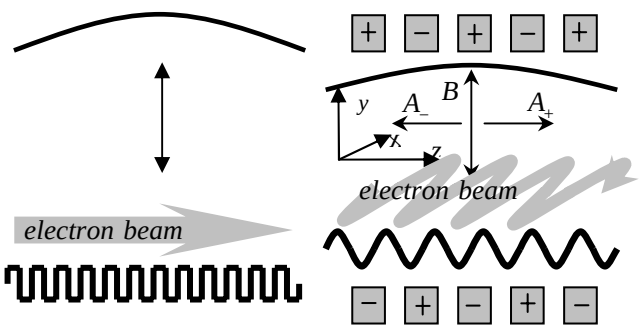

Fig.1. Schematic of the orotron (a) and FEL with orotron-type feedback (b).

A DESCRIPTION OF GUIDED FEL RADIATION WITH DIELECTRIC WAVEGUIDE EIGENMODES

E. Hemsing*, G. Andonian, J. Rosenzweig, Particle Beam Physics Laboratory, UCLA, USA
A.Gover, Deptartment of Physical Electronics, Tel-Aviv University, Israel

Abstract

We present a description of free-electron laser (FEL) radiation in the high-gain, small-signal regime through an expansion of eigenmodes of a virtual dielectric waveguide. A set of coupled differential equations is derived for the slowly-varying mode expansion coefficients and the electron beam density modulation amplitudes. The equations are decoupled into an algebraic matrix equation for solutions of the self-similar FEL supermodes that propagate with a self-similar profile. For a suitable choice of the form of the virtual dielectric, this virtual dielectric waveguide expansion (VDE) approach has the advantage of describing gain-guided FEL radiation over many Rayleigh lengths in terms of a basis that parallels the standard gaussian modes of free-space paraxial optics.

INTRODUCTION

The optical guiding of light in free-electron lasers (FELs) is a well-known phenomena that results during amplification as the coherent interaction between the electron beam (e-beam) and the electromagnetic (em) field introduces an inward curvature in the phase front of the light, refracting it back towards the lasing core of the e-beam[1, 2]. During the exponential gain process the e-beam can behave like a guiding structure that suppresses diffraction, reducing transverse power losses and enhancing the em field amplification (gain-guiding). The guided em field eventually settles into a propagating, self-similar eigenmode of the FEL system (supermode) with a fixed transverse profile distribution and spot size[3, 4].

Guided modes have been previously explored analytically by direct derivation of the eigenmode equations from the coupled Maxwell-Vlasov equations[3, 5, 6], and through expansions of the FEL signal fields in terms of hollow, conducting-boundary waveguide eigenmodes[4], step-index fiber modes[2], and free-space paraxial waves[7, 8]. Since, in an FEL, the e-beam operates simultaneously as an optical source and as a wave-guiding structure, an em mode description permits investigation of the coupling efficiency and guiding characteristics of individual modes to the e-beam. Of particular interest is the coupling to the well-known Hermite-Gaussian or Laguerre-Gaussian modes that describe free-space waves in the paraxial limit. The propagation and guiding of these modes over many Rayleigh lengths in an FEL interaction can be investigated directly by an expansion of the radiation field in terms of guided eigenmodes that have the form of paraxial modes evaluated at the waist. This connection is useful both in characterizing the free-space propagating radiation fields emitted from the FEL, but also in understanding input radiation coupling, as in the case of seed radiation injection.

FIELD EXPANSION AND MODE EXCITATION IN A WAVEGUIDE

In a structure of axial translational symmetry, the radiation fields can be expanded in terms of transverse radiation modes with amplitudes that vary only as a function of the symmetry axis, z. Neglecting backward propagating waves and approximating the fields as dominantly transverse, the radiation field expansion in terms of waveguide modes is,

$$\underline{\tilde{E}}_\perp(\underline{r}) = \sum_q C_q(z)\underline{\tilde{\mathcal{E}}}_{\perp q}(r_\perp)e^{ik_{zq}z}$$

$$\underline{\tilde{H}}_\perp(\underline{r}) = \sum_q C_q(z)\underline{\tilde{\mathcal{H}}}_{\perp q}(r_\perp)e^{ik_{zq}z}. \quad (1)$$

where $\underline{\tilde{\mathcal{H}}}_{\perp q} = (1/Z_q)\hat{e}_z \times \underline{\tilde{\mathcal{E}}}_{\perp q}$, k_{zq} is the q^{th} mode axial wavenumber, and $Z_q = (k/k_{zq})\sqrt{\mu_0/\epsilon_0}$ for TE modes. The modes are orthogonal and normalized to

$$\mathcal{P}_q = \frac{1}{2}\mathrm{Re}\Big[\int\int[\underline{\tilde{\mathcal{E}}}_{\perp \mathrm{q}}(\mathrm{r}_\perp) \times \underline{\tilde{\mathcal{H}}}^*_{\perp \mathrm{q}}(\mathrm{r}_\perp)] \cdot \hat{\mathrm{e}}_\mathrm{z}\mathrm{d}^2\mathbf{r}_\perp\Big]. \quad (2)$$

The mode $\tilde{\mathcal{E}}_{\perp q}$ is an eigenmode of a dielectric medium with transverse variation in the refractive index $n(r_\perp)$. Assuming $\nabla n^2 \ll k$, the eigenmode equation is

$$\nabla^2_\perp \underline{\tilde{\mathcal{E}}}_{\perp q}(r_\perp) + [n(r_\perp)^2k^2 - k^2_{zq}]\underline{\tilde{\mathcal{E}}}_{\perp q}(r_\perp) = 0 \quad (3)$$

where $k = \omega/c$. With equations (1) and (3) and under the paraxial approximation ($|d^2C_q/dz^2| \ll |k^2C_q|$) for the slowly-growing coefficients, the excitation equation for the mode q in the presence of a source current is given by,

$$\frac{d}{dz}C_q(z) = -\frac{1}{4\mathcal{P}_q}e^{-ik_{zq}z}\int\int \underline{\tilde{J}}_\perp(\mathbf{r}) \cdot \underline{\tilde{\mathcal{E}}}^*_{\perp q}(r_\perp)d^2\mathbf{r}_\perp - i\sum_{q'} C_{q'}(z)e^{-i\Delta k_{zqq'}z}\kappa^d_{q,q'} \quad (4)$$

where

$$\kappa^d_{q,q'} = \frac{\omega\epsilon_0}{4\mathcal{P}_q}\int\int[n(r_\perp)^2 - 1]\underline{\tilde{\mathcal{E}}}_{\perp q'}(r_\perp) \cdot \underline{\tilde{\mathcal{E}}}^*_{\perp q}(r_\perp)d^2\mathbf{r}_\perp \quad (5)$$

and $\Delta k_{zqq'} = k_{zq} - k_{zq'}$ is the difference between the axial wavenumbers of the modes q and q'. The term $\kappa^d_{q,q'}$ characterizes the mode coupling and represents the virtual polarization currents and charges that must be subtracted when using eigenmodes of a dielectric waveguide, since no such structure exists in the physical system.

* ehemsing@physics.ucla.edu

ENHANCING FEL POWER WITH PHASE SHIFTERS*

Daniel Ratner†, Stanford University, CA, 94305 USA
Alex Chao, Zhirong Huang, SLAC, Stanford, CA 94309 USA

Abstract

Tapering the undulator parameter is a well-known method for maintaining the resonant condition past saturation, and increasing Free Electron Laser (FEL) efficiency. In this paper, we demonstrate that shifting the electron bunch phase relative to the radiation is equivalent to tapering the undulator parameter. Using discrete phase changes derived from optimized undulator tapers for the Linac Coherent Light Source (LCLS) x-ray FEL, we show that appropriate phase shifts between undulator sections can reproduce the power enhancement of undulator tapers. Phase shifters are relatively easy to implement and operate, and could be used to aid or replace undulator tapers in optimizing FEL performance.

INTRODUCTION

Despite the projected six orders of magnitude increase in peak power for Self-Amplified Spontaneous Emission (SASE) x-ray FELs, some applications, including single molecule imaging, may require still higher photon flux [1]. To increase the power in higher harmonics, it is possible to shift the FEL electron phase relative to the radiation, suppressing the power in the fundamental wavelength and prolonging growth of the harmonics [2]. We have studied the related use of phase shifts to correct slippage at saturation and boost the power output of the fundamental wavelength. Similar methods have been mentioned in the past in connection with harmonic radiation [2] and numerical simulations [3]. Here we undertake a detailed analytical and numerical study of enhancing FEL power with phase shifters. We explore the relation between phase shifts and undulator tapers to calculate optimal phase shifts for SASE FELs in the saturation regime. The phase shift method, while equivalent to tapering the undulator parameter, provide an independent knob to maximize the FEL performance.

ONE-DIMENSIONAL ANALYSIS

The resonant condition

$$\lambda_1 = \lambda_u \frac{1 + K^2/2}{2\gamma_0^2} \tag{1}$$

sets the radiation wavelength, λ_1 for an FEL; after each undulator period, λ_u, the electron bunch slips behind the radiation by exactly λ_1. It follows that when the resonant condition holds, the phase, Ψ, between the electron bunch and radiation stays constant (up to 2π). Near saturation, the bunch loses significant energy to the radiation, and the FEL resonant condition begins to fail. As $\gamma_0 \to \gamma < \gamma_0$, the resonant wavelength increases, and the electrons slip more than one radiation wavelength during each undulator period. Introducing a phase shift (by means of a small chicane) can correct for the increase in slippage by shifting the bunch backwards into the previous bucket. (If, over many undulator periods, the bunch has accumulated extra slippage of $\Delta\theta$, then the chicane shifts the electrons an additional $2\pi - \Delta\theta$. There is no easy way to shift electrons forward.) After the shift, the electron bunch is once again in phase with the radiation, preserving the resonant condition farther into saturation.

To show that compensating for the additional slippage can optimize the radiation power in the undulator, we use a simplified 1-D FEL model and neglect the effect of detuning. The slowly varying radiation field $\tilde{a}$ is given by

$$\frac{d\tilde{a}}{d\bar{z}} = -\langle e^{-i\theta_j} \rangle \,. \tag{2}$$

The phases, $\theta \equiv (k + k_u)z - \omega t + \text{const}$, are the longitudinal positions of the electrons relative to the electron bunch given in units of $\lambda_1/2\pi = 1/k_u$. The variable $\bar{z} \equiv 2k_u\rho z$, is the scaled position along the undulator. Here ρ is the dimensionless FEL parameter [4]. Finally, the average in Eq. (2) is taken over all electrons. Taking $\tilde{a} \equiv Ae^{i\Psi}$, with Ψ the phase of the radiation relative to the electron bunch, we can separate out the magnitude and phase components of the radiation field:

$$\frac{d\tilde{a}}{d\bar{z}} = e^{i\Psi}\left[\frac{dA}{d\bar{z}} + iA\frac{d\Psi}{d\bar{z}}\right] . \tag{3}$$

Inserting Eq. (3) into Eq. (2) and separating real and imaginary parts gives

$$\frac{dA}{d\bar{z}} = -\langle \cos(\theta_j + \Psi) \rangle \,, \tag{4}$$

$$\frac{d\Psi}{d\bar{z}} = \frac{1}{A}\langle \sin(\theta_j + \Psi) \rangle \,. \tag{5}$$

Our strategy is to maximize A by introducing an arbitrary phase shift, ϕ between the radiation and electrons, and then maximize $\frac{dA}{d\bar{z}}$ with respect to ϕ at all points along the undulator. (A chicane delays all particles relative to the radiation, introducing an arbitrary change in relative phase of the bunch.) Our goal, then, is to choose ϕ to maximize the quantity $-\langle \cos(\theta_j + \Psi + \phi) \rangle$.

Adding the arbitrary phase, ϕ, gives

$$\frac{dA}{d\bar{z}} = \langle \cos(\theta_j + \Psi) \rangle \cos(\phi) - \langle \sin(\theta_j + \Psi) \rangle \sin(\phi) \tag{6}$$

*Work supported by Department of Energy contract DE–AC02–76SF00515.

† dratner@slac.stanford.edu

THREE-DIMENSIONAL THEORY OF THE CERENKOV FREE-ELECTRON LASER

H. L. Andrews* and C. A. Brau
Department of Physics and Astronomy, Vanderbilt University, Nashville, Tennessee, 37235, USA

Abstract

We present an analytical theory for the operation of a Cerenkov free-electron laser which includes diffraction of the optical mode in the direction transverse to the electron beam. Because the width of the optical mode depends on gain, the usual cubic dispersion relation is replaced by a 5/2-power dispersion relation, which allows two roots. These roots both have positive real parts, indicating that they are slow waves. For a narrow electron beam, the optical mode is much wider than the beam, thus reducing the gain by an order of magnitude from that predicted by the two-dimensional theory. In the limit of a wide electron beam, the two-dimensional theory is recovered.

INTRODUCTION

Compact narrow-band far-infrared, or terahertz (THz), sources have potential applications in a large number of fields including biology, chemistry, and materials science[1, 2]. The current THz sources in existence either produce short-pulsed broadband radiation, or require very large facilities. The exceptions to these are CO_2 pumped FIR lasers and backward-wave oscillators (BWOs). FIR lasers only have discreet lines, making them impractical for spectroscopy, and BWOs do not reach short enough wavelengths. Free-Electron Lasers (FELs) based on either the Smith-Purcell effect or Cerenkov radiation offer the possibility of a source capable of producing narrow-band THz radiation.

In a Cerenkov FEL the electron beam interacts with the evanescent wave of a single-sided dielectric waveguide. Since the wave has a forward group velocity, the instability is convective and the device works as an amplifier. Oscillation is achieved by feedback from reflections at the ends of the structure. The most powerful CFELs use ampere beams in cylindrical waveguides [3] but smaller devices can be constructed using milliampere beams in planar geometries [4]. The theory of cylindrical devices has been developed in detail, and the agreement with experimental results is good [3]. The theory for planar geometries has been worked out in two dimensions [5]. We extend this theory to three dimensions by including diffraction of the optical beam in the direction transverse to the electron beam, parallel to the surface of the dielectric [6]. We show that the gain is reduced by an order of magnitude and the fundamental nature of the conventional three-wave interaction is altered.

* heather.l.andrews@vanderbilt.edu

THEORY

To model the CFEL in three-dimensions we let the electron beam pass above a dielectric slab, bounded below by a conductor, as shown in Figure 1. The electron beam travels in $\hat{z}$, while $\hat{x}$ extends above the slab and $\hat{y}$ is the transverse direction. We assume a beam of width W, and a dielectric slab of depth H.

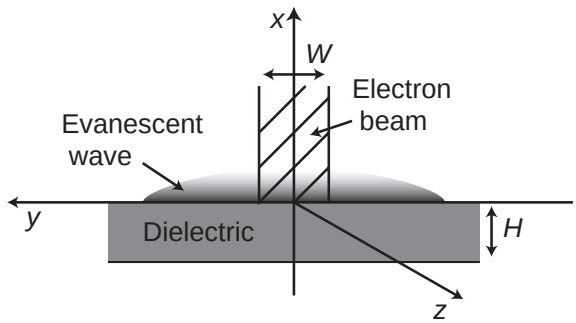

Figure 1: Geometry used for the three-dimensional model. The electron beam has a width W and is allowed to extend to infinity in x. The dielectric had a depth H and is wide compared to both the evanescent scale height and mode width.

To make the problem tractable, we start by making three assumptions. First, we assume the electron beam is uniform and extends infinitely far in $\hat{x}$. This introduces negligible errors to the theory because the electron beam height is actually on the order of the evanescent scale height. The assumption is corrected at the end of the calculation by using a filling factor. Next, we assume the operating frequency of the device is much larger than the plasma frequency or $\omega \gg \omega_e$. This is justified by considering the operating parameters of the most recent CFEL experiments at Dartmouth [4], shown in Table 1. For these parameters $\omega \approx 10^{12}$ Hz and $\omega_e \approx 10^9$ Hz. Finally, we assume that the mode width, Δy, is much greater than the evanescent scale height, Δx. For the Dartmouth parameters $\Delta x = \beta\gamma\lambda/4\pi \approx 80\mu$m, where βc is the electron beam velocity, $\gamma = 1/\sqrt{1-\beta^2}$ and λ is the operating wavelength. Diffraction arguments suggest that the evanescent mode width is on the order of $\Delta y = \sqrt{\beta\lambda Z_g/2\pi}$ ≈mm where Z_g is the gain length.

We find the fields within and above the dielectric by solving Maxwell's equations and requiring the solutions to meet the appropriate boundary conditions. Only TM modes

THREE-DIMENSIONAL THEORY OF THE SMITH-PURCELL FREE-ELECTRON LASER

J. D. Jarvis and H. L. Andrews,
Department of Physics and Astronomy, Vanderbilt University, Nashville, TN 37235, U.S.A.

Abstract

We present an analytic theory for the exponential-gain (growth) regime of a Smith-Purcell free-electron laser amplifier (oscillator), which includes the effects of transverse diffraction in the optical beam. The optical mode is guided by the electron beam, having a mode width that depends upon the gain length. For the case of a wide electron beam, the dispersion relation converges with that of the 2-D theory. When the electron beam is narrow, the conventional cubic-dispersion relation is replaced by a five-halves dispersion. The dispersive properties of the grating divide device operation into four distinct regions, two amplifier and two oscillator. The number and location of physically allowed roots changes depending on operating region. Additionally, in the narrow-beam case, new challenges arise in satisfying the boundary conditions required for operation as an oscillator

INTRODUCTION

The wide range of potential applications for THz radiation is currently driving interest in the development of intense, compact, tunable THz sources. Such applications include: resonant excitation and spectral analysis of chemical and biological molecules and systems, medical and industrial imaging, and investigations in materials science and nanostructures [1,2]. Electron-beam-based devices are very promising sources of THz radiation. These include synchrotrons, conventional FELs, and slow-wave devices, such as backward-wave oscillators. While synchrotrons and conventional FELs are large and expensive, slow-wave devices can be compact, laboratory-scale instruments.

Slow-wave structures support subluminal electromagnetic modes, which may interact resonantly with an electron beam passing in close proximity. This resonant interaction causes bunching in the electron beam and amplitude growth of an evanescent optical field. For an open-grating structure, superradiant Smith-Purcell radiation may be extracted at harmonics of the evanescent wave [3]. This configuration is known as a Smith-Purcell free-electron laser (SPFEL). The SPFEL may be operated as an amplifier (convective instability), or as an oscillator (absolute instability), depending on the sign of the laser wave's group velocity. The two-dimensional theory of such a device has been examined in detail for the exponential gain/growth regime [4,5,6,7], and is closely supported by PIC simulations [6,8,9]. A two-dimensional numerical treatment of device operation from startup to saturation, with one-dimensional electron dynamics, has also been performed [7].

In this work, we include the effects of transverse diffraction in the optical beam of an SPFEL. The approach used is similar to that used for the 3-D theory of the Cerenkov FEL [10]. As expected, three-dimensional effects increase the gain length and oscillator start current substantially. Furthermore, compared to the 2-D theory, their dependence on the beam current increases due to gain guiding. We find that diffraction of the optical beam in the periodic-grating structure subdivides device operation into two amplifier regions and two oscillator regions. For the amplifier and oscillator regions furthest from the Bragg point, we find the inclusion of a fast wave in the physically allowed solutions. This is very surprising, considering the nature of a guided system. For the oscillator region closest to the Bragg point there are only two physically allowed solutions. It is not known how the required boundary conditions on the electron and optical beams can be satisfied in this region.

DISPERSION

In an SPFEL, resonant energy exchange between the electron beam and bound surface modes gives rise to spatial modulations in the beam density. These density modulations lead to superradiant enhancement of the emitted SP radiation, and subsequent modification of its angular distribution [3]. In the following analysis we calculate the fields subject to the Maxwell equations and boundary conditions and solve for the dispersion relation. We then introduce the electron beam as a perturbation and calculate the resulting wavenumber and frequency shifts for solutions to the dispersion relation.

Table 1: Dartmouth grating and beam parameters

Grating period	173 μm
Groove width	62 μm
Groove depth	100 μm
Grating length	12.7mm
E-beam width/height	60 μm
E-beam current	1 mA
E-beam height above grating (measured from bottom of beam)	0 μm

For an electron beam energy of $150\ \mathrm{kV}$ and the grating parameters of Table 1, the intensity scale height of the evanescent wave is $\Delta x = \beta\gamma\lambda / 4\pi \approx 38\ \mu\mathrm{m}$, where $\beta \sim 0.43$ is the normalized electron velocity,

ON NMR PROBING OF THE KINETICS OF A FREE-ELECTRON LASER-INDUCED CHEMICAL EXCHANGE

S.P. Babailov, IIC SB RAS, Novosibirsk, Russia

Abstract

Determination of the rate constants of chemical exchange reactions (at dark conditions, Figure 1) and the quantum yields of photo-induced chemical exchange (PICE, in particular, molecular photoisomerization reactions) is an efficient application of NMR spectroscopy [1,2].

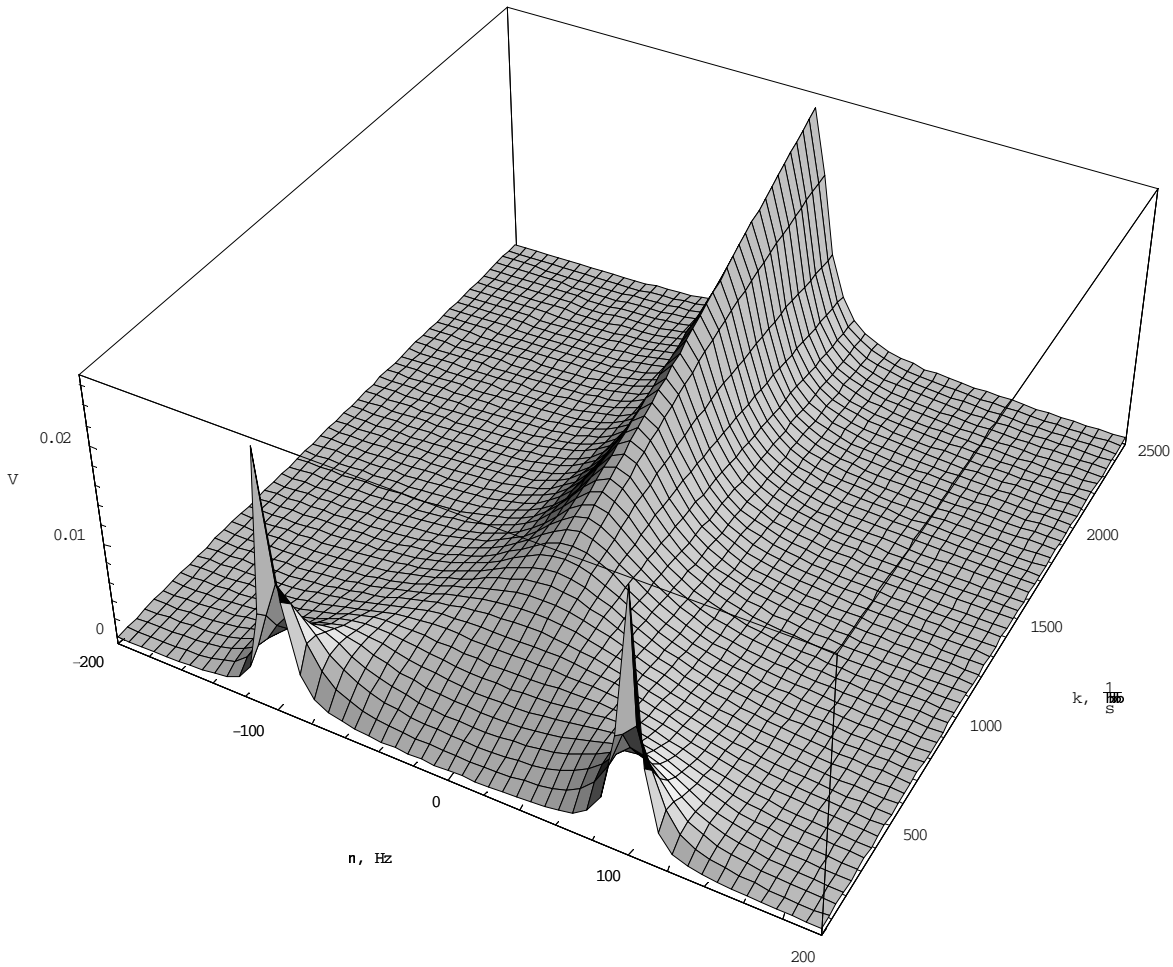

Figure1: Calculated NMR line-shape for a two-site chemical exchange at dark condition (T_1=T_2=10 c, Δν=200 Гц, the rate constant (k) changes from 38 to 2500 c^{-1}).

We are proposed a combined approach for study the kinetics of photo-induced chemical exchange (PICE) reactions (see (1), (2)), which involves a free-electron laser (FEL) and NMR spectroscopy [3].

$$A \underset{h\nu_2}{\overset{h\nu_1}{\rightleftharpoons}} B \qquad (1)$$

$$A + B \underset{h\nu_2}{\overset{h\nu_1}{\rightleftharpoons}} C \qquad (2)$$

Continuous and pulse irradiation of the chemical system in the presence of PICE can be achieved using FEL.

THEORETICAL

Based on the analytical equations derived in the work we consider the time-dependent dynamics of variation of the instant NMR line shape for two-site chemical exchange.

TERAHERTZ IMAGING AND RADIOSCOPY WITH 160X120 MICROBOLOMETER 90 FPS CAMERA*

A.L. Aseev, D.G. Esaev, M.A. Dem'yanenko, I.V. Marchishin, Rzhanov Institute of Semiconductor Physics SB RAS, 630090 Novosibirsk, Russia
B.A. Knyazev, G.N. Kulipanov, N.A. Vinokurov, Budker Institute of Nuclear Physics SB RAS, 630090 Novosibirsk, Russia.

Abstract

An uncooled micromolometer matrix camera has been developed for IR and THz high-speed imaging. The 120x160 matrix consists of resistive vanadium oxide elements on a silicon nitride bridge. The element size is 46x46 micron at the array period of 51 micron. We describe device fabrication process and matrix operational characteristics. Application of the camera in quasi-optical systems with Novosibirsk terahertz free electron laser as a radiation source is described. Recording rate up to 90 frames per second has been achieved.

INTRODUCTION

TERAHERTZ imaging is critically important for many applications. Appearance of high power terahertz sources, such as free electron lasers, enables using "parallel" recording techniques rather than recording images point-by-point with scanner. The last technique is routinely used in the time domain spectroscopy (TDS) systems, where recording an image takes minutes and hours. Recently commissioned Novosibirsk terahertz free electron laser generates terahertz radiation at the fundamental mode in a range of 120 – 240 μm with the average power 100 – 200 W at the repetition rate 5.6MHz and second and third harmonics with the average power of about several Watts. A number of imaging techniques employing the thermal effect of terahertz radiation were developed during past two years for recording images on the user stations [1 – 2]. These imaging techniques have many advantages, but each of them has at the same time certain drawbacks. One of them has a good spatial resolution, but pure sensitivity. Other being sensitive has no good spatial resolution. In this paper we describe the application of a microbolometer matrix to the recording of images in the terahertz spectral region.

MATRIX DESCRIPTION

The expansion of application sphere of thermal imager and others infrared (IR) devices along with increase of its sensitivity demands of decrease of cost, power consumption and weight, more convenience to use and high reliability. All these requirements are satisfied by uncooled focal plane array (FPA) actively developed last two decades. Microbolometer FPAs, based on thermoresistance effect have got the greatest expansion. Vanadium oxides (VOx) and amorphous silicon are mainly used as thermoresistance material. In the latter case process of microbolometer fabrication is carried out completely within the framework of usual silicon technology.

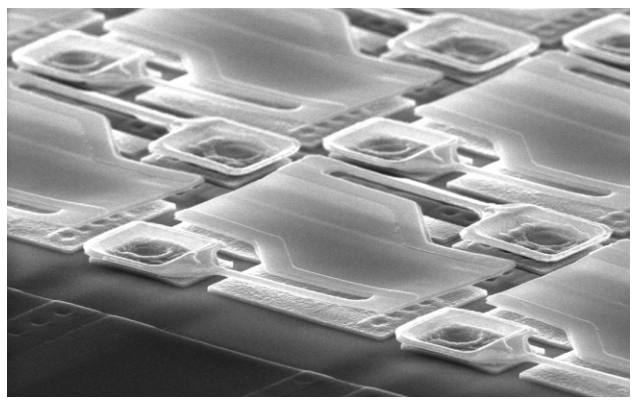

Fig. 1: Scanning electronic microscope photograph of 160x120 microbolometer FPA fabricated on silicon readout circuit.

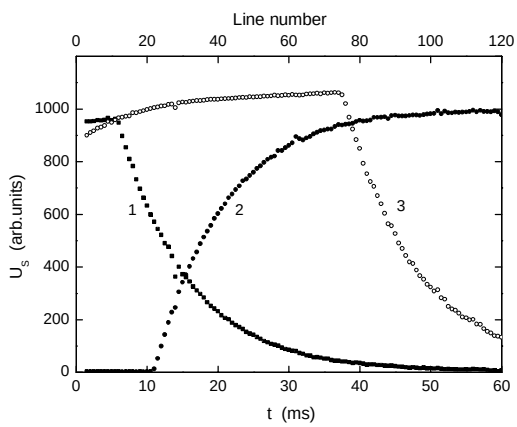

Fig. 2. Time dependence of 160x120 microbolometer FPA output signal normalized on sensitivity at pulse illumination. (1) the decay of FPA output signal after illumination: (2) the increasing of the signal during illumination, (3) is an intermediate situation.

*This work was supported in part by SB RAS under Integration Grant 174/6, by grant RNP.2.1.1.3846 from the Russian Ministry for Education and Science, and grant 07-02-13547 from Russian Foundation for Basic Research

SPECTROSCOPY AND SPECTRALLY RESOLVED RADIOSCOPY OF BIOLOGICAL SUBSTANCES USING TERAHERTZ FREE ELECTRON LASER RADIATION*

A. M. Gonchar, Institute of Cytology and Genetics SB RAS, Novosibirsk
V. V. Gerasimov, Novosibirsk State University
N.G. Gavrilov, B. A. Knyazev, Budker Institute of Nuclear Physics, SB RAS, 630090, Russia

Abstract

Osteoporosis is a major cause of morbidity of older people. Direct financial expenditure for the treatment of osteoporosis fracture in the U.S. is estimated at $10-$15 billion per year. Though there are a number of methods for diagnostics of osteoporosis, X-ray radioscopy, NMR, element analysis, densitometry, etc., the development of new methods, which are complementary to the existing ones, is highly desirable. We have carried out first experiments on the examination of spectroscopic characteristics of healthy and osteoporosis-affected bone tissues in the terahertz spectral range. The samples were prepared by pressing of grounded bone tissue obtained from the intact rats Wistar and from the senescence-accelerated rats OXYS. The OXYS rats suffered hereditary osteoporosis developed early in life are, therefore, a useful model for examining osteoporosis. The first experiments using a Fourier-spectrometer showed considerable difference in the bone tissue absorbance for two strains, though statistic tests are still required. Because the bone tissue is a highly-absorbing substance, the attenuated total reflection spectroscopy seems to be the most adequate method for detailed bone study. Imaging radioscopy of bone samples using a matrix of microbolometers as a sensor and the Novosibirsk free electron laser as a source of monochromatic terahertz radiation is described.

INTRODUCTION

Osteoporosis is a systemic skeletal disorder characterized by low bone mass and micro architectural deterioration of bone tissue, leading to enhanced bone fragility and an increased tendency to fracture. Osteoporosis has a long latent period and clinically reveals already in the presence of fractures when the bone mineral density is reduced significantly [1]. Thus, for preventing and treatment this disease the early diagnosis is necessary. Today there are several experimental techniques in diagnostic of the osteoporosis such as dual X-ray densitometry and computer tomography, NMR, etc. In spite of high developing and routine of such technique for bone research, the using of terahertz radiation can give complementary information about the bone tissue characteristics that can be valued for diagnostic of osteoporosis.

Recently, the capabilities of terahertz spectroscopy for bones research have been started to investigate. Until now, a few researches of bones using the terahertz time-domain spectroscopy (TDS) have been done. This technique allows obtaining information on the bone density and the complex refractive index. Bone A technique for the computer tomography of bones based on TDS had been demonstrated in the paper [2]. The information about the optical properties of three-dimensional (3D) structures of the investigated bone in the far-infrared region was obtained. Newly developed high-power terahertz sources, such as the Novosibirsk free-electron laser, open up new possibilities for bone radioscopy and imaging, including study of dynamical processes [3].

The goal of this study was the investigation of capabilities of osteoporoses diagnostics by comparison absorption spectra of normal and osteoporosis bone tissue. As a modal for the investigation two genetic strains of rats were chosen, Wistar (intact rats) and OXYS (senescence-accelerated rats with the early onset of osteoporosis). The strain OXYS was founded at the experimental animal laboratory of Novosibirsk Institute of Cytology and Genetics. The animals of this strain have a particularly short life span and accelerated development of age-

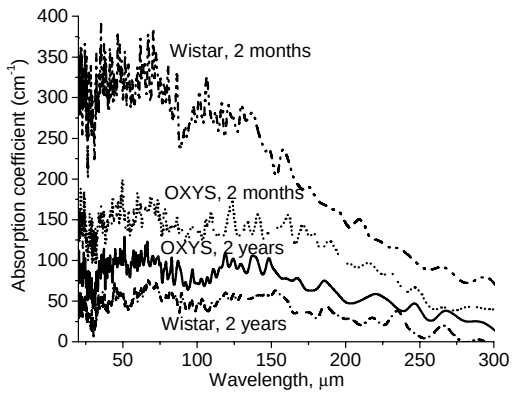

Figure 1: Absorbance vs. wavelength for the bone samples of intact (Wistar) and senescence-accelerated (OXYS) rats of different ages.

*This work is partially supported by Integration Grant 174/6 from SB RAS, by grant RNP.2.1.1.3846 from the Russian Ministry for Education and Science, and grant 07-02-13547 from Russian Foundation for Basic Research

DEVELOPMENT OF METAL MESH BASED QUASI-OPTICAL SELECTIVE COMPONENTS AND THEIR APPLICATION IN HIGH-POWER EXPERIMENTS AT NOVOSIBIRSK TERAHERTZ FEL*

S.A. Kuznetsov#, BINP SB RAS, Novosibirsk State University,
Novosibirsk, 630090, Russian Federation
V.V. Kubarev, P.V. Kalinin, B.G. Goldenberg, V.S. Eliseev, E.V. Petrova, N.A.Vinokurov
BINP SB RAS, Novosibirsk, 630090, Russian Federation

Abstract

In this paper we discuss main types of metal mesh based passive selective components of THz-quasi-optics required for applications in experiments at Novosibirsk terahertz free electron laser. The first experimental results on development of thin-film metal mesh polarizing beamsplitters and frequency filters by methods of photolithography and electroforming are presented. The technological aspects of the promising LIGA-technique being in progress in the Siberian synchrotron radiation centre and destined for production of thick metal mesh components with thickness compared to radiation wavelength are described.

INTRODUCTION

Successful realization of scientific programs of the Siberian Centre of Photochemical Research [1, 2] operating on basis of Novosibisk terahertz free electron laser (NovoFEL), which fundamental generation harmonics overlaps a spectral range 1.3÷2.5 THz, requires application in user experiments different types of passive quasi-optical selective devices intended for spatial and frequency gating of powerful beams of NovoFEL radiation. The necessary instrumentation includes beam-splitters, attenuators, frequency filters and some elements of focusing optics. Along with desired selective characteristics such devices should be capable of operating over a long period of time under high-power load conditions without noticeable degradation of their properties. It admits to employ in selective components only low absorbing and thermostable materials, such as high conductivity metals and special types of polymers. The best solution is in use of metal mesh structures with specially designed subwavelength topology of mesh cells. For minimizing absorption the metal structures should be wafer-free, however in case of non-self-bearing topology or small metallization thickness structure fastness requires presence of supporting thin-film polymeric substrates.

In this report we discuss selective properties of the main types of metal mesh structures required for NovoFEL experiments and present first results of development of metal mesh components by three different manufacturing techniques: a) contact photolithography; b) electroforming; c) LIGA. Dealing with a minimal topological size of the mesh pattern about a few microns, each of these techniques enables to produce mesh components within its own corresponding range of metallization thickness: a) ≤1 μ; b) ~10 μ; c) ~100 μ.

It should be elucidated that conventional photolithography is considered to be the most adequate, relatively cheap and well-proven technology for manufacturing metal mesh quasi-optical components traditionally used in low- and moderate-power THz-applications. In NovoFEL user experiments employment of such "photolithographic" components is restricted due to high average power of NovoFEL radiation, reaching 400 W nowadays and expected to be raised in the future. Small thickness of metallization and presence of dielectric carrier substrates in such components limit their surface and volumetric thermal conductivity resulting in danger of quick overheating and destruction under high-power load conditions. The best "high-power" alternative to "photolithographic" components (in case of self-bearing topology) are the components based on substrate-free self-supporting thick metal mesh structures manufactured by conventional electroforming and LIGA techniques. In spite of higher technological costs such components are of great interest for NovoFEL applications since they are much more thermostable and mechanically firm and have a much higher radiation destruction threshold. Another inherent and important feature of thick metal structures is much stronger low-frequency attenuation due to a waveguide cut-off effect that can be effectively used for solving problems of harmonics filtration and THz-beams intensity control discussed below.

THZ-COMPONENTS REQUIRED FOR NOVOFEL APPLICATIONS

By fundamental practical purpose influencing on choice of mesh pattern topology the metal mesh based selective components should be divided into three main groups (see Fig.1): 1) beam-splitters (attenuators); 2) frequency harmonics filters; 3) diffractive optical elements.

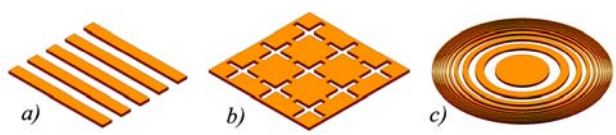

Figure 1: Fundamental types of metal mesh based components required for NovoFEL experiments: *a*) polarizing beam-splitter; *b*) frequency filter; *c*) diffractive optical element (amplitude transparency).

* This work is supported in part by the Russian Foundation for Basic Research (project No. 07-02-01459-a).
# sakuzn@inp.nsk.su

DIFFRACTION OPTICAL ELEMENTS AND OPTICAL SYSTEMS WITH A HIGH POWER MONOCHROMATIC TERAHERTZ SOURCE *

V.S. Cherkassky, A. V. Fanova, L.A. Merzhievsky, S.A. Zhigach, NSU, Novosibirsk, Russia
Young Uk Jeong, Hyuk Jin Cha, B.A., Korean Atomic Energy Research Institute
N.G.Gavrilov, B.A. Knyazev#, G.N. Kulipanov, I.A. Polskikh, N.A. Vinokurov, S.A., BINP, Novosibirsk, Russia.

Abstract

We have developed reflective diffraction optical elements (DOE) for focusing radiation of terahertz free electron lasers (FEL). Metal-dielectric Fresnel zone plates and metallic kinoform "lenses" were fabricated and tested using FEL radiation. A microbolometer camera (see the paper by Esaev et al. at this conference) sensitive to THz radiation had been applied for recording both terahertz beam caustic and terahertz images. Diffraction efficiency of a kinoform lens appears to be about unity. Quality of images obtained with the kinoform lens was studied. The lens was used as a key element for a Toepler optical system, which were used for studying condense matter non-uniformities and deformations. The experiments were performed at Novosibirsk and KAERI FELs.

INTRODUCTION

Imaging in the terahertz spectral region (1 – 10 THz) is a subject of special interest for many applications such as biological researches, medical diagnostics, study of materials, security systems and many other applications. Each optical system consists of a source of radiation, optical elements and an imager. In this paper we describe optical elements and recorders developed for imaging with free electron laser (FEL) as a source. Most of the experiments were carried out at high power Novosibirsk FEL. Some of them have been done at KAERI FEL.

Because the refractive optical elements can be damaged by high power terahertz radiation, we have developed a number of reflective diffraction optical elements (DOE). Large-scale reflection DOE are often used in the microwave spectral region, and the application of DOE in terahertz optical systems is, obviously, very prospective.

Previously [1 – 3] we have developed (or adapted) three recorders for the visualization of intense terahertz radiation: a near-IR thermograph, a thermal-sensitive Fizeau interferometer, and a "thermal image plate". In this paper we first used as a terahertz imager [4] a microbolometer matrix, initially developed for the MIR range 0. The matrix has higher sensitivity and better spatial resolution, than the imagers mentioned above.

*Work supported by Integration grants 174/6 and 22/6 from Siberian Branch of Russian Academy of Science, by grant RNP.2.1.1.3846 from the Russian Ministry for Education and Science, and grant 07-02-13547 from Russian Foundation for Basic Research.…
#knyazev@inp.nsk.su

TERAHERTZ OPTICAL ELEMENTS AND SYSTEMS

Fresnel zone plates

Three Fresnel zone plates (with zone numbers of 91, 46, and 30, respectively, and the first Fresnel zone radii of 5.2, 7.35 and 9.0 mm) had been designed and fabricated for focusing terahertz radiation with simultaneous reflection under the right angle. The elliptically shaped plates with the minor semi-axis of 5 cm and the aspect ratio of 1:1.41 were formed by etching a copper foil clad on a fiber-glass plastic. The central zone of each plate was reflecting.

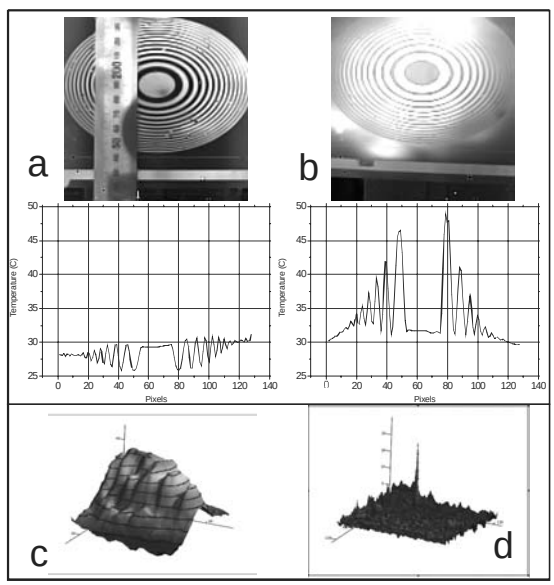

Figure 1: A thermographic image of a zone plate recorded with no radiation (*a*) and with THz irradiation (*b*); plots – effective temperature distribution along the major ellipse axis. Intensity distribution in the initial THz beam (*c*) and in the zone plate focus (*d*) recorded with the thermal image plate.

The images of a zone plate taken at 2.5 – 3.0 μm with the thermograph (Fig.1) show growing the temperature of the dielectric zones up to 55 C, nevertheless, the zone plate focuses THz radiation well. The focal lengths for all zone plates exactly correspond to designed values. Since the principle focal length of a zone-plate is inversely proportional to the radiation wavelength, $f_1 = r_1^2/\lambda_0$, it can be used at arbitrary wavelength, but low diffractio efficiency (~10%) constrains its application.

DIAGNOSTICS OF AN ELECTRON BEAM USING COHERENT CHERENKOV RADIATION*

R. Tikhoplav#, P. Musumecci, J. Rosenzweig, S. Tochitsky, UCLA, Los Angeles, CA 90095
G. Gatti INFN/LNF, 00044 Frascati (RM) Italy

Abstract

The use of coherent Cherenkov radiation as a diagnostic tool for longitudinal distribution of an electron beam is studied in this paper. This method will be employed for the 7th harmonic bunching experiment at Neptune linear accelerator facility at UCLA. Coherent Cherenkov radiation is produced in an aerogel with an index of refraction close to unity.

THEORETICAL BACKGROUND

Radiation due to a relativistic electron beam traversing a medium, such as transition radiation (TR), has proved itself to be a powerful tool for beam diagnostics, e.g., determining the transverse distribution and position of an electron beam as in TR screen technique. Such radiation could also be used for reconstruction of the longitudinal profile of the electron beam if the coherent part of such radiation is known [1].

Regardless of the source of radiation (Cherenkov (CR), Synchrotron (SR), or TR), the spectral response of the electron bunch can be represented as following [2],

$$T(\lambda) = S(\lambda)\left(N + N(N-1)\left|F_{3D}(\lambda)\right|^2\right) \quad (1)$$

where $S(\lambda)$ is the spectrum of a single particle, λ is wavelength, N is the number of particles in the bunch, F_{3D} is the 3-D Fourier transform of the bunch particle distribution, called the form factor,

$$F_{3D}(\lambda) = F(\lambda)F_T(\lambda) \quad (2)$$

where F and F_T are longitudinal and transverse form factors respectively. Coherent part of radiation is proportional to the number of emitters squared, thus it gives a much stronger signal than the incoherent part. It is also a function of a form factor which depends on the shape of the bunch. If a longitudinal modulation of a certain period λ_0 (micro-bunching) is introduced to the bunch with longitudinal Gaussian distribution of rms size σ, such modulation would change the form factor resulting in enhancement of a corresponding frequency of radiation and its harmonics.

$$F(\lambda) = \exp\left(-2\pi^2\sigma^2/\lambda^2\right)\left(1 + \sum_n h_n(\lambda_0)\right) \quad (3)$$

where $h_n = a_n \exp\left(-2n^2\pi^2\sigma^2/\lambda_0^2\right)\cosh\left(4n\pi^2\sigma^2/\lambda\lambda_0\right)$ is the modulation factor, n and a_n are the harmonics number and its weight respectively. Such radiation would be analyzed and a temporal distribution of the electron beam could be deducted.

Coherent Cherenkov Radiation in the Aerogel

Cherenkov radiation induced by a single particle can be expressed in terms of number of photons per unit frequency,

$$\frac{\partial N_{ph}^{Ch}}{\partial k \partial \theta} = L\alpha\theta_c^2\delta(\theta - \theta_c) \quad (4)$$

here α is the fine structure constant, θ_c is Cherenkov angle, L is the length of the electron path in the medium. In the case of a bunched electron beam, the total number of photons for Coherent Cherenkov Radiation (CTR) can be expressed as the following,

$$N_{ph}^{Ch} \approx \sqrt{\pi}LN^2\frac{\alpha}{\sigma}a_n^2\theta_c^2\left|F_T(\lambda)\right|^2 \quad (5)$$

We are particularly interested in using the aerogel as a medium for CTR. Aerogel, or 'frozen smoke' is a low-density solid-state material made by high temperature and pressure-critical-point drying of a gel composed of colloidal silica structural units filled with solvents [3].

Table 1: Aerogel Parameters

Parameter	**Value**
Material	SiO_2
Density	20 kg/m^3
Refractive Index, n	1.008
Cherenkov Angle, θ_c	7.25^O
Melting Point	1200^{O}C

Its low density provides nearly non-destructive tool for the electron beam diagnostics (see Table 1) and its small refractive index $n=1+\Delta$ gives a small Cherenkov angle $\theta_c \approx \sqrt{2\Delta}$.

The form factor (and consequently, the enhancement of coherent radiation) depends on the transverse shape of the electron beam as well. A Gaussian transverse distribution $f(\rho) \propto \exp(\rho^2/2\sigma_T^2)$ leads to suppression of shorter wavelengths (see Fig. 1), unless the transverse size σ_T is infinitely small. The corresponding form factor is given by the following:

$$F_T(\lambda) = \exp\left(-2\pi^2\theta_c^2\sigma_T^2/\lambda^2\right) \quad (6)$$

This could be overcome if other transverse shapes are employed. For example, transverse hard-edge distribution

*Work supported by US Department of Energy
#rodion@ucla.edu

FIRST EXPERIENCES WITH THE FIR-FEL AT ELBE

U. Lehnert, P. Michel, W. Seidel, G. Staats, J. Teichert, R. Wünsch
Forschungszentrum Dresden-Rossendorf e.V., 01314 Dresden, Germany

Abstract

We show the design and the parameters of operation of the long-wavelength (U100) FEL at ELBE. First lasing has been shown in August, 2006. Since then, the laser has undergone thorough commissioning and is available for user experiments since fall, 2006. Besides in-house users the IR beam is available to external users in the FELBE (FEL@ELBE) program witch is a part of the integrated activity on synchrotron and free electron laser science in the EU. At the beginning of 2007 lasing in the full designed wavelength range from 20 µm to 200 µm was demonstrated. The laser power typically reaches several Watts in cw operation but drops for very long wavelengths depending on the size of the used out-coupling hole. However, there exists a serious problem with small gaps in the wavelength spectrum. We attribute this behaviour to the transmission characteristics of the overmoded partial waveguide used from the undulator entrance to the first mirror.

INTRUDUCTION

At Forschungszentrum Dresden-Rossendorf, Germany, the radiation source ELBE (Electron Linac with high Brilliance and low Emittance) operates on the basis of a superconducting linear accelerator for electron energies up to 40 MeV with an average beam current of 1 mA in quasi continuous wave (cw) mode. The electron linac serves as a driver to generate several kinds of secondary radiation and particle beams. Two free-electron lasers generate radiation in the mid and far infrared for a very large field of applications reaching from semiconductor physics to biology. In addition, MeV Bremsstrahlung for nuclear (astro) physics, monochromatic hard-X-ray channelling radiation for radiobiological experiments, and in near future also neutrons and positrons for studies in nuclear reactor science and materials research are provided. The quality and range of the provided beams will be extended even further when the superconducting photo-electron gun [1] which is tested at present will become operational. The first FEL to become operational at ELBE was the mid-IR FEL [2] using two undulators with 27.3 mm period. With the available beam energies it covers a wavelength range from 3-24 µm. To extend the wavelength range into the far-IR a second FEL with a 100 mm period [3] undulator was installed. It now provides laser light from 20-200 µm. After first lasing in August, 2006 it is in routine user operation since fall, 2006. The relevant user facilities comprise 6 optical laboratories. Some of these are also used by in-house groups, mainly in the areas of semiconductor physics, and radiochemistry, and experiments there will require a certain level of collaboration with the in-house researchers. In particular noteworthy is the fact that a number of additional optical sources from the visible to the THz frequency range are available, e.g. for two-colour pump-probe experiments. These sources (Ti:sapphire laser and amplifier, OPO, OPA, broad-band THz generator) are all based on Ti:sapphire oscillators which are synchronized to the FEL with an accuracy better than a ps. Two laboratories are intended to provide users with utmost flexibility for their own experiments, also in scientific areas not covered by in-house groups (e.g., surface physics, molecular physics).

U100-FEL SETUP

The FIR-FEL at ELBE (see Fig. 1) uses a hybrid undulator with 100 mm period length. It consists of 38 periods equipped with SmCo magnets which were chosen due to their better radiation resistance with respect to NdFeB. With a minimum gap of 24 mm a maximum K_{rms} parameter of 2.7 is reached. The whole wavelength range from 20-200 µm is covered with electron beam energies from 20-35 MeV. To allow small undulator gaps a waveguide optical beam transport through the undulator is necessary. The ELBE FIR-FEL uses a partial waveguide spanning from the undulator entrance to the downstream mirror. The interior height was chosen to 10 mm. In horizontal direction the waveguide is wide enough to allow essentially free propagation. Thus, an overmoded parallel-plate waveguide is formed which shows low losses for the principal mode. The downstream mirror was placed as a cylindrical mirror inside the waveguide. On the upstream side the optical beam propagates freely through the focusing quadrupoles and the dipole to a toroidal mirror. To optimize the coupling between the waveguide mode and the free propagation the horizontal curvature of both mirrors was chosen to correspond to a Rayleigh range of 180 cm. The vertical curvature of the upstream mirror, however, equals its distance of 361 cm from the waveguide entrance. Round-trip optical losses inside the U100 resonator were computed using the GLAD [4] code. The mode conversion between waveguide and free propagation was approximated taking only the fundamental waveguide mode into account. The efficiency computed this way is above 94 % for all wavelengths yielding a reasonably high Q of the optical resonator. To allow for a near-optimum out-coupling over the whole wavelength range the upstream mirror chamber is equipped with three interchangeable mirrors of identical curvature but with 2.0, 4.0 and 7.0 mm out-coupling holes.

A STUDY OF DETECTION SCHEMES IN ELECTRO-OPTIC SAMPLING TECHNIQUE*

Y. W. Parc#, I. S. Ko, POSTECH, Pohang 790-784, Korea
J. Y. Huang, C. Kim, PAL, Pohang 790-784, Korea

Abstract

Electro-Optic Sampling (EOS) is the ingenious tool for the measurement of the electron beam. There are two traditional detection schemes: one is the crossed polarizer scheme and another is balanced detection one. A new detection scheme called 'Near Crossed Polarizer' (NCP) scheme in the EOS technique is developed to increase the signal to noise ratio (SNR) in the experiment. The new detection scheme is studied in detail and the 3D scanning result with electron beam in FLASH is compared with the detection scheme.

INTRODUCTION

The detection schemes for EOS measurement are studied in theoretically and experimentally also. Two traditional detection schemes are the crossed polarizer and the balanced detection scheme. Those have each difficulty to be applied in real diagnostic in the EOS measurement of the electron beam. To overcome those difficulties, new detection scheme called 'Near Crossed Polarizer' scheme is developed. In this letter, the detail study of the NCP scheme is shown with 3D scanning result of the EOS measurement.

THEORY

EO crystals such as ZnTe and GaP have a character of birefringence materials when the electric field is applied to the crystal. The refractive index of the crystal can be calculated from the constant energy surface in the electric displacement vector space and the impermeable tensor that is linear to the electric field strength. The refractive index can be found from the refractive index ellipsoid equation by a principal-axis transformation [1, 2]. The two main refractive indices n_1, n_2 of the crystal along the principal axes are given by

$$n_1 = n_0 + \frac{n_0^3 r_{41} E}{2}, \qquad n_2 = n_0 - \frac{n_0^3 r_{41} E}{2} \qquad (1)$$

where n_0 is the initial refractive index, r_{41} is the electro-optic constant, and E is the electric field applied to the crystal. The difference of the propagation speeds of each laser component, which is due to the different refractive indices, changes the polarization of the incident laser pulse. This brings the relative phase shift, Γ, between the horizontal component of the laser pulse and the vertical one, which is given by

$$\Gamma = \frac{\omega_0 d}{c}(n_1 - n_2) = \frac{\pi d}{\lambda_0} n_0^3 r_{41} E \qquad (2)$$

where d is the crystal thickness, ω_0 is the mean angular frequency of the laser pulse, c is the speed of light, λ_0 is the mean wavelength of the laser pulse, and E is the electric field applied to the crystal.

Detection schemes

There are two traditional methods to detect the polarization change; the crossed polarizer scheme and balanced detection one. In the crossed polarizer scheme, the laser intensity is measured by a polarizer and a detector. The analytic expression of the intensity difference ΔI in the case of the crossed polarizer scheme is given by [1, 2]

$$\Delta I = I_0 \sin^2(\Gamma/2) \qquad (3)$$

where Γ is the relative phase shift between the two polarized parts of the laser field and the I_0 is the initial intensity of the laser pulse. There is another method to detect the polarization change called balanced detection scheme. In the balanced detection scheme, the laser intensity is measured by a quarter-wave plate, a polarizer and two detectors. The quarter-wave plate enhances the relative phase shift by a quarter of one wave length. The analytic expression of the intensity difference ΔI in the case of balanced detection scheme is given by [1, 2]

$$\Delta I \equiv I_h - I_v = |\mathrm{E}_h|^2 - |\mathrm{E}_v|^2 = I_0 \sin(\Gamma) \qquad (4)$$

where all parameters are same with above Eqs., h and v represent 'horizontal' and 'vertical' each. When the relative phase change Γ is 7° in the crossed polarizer scheme, the change of the initial laser intensity is merely 0.37% from Eq. (3). This signal change is too low to be detected in real diagnostics setup. However, in the balanced detection scheme, there is 12% change of the initial laser intensity from Eq. (4) for the same Γ. The signal level is high enough to detect, but the balanced method is difficult to apply in real diagnostic setup. To overcome those difficulties, a new method called Near Crossed Polarizer (NCP) scheme is developed. In the new detection scheme, the laser intensity is measured by a quarter wave plate, a half wave plate, a polarizer, and a detector. The intensity with NCP scheme is calculated by the multiplication of the Jones matrices of the each wave plate [3]. The calculated intensity is given by

COMPARATIVE STUDY OF ELECTRO-OPTIC EFFECT BETWEEN SIMULATION AND MEASUREMENT *

Y. W. Parc#, I. S. Ko, POSTECH, Pohang 790-784, Korea
J. Y. Huang, C. Kim, PAL, Pohang 790-784, Korea

Abstract

Electro-Optic Sampling (EOS) is a promising method to measure various properties of the electron beam non-destructively. In this Letter, a rigorous analysis procedure of the electro-optic (EO) measurement is introduced. The measured data of electron beam by electro-optic technique is analyzed in terms of the relative phase shift between the horizontal and the vertical components of the laser. A simulation study is done with the pulse propagation method, which utilizes Fourier transform to investigate the evolution of an electromagnetic pulse inside the EO crystal. The analysis result of the EO measurement expressed in terms of the relative phase shift is compared with the simulation, and they show a good agreement.

INTRODUCTION

Non-destructive measurement of the electron bunch length with femtosecond resolution is one of essential issues to operate XFEL facilities successfully [1]. During last several years, the EOS method has been successfully implemented to measure femtosecond electron bunches and arrival time at FELIX, SPPS, and FLASH facilities [2-8].

THEORY

EO crystals such as ZnTe and GaP have a character of birefringence materials when the electric field is applied to the crystal. The refractive index of the crystal can be calculated from the constant energy surface in the electric displacement vector space and the impermeable tensor that is linear to the electric field strength. The refractive index can be found from the refractive index ellipsoid equation by a principal-axis transformation [9, 10]. The two main refractive indices n_1, n_2 of the crystal along the principal axes are given by

$$n_1 = n_0 + \frac{n_0^3 r_{41} E}{2}, \qquad n_2 = n_0 - \frac{n_0^3 r_{41} E}{2} \tag{1}$$

where n_0 is the initial refractive index, r_{41} is the electro-optic constant, and E is the electric field applied to the crystal. The difference in the propagation speeds, which is due to the different refractive indices, changes the polarization of the incident laser pulse. This brings the relative phase shift, Γ, between the horizontal component of the laser pulse and the vertical one, which is given by

$$\Gamma = \frac{\omega_0 d}{c}(n_1 - n_2) = \frac{\pi d}{\lambda_0} n_0^3 r_{41} E \tag{2}$$

where d is the crystal thickness, ω_0 is the mean angular frequency of the laser pulse, c is the speed of light, λ_0 is the mean wavelength of the laser pulse, and E is the electric field applied to the crystal.

Detection scheme

A new method called Near Crossed Polarizer (NCP) scheme is developed. In the new detection scheme, the laser intensity is measured by a quarter wave plate, a half wave plate, a polarizer, and a detector. The intensity with NCP scheme is calculated by the multiplication of the Jones matrices of the each wave plate [11]. The calculated intensity is given by

$$I(\theta, \varphi, \Gamma)/I_0 = \left[1 - \cos(\Gamma)\cos(4\theta - 2\varphi)\cos(2\varphi) + \sin(\Gamma)\sin(4\theta - 2\varphi)\right]/2 \tag{3}$$

where θ is angle of the half wave plate, φ is angle of the quarter wave plate, and I_0 is the initial laser intensity incident on the EO crystal. The signal level and the background are also changed according to the angles of the half and the quarter wave plates. The signal to noise ratio can be increased by the control of the angle of the plates [12].

EXPERIMENT

At the FLASH facility in DESY, there is an EO diagnostic section called Timing Electro-Optic (TEO) setup to measure the electron beam properties. The TEO setup is used to measure the bunch length and the timing jitter of the electron beam by the spatial decoding method with GaP crystal as shown in Fig. 1 [8].

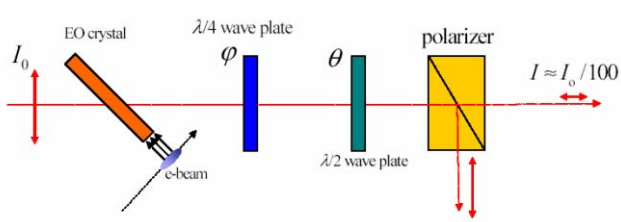

Figure 1. Layout of the electro-optic sampling.

In the spatial decoding method, the laser pulse is propagated through the EO crystal with 45° angle, and the timing information of the electron beam is converted to the spatial information of the image measured by the ICCD camera [5, 8].

LOSSES IN OPTICAL RESONATOR OF NOVOSIBIRSK TERAHERTZ FEL: THEORY AND EXPERIMENT

V.V. Kubarev#, BINP, Novosibirsk, Russia

Abstract

A direct comparison of the simple universal analytical theory used earlier to design an optical resonator for the Novosibirsk terahertz free electron laser (NovoFEL) and numerous subsequent experiments is presented. A good agreement of the theory with the experiments is shown. A possibility of future optimization of the optical resonator is described.

INRODUCTION

Round trip losses are the main parameter of most laser resonators. There are many different numerical methods to calculate losses of resonators with given geometries. However, an optimal geometry is not known when a new resonator is being created. A simple search for different geometries is ineffective. In this case we need some analytical theory. In [1], the author of this paper proposed a simple universal analytical method to calculate small losses in stable open laser resonators. A comparison of the method with well-known papers in which numerical [2, 3] and cumbersome analytical [4] methods were used only for certain types of losses and geometries shows a good agreement.

On the other hand, the free electron laser gives us a unique possibility of direct experimental measurement of such losses, which is practically impossible in conventional lasers due to the inertia of their active media. First measurements of this type on NovoFEL with the start optical resonator were published in [5]; they shown a good agreement of the theory and experiment. In this paper, a nominal optical resonator with larger output coupling was investigated in a wider spectral range.

THEORY

Diffraction losses c_i caused by different small perturbations at the center of a Gaussian mode (openings) and at its periphery (mirror apertures, diaphragms, scrapers) are equal, according to [1], to double "geometrical" losses $c_i = 1 - (1 - c_g)^2 \approx 2c_g$. Geometrical losses c_g are a part of the mode cross-section overlapped (cut) by a perturbation. The total resonator losses can be evaluated as:

$$c_\Sigma = 1 - \prod_i (1 - c_i) \approx \sum_i c_i \qquad (1)$$

This property of additivity for losses at the openings and outer apertures of mirrors is shown in paper [1]. For one-type aperture losses at the periphery of a beam (mirrors, diaphragms, scrapers), the additivity condition is satisfied if the elements with losses are divided by a distance exceeding the length $L_a = d \cdot \delta/\lambda$, where d and δ are typical sizes of the mode and perturbation, and λ is the wavelength. The mode fills the cutoff part of its periphery at this distance. This condition is satisfied for the main components of our resonator losses. The losses in other sections of the resonator can be ignored because of the exponential sensitivity of the Gaussian beam to narrower diaphragms.

The calculation model of our optical resonator after some optimization of diaphragm diameters and their positions is shown in Fig.1. Values of the diameters and axial distances between the resonator center and the diaphragms are presented in Table 1. We assume that the diaphragms are full absorbing because many of them have a special absorbing ceramic coating [5] and the cross-section of vacuum pipes of our resonator is sufficiently large.

Thus, the resonator losses per round trip (for removed scrapers and symmetrical positions of all diaphragms to the resonator center) are:

$$c_\Sigma = 1 - (1 - c_{mo})^2 (1 - c_{md})^4 (1 - c_{mh1})^2 (1 - c_{mh2})^2 \times \times (1 - c_{d1})^8 (1 - c_{d2})^8 (1 - c_{d3})^8, \qquad (2)$$

where c_{mo} and c_{md} are the ohmic and outer aperture losses of mirrors; c_{mh1} and c_{mh2} are the losses on openings in the mirrors; c_{d1}, c_{d2} and c_{d3} are diaphragm losses (pick-up sensor aperture, banding magnet camera aperture, and undulator aperture, respectively). For simplicity, we use one-index numeration of the losses in Fig.1, Table 1, and Fig.6, according to equations (1) and (2).

From the well-known experimental data for optical properties of solid gold, we can obtain the ohmic losses of our mirrors with gold coating: $c_{mo} = 10^{-2}(0.71 - 1.2\lambda$ [mm]).

For losses of the Gaussian TEM_{00} - mode with the radial field distribution $E \sim exp(-r^2/r_0^2)$; $r_0 = \{\lambda L_f/\pi [1 + (z/L_f)^2]\}^{1/2}$, where L_f is the Rayleigh length, one can obtain the following formulas:

$$c_{dk,md} = exp\{-\pi d_k^2 L_f/[2\lambda(L_f^2 + z_{dk,md}^2)]\} \qquad (3)$$

$$c_{mh} = \pi d_{mh}^2/\{2\lambda L_f[1 + (L_0/2L_f)^2]\}, \qquad (4)$$

where $k = 1, 2, 3$; d is the diameter of the losses component, and $L_0 = 26.589$ m is the resonator length.

The dependences of total losses as functions of wavelength for different Rayleigh lengths are shown in Fig.2. The value $L_f = 5$ m and mirror radiuses $R = L_0[1 + (2L_f/L_0)^2]/2 = 15$ m were chosen as optimal in the

CONTROL AND DIAGNOSTIC SYSTEM FOR NOVOSIBIRSK FEL RADIATION

V.V.Kubarev, E.V.Makashov, K.S.Palagin, S.S.Serednyakov. Budker Institute of Nuclear Physics, 630090, Novosibirsk, Russia.

Abstract

The architecture and main capabilities of the control and diagnostic system for the Novosibirsk FEL coherent radiation are described. The software managing this system employs a client-server model. The software developed is able to work both in client and server modes. It can also control various equipment – from the FEL optical cavity mirrors to the local equipment of user stations. The mode of control program operation and controlled equipment are determined by external configuration files. Some results of the system operation are also presented.

INTRODUCTION

The first stage of the free electron laser (FEL) based on energy recovery linac is now working at Budker Institute of Nuclear Physics [1]. Generation of coherent radiation in the wavelength range of 120 to 200 microns has been achieved. This radiation is applied in a number of user and diagnostic experiments. To apply the radiation successfully, it is necessary both to know its main parameters and to transmit them to the user stations and FEL control panel. In addition, it is necessary to control some radiation parameters (wavelength) and to set up the system.

To solve these and some other tasks, a control system has been developed. It performs the following:

1. Measurement and diagnostics of the main radiation parameters, i.e. wavelength, power and transversal shape of radiation beam.
2. Control over some FEL components (optical cavity) as well as over the radiation wavelength.
3. Real-time transmission of the main radiation parameters to the computers of user stations.

Operation of this system is considered in more details below.

SYSTEM ARCHITECTURE

This system consists of a certain set of equipment (ADCs and controllers of step motors) and a program to manage this equipment. Besides, the program uses a remote control interface for a set of parameters of the energy recovery linac as well as reading some parameters necessary for users. Figure 1 presents a scheme of the entire system. The program can work in client and server modes. The program mode and configuration of equipment to control (step motor controllers, numbers of ADC channels, etc.) are set in external configuration files. Thus, applying various configuration files, the program can work in various modes and control different equipment.

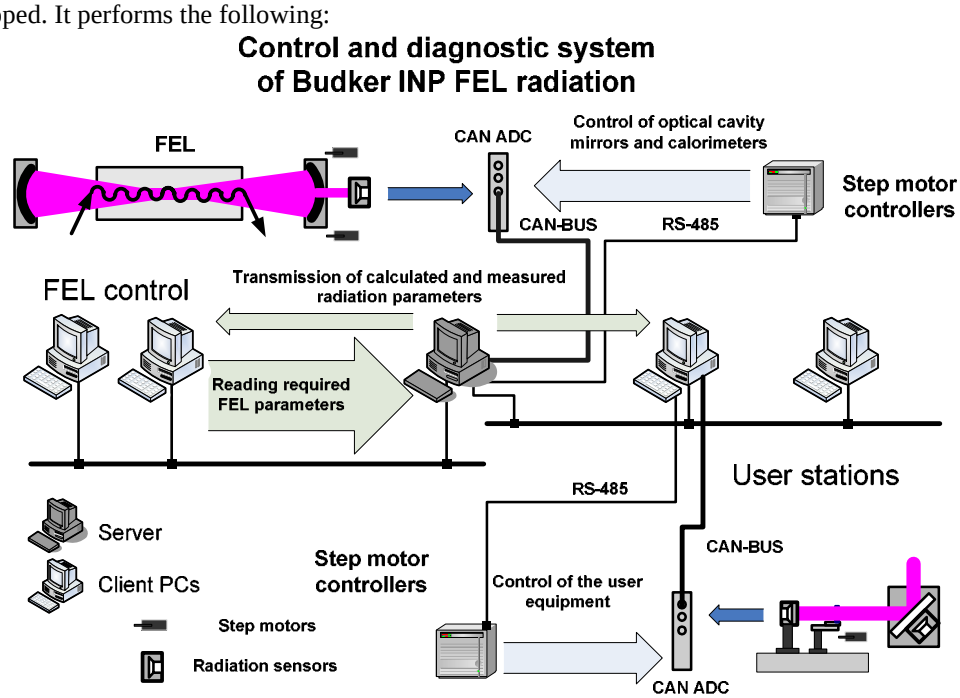

Figure 1: Scheme of the system

OPERATION OF NEAR-INFRARED FEL AT NIHON UNIVERSITY*

K. Hayakawa#, Y. Hayakawa, K. Nakao, K. Nogami, T. Tanaka, LEBRA, Funabashi, Japan
A. Enomoto, S. Fukuda, K. Furukawa, S. Michizono, S. Ohsawa, KEK, Ibaraki, Japan
M. Inagaki, T. Kuwada, T. Sakai, I. Sato, Nihon University, Tokyo, Japan

Abstract

The near-infrared FEL at Laboratory for Electron Beam Research and Application (LEBRA) in Nihon University has been operated for a variety of scientific applications since 2003. The stability of the FEL power was improved appreciably by the advanced stability of the 125MeV electron linac. Currently fundamental FEL wavelength ranges from 1 to 6 microns, which is restricted by the electron energy and the optical devices. The higher harmonics in the visible region is also available [1]. The maximum macropulse output energy of 60mJ/pulse has been obtained at a wavelength of 1725 nm. The short FEL resonator length at LEBRA results in relatively high optical energy density on the surface of the resonator mirrors; present copper-based Ag mirrors in use at LEBRA are not durable enough for long-term operation. Generation of intense harmonics by means of nonlinear crystals has been tested. The preliminary results have demonstrated the conversion efficiencies of 3 to 9% for the second harmonic generation by the fundamental FEL in the wavelength region from 1400 to 1800nm.

INTRODUCTION

The electron linac at LEBRA has a conventional configuration. It consists of the DC electron gun with a dispenser cathode, the prebuncher which is a 7-cell travelling wave structure, the buncher which is a 21-cell travelling wave structure and three 4-m long regular accelerating sections. The specifications of the electron linac are listed in Table 1. Schematic layout of the accelerating structures, the RF system and the beam lines for FEL and parametric X-ray (PXR) generations are shown in Fig. 1.

The FEL beam line and the optical resonator system have been installed to provide the near-infrared FEL for various studies [2]. To increase the FEL gain, magnetic bunch compression has been performed in the 90-degree bending system [3].

Table 1: Main parameters of the LEBRA linac.

Accelerating rf frequency	2856	MHz
Klystron peak output rf Power	30	MW
Number of klystrons	2	
Electron energy	30~125	MeV
Energy spread (FWHM)	0.5~1	%
Macropulse beam current	200	mA
Macropulse duration	20	μsec
Repetition rate	12.5	Hz

Table 2: LEBRA undulator parameters.

Resonator length, *L*	6.718	m
Undulator period	48	mm
Undulator length	2.4	m
Number of periods	50	
Maximum *K* (rms)	1.35	

To generate a monochromatic and spatially coherent X-ray beam, the PXR beam line has been installed next to the FEL beam line.

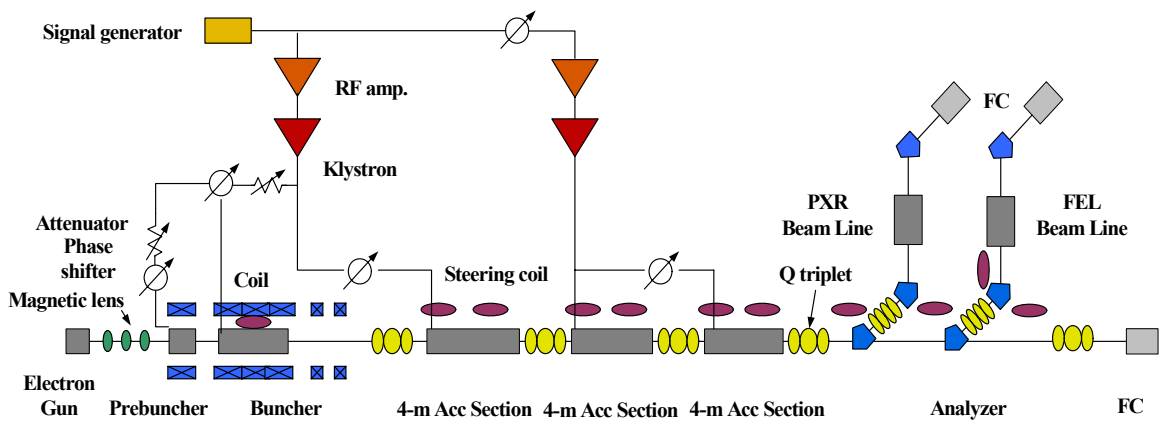

Figure 1: Schematic layout of the accelerating structures, RF system and the FEL and the PXR beam lines

*"Academic Frontier" Project for Private Universities: matching fund subsidy from MEXT, Japan, 2005-2007
#hayakawa@lebra.nihon-u.ac.jp

ARC-EN-CIEL project electron beam dynamics

C. Bruni *, A. Loulergue, M. E. Couprie, Synchrotron SOLEIL, Saint-Aubin, France

Abstract

ARC-EN-CIEL project is based on the development of fourth generation tunable light source of high brilliance in the VUV to soft X-ray wavelength domain. The project will evolved into three phases : first and second phases are in single pass configuration, while third phase comports recirculation loops. For delivering a high brilliance light source with high peak power short pulses, the high charge electron beam should have subpicoseconde duration with low emittance and energy spread. In order to keep optimal slice characteristics for light production, phase space non linearities due to optics aberrations and collective effects should be minimized. In ERL configuration, the accelerator scheme and focusing should be optimized to take into account collective effects as Beam Break Up instability.

INTRODUCTION

This project is based on the development of a fourth generation subpicosecond light source, with a high brilliance and tunable in the VUV to soft X-ray wavelength domain[1]. ARC-EN-CIEL views two simultaneous modes of operation :

- A high charge, low emittance electron beam for HGHG (High Gain Harmonic Generation) operation : a 1 nC electron bunch charge compressed by two chicanes, with 1 to 10 kHz repetition rate and 1 to 10 μA average current,
- A high average current electron beam for synchrotron radiation operation : a 0.2 to 1 nC electron bunch charge, with 1 to 100 MHz repetition rate and 1 to 100 mA average current.

The HGHG based FEL sets requirements on the beam : high charge, sub-picosecond duration, and low emittance. Optics aberration or collective effects, which are accentuated by high charge, are able to generate non linearities, which damage beam characteristics [2, 3].

Adding recirculation loops allows high average current operation and the energy to be increased by keeping high densities subpicosecond bunch. However, collective effects as Beam Break up instability, form a feedback loop between electron beams and RF cavities. Then, hereafter a threshold current, the oscillation amplitude of the beam transverse position exponentially grows leading to the beam loss [4].

* christelle.bruni@synchrotron-soleil.fr

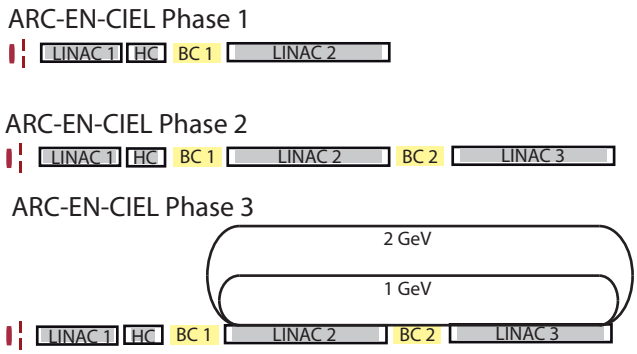

Figure 1: Representation of the ARC-EN-CIEL accelerator for the different phases. LINAC : Linear accelerator composed of cryomodules, HC : third harmonic cavity, BC : bunch compressor. To view all components, the representation is not scaled. Phase 1 is 70 m long, phase 2 : 200 m, phase 3 : 200 m with a radius of the arcs of 15 and 30 meters.

This paper presents the electron beam dynamics for the ARC-EN-CIEL project in single pass and ERL configuration, especially on the conditions for minimizing non linearities and Beam Break Up instability.

SINGLE PASS CONFIGURATION

ARC-EN-CIEL phase 1 and 2 (see fig. 1) aim at providing a 220 MeV and 1 GeV electron beam. The technology employed is a RF gun [5] followed by superconducting TESLA type [6] cryomodules. Chicanes are used to compress the beam duration. In this section, simulations realized for both single pass cases of ARC-EN-CIEL are presented by pointing out the optimisation for the light production.

The RF gun and the cavity modules have been simulated using ASTRA [7]. The laser, which lights the photocathode is 20 ps long (2.1 mm rms) with a cylindrical uniform distribution. To take into account the Coherent Synchrotron Radiation (CSR) in the chicane, the CSRTrack code [8] has been employed to model the compression scheme.

ARC-EN-CIEL phase 1

The RF gun produces a 1.1 π mm $mrad$ total emittance with a total charge of 1 nC. Then a first cryomodule (LINAC1) leads to an energy of 120 MeV. A third harmonic cavity (HC) tuned in order to suppress non linearities (RF and magnetic) is placed before the chicane [9]. Figure

STATUS OF THE UNDULATOR SYSTEM OF THE SEEDED HGHG-FEL TEST BENCH AT MAX-LAB*

J. Bahrdt, W. Frentrup, A. Gaupp, K. Goldammer, K. Holldack, M. Scheer,
BESSY, Berlin, Germany
M. Brandin, F. Lindau, D. Pugachov, S. Thorin, S. Werin, Lund University, Lund, Sweden,
J. Kuhnhenn, Fraunhofer INT, Euskirchen, Germany

Abstract

Within the EUROFEL Design Study a seeded HGHG-FEL will be set up at the 450 MeV linac at MAX-lab. The undulators and the dispersive section have been installed. Two different glass fiber based radiation dose monitors have been integrated. We report on the performance of these components. The impact of electron losses on undulator magnets and the Cherenkov fibers have been simulated. The THz radiation as produced by the bunched electron beam in the dump magnet can be used as a measure of the longitudinal and transverse overlap of the electron beam and the laser beam which has been concluded from simulations.

INTRODUCTION

Within the European FEL Design Study a single stage seeded HGHG FEL [1] test bench is currently set up at MAX-lab [2]. The electrons will be accelerated in the injection linac of the MAX-I-III rings. The FEL experiment is located inside the MAX-II storage ring and the electron beam will be available between the injections into the MAX-lab rings. A new low emittance photocathode gun [3] will be installed at the end of 2007. The commissioning of the complete setup will start in September 2007 using an existing gun which provides a bunch charge of 0.08nC.

BESSY has built and installed the two permanent magnet undulators (modulator and radiator) and the electromagnetic chicane. Permanent magnets are sensitive to radiation damage and the deposited doses have to be monitored. For this purpose two glass fiber systems have been implemented: i) A Cherenkov system delivers fast signals which will be used for a laser interlock system in case of an electron beam missteering. ii) Absolute dose measurements are done with a powermeter system which is based on another type of glass fiber. A detailed study and comparison of both measurements systems in combination with numerical simulations will be very helpful for the design of future FEL sources.

The alignment of the electron beam with respect to the laser beam is crucial for a reliable operation of the seeded FEL and a robust diagnostic is required. Simulations show that the spectral distribution of the THz radiation as produced by the electron bunch in the dump magnet changes significantly if the seed laser interacts with the electron beam. Thus, the THz will be helpful in the commissioning phase and also later during normal operation as an input for feedback systems.

*This work has been partially supported by the EU Commission in the Sixth Framework Program, Contract No. 011935 – EUROFEL.

THE UNDULATORS

The parameters of the undulators and the chicane have been described in [4]. The electron beam height at the FEL location of 520mm requires a horizontal operation of the two undulators. The undulators have been measured and shimmed in the vertical position at the BESSY field measurement bench. After shimming the devices have been rotated by 90° and mounted onto three columns each. Fig. 1 shows the radiator in operating position at MAX-lab. In the final position the field integrals will be checked with a pulsed wire system and air coils at the undulator ends will be used to compensate residual field errors.

Figure 1: Radiator of the APPLE II type in operating position without vacuum chamber. Four power meter sensors (see below) at each undulator end (orange cable) are installed.

THE CHICANE

The chicane consists of four electromagnets (Fig. 2). Each magnet is made of two low carbon steel pieces (C < 0.01%) which are bolted together. The poles have been wire cut. The number of windings per coil is 432. The measured field integrals per Ampere for the four magnets are: 10.9, 10.9, 10.6, 10.7 Tmm / A.

The magnetic hysteresis of the four magnets as measured with a moving wire is ±0.25 Tmm (Fig. 3).

NONLINEAR HARMONIC GENERATION IN THE BESSY SOFT X-RAY FEL*

olda er, BESS , Berlin, er any

Abstract

Free Electron Lasers FELs do not only radiate at the funda ental fre uency, they ay also radiate coherently at higher har onics This process is referred to as nonlinear har onic generation or NH NH is of high interest, because it e tends the output wavelength of FELs to several har onics of the FEL resonant fre uency In cascaded High ain Har onic eneration H H FELs, har onic radiation ay be used to i prove fre uency-conversion and reduce the nu ber of H H -stages BESS proposes to build a cascaded H H FEL with three FEL lines 1 They cover a wavelength range of 51 n Low-Energy FEL to 1 2 n High-Energy FEL and consist of up to four H H -stages In this paper, we present studies of the BESS High-Energy FEL har onic content perfor ed with the upgraded version of the si ulation code enesis 1 3 2

INTRODUCTION

The BESS High-Energy HE- FEL uses a cascade of four H H stages to convert a seed laser of 297 5 n down to 1 24 n Each stage consists of a odulator, dispersive chicane and radiator Analytic studies 3 predict that the signal-to-noise ratio SNR in H H FELs decreases by the s uare of the har onic nbu ber used during conversion As the total conversion factor in the BESS HE-FEL is 225, degradation of the radiation due to noise is a critical issue In order to conserve the e cellent te poral coherence of the seeded FEL radiation, a new design is proposed that uses har onic radiation to reduce the nu ber of H H -stages Its prospects are investigated in this paper

Har onic radiation is intrinsically produced during the FEL process in planar undulators and leads to coherent e ission at higher har onics of the FEL resonance 4 It beco es signi cant in the high gain regi e of an FEL and typically provides for power levels in the range of 1 or 0 1 of the funda ental depending on the har onic nu ber

The new design uses har onic radiation fro the rst stage radiator Its fth har onic has a wavelength of 11 n and could hence be applied directly as a seed for the third stage odulator Figure 3 illustrates the idea

HARMONIC CONTENT OF FIRST STAGE

The BESS High Energy FEL rst radiator is a planar undulator with the period length of λ_u 92 and a total length of 3 69 The radiator has to be prolonged signi cantly to yield suf cient fth har onic power for seeding the third stage The har onic power in the rst radiator then evolves as depicted in Fig 2

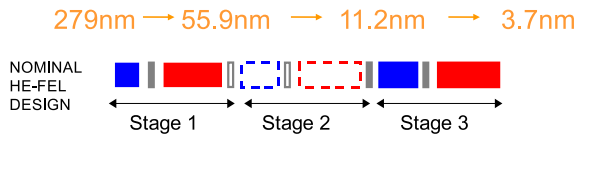

Figure 1 Sche atic picture of new proposal for BESS High Energy FEL har onic radiation fro rst stage radiator could be used to the seed third stage The second stage could be o itted Stages 1 to 3 depicted

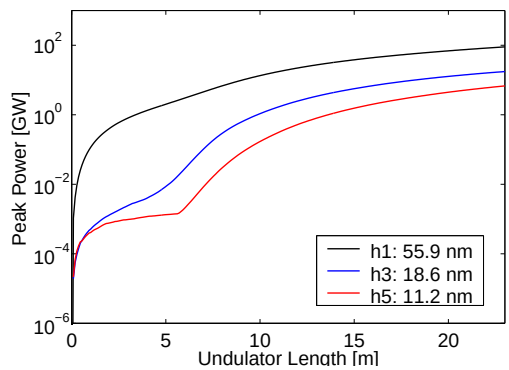

Figure 2 Si ulation of BESS High-Energy FEL radiation power along rst radiator Fro top to botto fun da ental, third and fth har onic radiation Si ulation perfor ed with new version of enesis 1 3 2

It can be observed that the har onics start later than the funda ental and enter their e ponential gain regi e after appro i ately 5 to 7 After that they rapidly reach a signi cant output power because they have a shorter gain length higher gain than the funda ental This corresponds well to analytic predictions 5

* Work supported by the Bundes inisteriu fur Bildung und Forschung, the State of Berlin and the ukunftsfonds Berlin

OUTPUT PERFORMANCE OF THE STARS HGHG DEMONSTRATOR AT BESSY*

B. Kuske †, K. Goldammer, A. Meseck, BESSY, Berlin, Germany

Abstract

BESSY is planning to construct a free-electron laser facility, STARS - **S**uper conducting **T**est-**A**ccelerator for **R**adiation by **S**eeding, to demonstrate cascaded high-gain harmonic generation (HGHG) FELs. A 325MeV superconducting linear accelerator will drive two HGHG-stages, where the second stage is seeded by the radiation from the first stage. Such a cascading of the HGHG scheme allows for a reduction of the STARS output wavelength down to the few 10nm range. This paper describes the layout and the expected performance of the facility, the achievable wavelength range, the harmonic content of the radiation, the potential of super-radiant pulses and first tolerance studies for bunch parameter mismatch.

INTRODUCTION

In 2004, BESSY presented the Technical Design Report for a 2.25GeV linac driven Free-Electron Laser (FEL) user facility, covering the VUV to soft X-ray spectral range [1]. The facility utilizes the high-gain harmonic generation principle (HGHG), first demonstrated at Brookhaven National Labratory, USA, in 2000 [2]. In order to reach the short wavelength range, several cascaded HGHG stages are foreseen. In 2006, the German Science Council recommended the construction of a demonstrator to investigate the possibility of cascading HGHG stages. A Conceptual Design Report for this demonstrator, 'STARS'- **S**uper conducting **T**est-**A**ccelerator for **R**adiation by **S**eeding, has been published in 2006 [3]. STARS will consist of a normal conducting RF gun, a superconducting 325MeV linac, a collimation and diagnosis section and a 27.5m undulator section [4]. It will produce pulses in the spectral range from 18eV to 31eV. For further details see [5]. This paper details the layout of the undulator section and presents the performance of STARS at different wavelengths and operational modes. A few preliminary calculations concerning the stability of the machine are shown.

MECHANICAL LAYOUT OF THE UNDULATOR SECTION

The undulator section will consist of two HGHG stages separated by a fresh bunch chicane, that delays the electron bunch so that the radiation of the first stage seeds a preceeding, fresh part of the beam. Each stage starts with a short undulator to modulate the energy of the electron bunch (modulator). It is followed by the dispersive section consisting of four identical dipoles. The adjacent undulator, called radiator, consists of two respectively three separated segments tunable to the harmonics of the modulators' resonant frequency. Table 1 lists the important parameters for all four undulators.

Table 1: Characterization of the STARS undulators (Modulators: M1, M2, Radiators R1, R2.)

	M1	**R1**	**M2**	**R2**
Type	planar	planar	planar	Apple III
Period [m]	0.05	0.05	0.05	0.022
No. Periods	10	2*40	30	3*150
Aper. [mm]	10	20	20	7
Max. B_y[T]	1.1	1.1	1.1	0.839
Max. B_x[T]	-	-	-	0.621
Length [m]	0.5	2* 2.0	1.5	3*3.3
Res. λ [nm]	800	160/200	160/200	40/50/66

The fresh bunch chicane is mechanically identical to the dispersive sections. In order to control the electron beam size along the length of almost 30m, a total of 9 quadrupoles are distributed, one before and after each chicane and one in between undulator segments. The matching into the section will be handled in the preceding collimator. The total length of the chicanes is 2.5m; the distance between undulator segments is 1.0m. The chicanes will also host all necessary diagnostics, as well as all vacuum components, which shall not be incorporated into the undulators. Phase shifters and further diagnostics are placed between undulators segments. The correctors necessary to control the trajectory of the bunch are incorporated into the quadrupoles.

OPERATIONAL MODES

A tunable 800nm Ti-Saphir laser will be used to seed the first modulator. There will be a small chicane right in front of the modulator as a port for the beam. The 4th or 5th harmonic of the beam modulation can be amplified in the following radiator by tuning the dispersive section and driving the undulator gap. After the radiator the electron bunch is delayed by 100 fs in the fresh bunch chicane. Thus, in the second modulator, the preceding, unused part of the bunch is seeded by radiation 160nm and 200nm. The second radiator can be tuned to the 4th or 3rd harmonic of the resonant frequency of the second modulator, so that the final output

* Funded by the Bundesministerium für Bildung und Forschung (BMBF), the State of Berlin and the Zukunftsfond Berlin

† Bettina.Kuske@bessy.de

SMALL-APERTURE VACUUM-CHAMBER DESIGN FOR STARS*

J. Bahrdt, V. Dürr, A. Meseck†, M. Scheer, G. Wüstefeld
BESSY GmbH, Berlin, Germany

Abstract

To demonstrate and investigate the cascaded high-gain harmonic generation (HGHG) scheme proposed for the BESSY Soft X-ray FEL, BESSY plans to build a test-facility called STARS consisting of two HGHG stages. The radiator in the second stage is planned as an APPLE III device which provides the highest field for a circular beam pipe. It's minimum Gap of 7 mm translates into a 5 mm inner diameter of the vacuum chamber, which leads to a higher pressure and an increase of the wakefields. An analysis of the impact of the wakefields and the expected vacuum profile is thus required. Results of this analysis and vacuum calculations and measurements are presented.

INTRODUCTION

To provide radiation with high power, short pulse length and full coherence in the VUV and soft X-ray regime, BESSY plans to build a seeded FEL facility based on the high-gain harmonic generation scheme [1, 2]. The technical design report of the BESSY Soft X-ray FEL facility [3] was evaluated in 2006 by the German Science Council and recommended for funding subject to the condition that its key technology, the cascaded HGHG scheme, be demonstrated beforehand. To address this issue, BESSY is proposing the proof-of-principle facility STARS [5] for a two-stage HGHG cascade which will serve as a user facility even after the commissioning of the BESSY FEL. The STARS is seeded by a tunable laser covering the spectral range of 700 nm to 900 nm. The target wavelength ranges from 70 nm to 40 nm with peak powers up to a few hundred MWs and pulse lengths less than 20 fs (rms). The polarization of the fully coherent radiation is variable. For efficient lasing a 325 MeV driver linac is required. It consists of a normal-conducting gun, superconducting TESLA-type modules modified for CW operation and a bunch compressor, for more details see please [4, 5, 6].

The STARS comprises a cascade of two HGHG stages each consisting of an undulator (acting as modulator) / dispersive chicane / undulator (acting as radiator) section. The two modulators and the first radiator of the STARS are planned as planar devices. The second (final) radiator needs to be helical to provide full polarization control of the output radiation. This radiator consists of three undulator modules and will be realized as an APPLE III [7] device.

The period lengths and the minimum gaps, i.e. free aperture between the magnet rows, of the undulators are chosen such that the desired wavelength range can be covered for an electron beam energy of 325 MeV. The planar devices have a period length of 50 mm and a minimum gap of 20 mm and 10 mm respectively. The period length of the final radiator amounts to 22 mm and the minimum gap is 7 mm. This small gap translates into 2.5 mm for the vacuum chamber inner radius.

Generally, the small conductance caused by such a small aperture leads to a higher pressure, which has to be counteracted by a suitable vacuum pumping scheme as far as possible. An other impact of the small aperture is the enhancement of the wakefields. In spite of the moderate peak current of 500 A predicted for STARS, an increase of the undulator wakefields can be expected.

The degradation of the electron beam quality due to the higher pressure and the change in the electron energy by the wakefields decline the FEL output radiaton. We present a analysis of their impact on the FEL performance.

CIRCULAR BEAM PIPE AND APPLE III TYPE RADIATOR

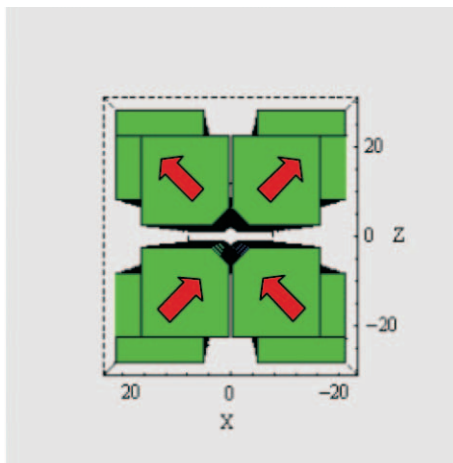

Figure 1: A sketch of the magnetic structure of an APPLE III device.

The second radiator will be realized as an APPLE III device providing full polarization control of the radiation. This APPLE type requires a round beam pipe to allow for more magnetic material located close to the electron beam, see Figure 1. For the second radiator of STARS, the free aperture between the magnets is 7 mm and the smallest vertical distance amounts to 4.4 mm which provides enough space for Hall probe measurements as well as for a fixture to support the vacuum chamber. An APPLE III type structure has been chosen for a number of reasons:

*Work supported by the Bundesministerium für Bildung und Forschung and the Land Berlin
† meseck@bessy.de

MEASUREMENT OF THE PROJECTED NORMALIZED TRANSVERSE EMITTANCE AT PITZ*

L.Staykov†, J. Bähr, C. Boulware, H. J. Grabosch, L. Hakobyan, M. Hänel, S. Khodyachykh, S. Korepanov, M. Krasilnikov, S. Lederer, A. Oppelt‡, B. Petrosyan, S. Rimjaem, A. Shapovalov§, F. Stephan, DESY, Zeuthen, Germany
J. Rönsch, Hamburg University, Hamburg, Germany
D. Richter, BESSY, Berlin, Germany
K. Flöttmann, DESY, Hamburg, Germany
G. Asova, K.Boyanov, I.Tsakov, INRNE-BAS, Sofia, Bulgaria

Abstract

The main objective of the Photo Injector Test facility at DESY in Zeuthen (PITZ) is the production of electron beams with minimum transverse emittance at 1 nC bunch charge. PITZ consists of a photo cathode RF gun, solenoids for compensation of the space charge induced emittance growth and a booster cavity. In order to study the emittance evolution along the beam line three Emittance Measurement SYstems (EMSY's) were installed downstream of the booster cavity [1]. In a first operation period in October 2006 the emittance was measured for gun gradients of about 40 MV/m. A new gun cavity is presently installed at PITZ and conditioning up to a gradient of 60 MV/m is ongoing. In this work we present recent results from measurements of the normalized projected transverse emittance of the electron beam. The emittance is measured using the so called single slit scan technique. Measurements are presented for different gun and booster gradients, solenoid strengths and initial beam size at the photocathode.

INTRODUCTION

Major goal of PITZ is the development and optimization of electron sources that fulfill the requirements for SASE FEL's such as FLASH and XFEL. The optimization process is conducted by extended numerical simulations using ASTRA [2], and closely followed by research and development of appropriate instruments for electron and laser beam characterization (see [3, 4]).

A simplified scheme of PITZ is shown on Figure 1. It consists (right-to-left) of a 1.5 cell L-band RF gun equipped with a Cs_2Te cathode, pair of solenoids for space charge compensation, low energy beam diagnostics, a booster cavity, high energy diagnostics including three EMSY's (installed at 4.3, 6.6 and 9.9 m downstream the cathode) and a beam dump. A photocathode laser system provides carefully shaped laser pulses with variable transverse diameter and flat hat longitudinal distribution (see [4, 5]).

In this paper we present results from the emittance measurements made in October 2006 and summer 2007 using two different gun cavities:

- prototype 3.1 conditioned in summer 2006 and optimized in October 2006 up to the maximum requirements for FLASH with a peak power of 3.5 MW resulting in gun gradient of about 40 MV/m [6];
- prototype 3.2 which was conditioned and optimized this summer with a peak power of up to 6.9 MW resulting in a gun gradient of $\sim$60 MV/m [7].

For gun prototype 3.1 the emittance was measured using the three existing EMSY's as a function of the main solenoid focusing current for various booster phases. For prototype 3.2 the emittance was measured only at the first EMSY (distance from the cathode 4.3 m) for various beam sizes at the cathode and different energy gain from the booster. In addition the optimized settings for gun 3.1 were applied to gun 3.2 and the emittance was measured, the results are compared and discussed.

EMITTANCE MEASUREMENT SETUP

The transverse emittance at PITZ is measured using the so called *single slit scan* technique. A schematic representation of the technique is shown on Fig. 2. For this technique the uncorrelated local divergence is estimated by cutting the electron beam into thin slices and measuring their size on a screen after propagation in a drift space. The so called sheared normalized RMS emittance is then calculated using the following definition [8]:

$$\varepsilon_n = \beta\gamma \cdot \sqrt{\langle x^2 \rangle \cdot \langle x'^2 \rangle}. \quad (1)$$

Here $\langle x^2 \rangle$ and $\langle x'^2 \rangle$ are the second central moments of the distribution of the electrons in the so called trace phase space where $x' = p_x/p_z$ represents the angle of a single electron trajectory with respect to the whole beam trajectory[1]. The RMS beam size is measured on an additional OTR or YAG screen at the position of the slits. The uncorrelated divergence is obtained by analyzing the profiles of

* This work has partly been supported by the European Community, Contract Number RII3-CT-2004-506008, and by the 'Impuls- und Vernetzungsfonds' of the Helmholtz Association, contract number VH-FZ-005.
† Presenting author, e-mail: lazaraza@ifh.de
‡ now at PSI, Vilingen
§ on leave from MEPHI, Moscow

[1] valid for small momentum spread within the bunch, otherwise more precise definition should be used (i.e. [9]).

STATUS OF THE SPARX FEL PROJECT*

C.Vaccarezza, D.Alesini, M.Bellaveglia, S.Bertolucci, M.E Biagini, R.Boni, M.Boscolo, M.Castellano, A.Clozza, L.Cultrera, G.Di Pirro, A.Drago, A.Esposito, M.Ferrario, D.Filippetto, V.Fusco, A.Gallo, A.Ghigo, S.Guiducci, M.Migliorati, L.Palumbo, L.Pellegrino, M.Preger, C.Sanelli, M.Serio, F.Sgamma, B.Spataro, A.Stella, F.Tazzioli, M.Vescovi, C.Vicario, INFN Frascati, Italy
F. Ciocci, G.Dattoli, A.Doria, F.Flora, G.Gallerano, L.Giannessi, E.Giovenale, G.Messina, P.L. Ottaviani, G.Parisi, L.Picardi, M.Quattromini, A.Renieri, C. Ronsivalle ,ENEA C.R. Frascati, Italy
S.Cialdi, C.Maroli, V.Petrillo, M. Rome, L.Serafini, INFN-Milano, Italy
L.Catani, E.Chiadroni, A. Cianchi, C.Schaerf, INFN-Roma II, Roma, Italy
P.Musumeci, M.Petrarca, INFN Roma, Italy
F.Alessandria, A.Bacci, F.Broggi, C.De Martinis, D.Giove, M.Mauri, INFN/LASA, Segrate, Italy
L.Ficcadenti, M.Mattioli, A.Mostacci, University La Sapienza, Roma, Italy
P.Emma, SLAC, Menlo Park, CA, U.S.A.
S.Reiche, J. Rosenzweig, UCLA, Los Angeles, CA, U.S.A

Abstract

The SPARX project consists in an X-ray-FEL facility jointly supported by MIUR (Research Department of Italian Government), Regione Lazio, CNR, ENEA, INFN and Rome University Tor Vergata. It is the natural extension of the ongoing activities of the SPARC collaboration. The aim is the generation of electron beams characterized by ultra-high peak brightness at the energy of 1 and 2 GeV, for the first and the second phase respectively. The beam is expected to drive a single pass FEL experiment in the range of 13.5-6 nm and 6-1.5 nm, at 1 GeV and 2 GeV respectively, both in SASE and SEEDED FEL configurations. A hybrid scheme of RF and magnetic compression will be adopted, based on the expertise achieved at the SPARC high brightness photoinjector presently under commissioning at Frascati INFN-LNF Laboratories [1,2]. The use of superconducting and exotic undulator sections will be also exploited. In this paper we report the progress of the collaboration together with start to end simulation results based on a combined scheme of RF compression techniques.

THE SPARX LAYOUT

A spectral range from 13 nm to 1 nm has been considered for the radiation. SASE-FEL's in this wavelength range require high brightness beam at the undulator entrance. In Table 1 the electron beam parameter list is reported for such a source, while in Fig. 1 the schematic layout of the accelerator is shown. A 150 MeV SPARC-like photoinjector [1] is meant to provide a 300-500 A beam, adopting the velocity bunching compression scheme. A first linac section L1 rises the beam energy up to 300 MeV, where a first magnetic chicane is foreseen mainly for comparing the overall efficiency between the two compression methods at low energy. After a second linac section L2, i.e. at the energy around 0.6 GeV, the main magnetic compressor BC2 is located rising the beam peak current up to I_{pk}≈1 kA, according to a 'hybrid' compression scheme consisting in one RF compression stage at low energy, plus one magnetic chicane at 0.6 GeV. A third accelerating section L3 brings the beam energy up to E≈1GeV and a first extraction dogleg DL1 drives the beam through a diagnostic section and to the first undulator where both SASE and seeding experiments in the radiation wavelength range of λ_r≈ 13 ÷5 nm are foreseen. This is what is meant for the first phase of the SPARX project. For the Phase II another linac section will bring the beam energy up to 1.5 GeV where a third magnetic chicane BC3 is foreseen to compress the beam and reach peak currents of the order of I_{pk}≈2÷2.5 kA. The last linac L4 brings the final energy up to E=2GeV. A second extraction dogleg DL2 provides the beam diagnostics and delivery to the second undulator for the wavelength range λ_r≈ 5÷1.5 nm

Table 1: Electron beam parameters

Beam Energy	1÷2	GeV
Peak current	1-2.5	kA
Emittance (average)	2	mm-mrad
Emittance (slice)	1	mm-mrad
Energy spread (correlated)	0.1	%
Repetition Rate	50	Hz

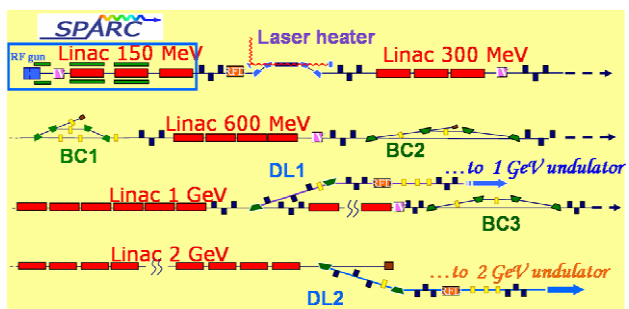

Fig. 1: SPARX Linac schematic layout

*Work partially supported by MIUR for the realization of "Grande Infrastruttura Laser ultrabrillante per raggi X multiscopo"

THE DRIVE LASER SYSTEM FOR CFEL

Li Weihua,Chen Yanan
Institute of Applied Electronics,CAEP,China

Abstract

A reliable and compact drive system is one of the key components for the stable operation of FEL.We have developed a solid-state drive laser system to meet the requirements of the CFEL(CAEP FEL) research.The system consisted of a passive mode-locked oscillator with a timing stabilizer,a regenerative amplifier and a frequency conversion part.After the 4-th harmonics,the duration of 15 picoseconds Gaussian pulses with wavelength 266nm at a repetition rate 54.17MHz were obtained.These micropulses were contained within a macropulses envelope as long as 1 to 6μs,which was emitted from the drive laser at a repetition rate at 3Hz,6Hz or 12Hz,one single micropulse energy as large as 4μJ was achieved.The design specifications, configuration and diode-pumped amplifier of the drive laser system are also described.

INTRODUCTION

A reliable and compact drive laser system is one of the key components for the stable operation of FEL.It will strongly affect the performance of the FEL,such as the specifications as following:the micropulse duration of electron beam,the micropulse current of electron beam,the jitter of micropulse-peak-current,and so on[1].We have developed a all-state-solid drive laser system to meet the requirements of the CFEL research,as shown in table 1.The laser stablility,e.g.,energy stability,timing stability and the pointing stability,was also requested stringently during the course of the research[2].

DRIVE LASER SYSTEM

The drive laser system,which was shown in Fig.1,was consisted of a passive mode-locked oscillator with a timing stabilizer,a regenerative amplifier and a frequency conversion part.

Oscillator

The seeding laser GE-100-XHP,is a passive mode-locked laser with a semiconductor absorber mirror (SESAM),developed by Time-Bandwidth Products Ltd, Switzerland[3].Its repetition rate is 54.167 MHz,equal to 1/24 of 1300MHz L-band radio frequency, which was used for the photocathode RF gun.The timing stabilizer measured the phase and the frequency offset between the laser pulses and the reference RF signal,and adjusted the cavity length to synchronize the two signals[4].

Regenerative Amplifier

It was composed of one-double-pass and two-single-pass stages.A Pockels Cell captured a “maropulse” from the continuous pulses output to increase the pulse energy.Every “macropulse” contains 50 to 300 micro-pulses,as long as 1us to 6us.

Harmonics Generator

This component coverted the fundamental output to the 4-th harmonics,which would illuminate the photocathode Cs_2Te.The net conversion efficiency was close to 20% from the fundamental to the 4-th harmonics.The UV energy was obtained up to 1.2mJ per “macropulse”,4uJ per micropulse.

LASER PERFORMANCE

Amplitude Uniformity

The amplitude uniformity from micropulse to micropulse in the same macropulse was quested stringently for the CFEL research.We have measured it at the port of regenerative amplifier,2-th harmonics and 4-th harmonics,as shown in Fig.2,Fig.3,Fig.4.The variation of amplitude uniformity from micropulse to micropulse was 3% rms or less.

Energy Stability

UV energy stability was measured for 300 shots by a power meter.The statistical results showed that the Energy fluctuation was 2.8%rms or less.The curve of energy deviation from the mean value was shown in Fig.5,which were 84 data from the 300 shots.

Timing Jitter

The timing jitter of the laser oscillator was estimated from the output of the phase detector in the feedback loop.A phase detector measured the phase difference between the fast photodiode signals of laser pulses and the reference RF signal,and generated an “error signal”.This phase difference was related to the timing jitter between the laser phase and the reference RF phase.The timing jitter of the oscillator was estimated as 0.4ps rms.

Pointing Stability

The pointing stability of 266nm output pulses was measured by a CCD camera.Beam profiles were measured on a screen plate at 30 meters away form the laser output port.Pointing stability of the beam centroid was estimated to be 0.1mrad rms in Y direction,and 0.01mrad rms in X direction,as showed in Fig.6 and Fig.7.The scale between the pixel to actual dimension was 13.7 pixels to 1mm.Fig.8 was the beam profile.

Other specifications and the laser performance were listed on Table 2.

DESIGN OF THE PAL TEST FEL MACHINE

Mungyung Kim*, Jinhyuk Choi, Jung Yun Huang, Heung-Sik Kang, In Soo Ko, Tae-Yeon Lee, Jong-Seok Oh, Sung Ju Park, PAL, Pohang, South Korea

Chang-Mook Yim, POSTECH, Pohang, South Korea

Abstract

In order to the PAL-XFEL, the 1st stage will be to build a test machine, whose design parameters are presented here. It will be a 200 MeV machine that has the target wavelength of visible range. The design details and simulation results are shown in this paper.

INTRODUCTION

The Pohang Accelerator Laboratory (PAL) is going to build a new X-ray free electron laser (XFEL) machine based on the self-amplified spontaneous emission (SASE) scheme [1]. For the first step of the project, a test machine is considered to build. But it means extra time and budget is required. Fortunately, we have found sufficient area in the linac building. Usually PAL linac is operated as an injector for the 2.5 GeV storage ring. So another linac, test linac, beside of the preinjector area in the linac building, is operated for low energy experiments with 60 ~ 100 MeV. Furthermore RF cathode gun system is installed to test as an injector of the PAL FEL in the assembly room of the building. The injector consists of two accelerator columns with about 80 MeV. If we combine with two machines, the test linac and the injector, we need only one acceleration column and one chicane to have a 200 MeV linac for the test machine of PAL FEL project. It means we can save time and budget to construct a building of the test machine. So the test machine is designed to install in the area. Fig 1 shows the structure of the PAL preinjector area and schematic layout of the test machine. In this paper, the simulation results and detail designs of the machine will be reported.

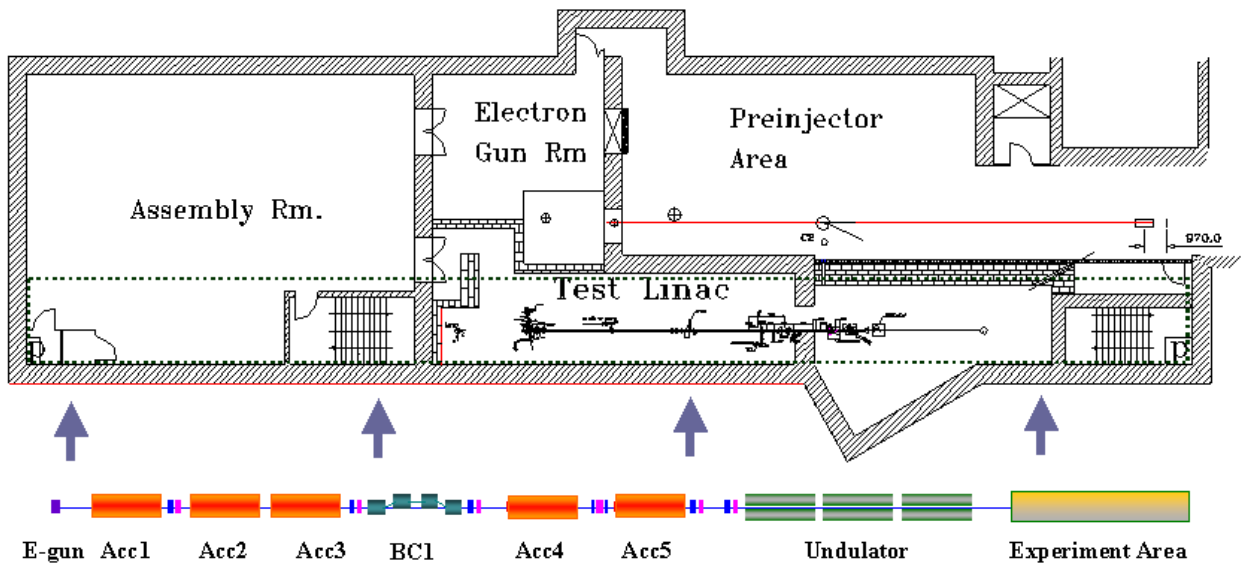

Figure 1: Drawing with preinjector area in the linac building and schematic layout of the test machine. The test machine is designed to install in the dashed block.

BEAM DYNAMICS DESIGN

The test machine consists of a 78 MeV injection part, linear accelerator with a chicane, beam transport line, SASE radiation area with three undulators and experiment area as shown in Fig. 1.

The injection part consists of a photo-cathode RF gun and two accelerating columns. The beam charge from the RF gun is 0.5 nC with 10 ps pulse length 60 Hz repetition rate in maximum, and the final energy of the injector is 78 MeV. After the injector, the beam pulse length is 777 μm, peak current is 60 A, energy spead is 0.3 % and rms normalized eimttances are 0.9 μmrad both direction with horizontal and vertical. PARMELA is used to simulate the injection part.

The linear accelerator is composed of two parts, bunch compressing and accelerating. The bunch compressing part consists of one accelerating column, L1, and one chicane bunch compressor BC1. At the exit of the injection part the electrons enter the L1 where they are

*mungyung@postech.ac.kr

FEATURES OF THE PAL-XFEL DESIGN*

T.-Y. Lee†, J. Choi, and H. S. Kang
Pohang Accelerator Laboratory, San 31, Hyoja-dong, Pohang, Kyungbuk 790-784, KOREA

Abstract

PAL-XFEL, the new XFEL project of Pohang Accelerator Laboratory, aim to emit hard X-ray of $1-1.5$ Å, although its beam energy is only 3.7 GeV. To achieve the goal, coherent third harmonic radiation will be utilized. This paper discusses schemes of hard X-ray generation with 3.7 GeV electron beam and concludes that use of the third harmonic is the only possible way.

INTRODUCTION

The storage ring based third generation light source has spread all over the world in the last twenty years and is now a useful and common facility for scientific research. However, even more advanced X-ray source, the XFEL facility, is not likely to be so. Apparently, the X-ray FEL (XFEL) is achievable only by a high energy electron beam. To make $1-1.5$ Å hard X-ray FEL, the electron energy has been chosen 14.35 GeV for the Linac Coherent Light Source (LCLS) in SLAC [1] that is under construction and 17.5 GeV for the European XFEL in DESY [2] that is approved. Not only the linear accelerator but also the undulator in XFEL is long; the LCLS undulator is 112 m long and the European XFEL undulator is even longer, 260 m. We may have to conclude that hard X-ray FEL is too expensive to be available in most countries. Is it possible to reduce the machine size? The SPring-8 Compact SASE Source (SCSS) project in Japan tries to reduce the whole facility size by using an in-vacuum undulator and the new technology of C-band linear accelerator [3]. It is going to need only 8 GeV electron beam to generate hard X-ray. However, building and maintaining an 8 GeV electron machine still costs a lot even with the new technology. A natural question is how compact an XFEL facility can be.

PAL-XFEL, the new XFEL project of Pohang Accelerator Laboratory (PAL) [4], tries to achieve the goal by utilizing the third harmonic SASE radiation. It will uses 3.7 GeV electron beam. Below it will be shown that $1-1.5$ Å hard X-ray FEL can not be achieved by 3.7 GeV electron energy, if we insist to use only the fundamental SASE radiation. Therefore, PAL-XFEL may be the lowest energy hard X-ray FEL machine. The only defect is that the transverse coherence of the PAL-XFEL third harmonic radiation would be far from perfect. Basic parameters of the PAL-XFEL are listed in Table 1 for unfamiliar readers.

Table 1: Parameters of PAL-XFEL

Beam Parameters	**Value**	**Unit**
Electron energy	3.7	GeV
Peak current	3	kA
Normalized slice emittance	1	mm mrad
RMS slice energy spread	0.01 %	
Full bunch length	270	fs
Undulator Parameters		
Undulator period	1.5	cm
Segment length	4.5	m
Full undulator length	80	m
Peak undulator field	1.19	T
Undulator parameter, K	1.49	
Undulator gap	4	mm
Average β-function	10	m
FEL Parameters		
Radiation wavelength	3	Å
FEL parameter, ρ	5.7×10^{-4}	
Peak brightness	5×10^{31}	1)
Peak coherent power	1	GW
Pulse repetition rate (Max.)	60	Hz
1D gain length	1.2	m
Saturation length, L_{sat}	45	m

1) photon/(sec mm^2 mrad^2 0.1%BW)

BEAM ENERGY DEPENDENCE OF XFEL FACILITY SIZE

To find the possibility of using low electron beam energy for an hard X-ray FEL, we need to know its beam energy dependence. To find out the beam energy dependence of an hard X-ray FEL, recall that the resonant wavelength of an undulator is given by

$$\lambda_r = \frac{\lambda_u}{2\gamma^2}\left(1+\frac{K^2}{2}\right), \quad (1)$$

where λ_r is the resonant wavelength, λ_u the undulator period, γ the Lorentz factor, and K the undulator parameter. K is defined by

$$K = 0.934 B_0[\text{Tesla}]\lambda_u[\text{cm}], \quad (2)$$

where B_0, the undulator peak magnetic field, depends not only on the undulator gap and period but also on the magnet material. If we consider a hybrid undulator with vanadium permendur, it is given by

$$B_0 = 3.694\exp\left[-5.068\frac{g}{\lambda_u}+1.520\left(\frac{g}{\lambda_u}\right)^2\right] \quad (3)$$

* Work supported by Korean Ministry of Science and Technology
† tylee@postech.ac.kr

POTENTIALITIES OF ELMI DEVICE FOR SUBMILLIMETER GENERATION BY STIMULATED INTERCAVITY SCATTERING IN PLANAR FEM *

A. V. Arzhannikov*, V. T. Astrelin, A. S. Kuznetsov, S. A. Kuznetsov, P. V. Kalinin, S. L. Sinitsky, V. D. Stepanov, BINP, Novosibirsk, Russia
N. S. Ginzburg, N. Yu. Peskov, A. S. Sergeev, V. Yu. Zaslavsky, I. V. Zotova, IAP, N-Novgorod, Russia

Abstract

Paper describes main features of a project on two-stage generation of submillimeter radiation at the ELMI device. This novel variant of a two-stage scheme is based on stimulated intercavity scattering. In accordance with the scheme, at the first stage a sheet electron beam drives a 2D Bragg free electron maser (FEM) of planar geometry to generate 4-mm pump wave. At the second stage this wave undergoes stimulated scattering at the supplementary electron beam to produce submillimeter radiation. In the paper we describe results of theoretical and experimental investigations of various aspects of the two-stage scheme and some testing experiments on units for realization of this scheme at the ELMI device.

INTRODUCTION

In recent experiments at the ELMI-device the single frequency operation of 4-mm planar FEM with 2D distributed feedback has been demonstrated [1]. These results created a basis for development of a two-stage generator for the sub-mm band. A key feature of the scheme proposed earlier in [2], is the use of two sheet beams with a few kAmps currents that transported in two parallel slit channels with a guiding longitudinal magnetic field, which are connected by a special waveguide. At the first stage one of the sheet beams passing in a slit channel with static undulator magnetic field drives 2D Bragg FEM of planar geometry to generate 4-mm pump wave as well as in the recent ELMI experiments. This intensive 4-mm radiation accumulated in the FEM resonator is transported through the special waveguide to the second slit channel where it is used as an EM-undulator for the secondary stage of sub-mm FEL.

The special waveguide connection will be realized in similar way as it was suggested earlier in the project of multibeam FEM with 2D distributed feedback where it was used for synchronization of radiation generated in different channels [3], [4]. Production of the two sheet beams by one accelerator diode with two cathodes is also similar to the process of operation of the multibeam diode described in Ref. [4].

SCHEMATIC OF PROPOSED EXPERIMENTS

At the first stage we plan to use a FEM with hybrid Bragg resonator which was developed in the recent experiments [1]. Hybrid two-mirror resonator consisting of upstream 2D and downstream 1D Bragg reflectors provides spatial coherence of radiation in a FEL driven by a large-size sheet e-beam [5], [6]. In the ELMI-experiments generated radiation has wavelength $\lambda_0 = 4$ mm with pulse duration up to 0.5 μs. The existence of regimes with high level of the mm-radiation spectral density near the frequency close to one of hybrid Bragg resonator eigen modes during all the pulse has been registered.

One of the typical shots shown in the Fig. 1 demonstrates the FEM operation on the mode with frequency 75.3 GHz. The single mode generation lasts 330 ns.

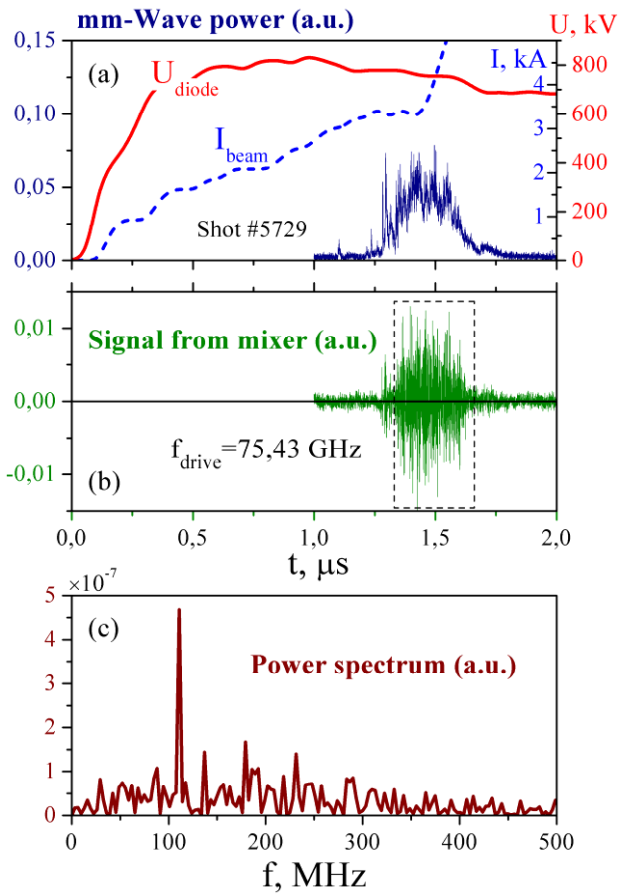

Fig. 1 Single frequency operation of 4-mm FEM: a) diode voltage (U_{diode}), beam current (I_{beam}) and mm-wave power; b) intercarrier frequency signal from heterodyne mixer (heterodyne frequency f_{drive}=75.43 GHz); c) mm-wave power spectrum.

*arzhannikov@inp.nsk.su

A PROJECT OF SC ERL AT KAERI

A.V.Bondarenko, S.V.Miginsky, Budker Institute of Nuclear Physics, Novosibirsk, Russia
B.C.Lee, S.H.Park, Y.U.Jeong, Y.H.Han, Korea Atomic Energy Research Institute, Daejeon, Korea

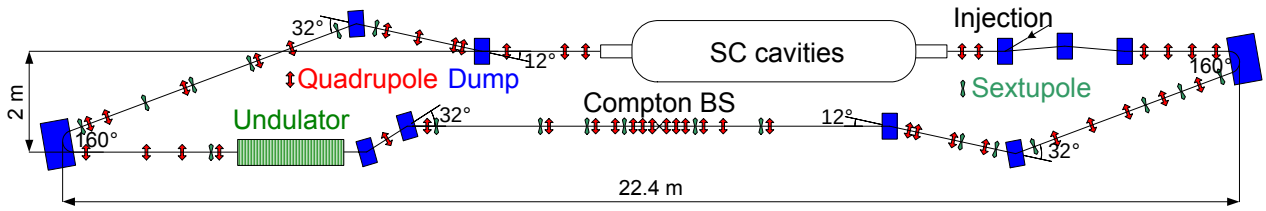

Figure 1. The layout of the ERL.

Abstract

A project of an ERL at Korea Atomic Energy Research Institute is described. The ERL will be connected to the existing machine without any modification. It consists of two 180° bents and two straight sections: one is for an FEL, another for a Compton X-ray source. One can choose the regime controlling the lenses. The total ERL is isochronous to avoid any problem with longitudinal beam instability. It will be possible to control both Sx and Sy transformation matrix elements independently to suppress longitudinal beam instability and allow the increase of beam current. Sextupoles will be installed in bents to suppress chromatic aberration. This design provides operation in FEL regime with high electron efficiency in the range of electron energies 12–22 MeV.

INTRODUCTION

At present time, a superconductive linear accelerator successfully operates at KAERI. It consists of an injector with injection energy 2 MeV, injection beamline, cryogenic accelerating module, which contains two cavities. Electron beam parameters are following:

- bunch duration: 100 ps;
- number of electrons per bunch: 10^{10};
- electron energy (full): 10 MeV;
- repetition rate: 5.6 MHz;
- emittance: 2π mm·mrad;
- energy spread (relative): $6 \cdot 10^{-3}$.

A future ERL based on this linac will be build at KAERI. An FEL and a Compton source will be driven by it. A project of the ERL should meet the following requirements:

- Accelerator should have two regimes, one for the FEL and the other for the Compton source. The regimes will be switched with magnets.
- The machine should operate in a wide energy range in order to provide broad band FEL retuning. The ERL will operate at the energy from 12 MeV up to 22 MeV.
- The possibility to control both S_x and S_y transport matrix elements independently and total isochronism of the ERL is necessary to suppress longitudinal and regenerative transverse beam instability. This possibility permits to increase the beam current and the FEL power.
- Low beam emittance degradation in the beamline is necessary for successful FEL operation and beam

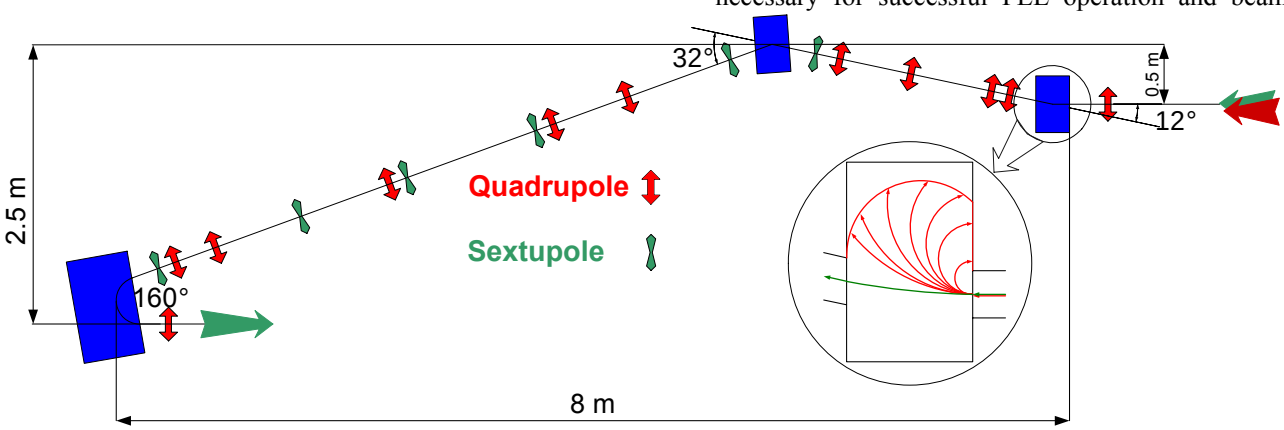

Figure 2. The layout of the first bent.

THE NIJMEGEN FEL, A FEL OSCILLATOR WITH HIGH SLIPPAGE

P.J.M. van der Slot*, E. van Geijn, K.J. Boller
Mesa+, Department of Applied Technology, University of Twente, Enschede, NL
J. Jalink, W.J. van der Zande, IMM, Radboud University Nijmegen, Nijmegen, NL

Abstract

The Nijmegen Free-Electron Laser (FEL) aims at producing narrow bandwidth radiation for high resolution spectroscopy in the THz regime. To this end, the radio frequency accelerator based FEL will produce a train of phase locked optical pulses. We use the Medusa1D code to simulate the performance of this system at various wavelengths and undulator lengths and estimate the power available in a single line of the phase locked spectrum.

INTRODUCTION

The High Field Magnetic Laboratory at the Radboud University Nijmegen, and other such laboratories worldwide, have made it possible to study molecules in materials in fields with strengths approaching 40 Tesla. All elementary excitation energies increase proportionally. As a consequence strong (> 100 W) and coherent radiation sources are needed from 100 μm to 1.5 mm, the so-called THz gap. Narrow bandwidth radiation is best suited for coherent, saturation, and pulse-echo studies. Pulsed intense radiation is best suited for non-linear and time-resolved studies. The parameters of the Nijmegen Free-Electron Laser (NijFEL) have been chosen to provide such a radiation source. An RF accelerator based electron source will provide short electron bunches creating a train of intense micropulses of picosecond duration. A narrow bandwidth, ($\Delta\lambda/\lambda \simeq 10^{-5}$), equals the generation of bandwidth limited pulses (BWL) of hundreds of nanosecond duration. This is achieved by ensuring that the micropulses in the macropulse are fully coherent, either using spontaneous coherence or forcing coherence using an intra-cavity interferometer. It is expected that spontaneous coherence is helped by using electron pulses with lengths comparable to the wavelength to be generated. This implies the design of a FEL oscillator with high slippage.

The zero design parameters to achieve this performance with NijFEL are shown in table 1, and fig. 1 shows the resonant wavelength of NijFEL as a function of the undulator parameter K for different values of the electron beam energy E_b. The ratio of the electron bunch length l_e to the slippage distance Δz_s ($= N_u\lambda$ at resonance) varies approximately from 0.015 to 0.3 depending on the actual number of undulator periods and wavelength used. The performance of the NijFEL system is therefore highly dominated by short pulse effects [1]. Because of the long wavelengths (see fig. 1), NijFEL will use a half open resonator that provides waveguiding between the poles of the undulator.

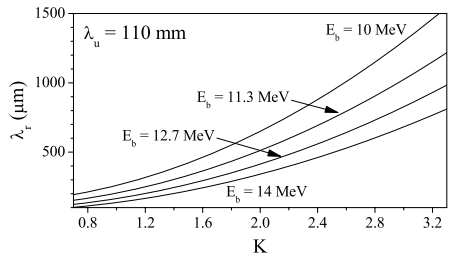

Figure 1: FEL resonant wavelength λ_r as a function of the undulator K parameter for different values of the electron beam energy E_b.

To determine the performance for various undulator lengths and wavelengths, we use the Medusa1d code. This code retains, in the 1d approximation, all the features of the 3D Medusa code [2, 3]. It includes a simple oscillator model where the the radiation output at the undulator's

Table 1: Zero design values for NijFEL. $L_u = N_u\lambda_u$ is the undulator length

Accelerator			
RF frequencye	f_{RF}	3	GHz
Bunch charge	Q_b	300	pC
micro pulse duration	t_p	3	ps rms
Beam energy	E_b	10-14	MeV
Emittance (norm.)	ϵ_n	50	mm mrad
Energy spread (rms)	$\Delta\gamma/\gamma$	0.25	%
Duration macropulse	T_m	10-12	μs
Rep. rate macropulses	f_{rep}	≤ 5	Hz
Undulator			
Period	λ_u	110	mm
K (rms)	K	0.7-3.3	
Number of periods	N_u	30-40	
Oscillator & radiation			
Wavelength	λ	0.1-1.5	mm
Final rel. bandwidth	$\Delta\lambda/\lambda$	10^{-5}	
Power (after filtering)	P_u	>100	W
Total roundtrip loss	α_L	5-20	%
Waveguide heigth	h	10	mm
Length	L_r	L_u+2	m

* p.j.m.vanderslot@tnw.utwente.nl

3D MODELLING OF THE ERLP IR-FEL

D.J. Dunning, N.R. Thompson and J.A. Clarke, ASTeC, STFC Daresbury Laboratory, UK.
B.W.J. M[c]Neil, SUPA, Department of Physics, University of Strathclyde, Glasgow, UK.

Abstract

The Energy Recovery Linac Prototype (ERLP) facility is currently being commissioned at Daresbury Laboratory. It serves as a testbed for technologies to be used in the proposed 4th Generation Light Source (4GLS) facility. As part of the ERLP facility, an infra-red oscillator FEL is due to be commissioned early in 2008. In this paper we present full three dimensional, time-dependent modelling of the ERLP IR-FEL using Genesis 1.3 in combination with a paraxial optical propagation code (OPC). We also discuss how this work will be used to inform commissioning of the FEL.

INTRODUCTION

The full details of the design for the ERLP IR-FEL are presented in [1] and summarised in Table 1 and a plan of the FEL is shown in Figure 1. Commissioning of the FEL is scheduled to begin early in 2008, and in preparation for this, full three dimensional modelling of the FEL has been carried out using Genesis 1.3 [2] in combination with a paraxial optical propagation code (OPC [3]). Both steady state and time-dependent simulations have been performed for three different modes of operation of the FEL. The results detailed in this paper will serve as a guide to the expected performance of the FEL during the commissioning period and will allow a comparison with experimental results so as to better inform FEL modelling for the 4GLS project.

Table 1: ERLP IR-FEL design parameters.

Parameter	Value
Wiggler period	0.027 m
Gap (fixed)	12 mm
Number of periods	40
Wiggler length	1.08 m
Deflection parameter, K	1.0
Nominal electron beam energy	35 MeV
Bunch charge	80 pC
Bunch length (rms)	<0.6 ps
Normalised emittance	10 mm-mrad
Energy spread (rms)	0.1 %
Optical cavity length	9.22438 m
Radiation wavelength (at 35 MeV beam energy)	4.394 μm

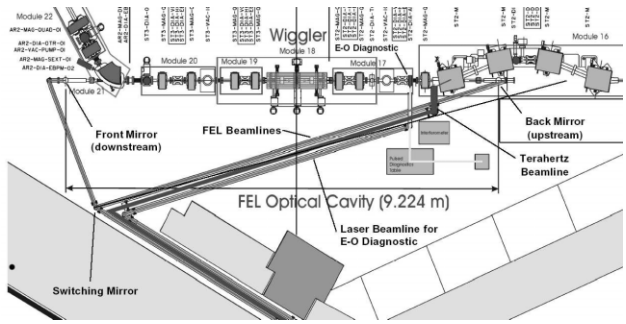

Figure 1: Plan of the FEL.

Operating Modes

The three proposed operating modes of the FEL are as follows: **normal mode**, **commissioning mode**, and **transmissive outcoupling mode**. A summary of the parameters for the different operating modes is given in Table 2. In transmissive outcoupling mode the electron bunch length is doubled, apart from this, the differences between different modes are in the mirror radii of curvature (ROC) and outcoupling method.

NORMAL MODE

The normal operating mode is designed to have maximum gain [4] and optimum output power. Details of this optimisation are included in the next section. The cavity is of a symmetric near-concentric design, of length $D = 9.22438$ m, with mirror ROC $R = 4.75$ m. The mirror angular alignment tolerance is $\ll 76$ μrad. Outcoupling is via a 1.5 mm radius hole in the downstream mirror, giving a 12 % outcoupling fraction (chosen to maximise the output power).

The optical mode radius at the centre of the wiggler is $w_0 = 1.04$ mm. At this location the matched electron beam radii are $\sigma_x = 0.24$ mm and $\sigma_y = 0.30$ mm. The electron beam jitter (in transverse position) is expected to be no more than 10 % of the beam radius. This means that the jitter in electron beam position is no greater than 3 % of the optical mode size and ensures the coupling between electrons and radiation is near-optimal. The optical mode radius on the mirror surface, assuming the fundamental transverse mode TEM_{00} is $w_{mirror} = 6.15$ mm compared to a mirror aperture radius of $a = 19$ mm. The ratio $a/w_m \approx 3{:}1$: this is large enough to ensure that diffraction losses from the fundamental mode are minimal. All higher order transverse modes are wider, and will therefore suffer more diffraction loss - this is advantageous because it encourages lasing at the fundamental mode. In effect the limited mirror aperture acts as a crude method of transverse mode control.

THE IR-BEAM TRANSPORT SYSTEM FROM THE ELBE-FELs TO THE USER LABS

W Seidel, E rosse, M ustus, -W Leege, Proehl, R Schlenk, A Winter, Wohlfarth, R Wuensch
Forschungszentru resden-Rossendorf, resden, er any

Abstract

In the Forschungszentru resden-Rossendorf, two free-electron lasers FELs have been put into operation They produce laser light in the ediu and the far infrared wavelength range 4-150 μ The IR ligh is transported to several laboratories in the sa e building and to the adjacent building of the High Magnetic Field Laboratory as well, where the e peri ental setups are up to 70 away fro the FELs Constructional peculiarities, the large wavelength range, the high average power in cw regi e, and the bea property re uire ents of the users pose a challenge to the bea line design The transport syste includes vacuu pipes, diagnostic ele ents, plane and toroidal gold-covered copper irrors, and e it windows The designed transport syste produces a bea waist at selected spots in each laboratory representing a agni ed i age of the outcoupling hole Spot size and position are independent of the wavelength

INTRODUCTION

The Radiation Source ELBE 1 at the Forschungszentru resden-Rossendorf is centered around a superconducting Electron Linear accelerator of high Brilliance and low E ittance ELBE , constructed to produce cw electron bea s up to 1 A bea current at 12-34 Me The electron bea is used to generate various kinds of secondary radiation, ainly to drive two free-electron lasers in the infrared region 4-150 μ Starting in the su er 2005, bea ti e is offered to e ternal users in the fra e of the EC funded Integrating Activity on Synchrotron and Free Electron Laser Science FELBE project 2

The IR radiation is produced in one of the two hybrid ag-net undulators U27 and U100 Changing the undulator gap or the electron energy the wavelength of the produced IR bea can be varied fro 4 to 22 μ U27 and fro 20 to 150 μ U100 Additionally, a 633 n bea fro a HeNe laser used for irror align ent has to be transported by the bea line

The outcoupled laser power to be transported by the bea line depends strongly on the para eters of the electron bea and of the FEL undulator and resonator Till now a a i u average cw power of 25 W has been obtained Theoretical esti ates predict a a i u cw power of about 35 W

The IR light is transported to several laboratories in the sa e building and to the adjacent building through a tunnel which is 27 long of the resden High Magnetic Field Laboratory HL , 3 as well, where the e peri-ental setups are up to 70 away fro the FELs

The bea arriving at the user laboratories should be sufciently narrow a few illi eters Its Rayleigh range should be long enough 10 c at ini u The pro le should be circular with a aussian shape It should not vary to uch with the wavelength, with the size of the outcoupling hole and the used FEL Linear polarization in horizontal or vertical direction should be conserved

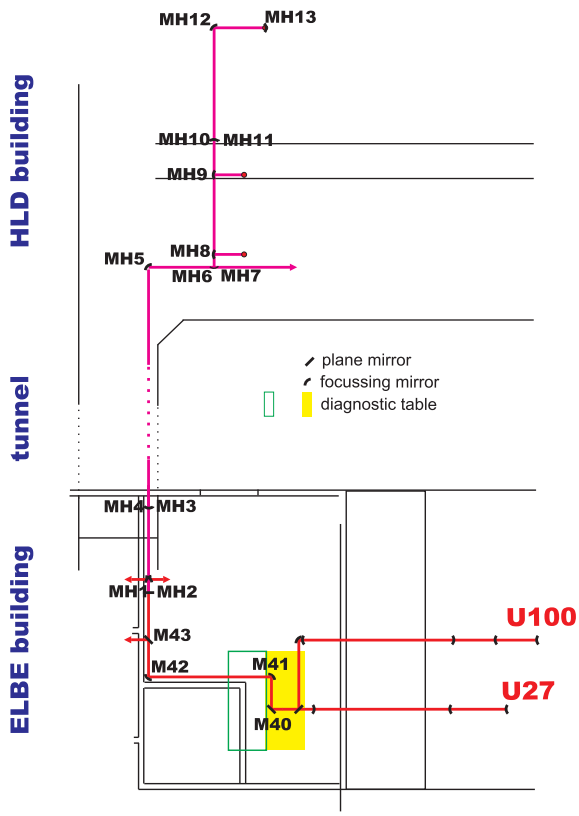

Figure 2 Top view of the bea line fro the U100 and U27 FEL in the ELBE building to the user station in the HL building via diagnostic table and tunnel

DESCRIPTION OF THE BEAM LINE

The designed bea line is able to transport IR light in the wavelength range between 4 and 200 μ without noticeable diffraction and absorption losses The HeNe adjust ent bea is visible in the whole transport syste To avoid the absorption of IR light in the a bient air the bea is guided in pipes which are either evacuated or purged with

THERMAL AND NON-THERMAL LASER CUTTING UTILIZING ADVANCED INDUSTRIAL LASERS AND ERL-FELS *

Eisuke J. Minehara,
JAEA, 2-4 Shirakata-shirane, Tokai, Naka, Ibaraki 319-1195, JAPAN.

Abstract

The JAEA and JLAB energy-recovery IR free-electron lasers (ERL-FEL) have successfully demonstrated their capabilities of a sub ps pulse, high efficiency, GW high peak power, kW average power, and wide tunability. Utilizing the high power FEL and ERL technologies, we could realize a more powerful and more efficient FEL than 20kW and 25%, respectively, for nuclear industry, pharmacy, medical, defense, shipbuilding, semiconductor industry, chemical industries, environmental sciences, space-debris cleaning, power beaming and so on very near future. We have performed their thermal and non-thermal cutting experiments using advanced industrial lasers like fiber, and water-jet guided ones and the ERL-FELs, and have characterized them according to their resultant effects.

INTRODUCTION

Two nuclear power plants of the 166MW Tokai power station and 165MW Fugen power stations have been prepared and partially started to decommission in Japan recently. The Tokai power station is the first nuclear power plant for commerce in Japan and decommissioning of the Tokai power station is the first project of the nuclear power plant for commerce in Japan. The Fugen is the advanced thermal reactor prototype using heavy water moderator, light water cooling, and dense piping structure in the core. Feasibility studies of laser cutting are discussed here to compare a few kinds of commercially-available advanced industrial lasers and ERL-FELs with each other.

The currently-available CW lasers like CO_2, YAG, and fiber lasers are widely used to cut, to drill and to peel-off the material sheet, rod, and pipes of stainless steel, zirconium alloy, and others in the power plants, factories and laboratories. Cutting mechanisms of all the lasers listed above to machine the materials are blown off or burn out the melted one by feeding the assisting gases of highly-pressurized inert gases and oxidation gases like N2, O_2 and others. Therefore, we can easily expect that there are some intrinsic difficulties to cut, to drill and to peel-off the materials wherever and whenever we cannot feed either one of the laser power and pressurized gases to the machining point. We can cut the stainless steel sheet at the speed of 10 meter per minute or even the higher one whenever we can feed enough amounts of the laser power and gas at the cutting point. Double-layered, and multi-layered sheets, and rod and pipe bundles are intrinsically difficult to cut completely using the mechanism discussed here and all the lasers being commercially-available in the world. Therefore, we have to give up cutting the layered sheets and bundles at once simply using the mechanism and all the lasers. We can only cut the layered sheets layer by layer, and bundles step by step after removal of the cut layer, cut rod, and cut pipe as long as we will use all the commercially-available lasers. The layer by layer and step by step cutting with all the lasers is not so quick enough to decommission the power station facilities. There is no commercially-available sub-ps or a few ps ultra-fast, GW peak power, kW average power free-electron lasers [1] to cut the multi-layered and bundled structures at once. As they have been under development over last 10 years, they will be commercially available next 10 years.

ADVANCED INDUSTRIAL LASERS

The figures 1 and 2 show the fiber laser device and cut sample as one of the typical industrial laser examples.

Figure 1: 1 to 50kW CW Ytterbium fiber lasers are manufactured by IPG Photonics. A typical example of the commercially-available advanced industrial CW lasers.

*Work supported by in part by Grants-in-Aid for Scientific Research (A19206103).
minehara.eisuke@jaea.go.jp

PRELIMINARY DESIGN OF THE PROPOSED IR-FEL IN INDIA

Srinivas Krishnagopal*, Vinit Kumar
RRCAT, Indore, M.P. 452013, India

Abstract

We discuss preliminary design studies of an infrared (IR) free-electron laser (FEL) proposed to be built at the Raja Ramanna Centre for Advanced Technology (RRCAT). The design calculations and optimisations have been performed using the three-dimensional time-dependent oscillator code GINGER [1].

INTRODUCTION

A terahertz free electron laser, the CUTE-FEL, designed to lase around a wavelength of 80 μm using a 10 MeV linac is in an advanced stage of construction at RRCAT [2]. In the next step in our FEL activities, we have proposed to build an IR-FEL. In this context, we have performed design studies of an IR FEL to lase between 12-50 μm, which will use a 15-25 MeV linac. In this paper, we focus mainly on 30 μm simulations and briefly discuss the results at 12.5 μm and 50 μm also. The high power, short pulse and widely tunable coherent radiation from this IR-FEL can be used for performing a wide range of interesting research applications that include experiments on direct as well as indirect band-gap semiconductors, IR microscopy of biological samples, multi-photon dissociation experiments, isotope separation, reaction dynamics studies, etc.

In the next section, we discuss the basic design considerations and then in the following section, we discuss design simulation results. We finally conclude in the last section.

DESIGN CONSIDERATIONS

After preliminary consultaions with users, we found that a wavelength range of 12-50 μm is interesting for a wide range of many interesting experiments. Using a 15-25 MeV electron beam from an electron linac, and an undulator having period (λ_u) of 40 mm and undulator parameter K in the range 1-2, it should be possible to cover this wavelength range, as can be seen from the following formula:

$$\lambda_R = \frac{\lambda_u}{2\gamma^2}(1 + \frac{K^2}{2}), \tag{1}$$

where λ_R is the radiation wavelength, γ is the electron energy in units of its rest mass energy and $K = eB_u\lambda_u/2\pi mc$, B_u is the peak undulator field, m is the rest mass of electron and c is the speed of light. Note that we have chosen maximum value of $K = 2$ such that we get a wavelength tunability up to a factor of two by varying K in the range 1-2. We will use a Halbach configuration of pure permanent magnets for the undulator, where the dependence of peak magnetic field on the gap g between the jaws of the undulator is given by[3]

$$B_u = 1.43B_r \exp(-\pi g/\lambda_u). \tag{2}$$

Here B_r is the remanent field of the permanent magnet used in the undulator. Using B_r = 1.2 T for NdFeB magnets, we obtain the gap to be 15 mm for $K = 2$. We therefore will need to use an undulator vacuum pipe having inner diameter (ID) of 11 mm.

The number of undulator periods N_u is chosen to be 60 on the basis of gain considerations. The 2.4 m long undulator will be immersed in a 4.1 m long optical cavity. The undulator will be asymmetrically placed in the optical cavity such that we have 1.05 m of space available for beam transport and diagnostic on the upsteam side and 0.65 m of space available on the downstream side. Assuming a Rayleigh range of 0.8 m, which is one third of the undulator length, the rms optical beam size at the waist is 1.4 mm. We therefore chose the rms electron beam horizontal size σ_x at the waist to be around 1 mm for good overlap with the optical beam. The rms electron beam size σ_y in the vertical direction is taken to be the matched beam size in the undulator given by [3]

$$\sigma_y = \sqrt{\frac{\epsilon_n\lambda_u}{\sqrt{2}\pi K}}, \tag{3}$$

where ϵ_n is the normalized rms electron beam emittance. We choose ϵ_n = 30 mm-mrad for our design calculation.

For the electron beam, we will use a micropulse charge in the range 0.2-0.5 nC. The electron beam rms pulse width is taken to be 4 ps and the relative rms energy spread is taken to be 0.5%. These parameters are easily acheivable. In the next section, we present the results of design simulations.

DESIGN CALCULATIONS

For performing the design simulations, we have used the FEL code GINGER [1], a multidimensional [full 3D for macroparticles and 2D ($r - z$) for radiation], time-dependent code to simulate the FEL interaction in single-pass amplifier as well as oscillator configurations. GINGER utilizes the KMR [4] wiggle-period-averaged electron-radiation interaction equations and the slowly-varying envelope approximation (SVEA) in both time and space for radiation propagation. For propagation outside the undulator for oscillator problems, the code uses a Huygens integral method. Shot noise is modeled by giving a controlled amount of randomness to the initial longitudinal

* skrishna@cat.ernet.in

SHORT WAVELENGTH REGENERATIVE AMPLIFIER FREE-ELECTRON LASERS

N. R. Thompson and D. J. Dunning, ASTeC, Daresbury Laboratory, Warrington WA4 4AD, UK*
B. W. J. M^{c}Neil, SUPA, University of Strathclyde, Glasgow G4 0NG, UK

Abstract

In this paper we discuss extending the operating wavelength range of tunable Regenerative Amplifier FELs to shorter wavelengths than current design proposals, notably into the XUV regions of the spectrum and beyond where the reflectivity of broadband optics is very low. Simulation studies are presented which demonstrate the development of good temporal coherence in generic systems with a broadband radiation feedback of less than one part in ten thousand.

INTRODUCTION

A regenerative amplifier free-electron laser (RAFEL) is a high-gain resonator FEL which achieves saturation in a few round-trips of the radiation in a high-loss, and hence low feedback, optical cavity. Because the radiation feedback fraction is low it is feasible that the use of low reflectivity optics in the resonator makes the RAFEL a candidate for short wavelength operation [1]. Several RAFEL proposals have been made in the VUV [2, 3] and X-ray [4] and some experimental results obtained [5, 6].

There are several expected advantages of the RAFEL over other types of FEL. The RAFEL should be less sensitive to radiation-induced mirror degradation than a low gain oscillator FEL, and the small number of passes required to reach saturation should relax the longitudinal alignment tolerances. The optical feedback also allows the undulator length to be reduced compared to a Self Amplified Spontaneous Emission (SASE) FEL, and it is expected that because of the feedback a RAFEL source can deliver higher quality and more stable pulses than a SASE FEL.

The properties of the transverse modes within the cavity differ from those of a low-gain oscillator FEL. Because of the high loss of the resonator the radiation is not stored over many passes, and because of the high-gain of the FEL the radiation does not propagate freely within the cavity but experiences gain guiding. The cavity's primary function is to return a small field to the start of the undulator to seed the interaction with the subsequent electron bunch. For these reasons it is equally valid to refer to a RAFEL as a High-Gain Self-Seeding Amplifier FEL.

In this paper we present 1D modeling results for a system with a very low feedback factor that returns only $\sim 10^{-5}$ of the undulator output. Such low feedback may occur when mirror reflectivities are very poor, for example into the XUV and x-ray regions of the spectrum. The results are encouraging and suggest that, in principle, a low feedback RAFEL may prove a viable source at these photon energies.

* n.r.thompson@dl.ac.uk

A GENERIC HIGH-GAIN RAFEL

We now consider a generic high gain system shown schematically in Fig. 1 and investigate the properties of such a system when the feedback fraction is reduced to very low levels. First we optimise the feedback fraction using two criteria—the output power and the pulse temporal coherence should both be maximised. We work in the units of the universal scaling [7] where $\bar{z} = z/l_g$ and $l_g = \lambda_w/4\pi\rho$ is the nominal gain length, with λ_w the undulator period and ρ the FEL parameter.

It can be shown from [8] that the electron beam equivalent shot-noise power is:

$$|A_0|^2 \approx \frac{6\sqrt{\pi}\rho}{N_\lambda\sqrt{\ln\left(N_\lambda/\rho\right)}}, \tag{1}$$

where N_λ is the number of electrons per radiation wavelength. In the exponential gain regime the radiation intensity after a single pass through an undulator of scaled interaction length $\bar{z}$ is then given by

$$|A_1|^2(\bar{z}) \approx \frac{|A_0|^2}{9}\exp(\sqrt{3}\bar{z}) \tag{2}$$

and after returning a fraction F of the output power to the start of the undulator, via some as yet undefined optical system, the seed power at the start of the second pass is $F \times |A_1|^2$. The necessary condition for the development of longitudinal coherence is that this seed power is greater than the shot noise power, i.e.

$$F \times |A_1|^2 > |A_0|^2.$$

A feedback factor criterion to dominate the shot noise can then be defined as:

$$F_N > 9\exp(-\sqrt{3}\bar{z}). \tag{3}$$

The feedback factor necessary to optimise the output power in the steady state regime only has been determined from 1D simulations, with the results shown in Fig. 2. A fit to the numerical data, valid over the range $3 \leq \bar{z} \leq 12$, gives

$$F_P \approx 25\exp(-\sqrt{3}\bar{z}). \tag{4}$$

It is seen from comparison of (3) and (4) that $F_P \simeq 3F_N$ implying that optimising feedback to maximise the output power will necessarily prove sufficient to dominate the

NUMERICAL SOLUTION OF THE FEL CORRELATION FUNCTION EQUATION

O.A. Shevchenko[#], N.A. Vinokurov,
Budker Institute of Nuclear Physics, 11 Acad. Lavrentyev Prosp., 630090, Novosibirsk, Russia

Abstract

The equation for two-particle correlation function in FEL was derived recently to provide a new way of noise calculations in SASE FELs [1]. In this paper this equation is solved numerically for the simplest case of narrow electron beam. Time independent solution with saturation is obtained. It is compared with the results of quasilinear theory and results of previous SASE linewidth estimates.

INTRODUCTION

High gain FELs operated in SASE mode are considered now as one of the most perspective high-brightness radiation source in the x-ray region. Therefore it is very important to know the radiation properties of such FELs. Parameters of radiation in a single shot are determined by the shot noise in the beam current which has stochastic nature. Because of that these parameters fluctuate from shot to shot and they can not be determined without exact solution of the particle motion and Maxwell equations. On the other hand the parameters averaged over many shots can be found by the methods of statistical mechanics.

The statistical approach has been treated by many authors but usually it was limited to the linear case when one can introduce the Green function and the averaging becomes straightforward [2,3]. Some authors considered the averaged results of simulations obtained by macroparticle based codes [4]. But in this case it is not evident that artificially constructed initial distribution of macroparticles leads to correct results at saturation stage.

The regular nonlinear approach to the start-up from noise has been proposed in [1]. It is based on the BBGKY set of equations which is truncated to two equations for single-particle distribution function and two-particle correlation function. In this paper we obtain the numerical solution of these equations for the simplest model of narrow beam comprised of charged disks with Gaussian transversal charge distribution.

BASIC EQUATIONS

In the case of the charged disks model the equations (4-5) of [1] for the single-particle distribution function and two-particle correlation function have the following form:

$$\left(\frac{\partial}{\partial\theta}+\nu_1\frac{\partial}{\partial z_1}\right)F(1,\theta)=-N\int d\{2\}\Phi(1,2)\frac{\partial}{\partial\Delta_1}G(1,2;\theta) \qquad (1)$$

$$\left(\frac{\partial}{\partial\theta}+\nu_1\frac{\partial}{\partial z_1}+\nu_2\frac{\partial}{\partial z_2}\right)G(1,2,\theta)=-N\frac{\partial F(1)}{\partial\Delta_1}\int\Phi(1,3)G(2,3,\theta)d\{3\}-$$
$$-N\frac{\partial F(2)}{\partial\Delta_2}\int\Phi(2,3)G(1,3,\theta)d\{3\}-\left(\Phi(1,2)\frac{\partial}{\partial\Delta_1}+\Phi(2,1)\frac{\partial}{\partial\Delta_2}\right)F(1)F(2) \qquad (2)$$

where $(i)=(z_i,\Delta_i)$, $d\{i\}=dz_i d\Delta_i$, $\nu_i=(1+2\Delta_i)$, Δ_i - relative electron energy deviation, z_i - electron longitudinal coordinate in undulator, N - number of electrons in the beam, $\theta=2\gamma_\parallel^2(t-z),(c=1)$ - "time" variable and $\gamma_\parallel$ - relativistic factor of electron longitudinal motion. The longitudinal interaction force $\Phi(1,2)$ can be determined from eq. (6) of [1]. In the considered model it should be averaged over transversal distribution:

$$\langle\Phi(1,2)\rangle_\perp=-\frac{r_e}{2\sigma^2k_w\gamma}\frac{K^2}{1+K^2}\left(\frac{e^{ik_w(z_1-z_2)}}{1+i\alpha k_w(z_1-z_2)}+c.c.\right) \qquad (3)$$

here σ is r.m.s transversal beam size, r_e - classical electron radius, $\alpha=1/2k_0k_w\sigma^2$ - small dimensionless parameter which characterizes the beam "thickness", k_0 - radiation wave number and k_w - undulator wave number. We assume that undulator has constant deflection parameter K and helical symmetry.

From this point we shell consider stationary case, therefore the time derivative in Eq. (1-2) can be omitted and N should be replaced by the number of electrons per unit of length. In this case the single-particle distribution function has to be renormalized the following way:

$$\int\nu_1F(z_1,\Delta_1)d\Delta_1=1$$

To eliminate the fast oscillating terms it is convenient to introduce the slow varying complex amplitude $\tilde{G}$ of the correlation function:

$$G(z_1,\Delta_1;z_2,\Delta_2)=2\,\mathrm{Re}\left(\tilde{G}(z_1,\Delta_1;z_2,\Delta_2)e^{i(z_1-z_2)}\right) \qquad (4)$$

Here we have replaced k_wz_i by dimensionless variable z_i. Substituting (4) into (1-2) and neglecting fast oscillating terms we obtain the final system of equations:

[#]O.A.Shevchenko@inp.nsk.su

NUMERICAL PROPAGATION SIMULATIONS AND COHERENCE ANALYSIS OF SASE WAVEFRONTS*

O. Chubar#, M.-E. Couprie, F. Polack, SOLEIL, 91191 Gif-sur-Yvette, France
M. Labat, G. Lambert, O. Tcherbakoff, CEA, DSM/SPAM, 91191 Gif-sur-Yvette, France

Abstract

Examples of wavefront propagation simulation and coherence analysis of Self-Amplified Spontaneous Emission (SASE), seeded and started-up from noise, are presented. The calculations are performed using SRW – the wave-optics computer code optimized for Synchrotron Radiation (SR), and the 3D FEL simulation code GENESIS. To ensure easy inter-operation and data exchange between the two codes, GENESIS has been integrated into the "emission" part of the SRW, which is dedicated for calculation of initial wavefronts in the form ready for subsequent propagation simulations. After each run of GENESIS in time-dependent mode, the resulting electric field is transformed from time to frequency domain, and the wavefront obtained this way is numerically propagated, using Fourier-optics methods implemented in SRW, from the exit of FEL undulator to a destination plane of a beamline containing several optical elements separated by drift spaces. Interferometer-type optical schemes, which allow for "probing" spatial and temporal coherence of SASE wavefronts, are used in the examples. Intensity distributions of the propagated radiation are extracted and analysed in time and frequency domains. The presented examples show that the SRW code can be used for optimization of optical beamlines for 4th generation synchrotron radiation sources, which require accurate treatment of wave-optical phenomena in frequency and time domains.

INTRODUCTION

Synchrotron Radiation emitted by relativistic electrons in magnetic fields of storage ring sources of the 3rd generation is a proven tool for research in many areas of science, from physics and chemistry to biology and medicine. An outstanding feature of the SR is a very broad emission spectrum extending from far infrared to hard X-ray range. Besides, undulator-based 3rd generation SR sources offer relatively high average spectral flux, brightness and degree of spatial coherence of the output radiation, and a possibility to use this radiation simultaneously for various experiments at a large number of beamlines.

The new emerging sources of the 4th generation – free-electron lasers and energy-recovery linacs – extend the domain of SR applications to time-resolved research, by providing femtosecond and, prospectively, even attosecond time scale pulses of radiation with extremely high peak brightness [1, 2].

To fully exploit all great SR features in the 3rd and 4th generation sources, high-accuracy simulation tools for the processes of emission and wavefront propagation through various optical elements of a beamline should be used. In the frame of classical electrodynamics, such simulation tools, dedicated both for the emission and propagation parts, would operate with 3D electric field of radiation [3]. Whereas this requirement seems absolutely natural for the emission part, it is much less evident for the propagation, where simple geometrical optics based approximation exists and is extensively (and successfully) used for incoherent sources and systems dominated by optical aberrations. Nevertheless, with decrease of electron beam emittance in storage rings [4] and continuous progress in the quality of optical elements [5-7], the radiation gradually approaches diffraction limit for shorter and shorter wavelengths, making physical-optics approaches to simulation of wavefront propagation increasingly important.

Two physical-optics based approaches to wavefront propagation simulation are currently popular: Fourier optics [8] and asymptotic expansions (mainly, the stationary phase method) [9, 10]. This paper deals with the Fourier optics approach, as it is implemented in the SRW computer code [11, 12].

The following are proven "strong points" of the Fourier optics method:

- very high CPU efficiency;
- possibility to take into account multiple diffractive/ refractive/ reflective optical elements in "uniform" way without any increase of the overall complexity;
- stability in case of "noisy" wavefronts (these methods are extensively used for simulation of scattering);
- availability of large amount of data on electric field after only one propagation pass.

Among "weak points" of this method one can mention:

- large amount of memory required for "standard" near-field propagator through free space, and
- poor accuracy of the "thin" element approximation for simulating grazing incidence optics and/or optics with very wide angular apertures.

We note that for the 3rd generation sources, it is often enough to simulate wavefront propagation through a beamline only in frequency domain – at one central or eventually at several different frequencies / photon energies. On the other hand, the 4th generation sources require a combined frequency- and time-domain analysis because of the necessity to preserve (or at least to keep track of) temporal characteristics of propagating wavefronts. To profit of CPU efficiency of the Fast Fourier Transforms (FFT), which are used by the free-space propagator and at changing the electric field representation between the frequency and time domains, it is preferable to keep in memory at each step of

*Work supported by EuroFEL
#oleg.chubar@synchrotron-soleil.fr

IMPACT OF LONGITUDINAL SPACE-CHARGE WAKE FROM FEL UNDULATORS ON CURRENT-ENHANCED SASE SCHEMES

G. Geloni, E. Saldin, E. Schneidmiller and M. Yurkov
Deutsches Elektronen-Synchrotron (DESY), Hamburg, Germany

Abstract

We present a description of longitudinal wake fields in XFELs that is of relevance in relation with Enhanced Self-Amplified Spontaneous Emission (ESASE) schemes. We consider wakes in XFELs, in the limit when the electron beam has gone inside the undulator for a distance longer than the overtaking length (the length that electrons travel as a light signal from the tail of the bunch overtakes the head of the bunch). We find that the magnitude of the resulting energy chirp constitutes a reason of concern for the practical realization of ESASE schemes. **A more detailed report of our study is given in [1]**.

INTRODUCTION

This article presents a description of longitudinal wake fields in XFELs. Our study is of importance in connection with ESASE schemes, demanding for a detailed study of longitudinal wake fields arising after the dispersive section. For XFEL setups, the undulator parameter K obeys $K^2 \gg 1$. As a result, the average longitudinal Lorentz factor $\bar{\gamma}_z = \gamma/\sqrt{1+K^2/2}$ is such that $\bar{\gamma}_z^2 \ll \gamma^2$, γ being the Lorentz factor of the beam. Based on $\bar{\gamma}_z^2 \ll \gamma^2$, we demonstrate that the presence of the undulator strongly influences the space-charge wake. In contrast to this, in literature, wake calculations for the LCLS case are given in free-space, as if the presence of the undulator were negligible. In this paper we pose particular attention to the LCLS case, for which ESASE schemes have been first proposed. We thus restrict our attention to a specific region of parameters. First, the longitudinal size of the beam is much larger than the FEL wavelength, i.e. $\sigma_z \simeq \lambda \gg \lambda_r$. Second, we assume a long saturation length compared with the overtaking length, i.e. $L_s \gg 2\bar{\gamma}_z^2\lambda$. Third, effects of metallic surroundings can be neglected, i.e. $a \gg \bar{\gamma}_z\lambda$. We present a general theory based on these three assumptions. These are satisfied for the LCLS case, together with an extra-assumption on the transverse electron-beam size $\sigma_\perp$: $\sigma_\perp^2 \gg \lambda\lambda_w$, λ being the reduced wavelength. Due to this last condition, major simplifications arise in the general theory. Radiation from the undulator is drastically suppressed and calculations of impedance and wake function can be performed considering a non-radiating beam, and thus accounting for space-charge interactions only. Space-charge impedance and wake function is found to reproduce the free-space case. Only, γ must be consistently substituted with $\bar{\gamma}_z$. We apply our theory to the ESASE setup referring to the LCLS facility. We calculate the energy chirp associated with wakes inside the undulator and between dispersive section and undulator. Subsequently, the magnitude of their effect is estimated by calculating the linear energy chirp parameter. We find that the gain of the FEL process is sensibly reduced, and that longitudinal wake fields constitute a reason of concern regarding the practical realization of ESASE schemes.

FIELD CALCULATION

Calculation of longitudinal wake field and impedance from an FEL undulator first demand characterization of the electric field generated at a given position by the bunch. We perform an analysis in terms of harmonics, i.e. $\vec{E} = \vec{E}(\vec{r},\omega)\exp[-i\omega t] + C.C.$, the symbol "C.C." indicating complex conjugation[1]. The complex amplitude $\vec{E}(\vec{r},\omega)$ can be considered as the electric field in the space-frequency domain, "the field". Transverse and longitudinal fields can be found by solving paraxial Maxwell's equation in the space-frequency domain: $\mathcal{D}[\vec{\bar{E}}(z,\vec{r}_\perp,\omega)] = \vec{g}(z,\vec{r}_\perp,\omega)$. Here $\vec{\bar{E}}_\perp = \vec{E}_\perp \exp[-i\omega z/c]$ is the electric field envelope that does not vary much along z on the scale of the reduced wavelength $\lambda = \lambda/(2\pi)$. The differential operator $\mathcal{D}$ is defined by $\mathcal{D} \equiv (\nabla_\perp{}^2 + (2i\omega/c)\cdot\partial/\partial z), \nabla_\perp{}^2$ being the Laplacian operator over transverse cartesian coordinates. The source-term $\vec{g}(z,\vec{r}_\perp)$ is specified by the trajectory of the source electrons, and can be written in terms of the Fourier transform of the transverse current density, $\vec{\bar{j}}(z,\vec{r}_\perp,\omega)$, and of the charge density, $\bar{\rho}(z,\vec{r}_\perp,\omega)$, as $\vec{g} = -4\pi\exp[-i\omega z/c](i\omega/c^2\vec{\bar{j}} - \vec{\nabla}\bar{\rho})$. Thus, we recognize current and gradient terms in the field. Here $\vec{\bar{j}}$ and $\bar{\rho}$ are regarded as given data. They will be treated as macroscopic quantities, and can be written as $\bar{\rho}(\vec{r}_\perp,z,\omega) = \rho_o(\vec{r}_\perp - \vec{r}'_{o\perp}(z))\bar{f}(\omega)\exp[i\omega s_o(z)/v_o]$ and $\vec{\bar{j}} = \vec{v}_o\bar{\rho}$. Here $f(\omega)$ is the Fourier transform of the longitudinal bunch-profile, while ρ_o is related with the transverse bunch-profile. $\vec{r}'_{o\perp}(z)$, $s_o(z)$ and v_o pertain a reference electron with Lorentz factor γ that is injected on axis with no deflection and is guided by the undulator field only. In particular, $r'_{ox}(z) = r_w\cos(k_w z)$ and

[1]For simplicity we will consider $\omega > 0$. Expressions for the field at negative values of ω can be obtained based on the property $\vec{E}(-\omega) = \vec{E}^*(\omega)$ starting from explicit expressions for $\vec{E}$ at $\omega > 0$.

SPACE CHARGE EFFECT IN AN ACCELERATED BEAM *

Stupakov and Huang
Stanford Linear Accelerator Center, Stanford University, Stanford, CA 94309

Abstract

It is usually assu ed that the space charge effects in relativistic bea s scale with the energy of the bea as γ^{-2}, where γ is the relativistic factor We show that for a bea accelerated in the longitudinal direction there is an additional space charge effect in free space that scales as E/γ, where E is the accelerating eld This eld has the sa e origin as the electro agnetic ass of the electron discussed in te tbooks on electrodyna ics We then consider the effect of this eld on a bea generated in an RF gun and calculate the energy spread produced by this eld in the bea

INTRODUCTION

Modern light sources such as free electron lasers and energy recovery linacs re uire high-peak current, s alle ittance bea s One of the i portant characteristics of such a bea is its energy spread It deter ines the li its of a possible bunch co pression, the stability against i crobunching, and properties of the bea as a radiator of photons There are several echanis s that contribute to the energy spread in radio fre uency electron guns with the do inant one, for nanocoulo b bunches, being the space charge effect

Traditionally in accelerator physics the space charge effect is co puted as a self eld of a bea oving with constant velocity along a straight line The longitudinal eld in such a bea causes the energy e change between the particles it typically scales with the bea energy as γ^{-2} 1, p 128 , where γ is the relativistic factor, and usually beco es s all for highly relativistic bea s In a broader sense, the space charge effect ight be understood as a self eld of the bea , even when it oves with acceleration With this understanding, acceleration adds to the bea self eld One such contribution, that attracted a lot of attention lately, is due to the coherent radiation of the bea and is called the coherent synchrotron radiation wake or CSR wake 2 The CSR wake is the radiation reaction force that keeps balance between the electro agnetic energy that is carried away by the radiation and the kinetic energy of the bea particles It occurs when the bea is being accelerated in the direction perpendicular to the bea velocity in bending agnets or undulators

Another type of radiation reaction force has been considered in recent papers 3, 4 it is a self eld that arises inside the bea during a violent longitudinal acceleration Such a eld can play a role in plas a acceleration e perients, where the pace of acceleration is uch larger than in a conventional RF cavities

In this paper we point out to a new co ponent of the space charge eld that arises during longitudinal acceleration of the bea We assu e that the acceleration is not strong enough to cause a noticeable radiation What it does, however, it changes the velocity of the bea Because the bea electro agnetic eld depends on how fast it oves, the electro agnetic energy of the bea eld changes during acceleration Si ilar to the case of a converging bea , one should e pect an additional co ponent of the self eld that keeps balance between the bea and the eld energy We call this eld the *acceleration field* Being proportional to the acceleration, on average, it is e uivalent to a renoralization of the ass it is discussed in te tbooks on electrodyna ics in connection with a so called electro agnetic ass of a point charge 5, 6 In this paper we are interested in the spatial distribution of the eld and, ore speci cally, the energy spread in the bea induced by the acceleration eld

The odel that we consider in this paper assu es that the bea does not change its shape during the acceleration We neglect a co ponent of self eld that is associated with the converging or diverging bea s see 7 and references therein

ENERGY OF ELECTROMAGNETIC FIELD OF A MOVING GAUSSIAN BUNCH

Consider a aussian bunch of charged particles oving with velocity v in the z direction with the particle distribution function given by

$$n(x,y,\zeta)=\frac{N}{(2\pi)^{3/2}\sigma_z\sigma_\perp^2}\exp\left(-\frac{r^2}{2\sigma_\perp^2}-\frac{\zeta^2}{2\sigma_z^2}\right), \quad 1$$

where N is the nu ber of particles in the bunch, $r=\sqrt{x^2+y^2}$, $\zeta=z-vt$, $\sigma_x=\sigma_y=\sigma_\perp$ is the r s bunch size in the transverse direction, and σ_z is the r s bunch length in the longitudinal direction The electro agnetic eld of such a bunch can be calculated using the Lorentz transfor ation fro the bea fra e, see, e g , 8 The integrated electro agnetic energy over the whole space

$$W=\int\frac{E^2+H^2}{8\pi}dV\,, \quad 2$$

grows with γ, as shown in Fig 1 Note that this energy tends to in nity when $\gamma\to\infty$ As a detailed analysis shows, at $\gamma\gg1$ the asy ptotic e pression for W is

$$W=\frac{Q^2}{\sqrt{\pi}\sigma_z}\log\gamma\,, \qquad \gamma\gg1\,. \quad 3$$

* Work supported by epart ent of Energy contract E AC02 76SF00515

ELECTRON OUTCOUPLING SCHEME FOR THE NOVOSIBIRSK FEL

A.N. Matveenko*, O.A. Shevchenko, V.G. Tcheskidov, N.A. Vinokurov
Budker Institute of Nuclear Physics, Novosibirsk, Russia

Abstract

One of the main problems of contemporary high power FELs is the mirror heating. One of the possible solutions of this problem is the use of electron outcoupling [1, 2]. In this case the mirrors of optical resonator are not transparent and the coherent radiation from an additional undulator in the FEL magnetic system is used. To provide the output of this radiation the electron beam in the auxiliary undulator is deflected from the optical resonator axis. To save bunching it is preferable to use the achromatic deflecting bend. The project of electron outcoupling for the Novosibirsk FEL is described. Simulation results are presented.

INTRODUCTION

The output power of high power oscillator FELs [3] are limited by mirrors heating, leading to surface distortion. Typical gain in oscillator FEL is tens per cent. Correspondingly, optical cavity "quality factor" must be of the order of 10 to make losses lower then amplification. Consequently, intracavity power is at least an order of magnitude higher, than extracted power, and optical cavity mirrors are most loaded compared to mirrors in the user beamlines. Electron outcoupling is one of the possible ways to decrease the power density on the mirrors at the same FEL output power.

The basic idea of electron outcoupling is to output the coherent radiation of the bunched electron beam in the second undulator section (see Fig. 1.), while the bunching is generated in the first section, which is put into optical cavity. In this case the lasing power in the first section can be limited some way (e.g. installing long undulator, or using beam scraper to control cavity losses), but the beam bunching can be preserved. An isochronous bend between the sections brings the beam into the second undulator.

The angle between undulators must be larger then undulator radiation divergence angle $\sim \frac{1}{\gamma}\sqrt{\frac{1+K^2/2}{2N}}$, where N is the number of periods in the undulator, γ is the relativistic factor, K is the planar undulator deflection parameter.

Lengths of the undulator sections are chosen from a condition $\frac{1}{N} \sim 4\pi\frac{\Delta E}{E}$, where ΔE is the r.m.s. energy spread of the electron beam.

Numerical simulations for different electron outcoupling schemes were performed earlier in [4-7]. Here we present design and simulation results for Novosibirsk high power FEL.

*A.N.Matveenko@inp.nsk.su

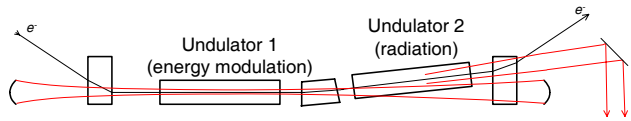

Fig. 1. Electron outcoupling scheme with two undulators and bending section between them. Electron beam path and laser output are shown.

ELECTRON OUTCOUPLING SCHEME OF NOFOSIBIRSK FEL

Electron outcoupling is planned to be used on the 4-th track of the second stage of Novosibirsk FEL. General layout of the second stage is shown in Fig. 2. Main electron beam and laser radiation parameters are summarized in Table 1.

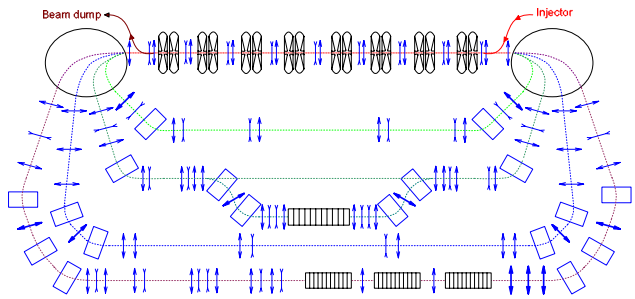

Fig. 2. Layout of the second stage of Novosibirsk FEL.

Table 1. Electron beam and laser radiation parameters.

Energy, MeV	40
Peak current, A	100
Electron beam emittance (normilized), μm	20
Maximum K	2
Undulator period, cm	6
Number of periods in each undulator	28
Deflection angle in second undulator, mrad	3
Relative energy spread	$3\cdot10^{-3}$
Radiation wavelength, μm	15
Optical cavity length, m	40
Mirror radius of curvature, m	25
Mirror reflectivity, %	90
Optical cavity β_x, β_y on mirrors, m	50
Optical cavity β_0 (Raleigh length), m	10

The scheme of the electron outcoupling of Novosibirsk FEL is shown in Fig. 3. It uses three undulators instead of two. The idea lying behind this modification is that in the basic scheme shown in Fig. 1 beam bunching reaches saturation at the end of the first undulator, therefore the efficiency of radiation in the second undulator is reduced. So, if one puts the third undulator (effectively, we divide the first undulator into two) one gets best beam bunching

MODELLING MIRROR ABERRATIONS IN FEL OSCILLATORS USING OPC

P.J.M. van der Slot*, J.G. Karssenberg, K.J. Boller
Mesa+ Institute for Nanotechnology, University of Twente, Enschede, NL

Abstract

Several high power free-electron lasers (FELs) are currently under design, operational or being upgraded. One central issue is the beam outcoupling and mirror deformation due to absorbed power. Here we present an extension to the OPC code that allows it to model mirror distorions. We use this code to model the high average power vacuum ultra violet FEL oscillator of the 4th generation light source. Both Genesis 1.3 and Medusa are used to calculate the gain provided by the undulator. Our findings indicate that the high gain oscillator is quite resilient to thermal mirror deformation and operation well into the kW range of average power can be expected.

INTRODUCTION

Several high average power Free-Electron Lasers (FELs) are currently operational [1, 2] or planned [3]. One of the issues in these devices is the thermal distortion of the mirrors that can alter the optical mode and degrade performance. Including this and other mirror distortions in simulation of these devices is important to understand and further improve these devices. Several attempts have already been made to model thermal mirror distortions [4, 5, 6, 7], however, a full integration of the FEL gain medium, optical propagation in the non-amplifying section and mirror distortions for both steady state and time dependent simulations is not readily available. Here we present an extension to the OPC package [8] that allows it to model mirror distortions. OPC implements paraxial optical propagation in the non-amplifying sections of a resonator, while either Genesis 1.3 [9] or Medusa [10] is used to simulate the gain provided by the undulator.

It is well know that various mirror distortions can be described using the circle polynomials of Zernike [11]. Within OPC these polynomials are used to calculated a phase difference $d\theta$ according to

$$d\theta = A_{nm} R_n^{|m|}(\rho) \times \begin{cases} cos(m\phi) & m \geq 0 \\ sin(m\phi) & m < 0 \end{cases} \qquad (1)$$

where $R_n^{|m|}$ is the circle polynomial of order (n,m), ρ is the scaled radial distance $\sqrt{x^2+y^2}/\rho_c$, ρ_c being a characteristic distance, ϕ is the angle $\tan^{-1}(y/x)$, and A_{nm} is the amplitude of the aberration. These aberrations define a phase mask that is applied to the optical field at the position of the corresponding optical component. The scaling constants A_{nm} and ρ_c can either be kept constant or made dependent on certain properties of the optical field, e.g., the total power or the root-mean-square (rms) width of the optical beam.

Different type of aberrations can be modeled using Zernike polynomials. For example, $n = 4$ and $m = 0$ corresponds to spherical aberration, $n = 3$ and $m = 1$ to coma and $n = 2$ and $m = 2$ to astigmatism [11]. A combination of Zernike polynomials can also be used to model a cylindrical lens. Here we focus on the the use of Zernike polynomials to model thermal mirror distortions [6, 4].

As an example of a high average power FEL we consider here the vacuum ultra violet FEL (VUV-FEL) oscillator that is part of the 4th generation light source (4GLS) project of Daresbury laboratory [3]. This high gain oscillator uses a low Q cavity to generate coherent output with photon energies in the range 3 to 10 eV. The VUV-FEL will operate in the 600 MeV high average current branch of the energy-recovery linac, and is driven by ~ 80 pC electron bunches at multiples of $4\frac{1}{3}$ MHz up to a maximum of 1.3 GHz. A system of distributed bunch compression along the beam line is expected to compress the bunch to lengths as short as 100 fs, generating a peak current of ~ 300 A before injection into the VUV-FEL. The main system parameters used in the simulations are given in table 1. Since the average output power will be of the order of 300 W or multiples thereof, and the mirror only reflects 60 % of the radiation falling on the surface, significant mirror heating is expected.

We will first briefly discuss the mirror thermal expansion and the resulting phase distortion. We then continue with a simulation of the VUV-FEL with and without the mirror expansion included.

MIRROR EXPANSION UNDER A THERMAL LOAD

The mirrors considered for the VUV-FEL oscillator consist of a protected aluminium coating on a silicon substrate. The reflectivity R of the mirror is expected to be 60 % [3]. Radiation is extracted at the downstream (DS) mirror through a hole with a radius of $r_h = 1.8$ mm. We approximate the mirror loading in the form of a train of optical pulses by an average power and determine the steady state displacement $\delta z(r)$ of the reflecting mirror surface under the assumption that the average absorbed power P_{abs} will have a Gaussian profile with rms width σ_m.

We use the finite element program MultiPhysics with the Structural Mechanics Module [12] to calculate the temper-

* p.j.m.vanderslot@tnw.utwente.nl

FLASH UPGRADED - PREPARING FOR THE EUROPEAN XFEL

H Schlarb* for the FLASH and the XFEL Project Tea ,
ES , -20607 Ha burg, er any

Abstract

Since 2005, the Free electron LASer in Ha burg, FLASH, has delivered a high brilliance photon bea to users with a wavelength range between 13 n and 40 n To eet the user de ands for 4 n wavelengths, sub-50 fs ti ing stability, and better pointing stability, the accelerator will be continuously upgraded within the ne t few years The upgrade to an energy of 1 3 e , the development of a transverse and longitudinal intra-train feedback syste , and a 3^{rd} har onic cavity at 3 9 Hz are key prototype tests for the European XFEL FLASH also serves as a test bench for an entirely new approach to accelerator facility synchronization involving optical pulses distributed in length stabilized bres Increased stabilization of the electron bea peak current and its arrival ti e should provide the possibility to reliably seed the electron bunch with higher laser har onics In this paper, an overview of the planned upgrades for FLASH will be presented with respect to their usefulness for the European XFEL

INTRODUCTION

Since 2005, the high-gain **F**ree electron **LAS**er in **H**a burg, FLASH, successfully delivers to user e perients in the U -wavelength range between 13 n and 40 n ultra-short photon pulses 10-25 fs FWHM with peak power at the igawatt level 1 The peak brilliance of the FLASH photon bea e ceeds that of state-of-the-art synchrotron radiation sources by seven orders of agnitude Observations of the high degree of transverse and longitudinal coherence, intensity stability of the self-a pli ed spontaneous e ission process, a pli cation gain easureents along the undulator and the content of high har onics down to 2 6 n are in full agree ent with theoretical prediction

The 13 n wavelength achieved with this FEL is li ited only by the 700 Me a i u electron bea energy and is an i portant ilestone for FLASH and the European XFEL as they set goals of reaching wavelengths of 6 n and 0 1 n , respectively Besides photon production for users, FLASH serves as a s all scale $\sim$ one tenth prototype for the larger XFEL facility The layouts of the facilities are shown in Fig 1 3, 4

The electron bea is produced in a laser-driven photoinjector using a nor al conducting RF gun The bea is accelerated in a linear accelerator co prised of eight 9-cell superconducting cavities housed in cryogenic odules The kilo-A pere s peak currents are achieved though two agnetic bunch co pressors before the bea enters the ain linac section Passing bea cleaning and protecting colli ators, the electron bunches of typically 100 fs duration produce the SASE-FEL photons in long undulators ey para eters of the achines are listed in Tab 1 3, 4

Most of the accelerator para eters i pacting the electron bea dyna ics, bea instru entation, echanical or RF tolerances are uite si ilar for the two facilities The ain differences are related to the electron bea energy, the accelerator and undulator length, the electron and the photon bea transport, and the photon diagnostics for Angstro wavelengths The large nu ber of devices in the XFEL - about 100 acceleration odules - re uires reliable ass-production by industry FLASH can provide for the prototyping of single XFEL units and, within certain li itations, can also provide long-ter reliability tests

Table 1 ey para eter of FLASH and the European XFEL

Parameter	FLASH	XFEL
nor e ittance	2 μ	1 4 μ
peak current	2 5 kA	5 0 kA
bunch rep rate	1 9 MHz	5 MHz
pulse rep rate	10 Hz	10 Hz
bunch charge	1 nC	1 nC
bea energy	1 0 e	17 5 e
photon wavelength	6 3 n	0 1 n
acc fre	1 3 3 9 Hz	1 3 3 9 Hz
at top duration	800 μs	650 μs
facility length	260	3 4 k
undulator length	30	250
orbit tolerance und	5 μ	3 μ

Bunch co pression for the XFEL takes place at bea energies that are $\sim$4 ti es higher than in FLASH The higher energies and the s aller R_{56} of the XFEL chicanes reduce the sensitivity to icro-bunch instabilities and rela the tolerances on the RF a plitude stability edicated diagnostics for te poral and spatial bunch pro ling up to the second bunch co pressor - the ost critical part of the accelerator - are essentially the sa e Therefore, al ost all critical accelerator sub-syste s can be tested and prototyped at FLASH, allowing for reduced costs, a rapid XFEL co issioning, and ini ized risk In this paper, the various FLASH upgrades relevant for the XFEL are described

ENERGY UPGRADE TOWARD 1.3 GEV

uring the spring shutdown of 2007, a new accelerator odule ACC6 - al ost the XFEL design odule - has been installed The average gradient of ACC6 is 28 5 M

* holger schlarb desy de

STATUS OF SCSS & X-RAY FEL PROJECT IN JAPAN

Tsumoru Shintake# and XFEL/SPring-8 Team
RIKEN/JASRI/SPring-8, Hyogo 679-5148 Japan

Abstract

The XFEL/SPring-8 project has been funded in FY2006, which is aiming at generating 1 Å coherent intense X-ray laser using 8 GeV normal-conducting accelerator. The construction period is scheduled 2006-2010, and FEL operation will start in 2011. XFEL/SPring-8 is based on unique concept of SCSS: SPring-8 Compact SASE Source. It requires low emittance and high peak current electron beam, i.e., normalized emittance of 1 π.mm.mrad and 3 kA peak current. We decided to employ the thermionic electron gun, which generates 1 A beam from single crystal cathode, followed by the multi-staged bunching system to achieve 3000 times compression. The design is based on the "Adiabatic Bunch Compression" scheme, i.e., compressing bunch length as inversely proportional to the beam energy, thus the bunch length on electron rest frame is kept constant, and as a result the low slice emittance is preserved. To prove this concept, the SCSS prototype accelerator of 250 MeV beam energy was build. On June 2006, the first lasing has been observed at 49 nm. From the FEL gain measurement, the beam brightness was determined as high as 300 A/(π.mm.mrad)^2, which is enough value for the beam quality for the 8 GeV XFEL/SPring-8 project.

INTRODUCTION

We started SCSS project in 2001[1] for developing technology required for X-ray FEL. SCSS stands for SPring-8 Compact SASE Source, in which by means of in-vacuum type short period undulator, the required electron beam energy becomes lower, additionally the C-band accelerator drives the beam at high gradient as high as 35 MV/m, as a result, the total system length becomes "compact", and it fits to available site length at SPring-8.

In the course of SCSS R&D, we developed a low emittance electron gun using single crystal CeB6 cathode shown in Fig. 2 and 500 kV gun driven by pulse modulator power supply: We also developed various hardware components required for SCSS: injector rf system, C-band klystron modulator with oil-filled compact design, high resolution beam position monitor, and digital rf signal processing system[2]. In order to check the developed hardware components and verify system performance, especially the low emittance electron injector, we constructed SCSS prototype accelerator in 2004-2005. The tunnel length is 60 m long, the maximum electron beam energy is 250 MeV, the shortest lasing wavelength is around 50 nm. In July 2006, we observed first lasing. The user beam run will start in October 2007.

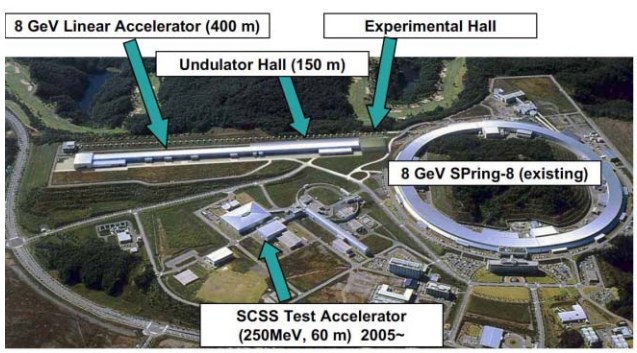

Fig. 1 The XFEL will be build at SPring-8 site.

On FY2006, the Japanese MEXT: Ministry of Education, Culture, Sports, Science and Technology has decided construction of XFEL at SPring-8 site. The project is aiming at generating 1 Å coherent intense X-ray laser, which is based on SASE using 8 GeV normal-conducting accelerator. A big benefit to have XFEL at SPring-8 site is to share human resources and facilities for sample preparation with existing 8 GeV synchrotron light source.

We have decided to use normal conducting linear accelerator technology at C-band frequency (5712 MHz), which was originally developed at KEK for the e+e- linear collider project. It is "warm" technology, not super conducting "cold" technology; therefore it can be constructed with much lower cost. The C-band accelerator is capable of running at high accelerating gradient, as high as 35 MV/m. The 50 MW C-band klystron was developed and it is now available from industries as a standard component. C-band accelerator technology is available right now.

CHOICE OF ELECTRON SOURCE

SCSS is unique and beneficial, however, it requires extremely low normalized emittance: ~ 1 π.mm.mrad and high peak current: 3 kA. We decided to employ the thermionic electron gun, which generates 1 A beam from single crystal cathode, followed by the multi-staged bunching system to achieve 3000 times compression (3000 = 20 x 5 x 10 x 3). The design is based on "Adiabatic Bunch Compression" scheme as shown in Fig. 3, i.e., compressing bunch length as inversely proportional to the beam energy, thus the bunch length on electron rest frame is kept constant, and as a result the low slice emittance is preserved. We carefully manipulate bunch length and avoid "over bunching", thus we do not mix particle between head and tail within bunch. The bunch length on the electron rest frame is kept almost constant, in practice it is about 30 cm long, while the diameter of the beam is a few mm only, therefore the electric field of space charge is fairly uniform and linear, and has only the radial component, as a result emittance break due to the space charge effect becomes negligibly small.

#shintake@spring8.or.jp

STARS—AN FEL TO DEMONSTRATE CASCADED HIGH-GAIN HARMONIC GENERATION*

M. Abo-Bakr, W. Anders, J. Bahrdt, K. Bürkmann, P. Budz, O. Dressler, H. Dürr, V. Dürr, W. Eberhardt, S. Eisebitt, J. Feikes, R. Follath, A. Gaupp, R. Görgen, K. Goldammer, S. Hessler, K. Holldack, E. Jaeschke, T. Kamps, J. Knobloch†, O. Kugeler, B. Kuske, P. Kuske, D. Krämer‡, F. Marhauser§, A. Meseck, R. Mitzner¶, R. Müller, A. Neumann, M. Neeb, K. Ott, D. Pflückhahn, T. Quast, M. Scheer, T. Schroeter, F. Senf, G. Wüstefeld
BESSY, Albert-Einstein-Strasse 15, 12489 Berlin, Germany

Abstract

BESSY is proposing a new facility to demonstrate the cascading of two high-gain harmonic-generation stages for the generation of FEL radiation. This facility, called STARS, is planned for lasing in the wavelength range 40 nm to 70 nm. A 325-MeV CW driver linac provides a peak current of 500 A at a bunch charge of 1 nC. The linac consists of a normal-conducting gun, three superconducting TESLA-type modules modified for CW operation, a third-harmonic unit to linearize the RF potential and a single-stage bunch compressor. This paper discusses the facility layout and the main operating parameters.

MOTIVATION

Femtosecond pulses from linac-based free-electron lasers are unique tools for future time-resolved experiments. In March 2004, BESSY published the TDR for a free-electron laser user facility that covers the VUV to soft X-ray range (BESSY FEL) [1]. This second-generation FEL facility is seeded and uses the high-gain harmonic generation (HGHG) [2] scheme to produce coherent radiation down to the 1-nm range. This scheme offers the possibility to generate photon pulses of variable femtosecond duration, gigawatt peak power, full shot-to-shot pulse reproducibility, wide-range tunability and full transverse and longitudinal coherence. To reach the highest energies, HGHG cascades with up to four stages must be employed.

Following the evaluation of the TDR in 2005/06 by the German Science Council, it was recommended that the BESSY FEL be realized on condition that its enabling technology, the HGHG *cascade*, be demonstrated beforehand.

To address this important issue, BESSY is therefore proposing to build a two-stage HGHG cascade with a superconducting driver linac called STARS (Superconducting Test Accelerator for Radiation by Seeding) [3, 4]. Although its primary purpose is to validate the cascading of HGHG stages, many components and technical issues are nearly identical to those of the BESSY FEL. Hence, STARS serves as an ideal test bed for operating CW superconducting technology, diagnostics, synchronization, and for studying beam generation, manipulation and transport.

To demonstrate the capabilities and potential of seeded, ultra-short-pulse FEL radiation, prototype user experiments will also be installed at STARS. The location of STARS is planned such that it will remain operational even after construction of the BESSY FEL. By expanding the experiments, STARS will therefore migrate towards a full user facility to enhance the BESSY FEL and to enable the exploration of new techniques before they are adopted for the BESSY FEL.

OVERVIEW

STARS will be located on the same site as BESSY-II in Berlin-Adlershof, making use of some of the existing infrastructure while leaving room for the BESSY FEL facility to be built later. The philosophy behind the layout of STARS, as depicted in Figure 1, is to adopt a conservative configuration that provides for "safe" operation in view of the main goal of demonstrating the cascading of HGHG at 70 nm. Hence, components for the driver linac and system parameters were adopted which have already been demonstrated experimentally elsewhere. Nevertheless, "optional upgrades" of the linac are included, some from the outset, that will enhance the FEL's performance to make STARS attractive for future user experiments.

A normal-conducting photoinjector generates high-brightness electron bunches. Three superconducting TESLA-type cryomodules, modified for CW operation, then boost the energy up to 325–380 MeV.[1] The cryomodules contain twenty 9-cell TESLA-type cavities with the possibility to add four further ones at a later date. Bunch compression is achieved in a magnetic chicane following the second module. A collimator and diagnostic beam line preceed the HGHG cascade, permitting linac commissioning before the beam is injected into the FEL section consisting of two HGHG stages and a fresh bunch chicane.

For bunch compression, off-crest acceleration is required. Non-linearities in the longitudinal bunch profile introduced by the RF potential result in a strongly peaked current distribution after compression. STARS thus in-

* Supported by the Bundesminsiterium für Bildung und Forschung, the State of Berlin and the Zukunftsfonds Berlin.

† knobloch@bessy.de
‡ now at GSI, Darmstadt
§ now at Jefferson Lab, Newport News
¶ Universität Münster

[1] The final energy depends on whether the third-harmonic cavities, discussed later, are in operation or not.

TOWARDS A LOW EMITTANCE X-RAY FEL AT PSI

A. Oppelt*, A. Adelmann, A. Anghel, R.J. Bakker, M. Dehler, R. Ganter, C. Gough, S. Ivkovic, F. Jenni, C. Kraus, S.C. Leemann, F. Le Pimpec, K. Li, P. Ming, B. Oswald, M. Paraliev, M. Pedrozzi, J.-Y. Raguin, L. Rivkin, T. Schietinger, V. Schlott, L. Schulz, A. Streun, F. Stulle, D. Vermeulen, F. Wei, A.F. Wrulich, Paul Scherrer Institute, 5232 Villigen PSI, Switzerland

Abstract

The Paul Scherrer Institute (PSI) in Switzerland is aiming to build a compact and cost-effective X-ray FEL facility for the wavelength range 0.1 – 10 nm. Based on the generation of very low emittance beams, it consists of a low-emittance electron source followed by high-gradient acceleration, and advanced accelerator technology for preserving the initial low emittance during further acceleration and bunch compression. In order to demonstrate the feasibility of the concept and the emittance preservation, a 250 MeV test facility will be built. This machine has been designed to be used as injector for the X-ray FEL at a later date. The accelerator design of the 250 MeV linac will be presented together with the status of the low emittance source and high gradient acceleration.

INTRODUCTION

In order to realize compact free electron lasers for the Angstrom wave length range, electron sources with high brilliance and ultra low emittance are required, allowing for low beam energies and short undulator length, and thus dramatically reducing the size and costs of such a project.
The proposed X-ray FEL at PSI is based on the development of new concepts that enable a substantial reduction in size and costs of the facility with respect to other existing designs.
The successful operation of such a FEL depends on the combination of high peak current, low energy spread, and high brightness of the electron beam. For the PSI-XFEL performance, in order to reach the Angstrom spectral range, a peak current of 1.5 kA, a relative energy spread around 10^{-4}, and a normalized transverse (slice) emittance as low as technically possible (i.e. $\varepsilon_n < 0.1$ mm mrad), are crucial. These stringent requirements shall be met by using new techniques, which include a low emittance source, a high gradient acceleration section, and a sophisticated bunch compression scheme.

LOW EMITTANCE SOURCE

Electrons emitted via field emission from micron sized metallic tips have an intrinsic low emittance due to the small source size. Using a double gated emitter geometry, parallel beamlets are produced from these tips. Combining the tips into a two-dimensional field emitter array (FEA), the required beam current can be reached with minor losses in emittance. Research at PSI focuses on developing suitable field emitter arrays emitting a total current of 5.5 A with an emittance of about 0.05 mm mrad. A scanning electron microscope (SEM) image of such an array, produced in-house at PSI, is shown in figure 1. Currents up to $\sim 10\mu$A per tip have been extracted from such a FEA in DC mode. The performances were studied at a 100 kV test stand [1].

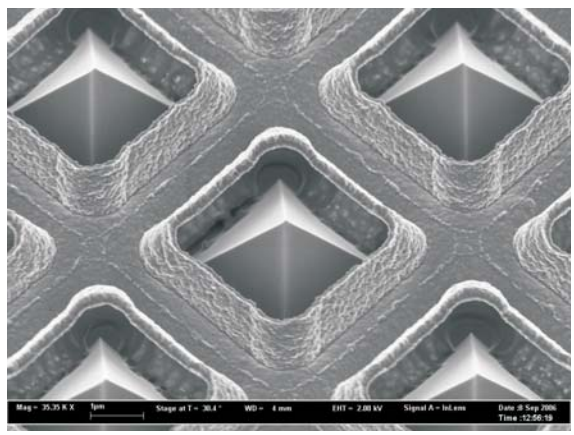

Figure 1: SEM picture of a FEA produced at PSI: the pyramidal shaped Mo tips and the gate layer are clearly visible.

Needle cathodes (single tip field emitters) are also investigated at PSI. Currents up to 470 mA were extracted from a ZrC needle via field emission (pulsed voltage, 2 ns FWHM, 30 Hz) [2]. Laser assisted field emission from needle cathodes allows increasing the extracted current further and offers the possibility of pre-bunching the electron beam. Figure 2 shows the measured current waveforms when applying different voltages (2 ns FWHM, 30 Hz) to a needle cathode in combination with laser illumination (266 nm, 6 μJ, 16 ps RMS). In this way, a peak current of 2.9 A was extracted [3]).
Since the fabrication and operation of the FEA [4] is very challenging, the option of using a conventional photo cathode is also investigated. With the proper choice of parameters (material, bunch charge, peak current), emittances of about 0.1 mm mrad should be reachable. Therefore, a Cu photo cathode will be chosen as start-up version for the injector. For both options, photo emission and field emission, the parameters were chosen equally such that the design of the following accelerator sections is not affected.

* presenting author: anne.oppelt@psi.ch

HIGH ORDER MODE ANALYSES FOR THE ROSSENDORF SRF GUN

V. Volkov, BINP, Novosibirsk, Russia
D. Janssen, FZD, Dresden, Germany.

Abstract

High Order Modes (HOM) excited by the beam in a superconducting RF gun (SRF gun) could destroy the quality of the electron beam. This problem is studied on the base of frequency domain description by considering of the equivalent RLC circuit contour for each HOM, periodical excited by a pulsed current source [1].

Expression for the voltage, the field amplitude and the phase of the excited HOM has been obtained. The equations for the coupling impedances of monopole TM-HOM and TE-HOM in the RF gun cavity has been derived. In this calculation the change of the particle velocity due to acceleration is taken into account.

Resonance frequencies, coupling impedances, unloaded and external quality factors, excitation voltages and field distributions for each HOM including trapped HOM are calculated for Rossendorf SRF gun up to the frequency of 7.5 GHz, using the complex field solver CLANS. The dependence of the calculated parameters from a cavity deformation has been studied.

The influence of the seven most dangerous HOM on the beam quality has been estimated by particle tracking using the ASTRA code.

DERIVATION OF THE THEORY

In the following considerations the electron beam is represented by a pulsed current with the repetition round frequency Ω. The time dependence of each pulse is given by the Delta-function [2].

Excitation Voltage

The voltage $\Delta U=\omega\cdot(R/Q)\cdot q$ of each HOM is excited when a bunch pass through the cavity. It can be presented as a vector in the complex space, which rotates with the round resonance frequency ω of the HOM:

$$U_0(t)=\Delta U\cdot e^{j\omega t-\omega t/2Q_L}, \qquad (1)$$

whereas R/Q is coupling impedance of the HOM; $\omega/2Q_L$ is attenuation factor; Q_L is loaded quality factor of the HOM and q is bunch charge.

The voltage U_N is the result of N bunch-HOM interaction, where the voltage is changed each time by the amount ΔU and N phase rotation ϕ between the interaction moments. This phase angle is determined by the HOM and the bunch repetition frequency and given by $\phi=2\pi\cdot Fraction(\omega/\Omega)$. Finally for U_N one obtains:

$$U_N(t)=\Delta U e^{i\cdot(\omega t+\varphi)}\sum_{n=0}^{N}\left(e^{i\cdot 2\pi\omega/\Omega-2\pi\omega/\Omega\cdot 2Q_L}\right)^n. \qquad (2)$$

where φ is phase angle at that time, when the bunch starts at cathode of the SRF gun. In the stationary limit $N\to\infty$ the amplitude of excitation voltage U(t) becomes constant. From (2) follows:

$$U(t)=U_N(t)\big|_{N\to\infty}=\frac{\Delta U}{1-e^{i\cdot 2\pi(\omega/\Omega)}\cdot e^{-2\pi(\omega/\Omega)/2Q_L}}\cdot e^{i\cdot(\omega t+\varphi)}, \qquad (3)$$

The time evolution of U in the complex plane is graphical represented in Fig.1.

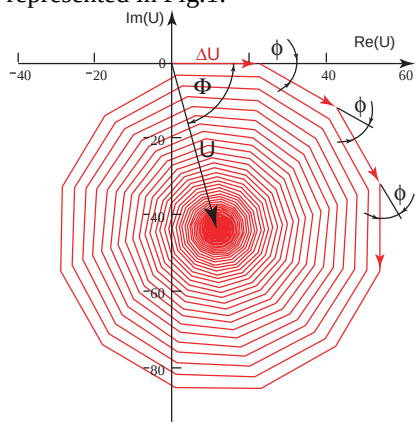

Figure 1: Evolution of excitation voltage of all bunches for low Q values of the HOM.

In the real cavity this excited voltage is equal to the change of the particle energy due to the interaction with the HOM field

$$U\equiv\int dW/e, \qquad (4)$$

whereas W is the change of the kinetic particle energy which can be measured in an experiment.

TM-HOM Excitation by Accelerated Beam

The energy exchange between the HOM and the particles moving through the cavity is defined as:

$$dW=\frac{1}{m\gamma}\cdot\left(dP_\theta\cdot P_\theta+dP_r\cdot P_r+dP_z\cdot P_z\right)=\frac{1}{m\gamma}\cdot\left(d\vec{P}\cdot\vec{P}\right) \qquad (5)$$

Here P_z, P_θ, P_r are particle momentum components which commonly depend from the accelerating and focusing fields in the cavity; The components of the $d\vec{P}$ are the momentum transfer due to the HOM-particle interaction. They are given by:

$$d\vec{P}=e\cdot\vec{E}\cdot dt+\frac{e}{m\gamma}\cdot\left[\vec{P}\times\vec{B}\right]\cdot dt, \qquad (6)$$

whereas e and m are the electron charge and the electron mass respectively, γ is relativistic factor, E and B is the electric and magnetic RF field of the HOM.

For the monopole TM HOM field at cavity axis the equations B=0; $\bar{E}=E_z(z)\cdot\sin(\omega t+\varphi)$ are hold. From (4) and (5) follow:

$$U=\int_0^T E_z(z)\cdot\sin(\omega t+\varphi)\cdot\beta(t)c\cdot dt \qquad (7)$$

The integration interval T is the time of HOM-particle interaction. $E_z(z)$ is the electric field distribution of the HOM on the cavity axis; β(t) and z=z(t) are the particle velocity and its coordinate determined by the acceleration

FEL POTENTIAL OF THE HIGH CURRENT ERLS AT BNL *

D. Kayran#, I. Ben-Zvi, V. N. Litvinenko, E. Pozdeyev,
Brookhaven National Laboratory, Upton, NY, USA,
A.N. Matveenko, O.A. Shevchenko, N.A. Vinokurov,
Budker Institute of Nuclear Physics, Novosibirsk, Russia.

Abstract

An ampere class 20 MeV superconducting Energy Recovery Linac (ERL) is under construction at Brookhaven National Laboratory (BNL) [1] for testing concepts for high-energy electron cooling and electron-ion colliders. This ERL prototype will be used as a test bed to study issues relevant for very high current ERLs. High average current and high performance of electron beam with some additional components make this ERL an excellent driver for high power far infrared Free Electron Laser (FEL). A possibility for future up-grade to a two-pass ERL is considered. We present the status and our plans for construction and commissioning of the ERL. We discus a FEL potential based on electron beam provided by BNL ERL.

INTRODUCTION

The R&D ERL facility at BNL aims to demonstrate CW operation of ERL with average beam current in the range of 0.1-1 ampere, combined with very high efficiency of energy recovery. The ERL is being installed in one of the spacious bays in Bldg. 912 of the RHIC/AGS complex.

The ERL R&D program is pursued by the Collider Accelerator Department (C-AD) at BNL as an important stepping-stone for 10-fold increase of the luminosity of the Relativistic Heavy Ion Collider (RHIC) using relativistic electron cooling of gold ion beams with energy of 100 GeV per nucleon. Furthermore, the ERL R&D program extends toward a possibility of using 10-20 GeV ERL for future electron-hadron/heavy ion collider, eRHIC [2].

These projects are the driving force behind the development of ampere-class ERL technology, which will find many applications including light sources and FELs.

The intensive R&D program geared towards the construction of the prototype ERL is under way: from development of high efficiency photo-cathodes [3] to the development of new merging system compatible with emittance compensation [4].

LAYOUT OF THE R&D ERL

Two operating modes are envisaged, namely the high current mode and the high charge mode. The high current (0.5 A) mode will operate electron bunches with lower normalized emittance, 0.7 nC charge per bunch at 703 MHz rep-rate. In this case, the full energy of electrons at gun exit is limited by the available RF power 2.5 MeV. In high charge mode electron beam will consist of bunches with charge up to 5nC per bunch at 10MHz repetition rate, 50 mA average current. The electrons energy at the exit of the gun can be pushed upto 3.0-3.5 MeV by the maximum field attainable in the super-conducting gun itself.

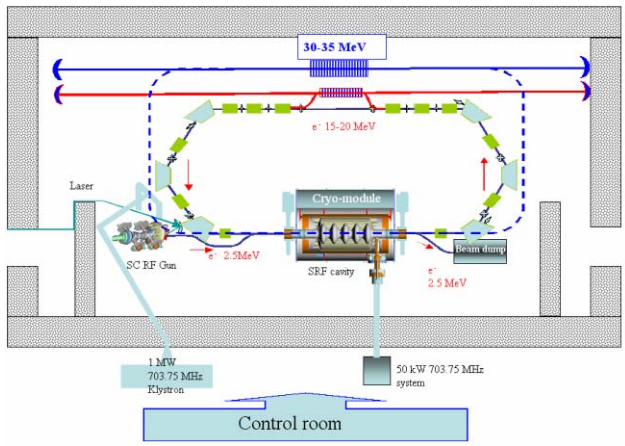

Figure1: Layout of the R&D energy recovery linac in the shielded vault with possible FEL setup. Dashed line shows considered second pass upgrade.

The ERL design (shown in Fig. 1) has one turn: electrons are generated in the superconducting half-cell gun and injected into the main superconductive linac. Linac accelerates electrons 15-20 MeV, which pass through a one turn re-circulating loop with achromatic flexible optics [5].

The photocathode is located in a high electric field for immediate acceleration of the electrons to as high energy as possible, reducing emittance degradation due to strong space charge force. Furthermore, linear part of space charge effects is compensated by applying a suitable external solenoid magnetic field.

In nominal recovery operation regime the path-length of the loop provides for 180 degrees change of the RF phase, causing electron deceleration (hence energy recovery) down to injection energy. The decelerated beam separates from the higher energy beam and goes to the beam-dump.

ERL Injector

The electron injector is a central part of any ERL that has to deliver high brightness electron beam. The BNL R&D ERL injector (see Fig. 2) consist of ½ cell superconducting RF gun with photocathode inside, solenoid, four dipoles and two solenoids turned on in opposite direction (in order to match the electron beam with linac entrance more accurately). The 4th dipole mergers the high and low energy beams.

* Work performed under the auspices of the US Department of Energy
# dkayran@bnl.gov

ELECTRON BEAM DYNAMICS UNDER COHERENT HARMONIC GENERATION OPERATION AT UVSOR-II

M Labat, CEA Saclay - 91 191 if-sur- vette, France
C Bruni, La bert, M E Couprie, Synchrotron SOLEIL - 91 192 if-sur- vette, France
A Mochihashi, M Shi ada, M atoh, U SOR Facility - Okazaki, apan
M Hosaka, Takashi a, Nagoya University - Nagoya , apan
T Hara, RI EN SPring-8 - Hyogo, apan

Abstract

In the Coherent Har onic eneration Free Electron Laser con guration, an e ternal laser source is seeded inside a rst undulator The interaction between the electron bea and this seed induces energy odulation of the bunch, further converted into a density odulation, producing coherent radiation in a second undulator The energy odulation enhances the energy spread of the electron bunch, converted by the achine optics into a odi cation of its longitudinal distribution In the case of a storage ring FEL, the electrons are re-circulating the sa e bunch keeps interacting with the seeded laser, and rela ation of the distribution is only allowed in between two laser injections Such speci c dyna ics has been studied on the CH FEL of U SOR-II storage ring apan The electron bea stored at 600 Me is seeded using a 2 5 , 1 kHz, 1 2 ps Ti Sa laser at 800 n wavelength, allowing radiation at 266 n third har onic A Streak Ca era is used to record the evolution of the longitudinal pro les as a function of the repetition rate and average power of the seeding laser, leading to bunch lengthening and distortion dyna ical analysis It appeared that because the heating induced by the interaction re ains local, the refresh ent process of the electronic distribution is odi ed The e peri ental results are co pared to si ulations

INTRODUCTION

The co bination of an intense fs laser with synchrotron electron bea s now allows delivery of sub ps light pulses in an e tendend spectral do ain fro TeraHertz 1 to X rays 2 The Coherent Har onic eneration Free Electron Laser CH FEL results fro this asse bly In the CH FEL 4, 5, 6 , the electron bea is odulated in energy by the laser pulse, within the agnetic eld of an undulator -so called odulator - Passing through a dispersive section converts this energy odulation into a density odulation, allowing in a second undulator -so called radiator-, coherent e ission at the seeding laser wavelength and its har onics Inversely to H H FEL con guration 7 , the injected seed does not interact with a fresh bunch but a re circulating synchrotron bea , which ay drive degradation in ti e of the electronic distribution, and eventually of the output radiation properties The effect of a ps laser pulse on an electronic distribution has already been studied in oscillator FELs physics lasing results fro the pass by pass a pli cation of the electrons spontaneous e ission which is stored in an optical cavity The light pulse increases the energy spread of the electron bea , the so called bunch heating 8, 9 , inducing bunch lengthening and shape distorsion 10, 11, 12, 13 , until saturation is reached epending on the longitudinal overlap between the electrons circulating in the ring and the laser pulse in the optical cavity, the FEL can be operated in continuous or pulsed ode In this last ode, the electron bea refreshes in between two pulses deliveries 14 -switch operation of oscillator FELs gave si ilar results on heating dyna ics and showed local effects on the electronic distribution 15, 16

In this paper, we investigate the dyna ical response of an electron bunch fro a storage ring to the e citation of an e ternal laser with shorter pulse duration by one order of agnitude and higher peak power, as it is the case for both Slicing and CH sche es A odel is given for si ulation of the electron-photon interaction inside the storage ring It is then used, together with e peri ental results obtained on U SOR-II CH FEL, to understand the evolution towards saturation of the electronic distribution under the laser heating Finally, local aspect of this interaction and its conse uence on the dyna ics are presented

BEAM HEATING SIMULATION

The electron bunch distribution is si ulated using a pass to pass odel following the stored particles in the longitudinal phase space 18 The initial code 13, 17 has been odi ed to include single pass interaction with an e ternal laser The evolution of the j^{th} particle at n^{th} pass is driven by

$$\tau_{n+1,j} = \tau_{n,j} - \alpha T_0 \epsilon_{n,j} \qquad 1$$

$$\epsilon_{n+1,j} = \epsilon_{n,j} - U_0 + V_{RF,n,j} - D_{n,j} + R_{n,j} + SE + W_{mod,n,j} \qquad 2$$

with $\tau_{n,j}$ its relative longitudinal position and $\epsilon_{n,j}$ its relative nor alized energy with respect to the synchronous particule Energy variation is converted by the achine optics into a longitudinal displace ent, which depends on the o entu co paction factor α and the revolution period T_0

Along each revolution, the particule losses energy by synchrotron radiation U_0 , rando e ission R and spontaneous e ission in the optical klystron SE 19 D is the da ping ter The interaction with the e ternal laser

ANALYTICAL STUDIES OF TRANSVERSE COHERENCE PROPERTIES OF X-RAY FELS

E.L. Saldin, E.A. Schneidmiller, and M.V. Yurkov
Deutsches Elektronen-Synchrotron, DESY, Hamburg, Germany

Abstract

The explicit solution of the initial value problem for a SASE FEL operating with a large ratio of electron beam emittance to the wavelength, $\hat{\epsilon} = 2\pi\epsilon/\lambda \gg 1$, is presented. The degree of transverse coherence is explicitly calculated, too. It is shown to be dependent on the ratio of the number of FEL gain lengths to the parameter $\hat{\epsilon}$. In particular, in the multi-mode limit the radiation from a SASE FEL has by the squared number of gain lengths higher degree of transverse coherence than a synchrotron radiation generated by a beam with the same emittance.

INTRODUCTION

Free electron lasing at wavelengths shorter than ultraviolet can be achieved with a single-pass, high-gain FEL amplifier. Due to a lack of powerful, coherent seeding sources short-wavelength FEL amplifiers work in so called Self-Amplified Spontaneous Emission (SASE) mode when amplification process starts from shot noise in the electron beam [1, 2, 3]. The first VUV FEL user facility FLASH ("F"ree-Electron-"LAS"er in "H"amburg) [4, 5] operates in SASE mode and produces GW-level, laser-like radiation pulses with 10 to 50 fs duration in the wavelength range 13-45 nm. Present level of accelerator and FEL techniques holds potential for SASE FELs to generate wavelengths as short as 0.1 nm [6, 7, 8].

The condition $\hat{\epsilon} < 1/2$ is often formulated as necessary one for an optimal design of a SASE FEL. It is meant that under this condition the radiation from SASE FEL has a full transverse coherence. However, as it is shown in [9], the maximal degree of transverse coherence (and brilliance as well) is achieved at $\hat{\epsilon} \simeq 1$. For smaller emittances the degree of transverse coherence decreases due to the effect discovered in [10]. Moreover, the above mentioned condition is strongly violated in the project parameters of hard X-ray FELs [6, 7, 8]: there the parameter $\hat{\epsilon}$ is in the range 2-5. Even without discussing exotic proposals [11, 12], one can notice a general trend towards lower energies of the electron beam, i.e. cost-saving solutions. Since achievable normalized emittance $\gamma\epsilon$ is limited by beam physics and technology issues, this would lead to a further increase of $\hat{\epsilon}$. Thus, theoretical understanding of properties of a SASE FEL, operating in this regime, becomes practically important. In this paper we present the main results of the theoretical analysis performed in Ref. [13] dealing with the limit $\hat{\epsilon} \gg 1$.

EIGENVALUE EQUATION

Let us have at the undulator entrance a continuous electron beam with the current I_0, with the Gaussian distribution in energy

$$F(\mathcal{E}-\mathcal{E}_0) = \left(2\pi\langle(\Delta\mathcal{E})^2\rangle\right)^{-1/2} \exp\left(-\frac{(\mathcal{E}-\mathcal{E}_0)^2}{2\langle(\Delta\mathcal{E})^2\rangle}\right), \quad (1)$$

and in a transverse phase plane

$$f(x,x') = (2\pi\sigma^2 k_\beta)^{-1} \exp\left[-\frac{x^2+(x')^2/k_\beta^2}{2\sigma^2}\right], \quad (2)$$

the same in y phase plane. Here $k_\beta = 1/\beta$ is the wavenumber of betatron oscillations and $\sigma = \sqrt{\epsilon\beta}$.

Using cylindrical coordinates, in the high-gain limit we seek the solution for a slowly varying complex amplitude of the electric field of the electromagnetic wave in the form [14]:

$$\tilde{E}(z,r,\varphi) \propto \Phi_{nm}(r)\exp(\Lambda z)e^{\pm \mathrm{i}\, n\varphi}, \quad (3)$$

where n is an integer, $n \geq 0$. For each $n > 0$ there are two orthogonal azimuthal modes and many radial modes that differ by eigenvalue Λ and eigenfunction $\Phi_{nm}(r)$. The integro-differential equation for radiation field eigenmodes [15, 16, 17] can be written in the following normalized form:

$$\left[\frac{\mathrm{d}^2}{\mathrm{d}\,\hat{r}^2} + \frac{1}{\hat{r}}\frac{\mathrm{d}}{\mathrm{d}\,\hat{r}} - \frac{n^2}{\hat{r}^2} + 2\,\mathrm{i}\,B\hat{\Lambda}\right]\Phi_{nm}(\hat{r}) =$$
$$-4\int_0^\infty \mathrm{d}\,\hat{r}'\hat{r}'\Phi_{nm}(\hat{r}')$$
$$\times\int_0^\infty \mathrm{d}\,\xi\frac{\xi}{\sin^2(\hat{k}_\beta\xi)}\exp\left[-\frac{\hat{\Lambda}_\mathrm{T}^2\xi^2}{2} - (\hat{\Lambda}+\mathrm{i}\,\hat{C})\xi\right]$$
$$\times\exp\left[-\frac{(1-\mathrm{i}\,B\hat{k}_\beta^2\xi/2)(\hat{r}^2+\hat{r}'^2)}{\sin^2(\hat{k}_\beta\xi)}\right]$$
$$\times I_n\left[\frac{2(1-\mathrm{i}\,B\hat{k}_\beta^2\xi/2)\hat{r}\hat{r}'\cos(\hat{k}_\beta\xi)}{\sin^2(\hat{k}_\beta\xi)}\right], \quad (4)$$

where I_n is the modified Bessel function of the first kind. The following notations are used here: $\hat{\Lambda} = \Lambda/\Gamma$, $\hat{r} = r/(\sigma\sqrt{2})$, $B = 2\sigma^2\Gamma\omega/c$ is the diffraction parameter, $\hat{k}_\beta = k_\beta/\Gamma$ is the betatron motion parameter,

COMPACT X-RAY FREE ELECTRON LASE BASED ON AN OPTICAL UNDULATOR

C. Maroli, V. Petrillo, Dipartimento di Fisica dell'Università di Milano-INFN Sezione di Milano Via Caloria,16, 20133 Milano, Italy
L. Serafini, A. Bacci, A Rossi, P. Tomassini, *INFN*-Sezione di Milano, Via Celoria,16, 20133 Milano, Italy

Abstract

The interaction between a very high-brilliance electron beams and a relativistically intense counter-propagating laser pulses produces X rays via FEL collective amplification. The phenomenon is, however, very selective, so that the characteristics of both electron and laser beam must satisfy tight requirements in terms of beam current, emittance, energy spread and laser amplitude stability within the pulse. The three dimensional equations governing the radiation phenomenon have been studied in both linear and non linear regime and solved numerically for the particular interesting values of wavelengths of 1 Ang, 1nm and 12 nm. The performance of the collective Thomson source has been compared with that of an equivalent static undulator.

INTRODUCTION

The collective effects that develop in the classical Thomson back-scattering give rise to intense X-ray pulses easily tunable and highly monochromatic at a level a few orders of magnitude larger than the incoherent radiation. Due to recent technological developments in the production of high brilliance electron beams and high power CPA laser pulses, it is now even conceivable to make steps toward their practical realisation.

The phenomenon of the impact between the electron beam and the laser pulse has characteristics similar to the free electron laser and has been studied in previous papers[1-2]. The lasing is rather difficult to start up and the power saturation level is lower than that achieved in conventional static wigglers. It is however large enough to be interesting for application as fast probing for chemical process, monochromatic X imaging, phase contrast imaging, deep probing for inertial fusion research, considering moreover the fact that this kind of set-up is compact and considerably less expensive than static FEL.

In this paper we present several details about this X-ray production phenomenon, analysing various beam lines producing different electron bunches as well as various situations relevant to the synchronization between the electron beam and the laser pulse. Finally, we have compared the results of the radiation levels obtained with our 'ad hoc' radiation code EURA (for Electromagnetic Undulator Radiation Analysis) with those provided by the code GENESIS 1.3 currently used in FEL simulations [3], which is however not presently able to model electro-magnetic undulators. The answers given by both codes are qualitatively similar and also the quantitative estimates of saturation power and gain length are very close, when magnetostatic undulators are considered.

NUMERICAL SOLUTION OF 3D EQUATIONS

We have first studied the use of a CO_2 laser of wavelength λ_L=10 micron. High power lasers of this frequency are characterized by 70-100 GW of power and up to 300 psec of time pulse length.

By fixing the mean energy of the electron beam around the value <E>=30 MeV, i.e. $<\gamma>=60$, using the resonance condition for the back-scattering Thomson, $\lambda_R=\lambda_L(1+a_{L0}^2)/4\gamma^2$ and assuming the laser parameter $a_{L0}\leq 0{,}5$, X rays of wavelengths λ_R of the order of 7-9 Angstrom can be obtained. For this case, collective effects and FEL instability develop when the beam transverse normalized emittance does not exceed the value ε_x=0.5, and if the energy spread $\Delta\gamma/\gamma$ is contained in few 10^{-4}. Values of this kind are out of the current state-of-the-art of high–brightness beams but represent an interesting challenge for a possible future operation scenario.

Our numerical simulations for the case of the electromagnetic undulator have been performed with the 3D code EURA, which is a three-dimensional, time dependent code that integrates equations (2-5) using a forth order Runge-Kutta method for the particles and an explicit finite difference scheme for the radiation equation. The bunching factor is calculated along the beam by selecting, around each point, a moving portion of the bunch including several buckets.

The data obtained with EURA for a static undulator have been compared with similar data produced with the code GENESIS 1.3 widely used in the FEL analysis. The comparison is presented in Fig 3 where data from EURA (black curve (b)) and from GENESIS 1.3 time dependent (red curve (a)) are reported.

The data chosen for the comparison are: undulator parameter a_w=0.3, undulator period λ_w=10μm, radiation wavelength λ_R=1.515 nm, ε_x=0.3 mm mrad, r.m.s. transverse dimension σ_x=12.5 μm (corresponding to a

PRODUCTION OF FEMTOSECOND PULSES IN A FREQUENCY DOUBLER AND PERSPECTIVES OF FLASH USER FACILITY FOR PUMP-PROBE EXPERIMENTS WITH FEMTOSECOND RESOLUTION

E.L. Saldin, E.A. Schneidmiller, and M.V. Yurkov
Deutsches Elektronen-Synchrotron (DESY), Hamburg, Germany

Abstract

Free Electron Laser in Hamburg (FLASH) operates successfully since the year of 2000. Permanent upgrades of the facility did allow to reduce operating wavelength from 100 nm in 2000 down to 13 nm in 2006. An upgrade of the year of 2007 is in the progress, and after its completition FLASH will reach design value of the wavelength of 6.4 nm. An attractive feature of FLASH is production of intense, ultra-short radiation pulses of sub-10-fs duration. In this paper we describe perspective upgrades of FLASH aiming at extension of the operating wavelength range while conserving the feature of ultra-short pulse production. We show that an upgrade of FLASH with a frequency doubler will allow to reduce the wavelength down to 3 nm, thus covering the "water window" – the wavelength range that is crucially important for the investigation of biological samples. We show also that recent installations at FLASH of far infrared undulator (FIR) and optical replica synthesizer (ORS) open up the possibility for implementation of schemes allowing to perform pump-probe experiments with 10 femtosecond temporal resolution.

INTRODUCTION

During last years we observe rapid progress of Self-Amplified Spontaneous Emission Free Electron Lasers (SASE FELs) [1–3]. Jump in the wavelength was by about three orders of magnitude, from 12 μm in 1997 down to 13 nm in 2006 [4–9]. Presently FLASH (Free Electron Laser in Hamburg) has produced unprecedented powers for EUV radiation at a fundamental wavelength of 13.7 nm, and harmonics with wavelengths as low as 2.75 nm [9]. After an energy upgrade to 1 GeV of the FLASH driving linac minimum wavelength in the fundamental harmonic of FLASH will be 6.4 nm.

FLASH demonstrated unique femtosecond mode of operation [6–9] which was not considered at an early design stage of the project [10]. Thorough analysis has shown that due to nonlinear compression and small local energy spread the short high-current leading peak (spike) in the bunch density distribution was produced by beam formation system. Despite strong collective effects (of which the most critical was the longitudinal space charge after compression) this spike was bright enough to drive FEL process up to the saturation for the wavelengths down to 13 nm. Analysis of the latest experimental results [9] indicate that the peak current in the spike is 2 to 2.5 kA, the FWHM length of the high current spike is approximately 30 fs and the normalized emittance is 1 to 1.5 mm-mrad. Note that the latter value is significantly less than the project one of 2 mm-mrad [10], and encouragingly approaches to the values predicted by start-to-end simulations. For FLASH this result is of crucial importance allowing to reach shorter wavelengths with fixed electron energy of 1 GeV. The first scenario for reaching "water window" at FLASH equipped with efficient frequency doubler has been analyzed a few years ago [11, 12]. That analysis has been based purely on refined start-to-end simulations. Now, with an experimentally proven update of the beam parameters we present further development of a concept of frequency doubling for generation of powerful femtosecond pulses. Application of frequency doubler at FLASH will allow to cover the water window (wavelength range between the K-absorption edges of oxygen ($\lambda = 2.34\mathrm{nm}$) and carbon ($\lambda = 4.38\mathrm{nm}$)) that is crucially important for the investigation of biological samples.

Two-color pump-probe experiments are very attractive for time-resolved studies. In this paper we show that present configuration of FLASH holds great potential for pump-probe experiments with 10 femtosecond temporal resolution. This potential stems from recent installation at FLASH of far infrared undulator (FIR) and optical replica synthesizer (ORS) [13–16]. In the case of FIR undulator optical pulses from FIR and XUV pulses from FEL are naturally synchronized since they are produced by the same electron bunch. In the case of pump-probe experiments with an external optical laser an ORS setup is used as a selection trigger for perfectly synchronized pump-probe pulses.

CONCEPT OF FREQUENCY DOUBLER

An idea of using two undulators, with the second undulator resonant to one of the harmonics of the first one, was considered in [17–19] (it is also referred to as the "afterburner" method). The first undulator is long enough to reach saturation and produce strong spatial bunching in harmonics. The bunched beam generates coherent radiation in the second undulator which follows immediately the first one. The main problem with this approach is the large induced energy spread which significantly degrades the performance of the radiator section at the harmonic fre-

GENERATION OF X-RAY FEL LIGHT USING LASER WAKEFIELD ACCELERATED ELECTRON BEAMS

O.A. Shevchenko[#] , N.A. Vinokurov, Budker Institute of Nuclear Physics, 11 Acad. Lavrentyev Prosp., 630090, Novosibirsk, Russia
Kim Ta Phuoc, Antoine Rousse, Laboratoire d'Optique Appliquée, ENSTA, CNRS UMR 7639, Ecole Polytechnique, Chemin de la Hunière, 91761, Palaiseau, France

Abstract

We consider a new class of high gain FELs based on femtosecond electron bunches with extra high current density produced by Laser Wake Field Acceleration (LWFA). The FELs of this kind can be used for generation of high power femtosecond x-ray pulses. We present the results of simulations of FEL operation with some reasonable beam parameters which will be obtained in future. We focus our attention on the advantages which can be gained from the unique possibility of the use of femtosecond hundred-kiloamperes bunches, generated by LWFA. We also consider the impact of the relatively poor electron beam properties on FEL characteristics.

INTRODUCTION

The possibility of the laser wake field acceleration (LWFA) of electron beams in plasma was explored in detail many years ago [1]. Until the present time practical application of this acceleration technique was impossible because of absence of lasers with required parameters. The rapid development of high power laser technique recently gave rise to intensive experimental investigation of LWFA [2]. At present one can obtain the laser peak power up to 1 PW with the pulse duration several tens of femtoseconds. This enables one to expect the creation of laser-plasma accelerators which can provide the peak currents several hundreds of kiloamperes with relatively small slice emittance and energy spread. Such accelerators could have very compact design as the gradient in the laser wake field can reach 300 GeV/m. They certainly would find many applications. One of them could be a source of electron bunches for the compact (tabletop) X-ray FEL [3].

The FEL operation may strongly depend on the details of the 6-D electron distribution function which can not be measured directly. Therefore it seems reasonable to make the LWFA experiments simultaneously with observation of the electron beam radiation from undulator. This way one can optimize the plasma accelerator parameters for the requirements of the X-ray SASE FEL.

In this paper we consider a possible scheme of the combined LWFA and SASE FEL experiment. We discuss some essential physical and technical problems of this experiment. They include space charge and wakefield effects, beam transport and undulator construction. Assuming some reasonable beam parameters which can be achieved in LWFA we obtain the FEL radiation parameters.

[#]O.A.Shevchenko@inp.nsk.su

DESCRIPTION OF THE ACCELERATOR AND FEL LAYOUT

Based on the X-ray FEL requirements one can imagine the scheme of the experimental setup which is shown in Fig. 1.

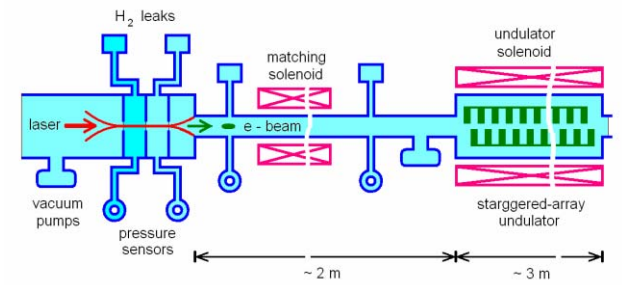

Figure 1. Possible scheme of the combined LWFA and X-ray FEL experiment.

In most of the existing LWFA experiments plasma volume is created in a gas jet or capillary and the transverse laser beam size does not exceed 10 microns [2]. For the laser pulse energy available now it seems worthwhile to increase the transverse laser beam size one order of magnitude and use the gas volume with optimized pressure profile. In addition one can use the gas focusing in the beam transport line after accelerator and inside undulator which matches very well with the electron acceleration in the same gas.

At the scheme presented in Fig. 1 the accelerator region is separated from the vacuum channel by narrow orifice through which the laser radiation is injected into the gas volume. To minimize multiple scattering the gas is hydrogen. The gas pressure is chosen to be $\sim 5\times10^{-3}$ atm so that acceleration up to 1 GeV occurs at the distance 10 cm. Additional diaphragms are placed along the accelerator axis. It allows to optimize the pressure profile.

For the compactness of the experimental setup it is desirable to obtain the FEL gain length no more then several tens of centimetres. The electron beam β-function in undulator should be of the same order of magnitude. It can be achieved by applying of gas focusing which works effectively at high beam peak currents. The focusing occurs because the beam electrical field is partly screened due to gas dielectric permeability and beam focuses itself by magnetic field (at high beam currents collective electric field may ionize atoms, and therefore effective permeability will increase). Usually the gas permeability

DIFFRACTION EFFECTS IN THE COHERENT TRANSITION RADIATION BUNCH LENGTH DIAGNOSTICS *

G. Kazakevich, V. Lebedev, S. Nagaitsev,
FNAL, P.O. Box 500, Batavia, Illinois 60510, USA

Abstract

Diffraction effects in the Coherent Transition Radiation (CTR) bunch length diagnostics are considered for the A0 Photoinjector and the NML injection module. The effects can cause a noticeable distortion of the measured CTR spectra depending on the experimental setup and the bunch parameters and resulting in errors of the bunch length measurenents. Presented calculations show possible systematic errors in the bunch length in measurements based on the CTR spectra at A0 Photo injector and the NML injection module.

INTRODUCTION

Application of the CTR diagnostics for the sub-picoseconds bunch length measurements was proposed more than 10 years ago and a number of articles have been devoted to the experiments in this field. The diagnostics employing the Transition Radiation (TR), [1], are based on the measurements of the CTR spectra to restore the bunch length through the Fourier transform. In this article we consider low-frequency TR range where the coherent part of the spectrum dominates and the wavelengths are about the bunch length. For such low-frequency harmonics one should not neglect the diffraction effects in the coherent radiation diagnostics, [2, 3, 4]. They can strongly distort the measured CTR spectra depending on the beam energy and the experimental setup. We discuss computations of the CTR diffraction effects in application to the measurements at A0 Photoinjector, [5], and the NML injection module [6].

ELECTRIC FIELD OF THE TR AND CTR

Most experimental techniques using CTR spectra for the bunch length measurements employ backward TR generated at 45^0 incidences of electrons on the mirror-quality metallic screen. This radiation has a spectral density practically similar to the one for the backward TR at the normal incidence. For simplicity we consider only this case. To estimate the diffraction effects we assume a finite radius *a* of the TR screen. Finite size of vacuum chamber we do not consider for sake of simplicity though it also affects the bunch longitudinal profile. We also assume that the screen is located at the origin of the cylindrical frame η: $(\rho, \phi, z = 0)$, and the *z* axis is directed along the momentum of the electron beam. The observation point is displaced at a distance *D>>a* along *z*. A derivation of required formulae generally follows to Ref. [4], where the consideration is based on the virtual-photon method applicable for ultra relativistic electrons.

The Fourier harmonic of the radial electric field for the incident single electron is expressed as, [7, 4]:

$$\tilde{E}_r(\omega,\rho) = \frac{-e\omega}{(2\pi)^{3/2}\varepsilon_0\beta^2c^2\gamma} K_1\left(\frac{\omega\rho}{\beta c\gamma}\right), \quad (1)$$

where: ε_0 is the permittivity of vacuum, $K_1(u)$ is the second kind modified Bessel function. We assume that the virtual photon constituting the electron self-field is converted into the real TR photon. Considering continuity of the normal components of the electric induction and tangential components of the electric field of the virtual and real (reflected) photons, [8], one can conclude that the amplitudes of the radial components of virtual and real photons are same, i.e. the electric field of an ultra relativistic electron is almost completely reflected from metal screen. The small element of the TR screen with coordinates $(\rho,\phi,0)$ gives following contribution to the field (this field is also radial) in the point of observation *(x,0,D)* :

$$d\tilde{E}_x(x,0,D,\omega) = \frac{-i\omega}{2\pi c}\tilde{E}_r(\omega,\rho)\cos\phi\frac{e^{\frac{i\omega R'}{c}}}{R'}\rho d\rho d\phi \cdot \quad (2)$$

Here: R' is a distance between the points $(\rho,\phi,0)$ and (*x*,0,*D*),

$$R' = \sqrt{D^2 + (x-\rho\cos\phi)^2 + (\rho\sin\phi)^2} \approx R - \frac{x\rho\cos\phi}{R} + \frac{\rho^2}{2R}, \quad (3)$$

and: $R = \sqrt{D^2 + x^2}$. Substitution (1) and (3) into (2) with $x/R = \sin\theta$ and integration over the TR screen area yields for the electric field in the point (*x*,0,*D*):

$$\tilde{E}_x(x,0,D,\omega) \approx \frac{ie\omega^2}{(2\pi)^{5/2}\varepsilon_0\beta^2c^3\gamma}\cdot\frac{e^{\frac{i\omega R}{c}}}{R}\times \int_0^a\left[\int_0^{2\pi}K_1\left(\frac{\omega\rho}{\beta c\gamma}\right)\cos\phi\cdot e^{\frac{-i\omega\rho\sin\theta\cos\phi}{c}}d\phi\right]\cdot e^{\frac{i\omega\rho^2}{2cR}}\rho d\rho \cdot \quad (4)$$

In this expression the integration over angle ϕ gives the first kind Bessel function $J_1(z)$:

$$\int_0^{2\pi} e^{\frac{-i\omega\rho\sin\theta\cdot\cos\phi}{c}}\cos\phi\cdot d\phi = -i2\pi\cdot J_1\left(\frac{\omega\rho\sin\theta}{c}\right),$$

That yields:

*Work supported by Fermi Research Alliance LLC. Under DE-AC02-07CH11359 with the U.S. DOE
#kazakevi@fnal.gov

SIMULATIONS FOR THE LCLS INJECTOR

C.Limborg-Deprey*, D.H. Dowell, P.Emma, R.Iverson, J.Frisch, H.Loos, J.Turner, J.Schmerge, J.Welch, J.Wu, Y.Ding, Z.Huang, J.Castro, G.Hays, P.Hering, S.Gilevich, A Miahnahri, W.White
SLAC[#], MS 18, SLAC 2575 Sand Hill Road, Menlo Park, CA , U.S.A.

Abstract

The Linac Coherent Light Source (LCLS) Injector has now been commissioned for five months. Measurements made at the end of the Injector beamline show that the beam quality meets the specifications. The transverse projected emittances at 135MeV are in the range of 1.2 mm-mrad for 1nC/100A and the horizontal slice emittances are below 1 mm-mrad. In this paper, we discuss the validity of both emittance and bunch length measurements by comparing them with results from simulations made with a multi-particle tracking code.

INTRODUCTION

The LCLS Injector commissioning started on April 5th 2007 after several years of design, manufacturing and installation. After a few months of commissioning, the beam quality at 135 MeV reached design performances with projected emittances varying from 1 to 1.5 mm-mrad at 1nC and peak current of 100A [1] .

A bunch charge of 1nC charge was obtained after "passive" and "active" laser cleaning were done. "Passive" cleaning is done at nominal laser fluence while operating. In particular, when the laser radius was decreased from 1.0 to 0.7 mm, to minimize the transverse emittances, a factor two increase in quantum efficiency was obtained after one week of operation at that new setting. "Active" cleaning was then performed switching off the RF and forcing the laser fluence to 2.5 times higher levels than nominal while scanning the cathode position. It then allowed us to reach 1nC at 300 μJ on the cathode and 30 degrees laser injection phase.

In this paper, we discuss the validity of transverse emittance numbers deduced from the measurements by comparing them to numbers obtained from simulated data after processing those latter following the same method as that applied to measured data. In the 135 MeV section of the LCLS Injector, the emittance can be obtained by either determining beam sizes at three screens (separated by 60 degree phase advance) or at a single screen while scanning an upstream quadrupole (quad scan). The beam sizes are measured using OTR screens or wire scanners. All combined, this gives at least four types of measurements. The rms beam sizes can be extracted following various algorithms which truncate the tails of the distributions at different levels. Similar truncation levels were applied to the simulated data. The first part of this paper shows that the emittance value rapidly decreases when long tails are truncated. Emittances as low as 1.2 mm-mrad in both planes for 1nC seem realistic for 90-95% of the particles constituting the core of the bunch.

* Corresponding author: limborg@slac.stanford.edu
# SLAC is operated by Stanford University for the Department of Energy under contract number DE-AC03-76SF00515

In the second part of this paper, we report on the effort made to benchmark the simulation code IMPACT [2] to the experimental data. Multi-particle tracking codes [3,4] had been used intensively at the design stage of the LCLS injector to specify tolerances of the beamline components and of the drive laser [5]. In this paper, we present results calculated with the 3D algorithm of the IMPACT code. 3D simulations are essential to represent our asymmetric beam. IMPACT can run on parallel processors, making 3D calculations time efficient.

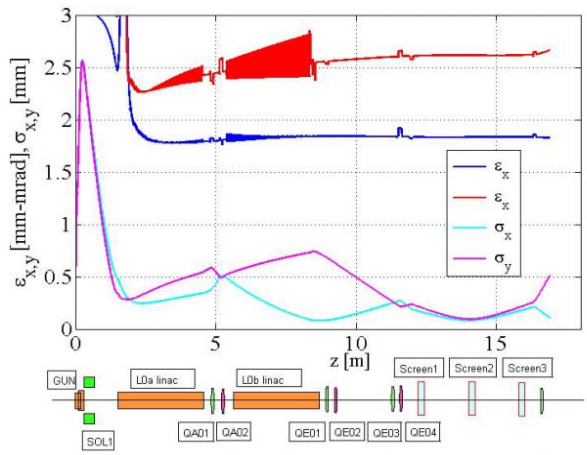

Figure 1: Beam size and 100% projected emittance for optimized beamline – the beam is matched to the 3-screens – the three OTR screen locations are shown

EMITTANCE

Transverse Tails

The initial distribution used in the simulations presented in this chapter uses the virtual cathode drive laser image as a transverse profile. The laser spot on the cathode, and thus the virtual cathode, is the image of an aperture limiting our transversally Gaussian laser profile. Even if the emission profile has hard edges, see figure2-a, the photo-electron beam develops large transverse tails. To evaluate the effect of those tails on the emittance calculations, simulations with 2 levels of meshing were used: 32 x 32 x 32 or 128 x 128 x 64. The first set was run with 200k particles and the second one with 4 million particles. No noticeable difference was seen in the generation of transverse tails and emittance results were within a few percent. In both cases some islands of higher density were preserved down the beamline as shown in the three screen profiles of figure 3. The 4 million particle distribution case shows finer structure in the profile than the 200k distribution. But, the 12μm

PRELIMINARY STUDY OF QUIET START METHOD IN HGHG FEL SIMULATION*

Y.Hao#, L.H.Yu, BNL, Upton, NY 11973, U.S.A.
Y.Hao, Indiana University, Bloomington, IN 47405, U.S.A.

Abstract

Quiet start scheme is broadly utilized in Self Amplified Spontaneous Radiation (SASE) FEL simulations, which is proven to be correct and efficient. Nevertheless, due to the energy modulation and the dispersion section, the High Gain Harmonic Generation (HGHG) FEL simulation will not be improved by the traditional quiet start method. A new approach is presented to largely decrease the number of macro-particles per slice that can be implemented in both time-independent and time-dependent simulation, accordingly expedites the high order harmonic cascade simulation or other small modulation HGHG cases.

INTRODUCTION

Great interest has been focused in single pass free electron laser (FEL) for many years for the capability of generating coherent radiation with high intensity and short pulse duration in short wavelength from deep ultraviolet (~100 nm) to hard x-ray (~0.1nm). The scheme, self amplified spontaneous radiation (SASE), has been carefully study in both theory and experiment. The simulation of SASE FEL process is achieved by using the quiet start method[1,2], which reduces the macro particle number and simulation time dramatically. However, SASE FEL is seeded by the shot noise of electron bunch; hence produce limited temporal coherence and large shot-to-shot intensity fluctuation.

An alternate approach for SASE FEL is the high gain harmonic generation (HGHG) FEL. As the first HGHG FEL experiment is accomplished successfully and overcome the limit of SASE FEL [3], increasing projects were proposed to produce fully coherent VUV and soft X-ray radiations sources using cascade HGHG scheme.

The Quiet Start scheme, which reduces the number of macro particles largely in SASE simulation, uses only small number of distinguished phase ψ (usually 4). Each phase is filled with identical macro particle distribution of other 5 dimensions (γ, x, y, p_x, p_y), which is generated by pseudo random number generator or Hammersley quasi-random sequence. However, the quiet start scheme does not lead to correct bunching factor in terms of HGHG process.

A quiet start method scheme for HGHG is introduced in [4]. In the article, we consider a more dedicate method to realize 'Quiet Start' initial particle loading in small modulation case when the modulator and dispersion sessions exist, in order to achieve correct bunching factor at the entrance of radiator. When energy modulation is small because of a weak seed laser, the beam energy spread is large or dispersion effect is large so that the beam is over bunched, the signal (bunching factor) generated by modulator and dispersion section will be small. Such small bunching factor will be overwhelmed by the noise of initial loading method such as Hammersley sequence, if the number of macro particles is not large enough. The quiet start loading method is to find a way to generate less noise with same number of macro particles compared with normal loading methods. To introduce our method on the small modulation HGHG FEL simulation, first we will derive the bunching factor errors produce by this quiet start scheme in 1-D case theoretically. Then 3-D scheme is carried out with utilizing Hammersley sequence on transverse dimensions to reduce noise. One example of small modulation HGHG scheme is demonstrated to show the effectiveness of the method in the last section.

ONE DIMENSION ANALYSIS

In the HGHG FEL scheme, the bunching factor after energy modulation and dispersion section can be calculated theoretically using a simplified one dimension model. Assuming that the phase space distribution is described by distribution written in variable $\gamma = E/mc^2 - \gamma_c$, $\theta = (k_0 + k_w)z - \omega_0 t$, where E is the energy of electron, mc^2 is electron mass, γ_c corresponds to the resonance energy, k_0 and ω_0 is the resonance wave number and resonance angular frequency, k_w is the undulator wave number.

The initial distribution function can be written as Eq. (1), with energy spread σ_γ,

$$f(\gamma_0, \theta_0) = \frac{1}{\sqrt{2\pi}\sigma_\gamma} \exp\left(-\frac{\gamma_0^2}{2\sigma_\gamma^2}\right) \tag{1}$$

After the modulator, the electron bunch energy is modulated to (γ', θ')

$$\begin{aligned} \gamma' &= \gamma_0 + \Delta\gamma \sin(\theta_0) \\ \theta' &= \theta_0 \end{aligned} \tag{2}$$

The energy modulation strength $\Delta\gamma$ can be calculated from the modulator strength and seed laser power.

The dispersion section gives rotation on the longitudinal phase space and change the energy modulation to density modulation. The new coordinate (γ'', θ'') is given by

$$\begin{aligned} \gamma'' &= \gamma' = \gamma_0 + \Delta\gamma \sin(\theta_0) \\ \theta'' &= \frac{d\theta}{d\gamma}(\gamma_0 + \Delta\gamma \sin(\theta_0)) + \theta_0 \end{aligned} \tag{3}$$

*Work supported by U.S.DOE under contract No DE-FG02-92ER40747 and NSF under contract No PHY-0552389
#yhao@bnl.gov

FREE ELECTRON LASERS AND HIGH-ENERGY ELECTRON COOLING*

Vladimir N. Litvinenko, BNL, Upton, Long Island, NY, USA#
Yaroslav S. Derbenev, TJNAF, Newport News, VA, USA)

Abstract

Cooling intense high-energy hadron beams remains a major challenge in modern accelerator physics. Synchrotron radiation of such beams is too feeble to provide significant cooling: even in the Large Hadron Collider (LHC) with 7 TeV protons, the longitudinal damping time is about thirteen hours. Two cooling methods (or combination of them) – stochastic cooling (CS) based on broad-back RF feedback(s) and electron cooling (EC) driven by energy recovery linac (ERL) – are under development for cooling high energy hadron colliders.

In this paper we focus on Coherent Electron Cooling (CEC), an unique technique which promising significantly better efficiency that the above-mentioned techniques, in a wide energy range. In the early 1980s, CEC was suggested as a possibility for using various microwave instabilities in an electron beam to enhance its interaction with hadrons (i.e., cooling them). The capabilities of present-day accelerator technology, ERLs, and high-gain Free-Electron Lasers (FELs), finally caught up with the idea and provided the all necessary ingredients for realizing such a process at energies typical for hadron colliders.

In this paper, we discuss the principles, and the main limitations of the CEC process based on a high-gain FEL driven by an ERL. We also present, and summarize in Table 1, some numerical examples of CEC for ions and protons in RHIC and the LHC.

INTRODUCTION

In contrast with electron- and positron-beams, hadron beams in storage rings (colliders) do not have strong loss mechanism (such as synchrotron radiation for electrons) and, therefore, do not have a natural damping mechanism to reduce their energy spreads and emittances.

There are several reasons why cooling high-energy hadron beams, mostly at the top energy range of a collider, is strongly desirable.

First, any increases in the longitudinal- and transverse-emittances of a hadron beam accumulated during multi-stage acceleration from a source to the store energy (collision) remain in the beam. Any instability causing the growth of emittance (for example, that of the electron cloud that is the limiting factor for most modern hadron colliders) may entail the need to discard accelerated beams and start the process again. In any case, present-day high-energy hadron colliders do not have control of beam emittances at the collision energy, and are forced to use beams as they are; this is not always the optimum approach.

The main figure of merit of any collider is its average luminosity, i.e., its average productivity for an appropriate branch of physics. Cooling hadron beams at top energy may further this productivity.

For a round beam, typical for hadron colliders, the luminosity is given by a simple expression:

$$\mathcal{L} = f_c \frac{N_1 N_2}{4\pi\beta^*\varepsilon} \cdot h\left(\frac{\sigma_s}{\beta^*}\right) \qquad (1)$$

where N_1, N_2 are the number of particles per bunch, f_c is their collision frequency, β^* is the transverse β-function at the collision point, ε is the transverse emittance of the beam, σ_s is the bunch length, and $h \le 1$ is a coefficient accounting for the so-called hourglass effect [1]:

$$h(x) = \frac{\sqrt{\pi}}{x} e^{1/x^2} erfc(1/x).$$

The hourglass effect is caused by variations in the beam's size $\sigma_r^2 = \beta^*\varepsilon\left(1 + s^2/\beta^{*2}\right)$ along the length of the collision region, which is defined by the bunch-length, σ_s. Accordingly, for h >0.75, β^* should be limited to values $\beta^* \ge \sigma_s$. Hence, longitudinal cooling of hadron beam may allow reduction of β^* and increase the colliders' luminosity. Plans are to use a non-zero crossing angle at the Large Hadron Collider (LHC) at CERN. In this case, reducing the bunch's length would directly contribute to increasing the luminosity and eliminating the necessity of having a complicated crab-crossing system.

The effect of transverse emittance cooling on the collider's luminosity is less straightforward, but is also important. For beams with limited intensities, the luminosity (1) grows as the transverse emittance decreases. Furthermore, reduction of the beam emittance (in combination with bunch shortening) provide favorite conditions for lowering β^* using final focusing quadrupoles with smaller aperture.

In many colliders luminosity is limited by beam-beam effects. In this case reduction of the transverse emittance would require also proportional reduction of the bunch intensities, N_1 (and sometimes N_2) in eq.(1), which may cause reduction of luminosity per bunch. Possible luminosity improvements in these cases are collider specific.

In eRHIC – BNL's plan for electron-hadron collider (EIC)- polarized electrons accelerated in an ERL will collide with hadrons stored in the RHIC's storage ring [2]. In this case, a reduction of the transverse emittance of the hadron beam engenders a proportional reduction of the electron beam's intensity while maintaining its ultimate luminosity constant [3]. Reduction of the electron beam's current has multiple advantages: reducing the strain on the polarized electron source, proportionally lowering synchrotron radiation (the main source of the

* Work performed under the auspices of the U.S. Department of Energy.
# Corresponding author vl@bnl.gov

COMMISSIONING RESULTS OF THE LCLS INJECTOR*

D. H. Dowell#, R. Akre, Y. Ding, P. Emma, J. Frisch, S. Gilevich, G. Hays, Ph. Hering, Z. Huang, R. Iverson, C. Limborg-Deprey, H. Loos, A. Miahnahri, J. Schmerge, J. Turner, J. Welch, W. White, J. Wu, *SLAC*, *Stanford*, CA 94309, USA,
L. Froelich, T. Limberg, E. Prat, *DESY*, *Hamburg*, Germany

Abstract

The Linac Coherent Light Source (*LCLS*) is a SASE x-ray Free-Electron Laser (FEL) project presently under construction at SLAC [1]. The injector section, from drive-laser and RF photocathode gun through first bunch compressor chicane, was installed in fall 2006. Initial system commissioning with an electron beam has recently been completed. The second phase of construction, including second bunch compressor and full linac, is planned for 2008. In this paper, we report experimental results and experience gained during the first phase of machine commissioning. This includes the cathode, drive laser, RF photocathode gun, linac booster section, S-band and X-band RF systems, first bunch compressor, and the various beam diagnostics.

INTRODUCTION

The months of April through August 2007 have been spent commissioning the *LCLS* injector. This is the first phase of machine commissioning, with the second phase starting in Dec. 2007 after a 3-month downtime, and the final phase in Nov. 2008, culminating in FEL light in 2009. First electrons from the new photocathode RF gun were observed on April 5 and beam was quickly established to the full (injector) energy of 250 MeV in the main SLAC linac on April 14, 2007 [2]. Over the next five months all the injector systems were commissioned and the beam accelerated to 15 GeV at the end of the SLAC linac. The bunch charge (1 nC) and the measured projected emittance of 1.2 microns meets the design requirements of LCLS.

DESCRIPTION OF THE INJECTOR

Figure 1 shows the major components of the LCLS injector at the 2 kilometer point of the 3 kilometer SLAC linac. The off-axis housing was built during the original construction of the linac in 1962 [3], anticipating future injection beamlines such as LCLS.

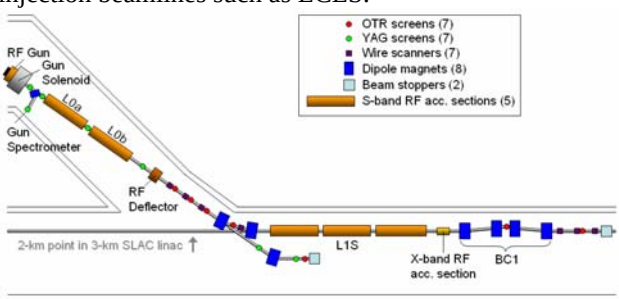

Figure 1: The injector for LCLS located in the off-axis housing at Sector 20, at the 2/3-point along the linac.

The LCLS injector begins with a photocathode RF gun followed by two modified SLAC linac sections producing a beam at 135 MeV, 100 amps peak current and transverse normalized emittance of 1.2 microns for 1 nC bunches. The cathode drive laser is located in a reconstructed alcove above the RF gun. The 135-MeV beam is deflected onto the main linac axis by a two-dipole 35 degree doubly achromatic bend or, with the first 17.5 degree dipole magnet turned off, the beam drifts to a 35 degree straight ahead spectrometer for energy and energy spread measurements. Once on the axis of the main linac, the electrons are accelerated to 250 MeV in three linac structures before entering the first chicane bunch compressor, BC1. Between the three linacs and BC1 is a short x-band structure whose 4th harmonic straightens the beam's longitudinal phase space for linear compression.

THE DRIVE LASER

The RF gun's copper cathode is illuminated by a UV laser operating at 255 nm delivering up to 450 microjoules per pulse at 120 Hz. In addition to the wavelength and energy, the laser must meet stringent stability and reliability requirements as well as strict transverse and longitudinal shaping specifications. The stability specifications were achieved with a pulsed Ti:sapphire system pumped by two quasi-cw, diode pumped Nd:YAG lasers (Figure 2); however the shaping requirements have not been met.

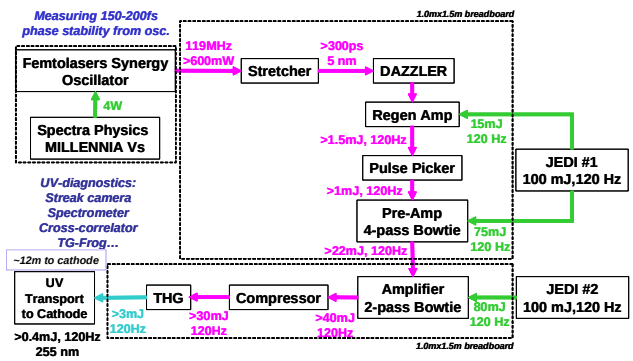

Figure 2: A block diagram of the RF gun drive laser designed and built by Thales Lasers.

The laser pulse shape is measured by combining a short pulse from the oscillator with the UV pulse in a non-linear crystal allowing back-conversion of the mixed signal to the second harmonic. A cross correlation measurement of the UV pulse sent to the cathode is shown in Figure 3.

* Work supported by US DOE contract DE-AC02-76SF00515.
# dowell@SLAC.Stanford.edu

DIRECT MEASUREMENT OF PHASE SPACE EVOLUTION IN THE SPARC HIGH BRIGHTNESS PHOTOINJECTOR*

E. Chiadroni[a†], D. Alesini[a], A. Bacci[c], M. Bellaveglia[a], R. Boni[a], M. Boscolo[a], M. Castellano[a], L. Catani[b], S. Cialdi[c], A. Cianchi[b], A. Clozza[a], L. Cultrera[a], G. Di Pirro[a], A. Drago[a], A. Esposito[a], M. Ferrario[a], L. Ficcadenti[e], D. Filippetto[a], V. Fusco[a], A. Gallo[a], G. Gatti[a], A. Ghigo[a], L. Giannessi[d], M. Incurvati[a], C. Ligi[a], M. Migliorati[e], A. Mostacci[e], P. Musumeci[f], E. Pace[a], L. Palumbo[e], L. Pellegrino[a], M. Petrarca[g], M. Quattromini[d], R. Ricci[a], C. Ronsivalle[d], J. Rosenzweig[f], A.R. Rossi[c], C. Sanelli[a], L. Serafini[c], M. Serio[a], F. Sgamma[a], B. Spataro[a], F. Tazzioli[a], S. Tomassini[a], C. Vaccarezza[a], S. Vescovi[a], C. Vicario[a]

[a]INFN-LNF, via E. Fermi, 40 - 00044 Frascati, Rome, Italy

[b]INFN-Roma "Tor Vergata", via della Ricerca Scientifica, 1 - 00133 Rome, Italy

[c]INFN-Milano, Via Celoria 16, 20133 Milan, Italy

[d]ENEA C.R., via E. Fermi, 00044 Frascati, Rome, Italy

[e]Università di Roma "La Sapienza", Dip. Energetica, via A. Scarpa, 14 - 00161, Rome, Italy

[f]UCLA - Dept. of Physics and Astronomy, 405 Hilgard Avenue, Los Angeles, California 90095, USA

[g]INFN-Roma I, p.le A. Moro 5, 00185 Roma, Italy

Abstract

The characterization of the transverse phase space for high charge density relativistic electron beams is a fundamental requirement in many particle accelerator facilities, in particular those devoted to fourth-generation synchrotron radiation sources, such as SASE FEL.
The main purpose of the SPARC initial phase was the commissioning of the RF photoinjector. At this regard, the evolution of the phase space has been fully characterized by means of the emittance meter diagnostics tool, placed in the drift after the gun exit.
The large amount of collected data has allowed for the first time a detailed reconstruction of the transverse phase space evolution downstream the RF, giving evidences of the emittance compensation process as predicted by theory and simulations.
In particular the peculiar behavior of a flat top longitudinal electron distribution compared to a gaussian distribution has been studied giving important insights for the correct matching with the following linac whose working point is based on the double emittance minimum effect.

INTRODUCTION

The SPARC project is an R&D activity oriented to the development of a high brightness photoinjector to drive SASE FEL experiments [1]. In the first phase, the SPARC layout (Fig.1) consisted of a 1.6 cell RF gun operated at S-band (2.856 GHz, of the BNL/SLAC/UCLA type) and high peak field on the cathode ($\simeq$ 120 MV/m) with incorporated Copper photo-cathode, generating a 5.6 MeV energy beam. The first few meters of beam propagation, where space charge effects and plasma oscillations dominate the electron dynamics, have been studied by means of the movable emittance meter [2]. This device, based on the 1D

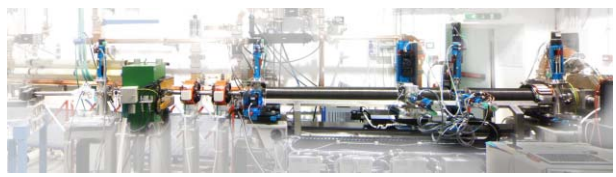

Figure 1: The SPARC photoinjector in the initial phase: from the right to the left, the RF gun with the solenoid, the emittance meter, quadrupoles and dipole magnets, the energy spectrometer and the beam dump.

pepper-pot technique, has allowed not only to measure the beam size and emittance, but also to reconstruct the transverse phase space at different positions along the direction of motion. Due to the high sensitivity of this method, a very precise emittance value can be calculated directly from the phase space analysis. For this reason, suitable data processing algorithms have been developed.
In the next phase of SPARC, which will start in Autumn, the beam emerging from the gun will be focused and matched into 3 accelerating sections of the SLAC type (S-band, TW), to boost the beam energy up to 155-200 MeV and to drive a SASE FEL at 530 nm.

SYSTEM DESCRIPTION AND OPTIMIZATION

To reach its goal SPARC requires a temporally flat, pico-second laser source. This source [3] is based on a Ti:sapphire oscillator that generates 100 fs pulses with a

* Work partially supported by the EU Commission in the sixth framework program, Contract No. 011935 EUROFEL-DS1 and from the MIUR Progetti Strategici DD1834.

† enrica.chiadroni@lnf.infn.it

SUPERCONDUCTING PHOTOINJECTOR

Ilan Ben-Zvi, Andrew Burrill, Rama Calaga, Xiangyun Chang, Ranjan Grover, Ramesh Gupta, Harald Hahn, Lee Hammons, Dmitry Kayran, Jorg Kewisch, Robert Lambiase, Vladimir N. Litvinenko, Gary McIntyre, Damayanti Naik, David Pate, David Phillips, Eduard Pozdeyev, Triveni Rao, John Smedley, Roberto Than, Robert J. Todd, Dan Weiss, Qiong Wu, Alex Zaltsman, BNL, Upton, Long Island, New York
Michael Cole, Michael Falletta, Douglas Holmes, John Rathke, Tom Schultheiss, Robert Wong, AES, Medford, New York
Alan Murray Melville Todd, AES, Princeton, New Jersey

Abstract

One of the frontiers in FEL science is that of high power. In order to reach power in the megawatt range, one requires a current of the order of one ampere with a reasonably good emittance. The superconducting laser-photocathode RF gun with a high quantum efficiency photocathode is the most natural candidate to provide this performance. The development of a 1/2 cell superconducting photoinjector designed to operate at up to a current of 0.5 amperes and beam energy of 2 MeV and its photocathode system are the subjects covered in this paper. The main issues are the photocathode and its insertion mechanism, the power coupling and High Order Mode damping. This technology is being developed at BNL for DOE nuclear physics applications such as electron cooling at high energy and electron ion colliders..

INTRODUCTION

In the past few years we are witnessing the growth of a new class of particle accelerators: high-power, high-brightness electron beams. This emerging technology is enabled by the combination of high-brightness electron sources and high-current SRF Energy Recovery Linacs (ERL). While the current state-of-the-art is at about 10 mA current [1] (the Jefferson Laboratory FEL upgrade), there is interest in much higher currents, in the range of 0.1 ampere to over 1 ampere CW, with emittances that are of the order of under 1 to a few 10's microns normalized rms, depending n the application, in particular on the bunch charge.

What are the applications driving this interest? First, as the Jefferson Laboratory example suggests, high power Free-Electron Laser (FEL) is one candidate. The high-brightness is required for the lasing conditions at UV or shorter wavelength, and significantly higher currents are desirable for high power FEL applications [2]. The energy required for such applications is not very high, in the range of 100 MeV to less than 1 GeV for UV high-power FELs.

The next application is also for the production of electromagnetic radiation, but for mostly spontaneous emission. This is the ERL based light sources [3,4]. For this application the current may be in the range of 100 mA, less for the extremely high brightness X-ray radiation or higher for flux dominant applications. The required energy is between 3 and 10 GeV.

Another application is in an altogether different field, electron ion colliders [5]. In this type of machine a current of hundreds milliampere electrons or polarized electrons is needed at energy of up to 10 or 20 GeV.

A somewhat specialized application is electron cooling of hadron storage rings, in particular heavy ion beams [6]. This application requires electron beams at currents of up to 0.1 amperes but relatively low energies of under 100 MeV. Finally, there are a host of other applications that have been demonstrated but are still under development: X-ray sources via Thomson scattering of laser on the electron beam and terahertz radiation a examples.

The electron gun and injector design is arguably the most critical part of the ERL. It is here that the ultimate performance of the ERL is determined: What will be its current, its bunch structure, and its transverse and longitudinal emittances. These parameters can only be degraded in subsequent parts of the ERL, never improved. The gun and injector are also the most dynamic elements, with rapid progress being made. It has some of the most intractable problems, in particular the issue of providing a good photocathode and dealing with severe space-charge interaction and limited space. The flip side of this is that any improvement made in this relatively small element affects the performance of the complete ERL and can easily lead to dramatic improvements.

In this paper we will look at the technology and challenges confronting the development of high-current, high-brightness electron sources and describe the approach taken by the few laboratories which are actively developing this technology: Brookhaven National Laboratory and Advanced Energy Systems, KF Rossendorf, the University of Peking and DESY.

THE CURRENT STATUS OF SRF GUNS

The first pioneering experimental work on a superconducting RF gun took place about 15 years ago in Wuppertal by Michalke [7]. The activity in the area of SRF guns around the world is growing steadily. Successful milestone operation of a SRF gun with a superconducting half-cell cavity were carried out in 2002

*Work done under the auspices of the US Department of Energy
#benzvi@bnl.gov

A COMPACT ELECTRON SPECTROMETER FOR AN LWFA*

A.H. Lumpkin**, R. Crowell, Y. Li, and K. Nemeth
Argonne Accelerator Institute, Argonne National Laboratory, Argonne, IL 60439, U.S.A

Abstract

The use of a laser wakefield accelerator (LWFA) beam as a driver for a compact free-electron laser (FEL) has been proposed recently. A project is underway at Argonne National Laboratory (ANL) to operate an LWFA in the bubble regime and to use the quasi-monoenergetic electron beam as a driver for a 3-m-long undulator for generation of sub-ps UV radiation. The Terawatt Ultrafast High Field Facility (TUHFF) in the Chemistry Division provides the 20-TW peak power laser. A compact electron spectrometer whose initial fields of 0.45 T provide energy coverage of 30-200 MeV has been selected to characterize the electron beams. The system is based on the Ecole Polytechnique design used for their LWFA and incorporates the 5-cm-long permanent magnet dipole, the LANEX scintillator screen located at the dispersive plane, a Roper Scientific 16-bit MCP-intensified CCD camera, and a Bergoz ICT for complementary charge measurements. Test results on the magnets, the 16-bit camera, and the ICT will be described, and initial electron beam data will be presented as available. Other challenges will also be addressed.

INTRODUCTION

One of the challenges of the laser wakefield accelerator (LWFA) project is generation of robust, quasi-monoenergetic electron beams. At the AAC06 Workshop a number of laboratories reported observation of such beams ranging in energies from 10s of MeV to 1 GeV with charges ranging from 10 s to 100 s of pC [1]. The Chemistry Division is currently using and developing an LWFA within their Terawatt Ultrafast High Field Facility (TUHFF) [2]. Although pulsed radiolysis chemistry experiments are the primary objective, an initiative to demonstrate an LWFA operating in the bubble regime [3] with quasi-monoenergetic beams is being driven by Strategic LDRD funds. A long-range goal of this project is to use the beam to drive an undulator for generation of ultrafast spontaneous radiation. Other laboratories have targeted the possible driving of a free-electron laser (FEL) [4]. As part of the present ANL project, characterization of the electron beams generated is a critical aspect. Towards this end an electron beam spectrometer is needed to measure the electron beam spectrum to look for the energy peak and energy spread. This is in addition to a basic charge measurement and a beam divergence measurement. The compact spectrometer design is based on that reported by Glinec et al. [5].

*Work supported by the U.S. Department of Energy, Office of Science, Office of Basic Energy Sciences, under Contract No. DE-AC02-06CH11357.
**lumpkin@aps.anl.gov

EXPERIMENTAL BACKGROUND

The 20-TW laser at TUHFF consists of a three-stage chirped-pulse amplified Ti:Sapphire laser system running at 10 Hz. The 15-fs (FWHM) seed pulse train from the oscillator is stretched to 440 ps in a double-pass single grating stretcher, and then a Pockels cell pulse picker is used to lower the repetition rate to 10 Hz. The beam passes through a three-stage amplifier and then is directed into a two-grating pulse compressor resulting in a 600-mJ, 30-fs (FWHM) pulse of 20 TW. A schematic is shown in Fig. 1. A more detailed description of the laser system can be found elsewhere [6]. The compressed laser beam is then directed into the interaction chamber and focused to about 30 μm size onto the 1.2-mm-diameter supersonic He gas jet. Electron pulses of relativistic energies are generated and pass through a rotating Cu disk that blocks the laser beam, but transmits the electrons to a sample or the electron spectrometer or other diagnostics.

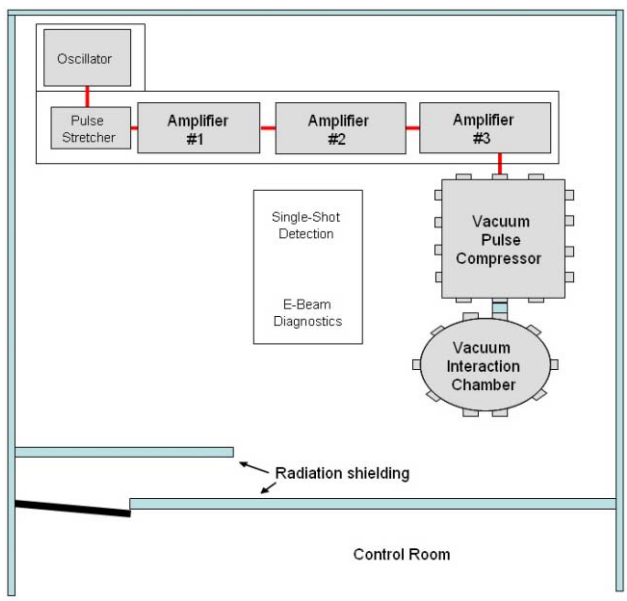

Figure 1: Schematic of the TUHFF with the Ti:Sapphire oscillator, pulse stretcher, three amplifiers, pulse compressor, and the interaction chamber.

Compact Electron Spectrometer

The major components of a compact electron spectrometer based on the Ecole Polytechnique University LOA design [3,5] are the permanent magnet dipole; the scintillator screen at the dispersive plane; the 16-bit CCD camera with optics, which views the screen; and an integrating current transformer (ICT) for complementary charge measurements.

Permanent Magnet Dipole: The two NdFeB magnets are 5 cm long by 2.5 cm wide by 1.2 cm thick. Magnet characterization was performed by the APS Magnetic

ADAPTIVE 3-D UV-LASER PULSE SHAPING SYSTEM TO MINIMIZE EMITTANCE FOR PHOTOCATHODE RF GUN AND NEW LASER INCIDENCE SYSTEM

H. Tomizawa, H. Dewa, T. Taniuchi, A. Mizuno, T. Asaka, K. Yanagida, S. Suzuki, T. Kobayashi, H. Hanaki, Accelerator Division, Japan Synchrotron Radiation Research Institute (JASRI/SPring-8), Kouto, Sayo-cho, Sayo-gun, Hyogo 679-5198, Japan
F. Matsui, Creative & Advanced Research Department, Industrial Technology Center of Fukui Prefecture, 61 Kawaiwashitsuka-cho, Fukui City 910-0102, Japan.

Abstract

We developed an adaptive 3-D shaping (both temporal (1D) and spatial (2D)) short pulse (80 fs~40 ps) UV-laser system as an ideal light source for yearlong stable generation of a low-emittance electron beam with a high charge (1~2 nC/pulse). In its current form, the laser's pulse-energy stability has been improved to 0.2~0.3% (rms; 10 pps, 0.4 TW in femtosecond operation) at the fundamental wavelength and 0.7~1.4% at the third-harmonic generation. Such improvement reflects an ability to stabilize the laser system in a humidity-controlled clean room. The pulse-energy stability of a mode-locked femtosecond oscillator has been continuously held to 0.3% (p-p) for 4.5 months (1% for 10 months), 24 hours a day. In addition, the ideal spatial and temporal profiles of a shot-by-shot single UV-laser pulse are essential to suppress emittance growth in an RF gun. We apply a deformable mirror that automatically shapes the spatial UV-laser profile with a feedback routine, based on a genetic algorithm, and a pulse stacker for temporal shaping at the same time. The 3D shape of the laser pulse is spatially top-hat (flattop) and temporally a square stacked chirped pulse. Using a 3D-shaped laser pulse with a diameter of 0.8 mm on the cathode and pulse duration of 10 ps (FWHM), we obtain a minimum normalized emittance of 1.4 π mm mrad with a beam energy of 26 MeV. We found that the last mirror in the vacuum to make normal incidence is an obstacle for the electron beam. Therefore, we developed the optical elements for a new hollow laser incidence with an axicon final focusing. We fixed temporal parameters with the present mechanical pulse stacker and prepared a new UV-pulse stacking system (fixed parameters) consisting of three birefringence α-BBO crystal rods.

INTRODUCTION

We have been developing a stable and highly effective UV-laser pulse as the light source of a photo-cathode RF gun [1] that in turn provides a high-brightness electron beam source to achieve future X-ray light sources (FEL (free electron laser), Compton back scattering, etc.) since 1996 at SPring-8 (Synchrotron Radiation Research Group). The electron source for several X-ray FEL projects [2-4] requires a very-low-emittance (high-brightness) electron beam as low as 1 π mm mrad. One of the most reliable candidates for this high-brightness electron source is a photocathode RF gun. This type of gun generates an electron beam pulse from a photocathode illuminated by a laser pulse. Our development of this gun is oriented toward a yearlong stable system for user experiments. It is necessary for the copper cathode of this RF gun to have a UV-laser pulse with a pulse width of ~10 ps and a photon energy of ~4 eV. Since we started to develop the laser test facility, two issues related to the laser light source have arisen. One is the energy stability of the UV-laser light source. Therefore, we have stabilized the third-harmonic generation (THG) of a CPA (chirped pulse amplification) Ti:Sapphire terawatt laser system (Figure 1) as the laser light source for the SPring-8 RF gun.

The other problem concerns the spatial and temporal laser profiles. To minimize the beam emittance of a photocathode RF gun, the laser pulse shape should be optimized three-dimensionally. Over the past six years at SPring-8's test facility for the photocathode laser light source, several 3-D shaping systems have been developed from combinations of spatial (transverse: x-, y-axes) and temporal (longitudinal: z-axis) pulse shaping methods (Figure 1). The spatial profile has to be modified with a microlens array [5] or a deformable mirror (DM) [6]. In addition, the temporal profile has to be modified with a spatial light modulator (SLM) [6-7] or the pulse stacker described in this paper. One of the candidates for a reliable 3-D laser pulse shape has been the cylindrical shape (spatially top-hat and temporally square pulse). With a square-shaped 9-ps laser pulse, the lowest beam emittance of 1.2 π mm mrad at 1.0 nC/pulse has already been achieved by J. Yang et al [7]. Previously, we have demonstrated a UV-laser spatial profile shaped as a quasi top-hat (flattop) with a deformable mirror used to automatically optimize it with a feedback routine based on a genetic algorithm. Using this top-hat laser pulse (diameter of 1.0 mm on the cathode) with a pulse duration of 5 ps (note: temporally, not square), we could obtain low-emittance beam generation of 1.7 π mm mrad [6] at a net electron charge of 0.1 nC/pulse. However, the beam emittance at high charge was much larger. This indicates that a 5-ps laser pulse is too short for the laser spot diameter of 1 mm. (The charge density is too high.)

PERFORMANCE TESTS OF THE PHOTON MONOCHROMATOR FOR SELF-SEEDING AT FLASH *

R. Treusch, U. Hahn, J. Viefhaus, DESY, Hamburg, Germany
H.K. Bechtold, J. Hartvig, H. Juul, V. Toft, Aarhus University, Aarhus, Denmark
S.V. Hoffmann ISA, Aarhus, Denmark
C. Knöchel, LBNL, Berkeley, California, U.S.A.
R. Reininger, Scientific Answers & Solutions, Madison, Wisconsin, U.S.A.
R. Follath, G. Reichardt, F. Senf, F. Siewert, BESSY GmbH, Berlin, Germany

Abstract

A single pass FEL amplifier can produce extremely intense and fully coherent radiation at short wavelengths if it is seeded by a coherent light beam resonant with the magnetic structure and collinear with the electron beam. Since at the present time a single pass SASE[1] FEL is the only source of sufficiently intense, tunable radiation in the soft X-ray region, it has been proposed to use such a source in combination with a narrow-band monochromator for seeding an FEL amplifier [1]. By means of such a "Self-Seeding", the soft X-ray free electron laser FLASH [2] at DESY will be modified so that it can provide coherent radiation in space *and* time in a wavelength range from about 60–6 nm (≈ 20–200 eV).

Here, we will focus on the performance of the photon monochromator beamline for the seeding which was set up and tested at the synchrotron radiation storage ring ASTRID in Aarhus. The optical and mechanical design will be described along with results on the resolving power of the monochromator which have been obtained scanning across rare gas resonance lines at various energies.

INTRODUCTION

Since August 2005 FLASH is providing SASE radiation for users, presently tunable from about 47–13 nm and soon from 60 down to 6 nm. The pulses possess a pulse length of a few 10 fs, almost full transverse coherence, limited longitudinal (temporal) coherence and pulse energies from about 10–100 μJ. By means of the Self-Seeding (or *Seeding Option*) FLASH will be modified in a way that it can provide fully longitudinally coherent, narrow-bandwidth radiation. The output radiation will then exhibit all the characteristic properties of conventional optical lasers but at much shorter wavelengths and with a continuous tunability between 6 and 60 nm. The enhanced beam properties will extend the range of possible applications, particularly for high resolution spectroscopy and for all experiments which need full longitudinal coherence.

The Self-Seeding consists of an additional undulator section, a bypass for electrons and a photon monochromator beamline. R&D in undulator design, FEL theory and electron beam dynamics, as well as on photon beam propagation and optical components were important parts of the project. The photon monochromator beamline aspect will be detailed here. More details, also on all the other components can be found in [3].

The general layout of the Self-Seeding is sketched in figure 1. The first undulator operates in the SASE mode

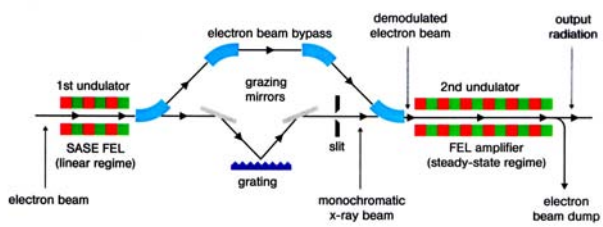

Figure 1: Schematic setup (side view) of the Self-Seeding for FLASH. Behind the first undulator, FEL radiation and electrons are separated. While the electrons travel through the bypass represented by the four blue dipole magnets in the upper part of the figure, the photons propagate across the photon monochromator beamline below in order to provide a narrow-bandwidth seed that is overlayed with the electrons again at the entrance of the second undulator.

in the "linear" (= exponential gain) regime, about 2–3 orders of magnitude below saturation. It produces intense, but structured light pulses as shown in the left part of figure 2. Subsequently electrons and photons are separated. Before they are overlayed again in the second undulator, the electrons travel through a magnetic chicane that is used to remove the longitudinal density modulation ("micro-bunching") of the electron beam which was induced by the FEL process in the first undulator. For the photons, a high resolution grating monochromator together with some matching optics is used as a narrow-band filter to provide the coherent radiation seed which is amplified to saturation in the second undulator section. The resulting spectral distribution is given in the right part of figure 2.

The requirements for the final seeding radiation pulse are obvious: its photon wavelength has to be within the gain bandwidth of the FEL amplifier, the photon bandwidth has to be narrow enough to provide a coherence length as long as the electron bunch length, and the intensity of the

* Work funded through HGF-Strategiefonds (01SF9935/1)
[1] Self-Amplified Spontaneous Emission

SINGLE-SHOT LONGITUDINAL BUNCH PROFILE MEASUREMENTS AT FLASH USING ELECTRO-OPTIC DETECTION: EXPERIMENT, SIMULATION, AND VALIDATION.

B Steffen*, E -A nabbe, H Schlarb, B Sch idt, P Sch user, ES , Ha burg, er any
W A illespie, P Phillips, undee University, undee, U
S P a ison, ASTEC, aresbury Laboratory, STFC, U
Berden, A F van der Meer, FELIX / FOM Insitute Rijnhuizen , Nieuwegein, NL
A M MacLeod, Abertay University, undee, U

Abstract

At the superconducting linac of FLASH at ES , we have installed an electro-optic EO e peri ent for single-shot, non-destructive easure ents of the longitudinal electric charge distribution of individual electron bunches The ti e pro le of the electric bunch eld is electro-optically encoded onto a chirped titaniu -sapphire laser pulse In the decoding step, the pro le is retrieved either fro a cross-correlation of the encoded pulse with a 30 fs laser pulse, obtained fro the sa e laser electro-optic te poral decoding, EOT , or fro the spectral intensity of the trans itted probe pulse electro-optic spectral decoding, EOS At FLASH, the longitudinally co - pressed electron bunches have been easured during FEL operation with a resolution of better than 50 fs The electro-optic process in galliu phosphide was nu erically si u-lated using as input data the bunch shapes deter ined with a transverse-de ecting RF structure In this contribution, we present electro-optically easured bunch pro les and co pare the with the si ulation

SINGLE-SHOT ELECTRO-OPTIC DETECTION

Precise easure ents of the te poral pro le of e - tre ely short electron bunches are essential for a detailed understanding of the bunch co pression and lasing ech-anis s in a SASE FEL Single-shot electro-optic EO de-tection techni ues are ideally suited for this purpose since they are non-destructive and per it correlation studies between the ti e pro le of electron bunches and the properties of FEL pulses produced by the sa e bunches

The transverse electric eld of a relativistic electron bunch passing close to an electro-optic crystal corresponds to a THz pulse traveling through the crystal This THz pulse induces a transient birefringence in the EO crystal which can be sa pled by a linearly polarized optical laser pulse In this e peri ent we use galliu -phosphide aP instead of the ore co on zinc telluride nTe as it offers a factor of two better ti e resolution The electro-optic te poral decoding EOT techni ue was applied 1, 2

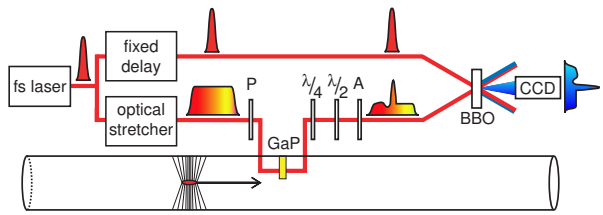

Figure 1 color Sche atic drawing of the electro-optic te poral-decoding EOT e peri ent at the FLASH linac For details see te t

yielding the best ti e resolution of the single-shot EO detection ethods

The sche atic setup is shown in Fig 1 The titaniu -sapphire Ti Sa laser a pli er pulse length 30 fs FWHM, central wavelength 795 n , pulse energy 0 8 , repetition rate 1 kHz is synchronized to the 1 3 Hz accelerator RF The laser bea is split into two bea s the probe bea and the gate bea The probe bea is stretched to 20 ps with a grating-pair optical stretcher and guided through a polarizer P to set the polarization parallel to the -1,1,0 a is of the EO crystal It is then injected into the linac vac-uu cha ber and passes through the aP crystal placed at a distance of 4-5 fro the electron bea The birefrin-gence induced by the Coulo b eld of the passing electron bunch is translated into a ti e-dependent elliptical polar-ization of the stretched probe bea This in turn is converted into an intensity odulation with a half wave plate and an analyzer A that is orthogonal to the polarizer P Any residual birefringence is re oved by a uarter wave plate The EO-induced intensity odulation of the probe pulse is easured through cross-correlation of probe and gate pulse in a fre uency-doubling BBO crystal By overlap-ping the two pulses non-collinearly, a spatially dependent ti e delay is introduced between the pulses The BBO light $\lambda \approx 400$ n is i aged by an intensi ed CC ca era, and the te poral pro le of the electron bunch is derived fro the light intensity as a function of position The intrinsic ti e resolution of the optical cross-correlator is $\sigma = 25$ fs r s

The electric eld of the bunch is also arranged to be parallel to the crystallographic -1,1,0 a is aligned in horizontal direction , so that the ain a is of the refractive

* e ail bernd steffen desy de

MAGNETIC MEASUREMENTS, TUNING AND FIDUCIALIZATION OF LCLS UNDULATORS AT SLAC*

Y. Levashov, V. Kaplunenko, A. Weidemann, Z. Wolf
SLAC, Menlo Park, CA 94025, USA

Abstract

A new Magnetic Measurement Facility (MMF) has been built at Stanford Linear Accelerator Center (SLAC) to measure, tune and fiducialize LCLS undulators. The climate controlled MMF utilizes two magnetic measurement benches and a large Coordinate Measurement Machine (CMM) to provide a throughput of one undulator per week. Magnetic measurement, tuning and fiducialization processes are presented and first tuning results are discussed.

INTRODUCTION

The Linac Coherent Light Source (LCLS) based on a Self-Amplified Spontaneous Emission Free-Electron Laser (SASE-FEL), is being built at Stanford Linear Accelerator Center (SLAC) by a collaboration of four US-DOE laboratories. A new injector and a part of the existing SLAC linac will be used as an electron source at energy of 13.64 GeV. The 120 m long LCLS undulator line consists of 33 segments. Each segment is a fixed-gap planar undulator assembled of permanent NdFeB magnets and canted poles. The undulator period is 3cm, gap at the beam line is 6.8mm, effective K value varies from 3.500 to 3.485 to account for beam energy loss, and the radiation wavelength will be 1.5A. A prototype of the segment and the first two undulators have been measured and tuned at the Advanced Photon Source (APS) in Argonne National Laboratory (ANL) [1],[2].

Requirements for LCLS undulator tuning and fiducialization are specified in a Physics Requirement Document [3]. The requirements must be met for all beam positions within ±2 mm horizontally and ±200μm vertically of the nominal beam axis. Trajectory excursions for one segment should be less than 2μm, r.m.s. phase errors and particle-wave slippage <10°, first field integrals $<40\times10^{-6}$Tm, second field integrals $<50\times10^{-6}$Tm², and K should be set to 1.5×10^{-4}. The position of the undulator magnetic axis, and the beam trajectory at the nominal K value should be known relative to external mechanical references to 50μm horizontally and 40μm vertically.

Because of their low electrical noise and small planar Hall effects, Sentron XZM12-3-0.6-2T Hall probes are used to sample magnetic fields along an undulator for beam trajectories and K calculations. Field integrals are measured by 3.6m long coils. Additional measurements are made with one period long λ -coils.

The semi-automated process of LCLS undulator tuning allows for a throughput of one undulator per week, which is required to meet the tight project schedule.

MAGNETIC MEASUREMENT LABORATORY

The main concern taken into consideration during construction of the MMF was the temperature. The remnant field of permanent magnet material typically changes by about 0.1% per degree Celsius, which requires the temperature to be constant at ±0.1C° level to meet the tolerance on the K. A high quality air conditioning system keeps the air temperature in the MMF within tolerance, as shown in figure1.

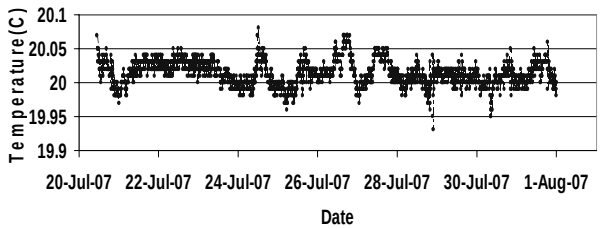

Figure 1. Ambient temperature in MMF

Each undulator stays inside the temperature controlled room for one week prior to the start of measurements to reach thermal equilibrium with the room temperature. During magnetic measurements and tuning, the undulator temperature is monitored by 5 sensors distributed along the length of the device. The difference between the background magnetic field in the laboratory and the magnetic field in the undulator hall at different LCLS tunnel locations was measured to be 0.1G. Many other metal objects, which could affect the ambient magnetic field components, should be taken into account during the tuning process. For that reason all undulators are covered by a μ-metal shield, shown in figure 2, which reduces the ambient magnetic field by a factor of 6. Also they are set in the same orientation in which the segments will be installed in the tunnel, and measured on the same steel support structure.

Initial mechanical acceptance checks and fiducialization measurements of an undulator are made on the 4 meter long CMM. Undulators are tuned on two separate magnetic measurement benches, which allow work to proceed in parallel. The measurement devices are mounted on precision x, y, z - stages with Heidenhain scales and encoders. The instruments are triggered by a National Instruments FPGA in a PXI-1031 chassis. Probe positioning accuracy w.r.t. reference indexes on the scales

* Work supported by US Department of Energy contract DE-AC02-76SF00515.

MAGNETIC MEASUREMENTS OF THE FLASH INFRARED UNDULATOR

N.Morozov*, A.Chesnov, E.Matyushevsky, D.Petrov, E.Syresin, JINR, Dubna, Russia,
O. Grimm, J. Rossbach, University of Hamburg, Germany,
Y.Holler, DESY, Hamburg, Germany

Abstract

The FLASH free-electron laser at DESY, Hamburg, has recently been equipped with an infrared electromagnetic undulator, providing radiation in the range 1-200 μm. It will be used both for electron beam diagnostics purposes and as a powerful source synchronized to the VUV and soft X-ray pulses of the FEL. The undulator was constructed at the Joint Institute of Nuclear Research (JINR). This paper summarizes the extensive magnetic measurements that where performed both at JINR and DESY prior to installation of the undulator.

INTRODUCTION

An important feature of the beam formation system of FLASH is the possibility to produce ultra-short (below 50 μm) electron bunches. Such short bunches produce powerful coherent radiation with multi-megawatt power level. Generation of two-colors by a single electron bunch reveals unique possibility to perform pump-probe experiments with VUV and IR radiation pulses [1,4]. Coherent radiation produced by the electron beam in the IR undulator strongly depends on the bunch profile, thus allowing the use of the device for longitudinal profile diagnostics

UNDULATOR MAGNET DESIGN

The undulator (Figure 1) magnetic system [2,3] consists of two ferromagnetic girders with 22 poles each. The exciting coils are set on poles. The coils of the top and bottom girders are connected sequentially and powered by a single electrical supply. Each main coil consists of four layers, and each layer consists of 16 turns. The windings are made of a square-shape copper pipe (8.5x8.5 mm^2) with a cooling channel of 5.3 mm diameter. The maximum current in the winding is 435 A (current density 8.7 A/mm^2). Each regular coil has an additional correction winding to provide fine regulation of the magnetic field. The number of turns in the correction winding is 270, and wire diameter is 1 mm. The corrector winding allows to regulate the number of Amper·turns within 2% of maximum value of the main winding. The correction coils permit to compensate a perturbation of the magnetic field related to an imperfection of magnetic system at its construction. The coils of two end poles differ from the coils of regular periods, and consist of 8 and 36 turns for the first and the second pole, respectively. End-pole coils have also a correcting winding for fine adjustment of the magnetic field.

Figure 1: View of the infrared undulator on the DESY magnetic field measurement bench

SCOPES OF THE MAGNETIC FIELD SHAPING

Undulator magnetic field measurements and correction were provided at the first stage in JINR (Dubna) and finally in DESY (Hamburg). At both sites a Hall probe magnetometer was used for the field measurement. The probe head was moved and controlled in three dimensions by stepping motors and a high accuracy linear encoder (~ some μm). The magnetic field monitoring was realized by reference Hall or NMR probe. During the magnetic field measurement campaign the following goals were realized:

- the first and second total integrals are I_1<200 G·cm and I_2<200 kG·cm^2;
- the first integral in each regular undulator period is I_1<200 G·cm;
- magnetic field reproducibility and long time stability for the first and second total integrals are I_1=±50 G·cm and I_2=±5 kG·cm^2;
- flat beam orbit;
- using one power supply for regular correction coils and as few as possible power supplies for the edge correcting coils.

The above undulator requirements have to be fulfilled in the range of the main coil excitation currents Io = 0 (remanent field) – 435 A (Bo=11000 G).

To achieve those goals, a large amount of simulation work was done at the initial stage of the project design by different codes (POISSON, ANSYS, TOSCA, RADIA) [2]. Those simulations have resulted in a flexible magnetic system with the possibilities to achieve the design goals.

*Corresponding author, email: morozov@nusun.jinr.ru

NUMERICAL CALCULATIONS OF THE RADIATION EMITTED FROM THE FLASH INFRARED UNDULATOR

O. Grimm*, J. Rossbach, University of Hamburg
V. Kocharyan, DESY, Hamburg, Germany

Abstract

The VUV and soft X-ray free-electron laser FLASH at DESY, Hamburg, has been complemented with an infrared undulator working in the wavelength range of 1 to 200 µm, providing pulses naturally synchronized with the FEL radiation. The results from the magnetic measurements prior to installation are used here as input for calculations of the expected radiation spectrum. Especially the behavior at small excitation currents is important for beam diagnostics using coherent radiation.

INTRODUCTION

Complementing the FLASH facility at DESY, Hamburg, with an undulator working in the mid- and far-infrared regime was first proposed in [1]. There is a strong interest in using such an undulator delivering up to 10 MW peak power in the THz-regime as a radiation source, allowing pump-probe experiments with high temporal resolution. Another equally important application lies within longitudinal bunch shape diagnostics [2, 3]. More details on the undulator have been reported in [4, 5].

The device has been build and installed in the FLASH accelerator, with first beam passing through expected in September 2007. In [6] results of the magnetic measurements that were performed prior to installation are reported. These are used for detailed numerical calculations of the radiation characteristics, some of which are reported in this paper. Such calculations are necessary input to optics codes to quantitatively analyze the transmission characteristics of the infrared beam line.

NUMERICAL CODES

Several numerical codes have been used to perform calculations of the radiation characteristics. Comparisons between the results from different codes are mandatory to get confidence about their validity.

Many calculations are performed with a custom-made code written in Matlab called SynchroSim. The code implements a full time-domain calculation based on using the general Liénard-Wiechert fields from an accelerated charge [7] and a subsequent Fourier transformation to get the spectrum. There are no approximations involved, however the calculation speed is low. Alternatively, a direct calculation in frequency-domain can be done using the paraxial approximation of synchrotron radiation emission [8], giving much higher speed.

The Synchrotron Radiation Workshop (SRW) code has also been used extensively [9]. Some cross-checks were performed with the SPECTRA code [10].

Perfect agreement was found for on-axis spectra calculated with SRW, SPECTRA and SynchroSim. The transverse intensity distribution at 61 µm wavelength and 1 GeV energy is compared between SRW and SynchroSim in Fig. 1. Also here very good agreement is found.

The horizontally asymmetric distribution and interference fringes result mainly from the undulator end poles. Some contribution results also from the inclusion of the dipole magnet that is installed downstream of the undulator. It has a field of about 0.45 T at 500 MeV and is used to dump the electron beam. It should be noted that further along the infrared beam line the relative contribution of the dipole will reduce, as the optics is optimized for the radiation contribution from the undulator.

Further comparisons confirmed the good agreement between different codes, thus calculations in the following were performed with the most convenient program.

SPECTRUM CALCULATIONS

The spectrum calculated for 200 A excitation current of the undulator at 511 MeV electron energy is shown in Fig. 2. On-axis a typical resonance spectrum is obtained containing only odd harmonics. When integrating over a transverse area of $60 \times 60\,\mathrm{mm}^2$ (corresponding to the beam line acceptance at that position), the spectrum acquires a clear baseline. This is an indication of the fact that only a small fraction of the total energy emitted by an electron ends up within the harmonics, see the estimation in the last section.

This effect becomes more pronounced at smaller excitation currents, as Fig. 3 shows for 30 A. This is due to the reduced opening angle of the harmonics at smaller K value, and thus larger contribution of non-resonant radiation when the acceptance aperture is fixed.

TRANSVERSE INTENSITY CALCULATIONS

The transverse distributions of the total radiation intensity (summed over both polarizations) with the undulator current set to the maximum value of 435 A is shown in Fig. 4 for the first and third harmonic (192 µm and 64 µm at 511 MeV, respectively). The 60 mm diameter aperture of

* Corresponding author. E-Mail: oliver.grimm@desy.de

MAGNET SORTING FOR THE XFEL HYBRID UNDULATOR—COMPARING STUDY

Yuhui Li, Bart Faatz and Joachim Pflueger
Deutsches Elektronen Synchrotron (DESY), Hamburg, Germany

Abstract

Current permanent magnet material quality is insufficient to obtain field qualities in undulators, which satisfy FEL requirements. Therefore position and orientation of magnets have to be carefully chosen in order to obtain mutual cancellation of field errors. In this paper we compare two different sorting schemes, simulated annealing and a straight forward paring method. They are applied to a 5m prototype structure built for the European XFEL facility. The algorithms of these two methods are described in detail and the sorting results and the expected field qualities are carefully compared.

Key words: undulator, sorting, annealing, pairing

INTRODUCTION

The European XFEL will be a user facility in the wavelength range from 0.1 to 1.6 nm [1]. It will use the so-called Self Amplified Spontaneous Emission (SASE) scheme to reach saturation in a single pass [2, 3]. The XFEL will use a technology similar to FLASH [4]. The electron beam is generated in an RF photo cathode gun, accelerated and compressed twice before it reaches its final nominal energy of 17.5 GeV. After acceleration and collimation, the beam will be distributed among several SASE undulators and wigglers for spontaneous emission. The radiation is distributed among 10 user stations. The wavelength can be changed by changing the electron beam energy or by changing the undulator gap.

Studies for FLASH have shown that the transverse overlap between radiation and electron beam has to be better than 20% of the beam size in order not to have a too large reduction in gain and therefore a too large increase in needed undulator length [5]. A similar criterion holds for keeping the resonance condition, i.e. keeping the phase shake within reasonable values. A typical rms deviation here is a few degrees. The undulator magnet quality needed to provide this overlap and phase shake without additional effort does not exist. Therefore, additional methods have to be used in order to guarantee a sufficiently good undulator quality.

Given the quality of the individual magnets, several methods can be used to obtain the appropriate undulator quality. One such method is magnet sorting, i.e. measuring the magnetic properties of the individual magnets and putting them into the structure such that errors in the magnet blocks cancel each other [6]. Another method which can be applied to correct the main field component of the structures that are discussed in this paper is pole-height adjustment [7]. This procedure, which has to take place in any case, is outside of the scope of this report and can only be applied to the main field. Therefore, our main aim is to correct the transverse field components that cannot be corrected by this method.

The structure for which the magnets are sorted is shown in Fig. 1. It consists of magnets separated by iron poles that focus the flux lines resulting in the main magnetic field. Of each magnet, several parameters have been measured: the magnetization in all three directions (M_x, M_y, M_z) and the main magnetic field at a given distance $(B_z^{(n)}, B_z^{(s)})$, thus giving the north-south inhomogeneous field. For a perfect magnet, $M_x = M_y = 0$ and $B_z^{(n)} = B_z^{(s)}$. In order to uniquely identify the orientation of the magnet, each of them is marked as in Fig. 1. Therefore, the direction of the field components is known independent of the orientation of the magnet.

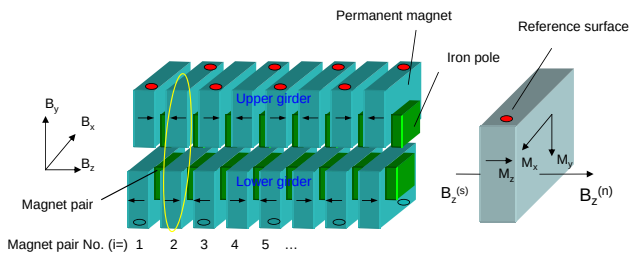

Figure 1: Coordinate system for the undulator and the magnet blocks. The red dot is used to determine the orientation of the magnet under any transformation that may be applied inside the magnetic structure. The arrangement shown here is referred to as the normal state.

With the magnet transverse flux M_x, M_y, the transverse undulator field can be evaluated by:

$$B_{x,i} \propto (F_{l,i} M_{x,l,i} + F_{u,i} M_{x,u,i})(-1)^i$$
$$B_{y,i} \propto F_{l,i} M_{y,l,i} - F_{u,i} M_{x,u,i} \quad (1)$$

The subscript l refers to magnets on the lower girder, u to magnets on the upper girder, i means pole position, F stands for a possible flip of magnet at a certain position, with $F = 1$ the magnet in its normal state and $F = -1$ in its flipped state. $B_{x,i}$ and $B_{y,i}$ are undulator transverse fields on each magnet pair, one in the upper girder, another in the lower girder (see Fig. 1).

In this paper, we will sort the magnets using two different methods, namely simulated annealing and pairing of magnets based on the magnetic measurements.

STUDY OF UNDULATOR TOLERANCES FOR THE EUROPEAN XFEL

Yuhui Li, Bart Faatz and Joachim Pflueger
Deutsches Elektronen Synchrotron (DESY), Hamburg, Germany

Abstract

For an X-ray FEL facility, error tolerance simulations for undulator systems are necessary. Previous work mainly took into account random errors for each pole and then simulate their impact. However, some errors, for instance the girder deformation, are not random but periodic. In this paper both random and periodic errors as well as a combination are studied. The results are limited to non-steering errors, i.e. a reduction in overlap between electrons and photon beam has been avoided throughout this study.
Key words: tolerance, undulator, XFEL

INTRODUCTION

In the European XFEL project, photons will be generated in the X-ray range of 3.1 keV to 12.4 keV [1]. High power radiation will be generated using Self-Amplified Spontaneous Emission (SASE). Saturation will be rezched within a typical length of 100 to 150 m [2, 3]. Undulator errors unavoidably exist in this long undulator system. A first estimate for an upper limit on these errors is related to the SASE-FEL bandwidth ρ:

$$\frac{\Delta\lambda_s}{\lambda_s} \approx \frac{2\Delta K}{K} < \rho \qquad (1)$$

With the value of ρ of the order of 10^{-4} for the European XFEL project, undulator gap variation should smaller than 1 μm and the temperature variation should be smaller than 0.08^oC [4]. If Eq. (1) could be satisfied, the power degradation and saturation length increase would be minimal. Because this is far from trivial and a mayor cost driving factor, a more detailed study is neccessary.

The European XFEL facility will supply 0.1 nm to 0.4 nm radiation. Wavelength tuning can be achieved by changing the undulator gap or the electron beam energy. Even though the tolerance level for different modes is different, their behaviour is similar. Therefore in this paper we only list the result of SASE1 with 0.1 nm mode which has the tighest tolerance requirement. A more complete study can be found in [5].

Two kinds of undulator field errors can be distinguished. One kind is random error on each undulator pole. This kind of error can be caused for example by the inhomogeneous field of magnet blocks [6]. Another kind of error changes along undulator as periodic or semi-periodic function. This kind of error exists for instance because of the girder deformation or gap tilt [7]. The previous tolerance simulation work concentrated mainly on the first kind of error. Thus this report only studies the latter one.

Some papers investigating the impact of undulator field errors show that beam wander and phase shake are the key reasons for the increase of gain length [8, 9]. Beam wander reduces the transverse overlap between electron beam and radiation. Phase shake indicates an electron ponderomotive phase variation and therefore a reduction in bunching. In this paper only the impact of phase shake is taken into account.

The FEL simulation code Genesis 1.3 is used for our simulations [10].

DESCRIPTION OF BASIC ERROR TYPES

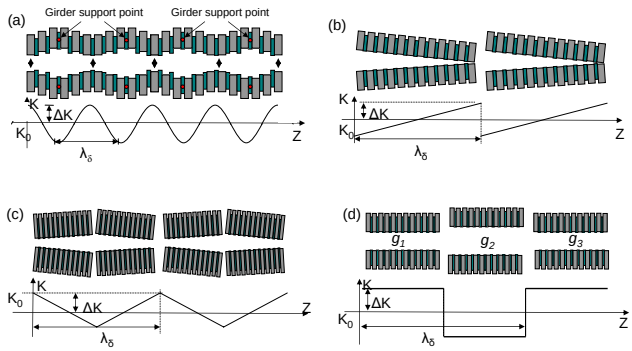

Figure 1: The induced undulator error by girder deformation and gap tilt (a) sinus, (b) sawtooth, (c) triangle and (d) constant

The periodic errors are divided into four basic types: sinus, triangle, sawtooth and (stepwise) constant. The sinus error is used to approximate undulator girder deformation due to the magnetic forces which can be compensated for one gap setting only. Fig. 1 (a) shows this effect. For the European XFEL, a four point support structure is used in order to minimize this effect. A periodic error can also be generated by the inhomogeneous movement of the undulator driving motors. Fig. 1 (b), (c) and (d) illustrate so generated three kinds of periodic errors (sawtooth, triangle and constant). The movement accuracy is assumed to be 1 μm.

Finite motor movement accuracy results some in residual random errors of which the importance has to be quantified. For this purpose, the same error model as shown in Fig. 1 is used, but in this case the resulting amplitude variation ΔK is random. In contrast to this, the undulator girder deformation is always homogeneous and thus a periodic error can always be expected. Therefore, in this paper the simulation of random sinus errors is not investigated. Fig 2 illustrates this random error.

MCP-BASED PHOTON DETECTOR WITH EXTENDED WAVELENGTH RANGE FOR FLASH

L Bittner, Feldhaus, U Hahn, M Hesse, U astrow, ocharyan, P Radcliffe, E L Saldin, E A Schneid iller, Tiedtke, B Ti ann, R Treusch, N von Bargen, M urkov
eutsches Elektronen-Synchrotron ES , Ha burg, er any
O I Brovko, harla ov, I Lokh atov, E A Matyushevskiy, A Shabunov, E M Syresin
oint Institute for Nuclear Research INR , ubna, Moscow Region, Russia

Abstract

E peri ental e perience gained at the e tre e ultraviolet SASE FEL FLASH ES , Ha burg has shown that successful operation of the facility strongly depends on the uality of the radiation detectors Here key issues are wide wavelength range 6 to 100 n for FLASH , wide dyna ic range fro the level of spontaneous e ission to the saturation level , and high relative accuracy of easure ents which is crucial for detection of a signature of a pli cation and characterization of statistical properties of the radiation In this report we describe MCP-based radiation detector for FLASH which eets these re uire ents ey ele ent of the detector is wide dyna ic range icro-channel plate MCP which detects scattered radiation fro a target With four different targets and MCPs in co bination with optical attenuators present detector covers operating wavelength range fro 6 to 100 n , and dyna ic range of the radiation intensities, fro the level of spontaneous e ission up to the saturation level of SASE FEL

INTRODUCTION

The free electron laser FLASH is in operation at ES since the year 2000 1 5 Several upgrades of the facility have been perfor ed, and after an upgrade of 2007 FLASH will cover a wavelength range fro 6 to 100 n Instruentation for photon bea characterization has been developed as well 6 11 An i portant piece of the photon diagnostics are detectors for easure ents of the pulse energy Originally FLASH has been e uipped with PtSi-photodiodes and ther opiles based on BCO High-Tc-superconductors HTSCs 6,7 These detectors helped to the rst signature of light a pli cation at FLASH 1 , but it has been realized soon that they have rather li ited possibilities The rst one refers to li ited dyna ic range, and the other one relates to the physics of interaction of powerful, ultrashort U radiation pulses with the detector In fact, nonlinearities and saturation effects started to occur in PtSi-photodiodes uch earlier with respect to calibrations perfor ed with conventional lasers To solve the proble of li ited dyna ic range and saturation effects we launched develop ent of MCP-based radiation detector 8 , and pretty soon succeeded to tune FLASH to saturation in 2001 2,3 An i portant feature of MCP-detector is high relative accuracy of intensity easure ents This is crucial for detecting the rst signature of light a pli cation and further ne tuning of the achine para eters for increasing the gain MCP detector is used for easureent of statistical properties of the radiation allowing to deter ine the pulse length and ode contents of the radiation 12 In 2004 the energy of FLASH accelerator has been increased to 700 Me , and a new MCP detector opti ized for wavelength down to 10 n has been installed, and beca e the pri ary tool for searching a pli cation, tuning the gain, and for statistical easure ents 4,5,9

In this paper we describe 3rd generation MCP detector at FLASH opti ized for the easure ent of SASE radiation with the wavelength down to 6 n

CURRENT EXPERIENCE WITH MCP-BASED DETECTOR AT FLASH

Photon detectors at FLASH are installed in a bea line downstrea the undulator The ost critical step of tuning lasing process is to nd the signature of light a pli cation The proble relates to a strong background of incoherent radiation produced by the whole bunch charge 0 5-1 nC

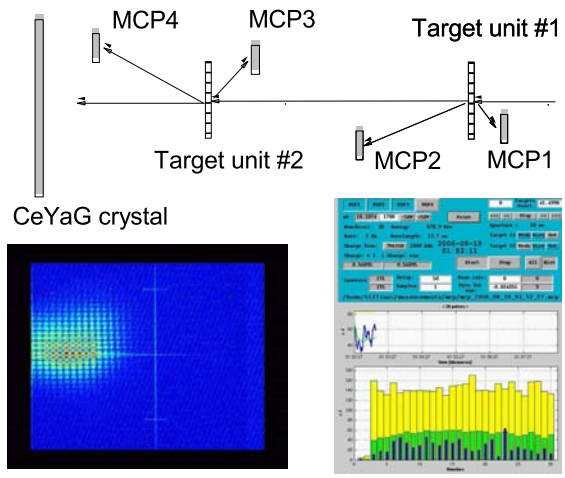

Figure 1 Top layout of MCP-detector operated at FLASH in 2004-2007 9 etector consists of two identical units for detection of radiation at ed angles The targets are se i-transparent gold esh and gold wire On-line tuning with this detector allows to have si ultaneously uantitative data and visual observation of the photon bea on Ce a crystal

MEASUREMENTS OF PROJECTED EMITTANCE AT FLASH

K. Honkavaara*, Hamburg University, 22761 Hamburg, Germany
F. Löhl, E. Prat, DESY, 22603 Hamburg, Germany

Abstract

FLASH is a SASE FEL user facility at DESY operating with photon wavelengths in the range from vacuum ultraviolet to soft x-rays. Although the slice emittance is a more appropriate parameter to characterize the SASE process, the projected emittance provides a useful measure of the electron beam quality. At FLASH, the projected emittance is measured at three locations along the linac: in the injector (130 MeV), after the collimator, and in the undulator section. The emittance is determined by using a multi-monitor method with OTR monitors and wire scanners. In this paper we describe the measurement set-up and procedure, and report recent results.

INTRODUCTION

FLASH is a SASE FEL user facility at DESY (Hamburg, Germany). It produces short (in order of 10 fs) laser like pulses in the wavelength range from the vacuum ultraviolet to the soft X-ray [1].

Figure 1 shows a schematic layout of the FLASH linac as operated in 2006 and the first half of 2007. Electron bunch trains with up to 800 bunches are generated by a laser-driven RF gun. The macro-pulse repetition rate is 5 Hz, and the bunch frequency 1 MHz. During the measurements reported here, the linac is operated with one or two bunches per bunch train. The bunch charge is 1 nC.

Five accelerating modules, with eight 9-cell superconducting TESLA cavities each, provide electron beam energies up to ∼730 MeV. The electron bunch is compressed by two magnetic chicane bunch compressors. At the location of the first bunch compressor, the beam energy is ∼130 MeV, and at the second one ∼370 MeV. During the measurements reported here, the total beam energy after acceleration is ∼500 MeV. The SASE radiation is produced by six undulator modules with length of 4.5 m each.

The SASE process requires a high quality electron beam in terms of transverse emittance, peak current and energy spread. In the characterization of this process, the slice parameters are the appropriate parameters to consider. However, also the projected emittance, which is relatively easy to measure compared to the slice emittance, provides an important measure of the electron beam quality. In addition to be able to produce a small emittance beam at the injector, it is important to conserve this small emittance up to the undulator, where the SASE radiation is produced.

* katja.honkavaara@desy.de

In this we paper describe the emittance measurements performed at three location along the FLASH linac: at the injector, after the collimation section and at the undulator. These measurements are also discussed in [2].

EXPERIMENTAL SET-UP

We measure the transverse projected emittance using a multi-monitor method. This method is based on measurements of the transverse beam distribution (shape and size) at several locations with fixed beam optics.

There are two diagnostic sections dedicated to emittance measurements along the FLASH linac (see Fig. 1). The first one is located downstream of the first bunch compressor. This section has four OTR (optical transition radiation) monitors combined with wire scanners mounted into a FODO lattice of six quadrupoles with a periodic beta function. Below, we refer this section as the 'BC section'. A second FODO lattice with four OTR monitors is located upstream of the undulator, referred here as the 'SEED section'. A fifth OTR monitor placed upstream of the FODO lattice is used as an additional monitor in the measurements. Along the undulator, the emittance is measured using wire scanners located in front of each undulator module. A seventh wire scanner station is downstream of the undulator.

OTR monitors

OTR monitors are based on detection of backward optical transition radiation. The OTR light is emitted when the electron beam passes through an aluminium coated silicon screen inserted at an angle of 45° with respect to the beam trajectory. The ligth is deflected downwards into an optical set-up consisting of three achromat doublet lenses, three neutral density filters, and a digital CCD camera. Each lens provides a fixed magnification, and can be remotely moved in and out of the optical axis. For accurate measurements we use the lens with the highest magnification (1:1). With this lens the measured resolution is 11 μm rms.

The digital CCD cameras with a firewire interface are connected to a PC in the accelerator tunnel. The PC is connected via local Ethernet to an "image server" in the control room. The read-out system, using a LabView based control software, provides beam images for the on-line visualization and for different applications.

More details of the OTR monitor system are in [3, 4].

RECENT MEASUREMENTS OF THE LONGITUDINAL PHASE SPACE AT THE PHOTO INJECTOR TEST FACILITY AT DESY IN ZEUTHEN (PITZ)*

Ronsch†, Rossbach, Ha burg University, 22761 Ha burg, er any
Asova‡, Bahr, C Boulware, H rabosch, M Hanel, Ivanisenko§, S hodyachykh,
S orepanov, M rasilnikov, S Lederer, B Petrosyan, A Shapovalov¶, T Scholz, L Staykov,
R Spesyvtsev‖, F Stephan, ES , 15738 euthen, er any
Richter, BESS , 12487 Berlin, er any
Rosbach, Hu boldt University Berlin, 12489 Berlin, er any
L Hakobyan, erPhI, erevan, Ar enia
A Onuchin, Budker Institut of Nuclear Physics, Novosibirsk 630090, Russia

Abstract

The Photo Injector Test facility at ES in euthen PIT was built to test and opti ize electron guns for short wavelength Free-Electron Lasers FELs like FLASH and XFEL at ES in Ha burg For a detailed analysis of the behaviour of the electron bunch, the longitudinal phase space and its projections can be easured behind the gun cavity The electric eld at the photo cathode was increased fro 40 M to 60 M to opti ize the transverse e ittance The o entu distributions for different gradients and gun phases will be presented In order to study e ittance conservation, a booster cavity and additional diagnostics were installed The evolution of the longitudinal phase space in the booster cavity will be investigated Measure ents of the o entu distribution and longitudinal distribution behind the booster cavity will be discussed

INTRODUCTION

The ain goal of PIT is to test and to opti ize L-Band RF photo injectors for Free-Electron Lasers The re uirements on such a photo injector are s all transverse e ittances, charge of about 1 nC, short bunches FWHM of about 20 ps and the possibility of long bunch trains of 800 pulses e itted with a fre uency of 1 MHz The heart of PIT is a copper gun cavity with a solenoid agnet that is used to focus the bea etailed analyses of the gun cavity at a gradient of 40-45 M were presented in 1, 2, 3 In order to decrease the effects of space charge forces and thus decrease the transverse e ittance, the gradient at the cathode was increased to 60 M E perience of the conditioning and the rst run period at high gradient are presented in 4, 5 In this paper the in uence of the higher gradient on the o entu distribution will be discussed

MOMENTUM

In order to understand the behaviour of the gun for higher gradients at the cathode, easure ents and si ulations for different gradients were done Figure 1 shows easure ents and si ulations of the a i u ean o entu reached for different powers in the gun The trend

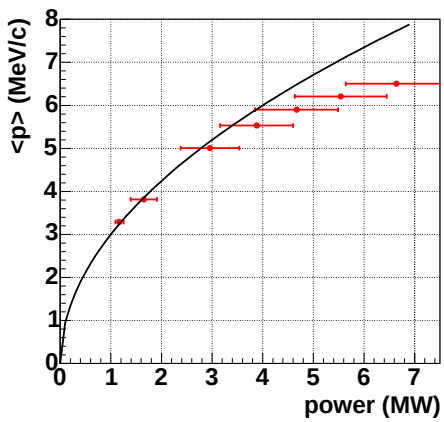

Figure 1 Measured ean o entu as a function of the power in the gun red dots the black curve describes the e pectation, it is tted with the s uare root of the power

of the easured ean o entu ts to the e pectations up to a power in the gun of about 3 5 MW For higher powers the ean o entu stays below the e pectation The power in the gun cannot be easured directly in the gun and the error of the power easure ent is uite large ± 0.5 MW One possible e planation would be that the easure ent of power the is not correct, it is for e a ple possible, that it easures higher order odes or the cavity is isshapen and eld balance could change Another possibility is, that we are loosing power between the point of

* This work has partly been supported by the European Co unity, contract nu bers RII3-CT-2004-506008 and 011935, and by the I puls- und ernetzungsfonds of the Hel holtz Association, contract nu ber H-F -005
† jroensch ifh de
‡ On leave fro INRNE, So a, Bulgaria
§ On leave fro IERT, harkov, Ukraine
¶ On leave fro MEPHI, Moscow, Russia
‖ On leave fro NSCIM, harkov, Ukraine

PHOTOCATHODE LASER PULSE DIAGNOSTICS AT PITZ*

M. Hänel#, J. Bähr, Y. Ivanisenko+, S. Korepanov, M. Krasilnikov, F. Stephan,
DESY Zeuthen, Germany

Abstract

The main objective of the Photo Injector Test facility at DESY in Zeuthen (PITZ) is the development of electron sources that meet the requirements for existing and future FELs such as FLASH or the European XFEL. The goal is the minimization of the transverse emittance of the produced electron bunches. In this respect one of the key issues is the cathode laser system, which should provide longitudinal and transversal flat-top pulses with an excellent long-term stability. In this work we present the full system of laser diagnostics that is currently used at PITZ to monitor the laser pulse parameters.

INTRODUCTION

Laser systems of photo injectors play a crucial role for generating electron bunches with optimum transverse emittance. In our case the laser must produce pulse trains with a repetition rate of 10Hz consisting of up to 800 micro pulses with 1MHz repetition rate. The laser pulses wavelength is 262nm and they have a temporal flat-top shape (FWHM 20ps, rise-/fall-times 6-8ps) as well as a transverse flat-top profile. To extract the required charge of 1nC from the photocathode (Cs_2Te) the laser must provide pulses with an energy of at least 1µJ (for 0.5% quantum efficiency). For further details on the laser system which was developed by the Max Born institute Berlin see [1].

In this paper we present the diagnostics system that is used to monitor the key laser parameters accompanied by recent results.

TEMPORAL LASER PROFILE

The currently used laser system is able to produce flat-top pulses (FWHM 20ps, rise-/fall-times 6-8ps) in the UV utilizing a pulse shaper which consists mainly of a grating stretcher and two birefringent crystals. The effects of the pulse shaper, the subsequent amplification stages, and the conversion of the infrared light into the UV combine to generate flat-top pulses. For tuning the temporal laser shape one can adjust the rotation angles of the birefringent crystals as well as their temperatures. For a detailed description on this pulse shaping technique see [2].

To measure the temporal profile of the laser pulses, a streak camera is used which has a temporal resolution of about 2ps in the UV (Hamamatsu C5680). In addition the measurements of the streak camera can be evaluated using a Matlab script which provides key parameters of the pulse from a fit procedure, i.e. the FWHM, rise- and fall-times as well as the depth of the modulations on the flat-top. Long-term observations show that this method of pulse-shaping is very robust due to its simplicity.

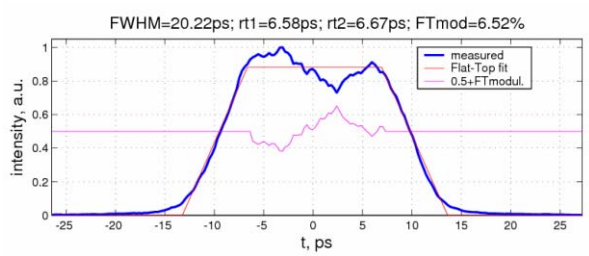

Figure 1: Typical temporal laser pulse shape used during 2007 run period evaluated by the mentioned Matlab script

SPATIAL LASER PROFILE

The spatial flat-top shape of the laser pulses is generated by cutting out a round spot from the center of the widened Gaussian intensity distribution which is produced by the laser. To provide various spot sizes a plate with several apertures of different diameters is mounted on a motorized stage which is remotely controllable. This almost flat-top distribution is then relay imaged onto the photocathode.

For monitoring the transverse profile three different virtual cathodes are used each having the same optical path length as the pulses to the real cathodes have. Two of these virtual cathodes are cameras with a rest-sensitivity in the UV so that the pulses can be shone directly onto the CCD chip. These cameras can be used in different intensity regimes due to different attenuations. The third virtual cathode consist of a Ce:YAG plate which converts the ultraviolet light to visible light. This virtual cathode was introduced recently to develop a method of measurement which does not rely on the rest-sensitivity of the CCD cameras in the UV. Experience shows that this sensitivity rapidly becomes inhomogeneous across the CCD chip. The method using Ce:YAG plates is described in a separate section.

In figure 2a one can see a typical image of the transverse laser profile shown in false colors. Figure 2b displays the same profile in a more intuitive 3D-representation. These images were taken using the direct measurement by shining the laser on the CCD chip. This method has a great disadvantage. Using standard settings for the shutter speed (1/60s) results in smear out effect for the profile. Instead of the one shown in figure 2 one meas-

*This work has partly been funded by the European Community, contract no. RII3-CT-2004-506008 and 011935 and by the 'Impuls- und Vernetzungsfonds' of the Helmholtz Association, contract no. VH-FZ-005.

#marc.haenel@desy.de
+on leave from IERT Kharkiv, Ukraine

INVESTIGATIONS ON THE THERMAL EMITTANCE OF Cs_2Te PHOTOCATHODES AT PITZ*

S. Lederer†, G. Asova‡, J.W. Baehr, K. Boyanov‡, C. Boulware, H-J. Grabosch, M. Haenel, Y. Ivanisenko§, S. Khodyachykh, S. Korepanov, M. Krasilnikov, B. Petrosyan, S.Rimjaem, T.Scholz, R. Spesyvtsev¶, L. Staykov, F. Stephan (DESY, Zeuthen, Germany)
L. Hakobyan (YerPhI, Yerevan, Armenia),
D. Richter (BESSY GmbH, Berlin, Germany)
J. Roensch (University of Hamburg, Hamburg, Germany)

Abstract

The main objective of the Photo Injector Test facility at DESY in Zeuthen (PITZ) is the production of electron beams with minimal transverse emittance. The lower limit of this property of electron beams produced with a photocathode in an RF-gun is determined by the thermal emittance. To understand this crucial parameter for high performance FEL's, measurements under RF operation conditions for cesium telluride (Cs_2Te) photocathodes are done. Results for various accelerating gradients and the dependence on the laser spot size in the cathode plane are presented and discussed in this work.

INTRODUCTION

The thermal emittance determines the lower limit of the normalized emittance of electron beams in injectors. Cesium telluride (Cs_2Te) photocathodes are used at PITZ as sources for electron beams because of their high quantum efficiency (QE) and their ability to release high charge electron bunches in a high gradient RF-gun. In the past several theoretical and experimental studies on the thermal emittance of semiconductor photocathodes like Cs_2Te were performed [1, 2, 3, 4].

In Figure 1 a simplified overview of PITZ is given. The 1.5 cell L-band RF-gun is surrounded by a main and bucking solenoid for compensation of emittance growth due to space charge forces. Under normal operation conditions electrons are emitted from the Cs_2Te cathode by illumination with flat-top laser pulses with temporal FWHM $\approx$ 20 ps and $\lambda = 262$ nm wavelength. A 10 MW klystron provides gradients of about 60 MV/m at the cathode. This gradient is a necessary step toward achieving the required emittance for the European XFEL [5]. More details on the PITZ set-up can be found elsewhere [6].

* This work has partly been supported by the European Community, contracts RII3-CT-2004-506008 and 011935, and by the 'Impuls- und Vernetzungsfonds' of the Helmholtz Association, contract VH-FZ-005.

† sven.lederer@desy.de
‡ on leave from INRNE, Sofia, Bulgaria
§ on leave from IERT, Kharkiv, Ukraine
¶ on leave from NSCIM, Kharkiv, Ukraine

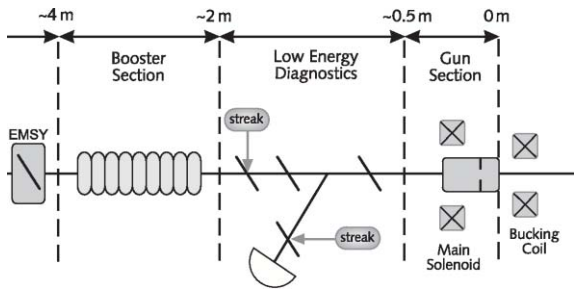

Figure 1: Simplified overview first part of PITZ

At PITZ it is not possible to measure the thermal emittance directly at the cathode. In order to estimate a thermal emittance, a normalized beam emittance has been measured for very low bunch charge and short laser pulses at the first emittance measurement system (EMSY1) 4.3 m downstream (Fig. 1) by the slit scanning technique [7].

In this contribution results from the emittance measurements performed at PITZ are presented for different rms laser spot sizes on the cathode and different accelerating gradients between 30 and 60 MV/m.

THEORETICAL ESTIMATIONS ON THE THERMAL EMITTANCE

The photoemission from semiconductors can be described by a three step model [8]. In the first step an electron from the valence band (VB) is excited to the conduction band (CB) by photon absorption. Due to the energy gap between the conduction and the valence band of $E_g = 3.3$ eV for Cs_2Te, the photon energy must be larger than 3.3 eV [8]. At PITZ a laser with a wavelength of $\lambda = 262$ nm ($E_{ph} \approx 4.72$ eV) is used for the electron excitation into the first density of states maximum in the CB, located 4.05 eV above the VB maximum [8]. The second step involves the electron transport to the surface. In the last step the electron is emitted into vacuum. For the emission process the electron has to overcome the potential barrier at the surface, which for semiconductors can be described by the electron affinity E_A (difference between

STATUS AND PERSPECTIVES OF THE PITZ FACILITY UPGRADE*

S. Rimjaem†, G. Asova‡, J.Bähr, C. Boulware, K. Boyanov‡, H.J. Grabosch, M. Hänel, Y. Ivanisenko§, S. Khodyachykh, S. Korepanov, M. Krasilnikov, S. Lederer, A. Oppelt¶, B. Petrosyan, S. Riemann, A. Shapovalov‖, T.Scholz, L. Staykov, R. Spesyvtsev**, F. Stephan, DESY, 15738 Zeuthen, Germany
K. Flöttmann, DESY, 22603 Hamburg, Germany
L. Hakobyan, YerPhI, Yerevan, Armenia
D. Richter, BESSY, 12487 Berlin, Germany
J. Rönsch, University of Hamburg, 22761 Hamburg, Germany
K. Rosbach, Humboldt University, 12489 Berlin, Germany

Abstract

The Photo Injector Test facility at DESY in Zeuthen (PITZ) has been established to develop and optimize electron sources that cover requirements of Free Electron Lasers (FELs) facilities such as FLASH and the European X-ray Free Electron Lasers (XFEL). A major upgrade of the facility is ongoing in steps, in parallel to the commissioning of the extended setup and first experiments. The new setup towards the final design mainly includes a photo cathode RF gun, a post acceleration booster cavity and several diagnostic systems. In order to fulfill the characterization of the high brightness electron source, the diagnostic systems will consist of three emittance measurement systems, two high-energy dispersive arms, an RF deflecting cavity and a phase space tomography module as well as bunch length diagnostics. In this paper, results of the commissioning of the new RF gun, which has been installed and conditioned at PITZ in spring and summer of 2007, the current PITZ status and details of the future facility upgrade will be presented.

INTRODUCTION

Source and injector development has been realized as one of the most important challenges in electron accelerator technology since several accelerators, e.g. FELs, XFEL or Linear Collider, demand excellent beam conditions right from the source. The main requirement for an electron injector is its capability to produce a high brightness beams. PITZ has been designed and built to serve this purpose in order to produce intense electron beams with very small transverse emittance and reasonably small longitudinal emittance. The main objective at PITZ is to generate a reliable electron beam, with transverse emittance of about 1 mm mrad with a bunch charge of 1 nC and an energy spread smaller than 1%. The possibility to achieve small beam emittance has been demonstrated during the successful commission of the facility in the first phase (PITZ1) [1] and intermediate upgraded phase (PITZ1.5) [2].

Further upgrade of the facility towards the final design PITZ2 has been continued to extend the ability to achieve a smaller beam emittance. The so called PITZ1.6 has been finalized and was taken into operation in 2006. PITZ1.6 has completed its tasks with characterization of two new gun cavities (prototype 3.1 and 3.2). Recent commissioning and experimental results from PITZ1.6 with gun 3.2 will be discussed in this paper. Furthermore, the facility upgrade towards the next phases will be described.

PITZ1.6 SETUP WITH RF GUN PROTOTYPE 3.2

The current PITZ setup (PITZ1.6) consists of a 1.5 cell normal conducting RF gun with a Cs_2Te photocathode and a Nd:YLF laser system, a normal conducting booster cavity for post acceleration and diagnostic systems upstream and downstream of the booster cavity. The RF gun and booster cavity are operated with separated L-band (1.3 GHz) RF power systems. The diagnostic sections include devices for characterize the electron beam, e.g. beam size, bunch charge, its position, transverse emittance, longitudinal phase space distribution, electron bunch length, beam momentum and momentum spread. The main upgrade from PITZ1.5 to PITZ1.6 comprises installation of three new emittance measurement systems [3] and a new screen station after the booster for bunch length measurements at electron energies between 4 and 40 MeV [4]. Gun prototype 3.1 was installed and operated up to the maximum requirements of FLASH with maximum peak power of 3.5 MW, resulting in $\sim$40 MV/m gun gradient at the cathode, with RF pulse length of 900 μs at 10 Hz repetition rate [5]. Gun prototype 3.2 was installed in the PITZ1.6 beam line and was taken into operation in April 2006. A main goal for its operation is to study and optimize its properties in the presence of a high accelerating gradient of up to 60 MV/m.

* This work has partly been funded by the European Community, contract no. RII3-CT-2004-506008 and 011935 and by the 'Impuls- und Vernetzungsfonds' of the Helmholtz Association, contract no. VH-FZ-005.

† sakhorn.rimjaem@desy.de
‡ On leave from INRNE, Sofia, Bulgaria
§ On leave from IERT, Kharkov, Ukraine
¶ Presently at PSI, Villigen, Switzerland
‖ On leave from MEPHI, Moscow, Russia
** On leave from NSCIM, Kharkov, Ukraine

PERFORMANCE OF THE FERMI FEL PHOTOINJECTOR LASER*

M. B.Danailov, A.Demidovich, R.Ivanov, I.Nikolov, P.Sigalotti
ELETTRA, 34012 Trieste, Italy

Abstract

The photoinjector laser system for the FERMI FEL has been installed at the ELETTRA laser laboratory. It is based on a completely CW diode pumping technology and features an all-CW-diode-pumped Ti:Sapphire amplifier system, a two stage pulse shaping system, a time-plate type third harmonic generation scheme and aspheric shaper based beam shaping. The paper will present experimental results describing the overall performance of the system. The data demonstrates that all the initially set parameters were met and some largely exceeded. We present what is to our knowledge the first direct measurement of the timing jitter added by a Ti:Sapphire amplifier system and show that for our case it is below 10 fs.

INTRODUCTION

The photoinjector laser (PIL) is known to be one of the very important sub-systems for all single-pass UV and X-ray FELs. The charge and quality of the electron bunch created at the photoinjector (PI) affect dramatically the operation of the FEL and can be a strong limitation in obtaining the expected FEL performance. This is especially true for the challenging projects that are now in construction phase (like LCLS, SLAC, European XFEL). A lot of attention has thus been devoted previously for studying the optimum parameters of the PIL. It is now well accepted that the UV beam should have a nearly flat top spatial profile, while the optimum longitudinal (temporal) shape may vary [1-3]. In addition, laser parameters like energy and beam pointing that may seem easier to control, have also to be very carefully optimised. The overall system design appears to be more difficult in the case of copper photocathode, because of the required very high UV energy (~0.5 mJ for extracting 1 nC). The implementation of beam and pulse shaping techniques at these energy levels in UV is quite challenging. In this paper we describe the schemes and technologic solutions developed at Elettra for the FERMI PIL. As it will be seen the system fully meets and in some aspects exceeds the requirements.

MAIN SYSTEM DESIGN

As it has already been discussed in earlier papers [4], the only laser technology that can meet all the PIL parameters requested for copper photocathode, and is enough mature and reliable, is the one based on Ti:Sapphire as an active material and regenerative amplifier/multipass chirped-pulse amplifier design. The amplifier system described here is a custom system constructed by Coherent Inc. This is in fact the first amplifier system of this type, reaching an energy level above 18 mJ in the infrared, with the use of entirely CW diode pumping technology, which is the base for the extremely high UV energy stability reported below. The amplifier design is shown on Figure 1.

As it is seen, the seed coming from a Ti:Sapphire oscillator (Mira), is stretched and amplified to a mJ level in a regenerative cavity, after which it is further amplified in two two-pass amplifier stages. Each of these is pumped by up to 45 mJ from two Evolution HE Nd:YLF Q-switched pump lasers. As mentioned above, they are pumped by diodes in CW. Table 1 summarizes some of the main laser parameters.

Parameter	Specs	Measured
IR output energy	> 18 mJ	> 18 mJ (~15 mJ in operation)
Pulse duration (Gauss.fit)	<100 fs	~90 fs
Center WL	780+/-5 nm	~783 nm
M^2 value	$M^2_{x,y}$<1.5	M^2_x~1.27, M^2_y<1.17
UV energy before shaping	>2 mJ	>2.3 mJ
Short term energy stability UV (500 shots), RMS	<3%	<0.6%
Long term energy stability UV (8 hours), RMS	<3%	<0.8%
Beam pointing stability	<10 µrad	<5 µrad
Timing jitter (10 Hz-10MHz), RMS	<350 fs	<180 fs

Table 1: Main laser parameters , left- specified, right-measured

We note that the system is capable of delivering >18 mJ energy per pulse in IR, however the reported 2.3 mJ of UV energy is obtained at ~15 mJ in the IR. This regime is preferred for everyday operation because of lower diode current (~19A) and also lower load on the optical components. Conversion efficiency to third harmonic (261 nm) is about 15% and has been fixed after careful balancing of spot-size and pulse duration. Both interferometer like and 'time-plate' designs of the THG unit have been tested with similar results. However, in the latter we have observed a deterioration of the calcite plate which pre-compensates the group velocity mismatch, so at present the interferometric version is in operation.

* This work has been partially supported by the EU Commission in the Sixth Framework Program, Contract No. 011935 EUROFEL

A LASER HEATER FOR FERMI@ELETTRA

S.Spampinati, S. Di Mitri, B Diviacco, Sincrotrone Trieste, Italy.

Abstract

To cure the microbunching instability in the FERMI@elettra FEL a laser heater is proposed. The one-dimensional model of the instability predicts a large energy modulation cumulating as the electron beam travels along the linac. According to analytical studies and simulations the longitudinal Landau damping provided by the laser heater is expected to help in suppressing the formation of such a modulation. The efficiency of the beam heating is studied as function of the transverse laser-electron beam mismatch in the laser heater undulator in case of a realistic transverse beam profile.

INTRODUCTION

The FERMI@elettra [1] project will upgrade the Elettra linac with the installation of a photoinjector, a laser heater, an X-band cavity and two magnetic bunch compressors. The linac will then be able to provide the high current, low emittance and low energy spread (high brightness) electron beam needed by the single-pass Free Electron Laser (FEL). In this paper we describe the laser heater.

LASER HEATER

The laser heater is planned to be installed in the linac at a point where the electron beam energy is roughly 100 MeV. This device will provide a controlled increase of the uncorrelated energy spread. According to analytical and numerical studies, the beam heating is expected to help in suppressing the microbunching instability through longitudinal Landau damping [2].

The laser heater layout is shown in Figure 1.

The laser heater consists of an undulator located within a small magnetic chicane that allows an external laser to seed the electron beam. There is space for further diagnostic devices beyond the exit of the laser heater undulator.

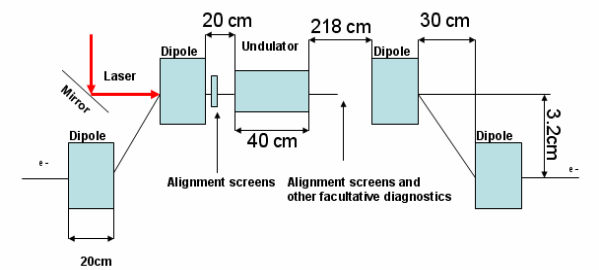

Figure 1: Schematic of the laser heater layout.

The particles interact with the laser in the short undulator and they gain an energy modulation with a periodicity on the scale of the optical wavelength. The corresponding density modulation is negligible; however, the induced energy/position correlation is smeared by the transverse motion in the chicane. As a result, the laser/electron interaction leads to an effective heating of the beam. The main laser heater parameters are listed in the Table 1.

The laser used for the heater will be split from the main beam of the Ti:Sa laser used for the photoinjector laser system. The maximum peak laser power available in the undulator is 10 MW. The IR laser will be stretched to reach a pulse duration of 20 ps. The pulse energy needed is <1mJ, therefore only a small part of the infrared light energy available (for laser heater and photocathode, >18mJ) will be needed for the laser heater. The induced energy spread must be in the rage 10 – 20 keV RMS [3].

Table 1: Mean laser heater parameters

Parameter	**value**
Undulator period	4 cm
Number of periods	12
Bending angle	3.5 degrees
Bending length	20 cm
Drift between bending	30 cm
Drift before undulator	20 cm
Drift after undulator	218 cm
Total length	418 cm

Neglecting changes in the laser and beam transverse dimensions during the interaction, the provided energy modulation for a “hard edge” undulator filed [4] is given by equation.(1):

$$\Delta\gamma_L(r)=\sqrt{\frac{P_L}{P_0}}\frac{K\,L_U}{\gamma_0\,\sigma_r}\left[J_0\left(\frac{K^2}{4+2K^2}\right)-J_1\left(\frac{K^2}{4+2K^2}\right)\right]\cdot e^{-\frac{r^2}{4\sigma_r^2}}\frac{\sin(\frac{\nu_0}{2})}{\frac{\nu_0}{2}}$$

with:

$$\nu_0 = 2\pi N\frac{(\lambda-\lambda_r)}{\lambda} \quad (2)$$

P_L is the laser peak power, $P_0 = 8.7GW$, r is the average radius of the electron beam transverse size, σ_r is the RMS laser spot size in the undulator and $\gamma_0 mc^2$ is the average total energy of the electron beam. J_0 and J_1 are the Bessel functions, K is the undulator parameter, L_u is the undulator length, λ_u is the undulator period, N is the number of periods of the

UV PERFORMANCES OF PULSED LASER DEPOSITION GROWN MG PHOTOCATHODES*

L. Cultrera, G. Gatti, F. Tazzioli (INFN/LNF, Frascati (Roma)), C. Ristoscu (INFLPR, Bucharest - Magurele), P. Miglietta, A. Perrone (INFN-Lecce, Lecce)

Abstract

We report a detailed description of the laser cleaning procedure and emission performance measurement on a Pulsed Laser Deposited Mg film. During the tests performed after the end of each cleaning operation we have evidenced an increase of Quantum Efficiency (QE) in time. Then the QE apparently stabilizes at a remarkably higher value. The study of this phenomenon is important because it determines both the working QE value and the lifetime of the cathode. Moreover, the stability of the QE has been revealed for a time scale of several days after each laser cleaning process, in our vacuum conditions.

INTRODUCTION

The electron injectors for the advanced projects of fourth generation X-ray sources, as SASE-FELs [1], and for future linear colliders [2], are mostly based on laser excited photocathodes. Metals have order of femto-second response and they are rugged in handling. Among them, Mg has premium QE, in the order of 10^{-3} at near UV wavelength (266 nm). However, bulk Mg cathodes have shown poor emission uniformity and failures in the high electric fields environment of RF guns. Moreover, the QE value degrades in time even in the UHV vacuum of RF guns.As an alternative, Mg films on copper substrates have been proposed and tested on the basis of their presumed better purity and uniformity [3]. Previous reports on Mg films grown by Pulsed Laser Deposition showed promising results in particular with respect to uniformity of emission, quantum yield, and adhesion to the substrate [4-6].

In order to reach the utmost QE value is necessary to remove the inevitable oxide layer that forms on the film surface. Only two techniques were used to perform such operation: laser cleaning and ionic etching [7]. The laser cleaning operation must be performed with particular care due to the limited thickness of the film and to avoid inducing surface roughness. It was evidenced that the cleaning irradiation may determine a variation of the film surface morphology [8].

The aim of this paper is to describe the film deposition conditions, the laser cleaning procedure and to evidence the performance of Mg films from photoemission point of view.

EXPERIMENTAL

Cathode preparation

The PLD technique is a well-known method for thin films deposition of several materials [9, 10]. The PLD apparatus used to deposit thin films is shown in figure 1. During the deposition the vacuum chamber was filled with pure He at a pressure of 5 Pa to reach the plume confinement regime leading to an increase of the deposition rate [11].

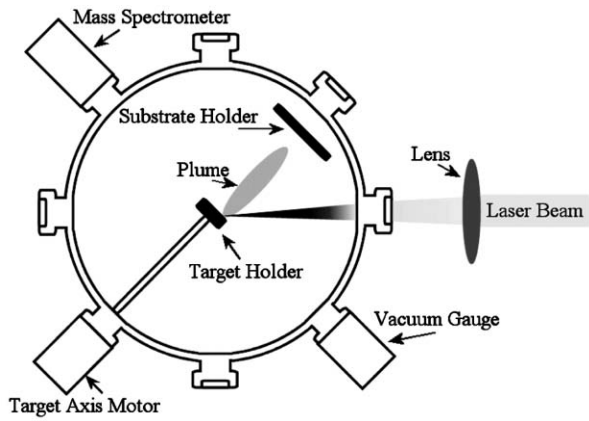

Figure 1: PLD experimental setup.

With the aim to clean the target surface, a pre-irradiation treatment was applied with 5,000 laser pulses. During this laser cleaning, the Cu substrate was shielded from the initial ablated material, which could contain impurities. Several films were prepared to optimize the deposition process. The deposition parameters of the tested sample are shown in table 1.

Table 1: Mg film deposition parameters.

Target	Mg
Substrate	Cu
Target-Substrate distance	3.5 cm
Laser spot size	1.0 mm^2
Base pressure	5 x 10^{-6} Pa
Laser pulses • Cleaning (5 x 10^{-6} Pa) • Deposition (in He at 5 Pa)	 5000 50000
Laser fluence	10 J/cm^2
Film thickness	2.5 μm
Film diameter	12 mm

Vacuum diode cell

The QE measurements were performed in a photodiode cell under UHV condition. The cathode and the anode separated at a distance of 3 mm were placed inside the photodiode cell (fig. 2). The Mg film occupied the cathode position and was electrically grounded. The anode plate was biased with high DC voltages up to 5 kV thus allowing the generation inside the gap of an intense electric field of about 1.7 MVolt/m.

* This work has been partially supported by the EU commission in the sixth framework program, contract no. 011935 EUROFEL and by MIUR, Progetti Strategici, DD 1834. December 4. 2002.

HIGH BRIGHTNESS C-BAND AND X-BAND PHOTOINJECTOR CONCEPTS AND RELATED TECHNOLOGICAL CHALLENGES

M. Ferrario, D. Alesini, V. Fusco, M. Migliorati, L. Palumbo, B. Spataro, INFN-LNF, Frascati, Roma, Italy.
L. Serafini, INFN-Mi, Milano, Italy.
J. B. Rosenzweig, UCLA, Los Angeles, CA, USA.

Abstract

Future light sources based on high gain free electron lasers, require the production, acceleration and transport up to the undulator entrance of high brightness (low emittance, high peak current) electron bunches. Wake fields effects in accelerating sections and in magnetic bunch compressors typically contribute to emittance degradation, hence the photo-injector design and its operation is the leading edge for high quality beam production. The state of the art photoinjector beam brightness can be in principle brought close and above the 10^{15} A/m^2 threshold with C-band and X-band guns and a proper emittance compensation scheme. We discuss in this paper optimized designs of split C-band and X-band photoinjectors and the further technological developments required to reach such an appealing goal.

INTRODUCTION

The optimization of a FEL source is quite a complicated task [1] but the main requirement for the electron beam in order to achieve short wavelength radiation in a reasonable long undulator (30-100 m) is clear: high transverse brightness. Transverse beam brightness is defined hereafter with the approximated [2] expression:

$$B_{\perp} \approx \frac{2I}{\varepsilon_{n,x}\varepsilon_{n,y}}$$

where I is the bunch peak current and ε_n is the bunch transverse normalized emittance. The expected transverse brightness for electron beams driving short wavelength SASE FEL facilities is of the order of $10^{15} - 10^{16}$ A/m^2. Wake fields effects in accelerating sections and in magnetic bunch compressors typically contribute to emittance degradation, hence the photo-injector design and its operation is the leading edge for high quality beam production. In a photoinjector the emitted electrons are rapidly accelerated to relativistic energies, thus partially mitigating the emittance growth due to space charge effects that is the dominant source of emittance degradation in a high brightness photoinjector. One of the key feature that make RF photoinjectors so actractive is that the emittance growth is reduced when operated at high peak field as the one achievable in the RF gun: up to 140 MV/m in a S-band gun. In addition the technique termed "emittance compensation" [3] has been experimentally verified in many laboratories and theoretically well understood [4].

A lot of efforts has been done in the last years at SPRING-8 and SLAC in the context of the high frequency normal conducting linear collider development, in order to achieve high accelerating gradient in C and X-band accelerating structures. Accelerating gradient in multi-cell TW accelerating structures as high as 40 MV/m (C-band) and 100 MV/m (X-band) has been so far achieved with low breakdown rate. In a different context an X-band standing wave 5.5 cells photoinjector has been developed at SLAC as a compact electron source for Thomson backscattering experiments. As reported in [5] a peak field on the cathode surface of 200 MV/m has been achieved.

The decision to adopt L-band superconducting technology for the next International Linear Collider (ILC) has somehow damped the effort towards high frequency structures development. More recently the choice to adopt X-band technology in the framework of the CLIC project [6], which has a less tight temporal time schedule than ILC, has open up again the interest towards X-band high gradient cavity R&D. FEL sources driven by high brightness linacs will certainly take profit from this new effort in the linear collider community, in particular for the possibility to develop high gradient photoinjectors. To this end we discuss in this paper possible designs of high frequency RF photoinjectors based on C-band or X-band technology, able to produce beams with brightness as high as 10^{15} A/m^2 directly from the injector and the related technological developments required to reach such an appealing goal

SCALING APPROACH TO HIGH FREQUENCY PHOTOINJECTORS

We decided to investigate a split photoinjector configuration, consisting in a 1.6 cells standing wave RF gun followed by a booster, because it is a well know scheme in the L and S band projects and also because is a promising design to achieve ultra-high gradients operating at higher frequency: the reduced wall surfaces implies a lower probability for surface defects that may cause RF breakdown. Another possible scheme has been presented in [17]. In addition following the matching condition discussed in [4] a working point very suitable to damp emittance oscillations has been found [7]. As any well optimised design it can be easily scaled [8,9] to any other frequency, gradient or charge design.

As a reference design we have taken the S-band (2856 MHz) SPARC [15] photoinjector. In its ideal configuration the beam consists in a uniform charge distribution inside a cylinder of length L and radius R, and we have scaled its parameters (charge Q, beam sizes

WAKEFIELD INDUCED ENERGY SPREAD IN THE FERMI UNDULATOR

A.A.G. Lutman*, M. Castronovo†, R. Vescovo*, Università degli Studi di Trieste, Trieste, Italy
C. Bonţoiu, P. Craievich‡, L. Rumiz, ELETTRA, Trieste, Italy

Abstract

The FERMI Project aims to achieve very high-brightness photon beam pulses of minimum bandwidth. These goals can be marred by the presence of large wakefields along the undulator small-gap vacuum chamber. Estimations of the induced energy-spread caused by the resistive wall and surface roughness wakefields along the FERMI FEL undulator are presented. The energy spread and losses induced by resistive wall wakefield are determined for three possible transverse geometries of the vacuum chamber, namely circular, rectangular and elliptic cross-section, while the energy spread and losses induced by the surface roughness wakefields are obtained for the circular cross-section case. In this last case in-house surface profile measurements carried on a spare vacuum chamber of ELETTRA are used to provide realistic estimates.

WAKEFIELDS IN THE UNDULATOR VACUUM CHAMBER

In the undulator vacuum chamber the finite conductivity of the metal wall and the roughness of the chamber inner surface wakefields are sources of wakefields. For the FEL effect, the main concern is the longitudinal wake which may impress an energy modulation on the electron bunch and consequently degrade the quality of the FEL radiation. Transverse wakefields are much less disruptive in the undulator and will be neglected.

Resistive Wall Wakefields

The interaction between the electron beam and the metal wall has been evaluated for circular, rectangular and elliptical cross-section vacuum chambers. Regardless of the shape of the cross-section, the chamber is modeled as an infinite pipe with finite conductivity σ, electron relaxation time $\tau > 0$ and infinite wall thickness. The relative longitudinal displacement from the bunch head will be denoted by z. The almost flat-top short bunches which will be used for the FERMI FEL contain very high frequencies components induced by the residual current spikes and thus require, as pointed out by Bane [1], the use of the AC conductivity model. In the following formulas the skin-depth related parameter $\lambda = \sqrt{\frac{Z_0 \sigma |k|}{2}}(i + sign(k))$ will be used, where Z_0 is the intrinsic impedance of the vacuum and k is the wave number.

Circular cross-section: For the circular cross-section, the calculations rely on the formula derived by Chao [2]. Denoting with b the radius of the pipe, the longitudinal coupling impedance is given in SI units by:

$$Z(k) = \frac{Z_0}{4\pi} \frac{1}{b} \frac{2}{\frac{\lambda}{k} - \frac{ikb}{2}} \tag{1}$$

Rectangular cross-section: For the rectangular shape the evaluation relies on the formulas given by Henke and Napoly [3]. Although the theory is elaborated for two conducting infinite parallel plates, we will use it for a rectangular cross-section neglecting the effects of the lateral walls. Denoting with b the half gap between the metal plates, the longitudinal coupling impedance, as given in [4] is in SI units:

$$Z(k) = \frac{Z_0}{4\pi} \int_{-\infty}^{+\infty} \frac{1}{\frac{\lambda}{k} \cosh^2 bx - \frac{ik}{x} \cosh bx \sinh bx} dx \tag{2}$$

Elliptic cross-section: For the elliptic cross-section shape a novel method that holds for AC conductivity and allows one to evaluate the wakes at very short range, has been developed. The fields are obtained by developing a system of solutions to the Maxwell's equations both in the vacuum and in the resistive wall and then imposing the boundary conditions on the wall surface similar to what has been done for the circular case. The longitudinal and transverse wake functions are then calculated using field expansions. Maxwell's equations have been solved in an elliptic cylindrical system of coordinates (u, v, z) (see Fig. 1), taking the source as an ultrarelativistic point charge travelling down the pipe, parallel to its axis, located arbitrarily in (u_1,v_1,0). On the cross-section the interface between the vacuum and the metal wall is the ellipse of equation $u = u_0$. With the observation that, due to causality, any field must vanish for $z > 0$, the Fourier transform of the electric and magnetic longitudinal fields in the vacuum, can be written as:

$$\begin{aligned} \tilde{E}_z &= \sum_{n=0}^{+\infty} A_n \cosh nu \cos nv + \sum_{n=1}^{+\infty} B_n \sinh nu \sin nv \\ c\tilde{B}_z &= \sum_{n=0}^{+\infty} B_n \cosh nu \cos nv - \sum_{n=1}^{+\infty} A_n \sinh nu \sin nv \end{aligned} \tag{3}$$

where A_n and B_n depend on k and are determined by imposing the continuity of the fields $\tilde{E}_z$, $\tilde{B}_z$, $\tilde{E}_v$, $\tilde{B}_v$. In the vacuum, the transverse fields behavior shows a coupling between different modes. In detail the components $\cos nv$,

* DEEI
† Dipartimento di Fisica
‡ paolo.craievich@elettra.trieste.it

WIDE BAND SEEDING AND WAVELENGTH COMPRESSION

Tsumoru Shintake, RIKEN/SPring-8, 679-5148 Japan

Abstract

The "wavelength compression" has a potentiality to generate seeding signal at the nano-meter wavelength by squeezing optical wavelength of the visible laser beam on a high energy electron beam. Applying energy chirp on the incoming electron beam and overlapping laser beam to produce micro-period energy modulation at optical wavelength, the velocity modulation can be converted into density modulation at shorter wavelength during the bunch compression in a chicane. Using 255 nm 4th harmonic YAG laser as modulation signal, and if we compress bunch length 20 times, we can generate coherent signal below 10 nm. By cascading multiple bunch compressors, higher compression ratio will be obtained. To go X-ray wavelength, we may use HGHG scheme after the wavelength compression. Since compression factor is variable, it becomes tuneable coherent source at X-ray wavelength, which is suitable to seeding the X-ray FELs.

Using femto-second laser at the modulator, it will generate atto-second pulse at short wavelength.

MOTIVATION

SASE-FEL: Self-amplified Spontaneous Emission Free Electron Laser, as it is named, the spontaneous radiation (noise power) is amplified in the long undulator line. If the undulator is long enough, power level reaches to saturation. Since its power level is extremely higher than conventional X-ray sources, even higher than 3rd generation light sources, many new scientific applications are expected with using this source. Also the short pulse feature in femto-sec range is expected to be an important feature for analysing fast chemical and physical reaction of condensed matter.

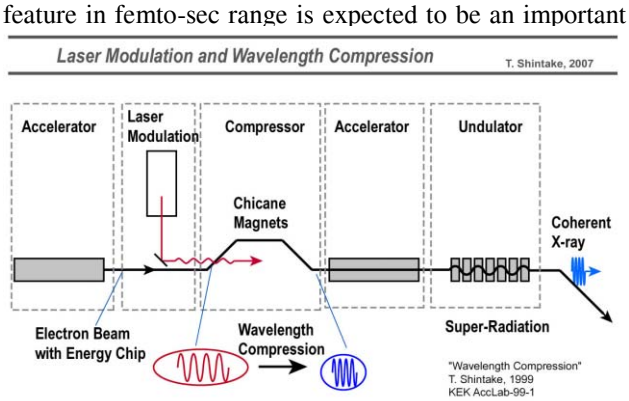

Figure 1: Laser optical modulation and wavelength compression. Applying both the energy chirp at rf wavelength and micro-period energy modulation at optical wavelength using laser beam, the modulation pattern can be compressed into short wavelength during bunch compression, which provides seeding signal to the downstream undulator. By combining with HGHG scheme in the downstream undulator line, an X-ray seeded FEL will be realized.

However, since SASE-FEL process starts from the spontaneous radiation, the resulting saturated radiation power varies shot-by-shot. And most importantly, there are many longitudinal modes, similar to old fashion ruby laser, temporal profile has many spikes, thus longitudinal coherence is quite limited.

If we seed a coherent signal from upstream undulator, the seeding signal will be amplified and saturated. It becomes (1) fully coherent, (2) temporally single-mode, (3) stable energy in pulse-to-pulse and (4) power level controllable. These features are favourable to all kind of scientific applications. Therefore, various proposals have been made on seeding schemes, including HGHG, TUHG,[3,4,5]. G. Lambert reported first observation of amplification of seeded FEL using higher harmonic generation in gas [HHG] at 160 nm in SCSS test accelerator[7].

They are also promising approach to generate coherent radiation at nano-meter wavelength. However they are not wavelength tuneable. In actual machine, a small wavelength shift was observed experimentally at DUV FEL at BNL[6]. However the observed wavelength shift was as low as 1%.

For fully tuneable seeding, the wavelength compression scheme was originally proposed by the author in 1999[1]. As shown in Fig. 2, a modulator, a short undulator was assumed as energy modulator, where a laser beam was introduced from upstream[2]. The velocity modulation is created through $E_t \cdot v_t$ coupling in the undulator. After the undulator, the electron bunch is accelerated at off-crest phase to apply energy chirp, then the bunch length is compressed. After accelerating the beam, the modulated electron beam is fed into undulator to generate coherent radiation. This scheme requires many hardware components, and also spontaneous emission in the upstream undulator cause additional energy spread on the incoming electron beam.

In the previous paper[2], the author proposed a scheme to generate energy modulation at optical wavelength using the focal point laser field. However, the laser beam has to be focused into a very small spot, and the fraction of overlapping the laser beam to the electron beam is fairly small, as a result overall modulation efficiency becomes small.

To overcome this difficulty, the author proposes a new scheme which provides higher coupling efficiency.

#shintake@spring8.or.jp

FEASIBILITY TEST OF LASER-INDUCED SCHOTTKY-EFFECT-GATED PHOTOCATHODE RF GUN

H. Tomizawa, Accelerator Division, Japan Synchrotron Radiation Research Institute (JASRI/SPring-8), Kouto, Sayo-cho, Sayo-gun, Hyogo 679-5198, Japan
M. Kobayashi, Research & Development Division, Nanophoton Corporation
A-509, Center for Advanced Science and Innovation, Osaka University, Osaka 565-0871, Japan.

Abstract

We propose a laser-induced Schottky-effect-gated photocathode RF gun using Z-polarization of the laser source. This concept of laser-induced Schottky emission can be applied to a photocathode DC gun (even for a polarized electron source). Radial polarized laser propagation modes exist theoretically and were recently generated practically. Focusing a radial polarized beam on the photocathode, the Z-polarization of the laser is generated at the focus point. The generated Z-polarization field can exceed an electrical field of 1 GV/m easily with fundamental wavelength from compact femtosecond Ti:Sa laser systems. According to our calculations (NA=0.15 60-% hollow ratio, inside-out Gaussian beam), the Z-field of 1 GV/m needs 1.3 MW at peak power for the fundamental (790 nm) and 0.32 MW for the second harmonic generation (SHG). In the field of 1 GV/m, the work function of copper cathode reduces ~2 eV. The quantum efficiency is pessimistically estimated to be $\sim 10^{-2}$ % at SHG by the Schottky effect associated with the 1 GV/m. This Schottky effect can be used as a gate of the photo-emission process. We report a feasibility study of this new concept of photocathode.

INTRODUCTION

There are three well-known types of electron guns; the thermionic gun, field emission gun, and photocathode gun. They are widely used for many applications. The future light sources based on linear accelerators such X-ray FEL [1,2,3] and ERL [4] required high brightness electron sources. One of the most promising candidates for such an electron source is a photocathode RF gun.

The photocathode RF gun needs a UV-laser source (~266 nm) for a long-lived metal cathode like copper and even for a higher quantum efficiency (QE) cathode such as Ce_2Te. At SPring-8 in collaboration with Hamamatsu Photonics K.K. a diamond cathode has been developed as the future transparent cathode candidate [5]. The diamond cathode is a robust and high QE cathode. However, it requires a laser wavelength below 197 nm for acceptable QE. For a robust cathode like copper and diamond, we need UV-laser light due to their high work functions. Consequently, the laser system becomes larger and complex. To make the laser source compact, we need to find a cathode with a lower work function and high QE. However, such a high QE NEA-cathode requires an ultra-high vacuum ($< 10^{-8}$Pa) and does not have a long life time.

One solution to make the work function lower is to apply a high field on the cathode. In the field of 1~2 GV/m, the work function of the copper cathode reduces 2~3 eV. To achieve such a high field (~1 GV/m) on the photocathode, the tungsten needle photocathode, the photo-assisted field-emission, was proposed and tested [6]. The dependence of quantum efficiency on a high electric field was investigated using a tungsten needle (radius: ~1μm) photocathode irradiated by the third harmonic generation (THG) of a Nd:YAG laser (353 nm) whose photon energies were lower than the work function of tungsten. The obtained QE of the needle tip is found to be proportional to the >10th power of the electric field over 500 MV/m, and it reached up to 3% at about 800 MV/m. This observed field-enhancement of QE is qualitatively explained with a field-emission process including the Schottky effect and photo excitation. However, such a needle cathode tip became round and broken in the cavity during rf conditioning.

Therefore, we started to investigate with a plane-field emitter assisted by laser radiation field. We have indirect evidence of such a laser field effect through comparison between normal and oblique incidences to the cathode. It is well known that the oblique incidence obtains higher QE than normal incidence. In the oblique incidence, the more intensive the laser illuminating the cathode, the higher a QE we obtain. It cannot be explained only with Brewster's angle. However, we have to think about multi-photon absorption in the case of intensive laser focusing on the cathode. The oblique incidence makes the laser spot elliptically larger on the cathode. However, we can obtain a higher QE. It indicates that the laser field can assist the Schottky effect on the cathode.

Radial polarized laser propagation modes exist theoretically and were recently generated practically. The radial polarization beam is a superposition of π/2 phase-shifted TEM_{01} and TEM_{10} mode in the case of a polarisation direction vertical to each other. Focusing a radial polarized beam on the photocathode, the Z-polarization of the laser is generated at the focus point. The generated Z-polarization can exceed an electrical field of 1 GV/m easily with fundamental wavelength from compact femtosecond laser systems. On the other hand, focusing an azimuth polarized beam on the photocathode results in zero Z-polarization field. Comparing the radial and azimuth polarization with focusing, we conduct a feasibility study of the laser-induced Schottky-effect on the photocathode.

BEAM PROPERTIES FROM S-BAND ENERGY COMPENSATED THERMIONIC RF GUN AND LINAC FOR KU-FEL

Toshiteru Kii, Hideaki Ohgaki, Kai Masuda, Satoshi Sasaki, Takumi Shiiyama, Heishun Zen

Institute of Advanced Energy, Kyoto University, Gokasho, Uji, Kyoto 6110011, Japan

Abstract

Beam properties after the accelerator tube of the KU-FEL system were measured to ensure the potential of the energy compensation technique to compensate for energy degradation in a thermionic RF-gun. Small growth of energy spread and emittance were observed, and its influence to the FEL gain and evolution of output power were estimated. It was found that the influence due to the amplitude modulation was so serious, because the small increase of the energy spread drastically reduces FEL gain. In addition to the amplitude modulation, phase modulation will be required.

INTRODUCTION

An MIR-FEL facility, KU-FEL, has been constructed for application of the energy science[1]. The KU-FEL consists of a thermionic RF gun and a 3-m accelerator tube and an undulator to generate 4-13 μm FEL as shown in fig. 1. As an electron injector, we chose a thermionic RF-gun because of its compactness and an easy-handling feature. However, a serious problem of back-bombardment limits macro-pulse duration up to several micro seconds. Then, we have tested an energy compensation technique[2], which uses an amplitude modulated rf pulse using remotely controllable pulse forming network of the Klystron modulator, to reduce the influence of the back-bombardment, and successfully extracted energy compensated electron beam of 4.0 μsec macro-pulse duration and numerically expected to extract electron beam with constant energy up to 8.0 μsec[3,4]. On the other hand, the amplitude modulated RF pulse will give rise to phase difference between RF-gun and accelerator tube, because timing of RF output from Klystron will be shifted to earlier timing because the velocity of the electrons in the Klystron tube is changed during macro-pulse. Moreover, time-varying beam loading will increase beam emittance due to space charge effect. Therefore, we have studied influence of the beam properties, such as temporal current profile, energy spread and emittance, at the exit of the accelerator tube. We have also studied on a figure-of-merit of average beam current and pulse duration, because higher beam current reduces macro-pulse duration.

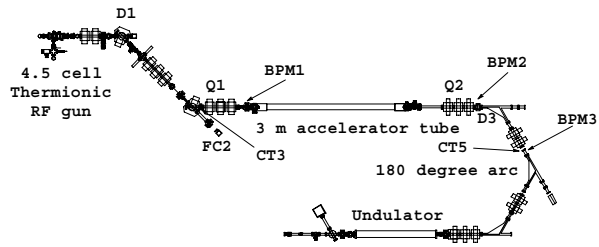

Fig. 1 Arrangement of the KU-FEL.

BEAM PROPERTIES

We have estimated the influence of the energy compensation technique from measurements of beam properties at the entrance and the exit of the accelerator tube. To estimate the influence of the technique clearly, two operational modes were selected. In the first mode, RF pulse of 3 μsec was fed to the RF-gun. Pulse duration after the first bending magnet was about 1.5 μsec. This mode was used to evaluate the beam properties without amplitude modulation. (Mode 1: Non-modulated mode) In the second mode, RF pulse of 7 μsec was fed. Pulse duration after the first bending magnet was about 5.2 μsec. This mode was used to evaluate the effect of the amplitude modulation. (Mode 2: Modulated mode) In these modes, average beam currents were set to around 30 mA, because if the electron beam with higher beam currents and shorter macro pulse duration is used as modulated mode, it is difficult to clear the differences between two modes.

Temporal Current Profile

Temporal profiles of the beam current at the entrance and the exit of the accelerator tube were measured using current transformers (CT3 and CT5 in fig. 1). As shown in figs. 2 and 3, acceleration was performed well in both modes. Although the most of electrons were accelerated in the modulated mode, macro-pulse duration was shortened after acceleration, and beam current was decreased by several percent in the latter part of the macro-pulse as shown in fig 3.

#kii@iae.kyoto-u.ac.jp

NUMERICAL EVALUATION OF OSCILLATOR FEL WITH MULTI-BUNCH PHOTO-CATHODE RF-GUN IN KYOTO UNIVERSITY*

Hideaki. Ohgaki#, Toshiteru Kii, Kai Masuda, Satoshi Sasaki, Takumi Shiiyama, Heishun Zen, Institute of Advanced Energy, Kyoto University, Gokasho, Uji, Kyoto 6110011, Japan
Ryunosuke Kuroda, National Institute of Advanced Industrial Science and Technology, Umezono 1-1, Tsukuba, Ibaraki 3058658, Japan
Masao Kuriki, Nobuhiro Terunuma, Junji Urakawa, High Energy Accelerator Research Organization, 1-1, Oho, Tsukuba, Ibaraki, 305-0801, Japan
Yoshio Kamiya, Masakazu Washio, Research Institute for Science and Engineering, RISE, Waseda University, 3-4-1, Okubo, Shinjuku-ku, Tokyo, 169-0072, Japan

Abstract

Numerical evaluations have been performed to install a photo-cathode RF-gun into an oscillator FEL system which has been developed in Kyoto University. The original FEL system was consisted of a 4.5-cell thermionic RF gun with S-band accelerator tube of 3-m to oscillate the mid-infrared FEL. The electron beam properties have been evaluated from an RF-gun to an FEL by using PARMELA and ELEGANT. On the other hand, the FEL parameters have been calculated with GENESIS which takes the optical cavity into account. The evaluated peak current of the electron beam was 10-50 times as high as those with the thermionic RF-gun. Since the oscillator FEL requires a multi-bunch electron beam, evaluation of the round-trip development of the FEL has been also performed by a 100 bunch train beam. The results showed that the FEL gain saturation was achieved within 3 round-trips.

INTRODUCTION

An infrared FEL (4-13 μm) facility for energy science is under construction at the Institute of Advanced Energy, Kyoto University [1]. The electron beam of 40 MeV and peak current of -10 A has been successfully accelerated by a linac system which consists of a 4.5-cell thermionic RF gun, a 'dog-leg' transport system, a 3m s-band linac, and a 180-degree arc bunch compressor [2]. Figure 1 shows the schematic view of the linac system which includes the photo-cathode RF-gun. To reduce the back-bombardment effect in the 4.5-cell RF gun, several attempts have been made, and the macro pulse duration of 5 μs has been achieved [3]. However, there still needs several efforts are needed both to extend the macro pulse duration and to increase the peak current to reach the FEL saturation [4]. Replacing the thermionic RF-gun to a photo-cathode RF-gun is the most promising way to obtain a high peak current electron beam. Therefore, we made a preliminary design study [5] and start to develop a 1.6-cell photo-cathode RF-gun [6]. Recently, the improved design of the

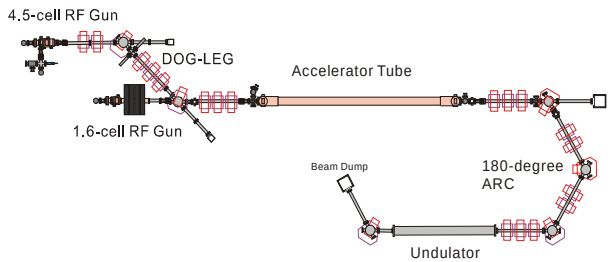

Figure 1: Schematic view of the KU-FEL driver linac.

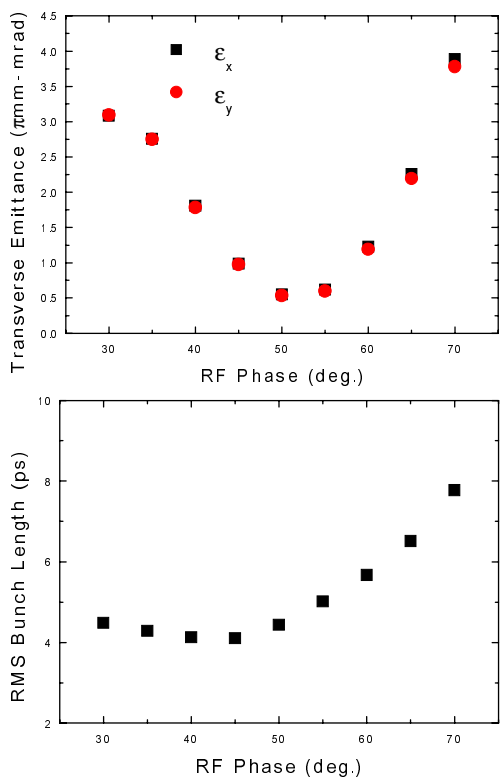

Figure 2: Transverse RMS emittance(a) and energy spread(b) of the electron beam from the gun as a function of the laser injection phase.

*Work supported by Promotion of Collaborative Research Programs in Universities of High Energy Accelerator Research Organization (KEK).
#ohgaki@iae.kyoto-u.ac.jp
+present address: International Center for Elementary Particle Physics, The University of Tokyo, 7-3-1 Hongo, Bunkyo-ku, Tokyo 113-0033, Japan

PRESENT STATUS OF FEL DEVELOPMENT IN KYOTO UNIVERSITY

Satoshi Sasaki, Heishun Zen, Takumi Shiiyama, Toshiteru Kii, Kai Masuda, Hideaki Ohgaki
Institute of Advanced Energy, Kyoto University, Gokasho, Uji, Kyoto, Japan, 611-0011

Abstract

We have constructed an infrared (4-13 μm) FEL facility for advanced energy researches in Kyoto University. The numerical studies on the expected FEL gain, which were based on the experimental measurements both of the undulator and of the electron beam parameters, were carried out. GENESIS code has been modified to simulate an oscillator FEL which took into account the chamber geometry and the mirror including hole coupling. Dependencies on a tilt angle and an offset of the mirror were evaluated by using this modified code, then for the first lasing the mirror parameter was optimized. At the present stage, we have installed the undulator and the mirror cavity. Measurements on spectrum of the spontaneous emission and electron beam characteristics were carried out. The measured spontaneous emission was consistent with the result of the calculation obtained with measured magnetic field of the undulator. Since the evaluated peak current of the electron beam was not enough for the lasing, LaB_6 cathode was ready to use.

INTRODUCTION

We have studied and developed an infrared (4-13 μm) FEL facility (KU-FEL) for advanced energy researches in Kyoto University. The KU-FEL consists of a 4.5-cell thermonic RF gun, 3 m accelerator, beam transport, Halbach-type undulator, and optical cavity. The RF gun and the accelerator operate at 2856 MHz (S-band), and produce electron beams up to 40 MeV.

To optimize the optical cavity, we calculated the FEL gain with the measured magnetic field of the undulator[1]. However, the treatment of the loss in the vacuum chamber and the light output from the cavity was truncated on the assumption of simple Gaussian distributions in transverse direction. On this assumption, the tolerance of the alignment errors of the optical cavity mirrors could not be evaluated. In this study, we carried out calculations of the light propagation taking into account of the duct shape and reflection/transmission of the light at the mirror for optimization of the optical mirrors and evaluation of the misalignment tolerance. For this purpose, we have modified a calculation code, GENESIS1.3[2].

Based on the re-optimized parameters in these calculations, we have installed the optical cavity and undulator in the KU-FEL system. We then observed the spectrum of the spontaneous emission, and compared it with the SRW[3] calculation.

Aiming at a higher peak current, we replaced the tungsten cathode in the RF gun by a LaB_6 cathode. In this paper, the preliminary experimental comparison will be also reported.

FEL GAIN CALCULATION

Calculation Code

We had calculated the FEL gain and round trip development to optimize the optical cavity parametes, by using TDA3D[4], but it didn't take into account the duct shape, reflection on mirror, absorption, and transmission of the mirror. In addition, the detuning parameter can hardly be handled.

To cope with these problems in this study, we modified GENESIS1.3 code taking in the realistic duct shape. We simulated a realistic FEL gain by using the modified code. The duct shape taken in the calculation is shown in Fig.1. The parameters of the electron beam used in the FEL gain calculation were optimized for the measured undulator parameters, and are listed in Table 1. The undulator parameters are listed in Table 2.

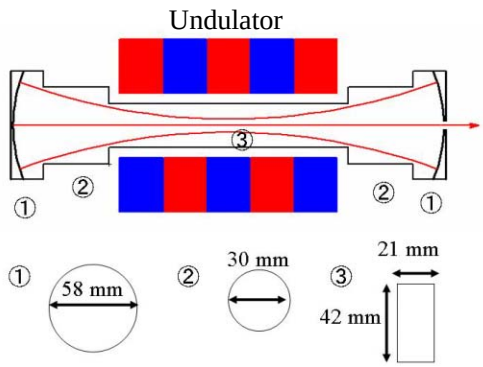

Figure 1: Duct shape

Table 1: Electron beam parameters

Emittance(x)	3.5 πmm-mrad
Emittance(y)	3.5 πmm-mrad
ΔE / E	0.5 %
Beam size(x)	0.6 mm
Beam size(y)	0.4 mm
Twiss parameter α_x	3.6
Twiss parameter α_y	0
Beam energy	25 MeV

Table 2: Parameter of Halbach type undulator

total length	1.6 m
Repetition	40
period	4 cm
gap	25.5 - 45 mm
Maximam magnetic field	0.26 - 0.0045 T
K value	0.99 - 0.17

A TRIODE-TYPE THERMIONIC RF GUN FOR DRASTIC REDUCTION OF BACK-STREAMING ELECTRONS

T. Shiiyama, K. Masuda, H. Zen, S. Sasaki, T. Kii, H. Ohgaki,
Institute of Advanced Energy, Kyoto University, Gokasho, Uji, Kyoto, 611-0011, Japan
K. Kanno, E. Tanabe, AET, INC., 2-7-6 Kurigi, Asaoku, Kawasaki, 215-0033, Japan

Abstract

We have proposed a triode-type thermionic RF gun with an additional small cavity replacing the conventional cathode, which provides the beam extraction phase independent of the main accelerating phase to suppress the back-bombardment effect drastically. In order to compensate the predicted degradation in transverse emittance, a design refinement was carried out by the use of numerical simulations in this study. The results showed that the back-bombardment power can be reduced by more than 80% and the peak current of the output electron beam will be enhanced greatly without emittance degradation. Also the cavity parameters, namely the quality factor and the coupling coefficient of the additional cavity with the RF feed coaxial cable were designed to ensure both the induction of the required cavity voltage and a wide frequency acceptance. The prototype design of the triode-type thermionic RF gun was completed and ready for experiments.

INTRODUCTION

We have used a 4.5-cell thermionic RF gun for the injector of MIR-FEL facility (KU-FEL: Kyoto University Free Electron Laser) at Institute of Advanced Energy, Kyoto University. As is well know thermionic RF guns suffer from the back-bombardment of electrons onto thermionic cathodes, which eventually leads to an output beam energy drop and limitation of the macro pulse duration [1, 2]. This effect is seen significant especially in the 4.5-cell RF gun in the KU-FEL because of its high coupling coefficient β and large number of cells. Some countermeasures were applied so far, such as the use of transverse magnetic fields [3] and the temporal control of the RF input for compensating time-varying beam-loading [4] with limited successes. A longer macro-pulse duration by a new technique against the back-bombardment effect is thus essential for the first FEL lasing.

For this purpose, we have proposed a triode-type thermionic RF gun [5, 6]. An additional small cavity with a thermionic cathode replaces the conventional cathode in the RF gun as schematically shown in Fig.1. An RF field induced at the short gap of the additional small cavity, and both the amplitude and the phase are controlled independently of the main accelerating cavities to minimize the back-bombardment of electrons onto the cathode.

Numerical studies so far have shown that the RF triode concept could reduce the back-bombardment power drastically (80% or higher) while it tends to induce inherent defocusing force at the same time, eventually resulting in an expense of the transverse emittance increase [7].

In this paper, design refinement of a triode-type thermionic cathode was carried out in order to suppress the transverse emittance increase. A wehnelt structure schematically shown in Fig.1 (b) was studied by PIC simulations to compensate the defocusing effect induced by the RF triode.

Also discussed in this paper is the selection of cavity parameters, namely the coupling coefficient β to the additional RF power feed, and the quality factor Q.

A potential feature of the RF triode concept is that the requirement of the RF power into the additional cavity is moderate, thus the cost for the RF system modification is low. For the first experiments we have installed a directional coupler to split the RF power from the existing klystron to feed < 40kW to the additional cavity.

To ensure a sufficient cavity voltage with the limited RF power and also expected resonant frequency shifts due to the beam loading effect and/or the cavity temperature change, the tuning curves were calculated by the use of an equivalent circuit model with the beam loading effect taken into account.

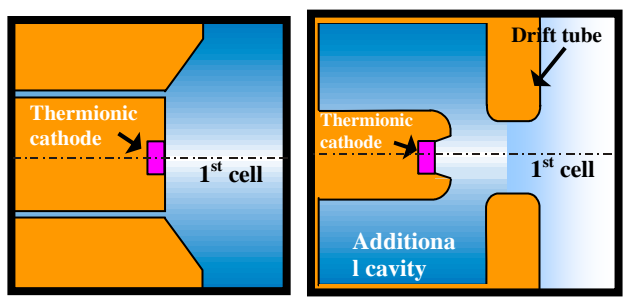

(a) Conventional type (b) Triode type

Figure 1: Schematics of RF cavity structures in the vicinity of the thermionic cathode in (a) a conventional, and (b) a triode-type RF gun.

NUMERICAL STUDY ON THE OPTIMUM CAVITY VOLTAGE OF RF GUN AND BUNCH COMPRESSION EXPERIMENT IN KU-FEL

H. Zen#, T. Kii, K. Masuda, H. Ohgaki, S. Sasaki, T. Shiiyama,
Institute of Advanced Energy, Kyoto University, Gokasho, Uji, Kyoto, 611-0011

Abstract

High peak current (~40 A) electron beams with the macro-pulse duration of 2-5 μs are required for the lasing of Kyoto University Free Electron Laser (KU-FEL). However, the bunch charge and macro-pulse duration in the facility have a trade-off relationship, and the bunch charge is limited to <30 pC when the macro-pulse duration is ~3 μs. Therefore, the optimization of operational condition of our thermionic rf gun and the bunch compression are necessary to achieve such a high peak current. Optimum field strength of our rf gun was surveyed by numerical simulation. The result indicates that the highest peak current is around 23 A with the average field strength of 24 MV/m. Under the same condition, bunch lengths of electron beams were measured by using a streak camera. The condition of bunch compression was also surveyed in experiment. The measured minimum bunch length was 2.0 ps, which was as short as the temporal resolution of the measurement system. Since the bunch charge was 14 pC, the highest peak current was estimated to be more than 7 A from the experimental result.

INTRODUCTION

A mid-infrared free electron laser facility (3-14 μm) named KU-FEL was constructed for the energy science in Institute of Advanced Energy, Kyoto University [1]. As shown in Fig. 1, the facility consists of an S-band 4.5 cell rf gun with a tungsten dispenser-type thermionic cathode, an energy filtering section (Dog-leg), a S-band accelerator tube (3 m), a bunch compression section (180-deg. arc), an undulator and an optical cavity. Electron beams were successfully accelerated up to 40 MeV [2]. However, due to the back-bombardment effect [3,4], the bunch charge and macro-pulse duration have a trade-off relationship and the bunch charge was limited to smaller than 30 pC with the macro-pulse duration of ~3 μs. Thus the bunch compression is necessary to obtain a peak current of ~40 A, which is required to achieve the FEL saturation [5] in KU-FEL. Another feature of the gun is that the higher average current is available after energy filtering section if the higher electrical fields are induced to its cavities. On the other hand, the nonlinearity of longitudinal phase space distribution, which enlarges a bunch length during a bunch compression, increases if too high electrical fields induced. It means that there is the optimum operational condition of the field strength of rf gun to obtain the highest peak current. In this study, first, the optimum field strength of the gun was surveyed by numerical simulation. Second, the bunch length was measured and the optimum bunch compression condition was determined under the gun condition in experiment. PARMELA [6] was used for particle tracking from the gun to the undulator. And ELEGANT [7] was used to find the achromatic sets of quadrupole magnets of dispersive section in simulation and experiment. And the code was also used to calculate and control the R_{56} of the arc.

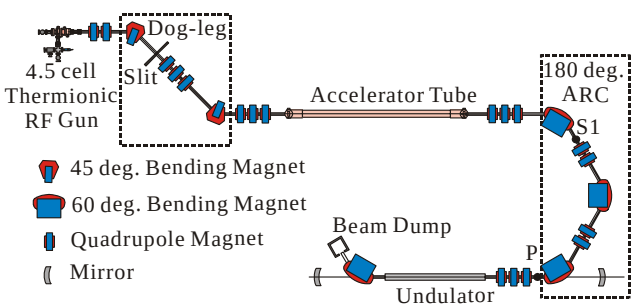

Figure 1: Schematic view of KU-FEL facility.

#heishun@iae.kyoto-u.ac.jp

STUDY ON THE OPTIMUM FIELD STRENGTH OF RF GUN

Dependences of the longitudinal emittance and the average current on the average field strength of the first half cell of the 4.5 cell rf gun were shown in Fig. 2. The field strengths of other 4 cells are about twice higher than that of the first cell. The longitudinal phase space distributions at the entrance of the accelerator tube were shown in Fig. 3. As mentioned in the introduction, the higher average current is available after the energy filtering section if the higher field strength of the cells is induced. As shown in Fig. 2 and 3, however, the nonlinearity of the longitudinal phase space distribution and the corresponding longitudinal emittance rise up if too high electric fields (>25 MV/m) are induced. High bunch charge and low longitudinal emittace are required to obtain high peak current after bunch compression.

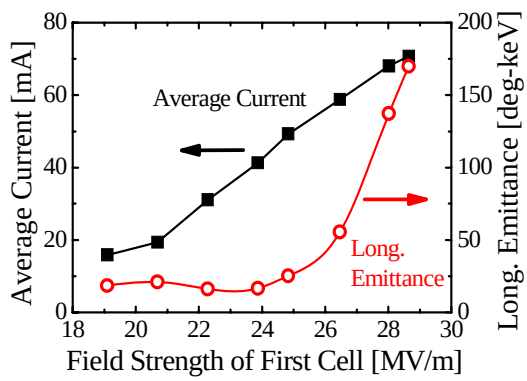

Figure 2: Longitudinal emittance and average current as a function of the field strength of first half cell.

DEVELOPMENT OF A COMPACT CHERENKOV FREE-ELECTRON LASER OPERATING IN TERAHERTZ WAVE RANGE

Nozo u Miyabe*,Akira Ikeda,Makoto R Asakawa,Mitsuhiro usaba, oshiaki Tsunawaki
ansai University, 3-3-35 a ate-cho, Suita, Osaka 562-8680, apan
Osaka Sangyo University, 3-1-1 Naka-gaito, aito, Osaka 574-8530, apan

Abstract

We designed a co pact Cherenkov Free-Electron Laser CFEL oscillator driven by 50ke electron bea The resonator, called double-slab resonator, consists of a rectangular waveguide partially lled with two lined parallel silicon slabs, whose dielectric constant ε e uals to 11 6 in the terahertz fre uency range The operation fre uency ranges fro 40 Hz to 1THz according to the thickness of the slabs Nu erical calculation predicted 100W-level output at 46 Hz by electron bea with 50ke 400 A

OPERATING FREQUENCY OF THE DOUBLE-SLAB RESONATOR

Our purpose is to develop a CFEL oscillator operating in the terahertz fre uency range driven by a low energy electron bea 1 We e a ine the operating fre uency of the double-slab resonator fed by 50ke electron bea in this section

Fig 1 shows the sche atic view of the double-slab resonator To si plify the proble , it is assu ed that its transverse di ensions are $2(D+d)$ and in nite, where D and d are the vacuu half width and the thickness of the dielectric slab with dielectric constant of ε, respectively

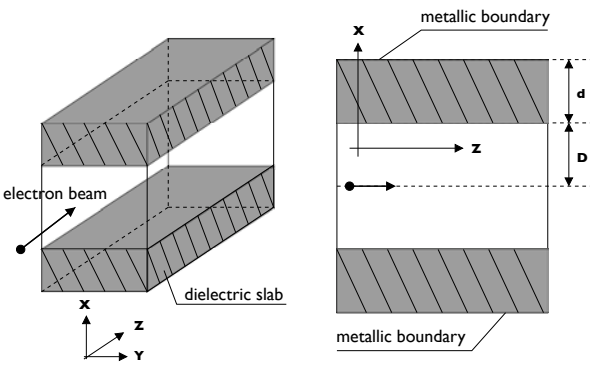

Figure 1 Sche atic for of the waveguide partially lled with two lined parallel dielectric slabs with the thickness of d Electron bea propagates along the -a is in the spacing of the slabs with the width of $2D$

In CFEL oscillator, the radiation is gained by the interaction between the longitudinal electric eld E_z and the straightly oving electron 2 TM odes whose E_z distributes in a sy etrical pattern to the x 0 plane are, therefore, of interest The electro agnetic eld of the sy etric TM ode, in concrete ter s TM_1, TM_3, TM_5 , is e pressed as following 3
In vacuu region $0 < |x| < D$

$$\mathbf{E}(x,z,t) = E_{z0}\begin{pmatrix} \frac{k_z}{p}\sinh px \\ 0 \\ i\cosh px \end{pmatrix} e^{i\theta}$$
$$\mathbf{H}(x,z,t) = E_{z0}\begin{pmatrix} 0 \\ \frac{k_0}{p}\sinh px \\ 0 \end{pmatrix} e^{i\theta} \quad 1$$

In dielectric region $D < |x| < D+d$

$$\mathbf{E}(x,z,t) = E_{z0}\begin{pmatrix} \frac{k_z}{\varepsilon p}\left(F\cos\theta' + G\sin\theta'\right) \\ 0 \\ -i\frac{q}{\varepsilon p}(F\sin\theta' - G\cos\theta') \end{pmatrix} e^{i\theta}$$
$$\mathbf{H}(x,z,t) = E_{z0}\begin{pmatrix} 0 \\ \frac{k_0}{p}\left(F\cos\theta' + G\sin\theta'\right) \\ 0 \end{pmatrix} e^{i\theta} \quad 2$$

where E_{z0} is the a plitude of E_z at x 0, k_z and ω are the wavenu ber and angular fre uency, respectively The transverse wavenu bers in the vacuu and dielectric regions are de ned as $p^2 = k_z^2 - \omega^2/c^2$ and $q^2 = \varepsilon\omega^2/c^2 - k_z^2$, respectively Here the free-space wavenu ber $k_0 = \omega/c$, the longitudinal phase of the radiation eld $\theta = k_z z - \omega t$, the transverse phase $\theta' = (x-D)q$, the constants deter ined by the resonator con guration $F = \sinh pD$, $G = \varepsilon\frac{p}{q}\cosh pD$

The dispersion relation is given by

$$\varepsilon\frac{p}{q}\cos qd\cosh pD - \sin qd\sinh pD = 0. \quad 3$$

Fig 2 shows the dispersion curves for TM_1 ode for slabs of silicon ε 11 6 with thickness d 0 65 and $30\mu m$ In CFEL, the radiation resonates with electron bea if the phase velocity w/k_z is e uals to the electron velocity Thus the intersections of the curves and the bea ode line $w = \beta_z k_z$ are the resonant points The resonant fre uencies are 46 0 Hz and 983 Hz for d 0 65 and $30\mu m$, respectively The nu erical calculations of the dispersion relations found that the resonant fre uency was al ost inversely proportional to the thickness d

On the other hand, the resonant fre uency suggests a little dependence on the width of vacuu region D as shown in Fig 3 It decreases only by 3 as the thickness D increases fro 0 325 to 1 3

However, the vacuu width D has a substantial effect on the radiation led strength of E_z in the vacuu region,

* sa6 051 edu kansai-u ac jp

DEVELOPMENT OF THE LONGITUDINAL PHASE-SPACE MONITOR FOR THE L-BAND ELECTRON LINAC AT ISIR, OSAKA UNIVERSITY*

R. Kato#, S. Kashiwagi, T. Igo, Y. Morio, G. Isoyama
ISIR, Osaka University, Ibaraki, Osaka 567-0047, Japan

Abstract

In order to measure the longitudinal phase-space profile of the high-brightness electron beam, we are developing the measurement system consisted of a profile monitor, a bending magnet and a streak camera. Instead of an optical transition radiation (OTR) monitor as previously considered, a Cherenkov radiator with a hydrophobic silica aerogel is used as a profile monitor. Due to the physical limitation at the installation location, we designed a simple radiator supported with a metallic mirror. The Cherenkov radiator has been designed, and it is in the process of production.

INTRODUCTION

The performance of the self-amplified spontaneous emission free-electron laser (SASE-FEL) strongly depends on beam parameters, such as a longitudinal beam profile, bunch charge, the transverse emittance and an energy profile. A correlation between longitudinal positions of electrons in a bunch and their energies has a crucial effect on the temporal evolution of the optical pulse of SASE. Several types of methods are extensively under study to evaluate the longitudinal phase-space profile of the electron beam [1-4].

A measurement system of the longitudinal phase-space distribution of electrons using the combination of a bending magnet, a profile monitor and a streak camera are currently under development at the Institute of Scientific and Industrial Research (ISIR), Osaka University. In the preliminary experiments using an optical transition radiation (OTR) monitor as the profile monitor, it was confirmed that the monitor had higher momentum resolution rather than the ordinary used momentum analyzer using a slit and a current monitor [5]. However, we could not get the efficient number of photons to obtain the phase-space images since, in addition to low photon yield, the angular distribution of the OTR is too large to concentrate in the electron energy region of 10 – 20 MeV, which is suitable energy for THz-SASE and THz-FEL experiments conducted at this laboratory [6-8]. In order to increase the number of photons, we try to use a Silica aerogel as a profile radiator using example from the results at PITZ [2]. In this report, we introduce the design of the longitudinal phase-space monitor using a Silica aerogel Cherenkov radiator and the system layout.

*Work supported by Japan Society for the Promotion of Science (JSPS), Grant-in-Aid for Scientific Research (C), 18540273, 2006-2007.
#kato@sanken.osaka-u.ac.jp

PROPERTIES OF AEROGEL AND ITS CHERENKOV RADIATION

Aerogel is a low-density light-weight solid material produced by replacing the liquid component in the gel with gas. Silica aerogel, which is a silica-based substance, is the most common type of aerogel and has extremely light weight, extraordinary thermal insulation abilities, etc as a feature. We use a hydrophobic silica aerogel manufactured by Matsushita Electric Works, Ltd. (MEW). They supply several types of aerogel as shown in Table 1. In high energy particle physics, these aerogels are also used as radiators in Cherenkov detectors of the Belle detector system at KEKB.

Table 1. Characteristics of hydrophobic silica aerogels.

Aerogel type	SP-15	SP-30	SP-50
index of refraction	1.015	1.03	1.05
density (g/cm3)	0.06	0.11	0.19

Cherenkov radiation is emitted when a charged particle passes through a medium at a velocity greater than the speed of light in that medium. Cherenkov radiation is emitted in a cone having a subtended angle $2\theta_{\mathrm{CR}}$, which is determined by the average index of refraction in the medium n and the particle velocity β as follows:

$$\cos\theta_{CR} = \frac{1}{\beta n}. \tag{1}$$

Figure 1 shows the emission angle of Cherenkov radiation in the aerogel radiator versus the electron energy. Above the electron energy of 10 MeV, the emission angle is almost constant. However, the angle is too large to gather all rays of light. The number of photons N_{CR} radiated as Cherenkov radiation with wavelengths between λ_1 and λ_2 per a distance d along the path of the electrons is represented as follows:

$$\begin{aligned} N_{CR} &= 2\pi\alpha d\left(\frac{1}{\lambda_1}-\frac{1}{\lambda_2}\right)\left(1-\frac{1}{\beta^2 n^2}\right), \\ &= 2\pi\alpha d\left(\frac{1}{\lambda_1}-\frac{1}{\lambda_2}\right)\sin^2\theta_{CR} \end{aligned} \tag{2}$$

where α is the fine structure constant. Figure 2 shows the number of photons emitted from the aerogel with different indices of refraction. In this case, the wavelength region is assumed to be equal to the sensitivity region of the streak camera (400 ~ 800 nm). The photon yield of Cherenkov

DEVELOPMENT OF A PRECISE TIMING SYSTEM FOR THE ISIR L-BAND LINAC AT OSAKA UNIVERSITY

Shigeru Kashiwagi*, Goro Isoyama, Ryukou Kato, Shoji Suemine
ISIR, Osaka University, 8-1 Mihogaoka, Ibaraki, Osaka 567-0047, Japan

Abstract

We are developing a free electron laser (FEL) in the infrared region and also conducting Self-Amplified Spontaneous Emission (SASE) experiment in the same wavelength region using the L-band linear accelerator at the Institute of Scientific and Industrial Research (ISIR), Osaka University. In order to conduct such studies, a stable operation of the linac is critical, so that we have developed a highly precise and flexible timing system for a stable generation of the high intensity electron beam with the energy region of 10-30 MeV. In the timing system, a rubidium atomic clock producing 10 MHz rf signal is used as a time base for a synthesizer which is used as the master oscillator for generating the acceleration frequency of 1.3 GHz. The 1.3 GHz rf signal from the master oscillator is directly counted down to produce the clock signal of the timing system at 27 MHz and the four rf signals for the linac and laser used in the beam experiments. The start signal for the linac is precisely synchronized with the 27 MHz clock signal. To make an arbitrary delayed timing signal, a standard digital delay generator is used to make a gate signal for a GaAs rf switch, which slices out one of the 27 MHz clock pulses to generate the delayed timing signal. Any timing signal can be made at an interval of 37 ns and the timing jitter of the delayed signal is less than 2 ps (rms). We will report the new timing system and its performance in detail.

INTRODUCTION

The L-band electron linear accelerator is used for studies on nanotechnology and beam science as well as for basic studies in the related fields at the Radiation Laboratory of the Institute of Scientific and Industrial Research (ISIR), Osaka University. The L-band linac can produce electron beams of different time structures, like a single-bunch, multi-bunch with 9.1 ns spacing and so on, corresponding to various beam experiments. The high intensity single-bunch beam is the most characteristic beam of this L-band linac and it is very useful for radiation chemistry studies by means of pulse radiolysis

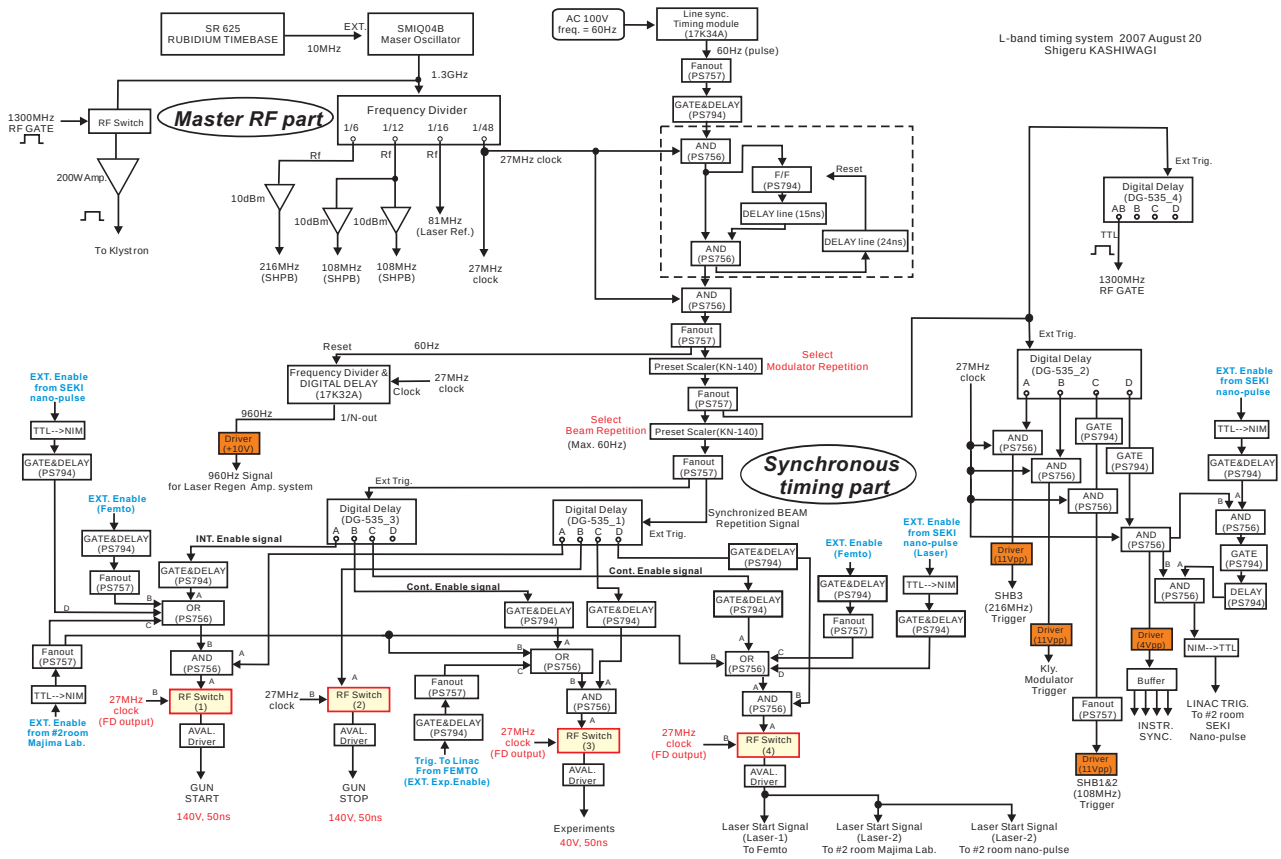

Fig. 1: Block diagram of the new timing system for the L-band linac at ISIR, Osaka University.

*shigeruk@sanken.osaka-u.ac.jp

DEVLOPMENT OF A LOW EMITTANCE DC GUN FOR SMITH-PURCELL BWO FEL

K. Kasamsook#, K. Akiyama ,K. Nanbu, M. Kawai , F. Hinode, T. Muto , T. Tanaka, M. Yasuda, Y. Mori, H. Hama, Laboratory of Nuclear Science, Tohoku University,
1-2-1 Mikamine, Taihaku-ku, Sendai 982-0826, Japan

Abstract

An electron DC gun capable for producing very low emittance beam is now under evaluation of beam qualities at Laboratory of Nuclear Science, Tohoku University. The DC gun employs a high voltage of 50 kV to extract electrons, which is suitable to drive Smith-Purcell backward wave oscillator free electron laser (BWO FEL) [1]. From a result of numerical simulation using a 3-D finite deference time domain (FDTD) method [2], the BWO FEL oscillation at the terahertz wavelength region maybe achieved by using the electron beam with an emittance lower than 1 π mm mrad. Average power is expected to be more than 100 W/mm^2.

In addition to which a very small cathode of LaB_6 single crystal is employed for the gun [3], the geometrical structure is optimized to produce the lower emittance beam. A numerical calculation of the electro-static model for the DC gun to solve equilibrated beam envelope predicts a normalized beam emittance of 0.3 π mm mrad will be possible for the beam current of a couple of hundreds mA. Particularly by applying additional bias voltage between the cathode and the wehnelt, the transverse distribution of electrons is possibly becoming to be an ideal Kapchinskij-Vladimirskij (K-V) beam [4], so that the space charge effect will be minimized.

INTRODUCTION

Smith-Purcell BWO FEL

In order to understand the characteristics of the BWO FEL and the interaction between the DC beam and the evanescent waves supported by a grating, an FDTD simulation has been performed. Nonlinear behavior of the Smith-Purcell radiation was already observed [5]. That was coherent and has been presumed to result from the beam microbunching effect due to interaction with the evanescent modes.

We have chosen a model grating for the simulation as indicated in Fig. 1. The period length λ_g = 400 μm, the groove width W = 200 μm, the groove depth d = 300 μm and the grating full width L = 2 mm, the number of period of 50 are employed, respectively. The sheet DC beam, which has the emittance of 1 π mm mrad for the both directions, is generated by very low horizontal and vertical beta functions of 6.25 cm and 0.4 mm, respectively. Since the evanescent wave is exponentially decreasing as the distance from the grating surface increases, the sheet beam has to travel just above the surface in order to have sufficient overlapping with the evanescent wave (here we have chosen 100 μm).

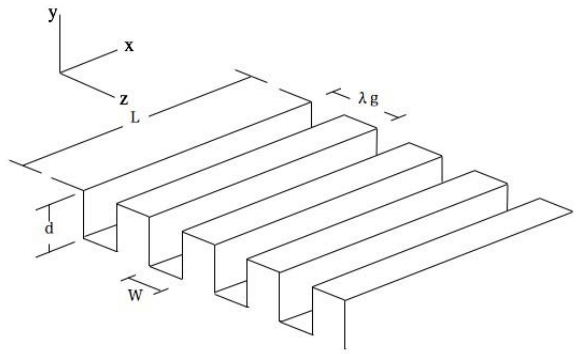

Figure 1: A model grating for FDTD simulations.

The Smith-Purcell BWO FEL is not driven by ponderamotive potential as conventional FELs with wigglers. The microbunching is occurred by the longitudinal electric field (E_z) in the evanescent wave, and the conventional Smith-Purcell radiation becomes coherent. The evanescent mode is much more excited by the bunched beam, so that the gain is yielded.

The FDTD simulation was performed with a DC beam current of 150 mA. To avoid beam brow-up the strong external longitudinal field (B_z ~ 1 T) applied. From the dispersion relation of the evanescent wave [6], the group velocity at the beam frequency negative, so that this is the backward-wave. Time dependent evolutions of radiated power observed at the grating upstream end are shown for two different emittance cases in Fig. 2.

We notice that for the normalized emittance of 1 π mm mrad case, the power increased up to several hundreds W/mm^2 and a damping oscillation was excuted after saturation. Meanwhile a larger normalized emittance case, such as 5 π mm mrad shown in Fig. 2(b), the FEL oscillation was not occurred. The results show the beam emittance is very crucial for the Smith-Purcell BWO FEL.

The frequency spectrum obtained Fourier transform of the power evolution of Fig. 2(a) is shown in Fig. 3. In this grating case, an intense sub-Terahertz radiation may be obtained.

ZZELECTRON- LINAC BASED FEMTOSECOND THZZZZZ ZRADIATION SOURCE AT PAL*

H S ang†, C M Li , W W Lee, B R Park, H i , S C i , ung, M S Lee, Park, Choi, and I S o
Pohang Accelerator Laboratory, POSTECH, Pohang 790-784, OREA

Abstract

A 60-Me electron linac for intense fe to-second THz radiation source is under construction at PAL, which is the bea line construction project to be co pleted by 2008 To get intense fe to-second THz radiation up to 3 THz, the electron bea should be co pressed down to below 100 fs The linac will use an S-band photocathode RF-gun as an electron bea source, two S-band accelerating structures to accelerate the bea to 60 Me , a chicane-type bunch co pressor to get fe to-second electron bunch, and an optical transition radiation OTR target as a radiator The PARMELA code si ulation result shows that the 0 2 nC bea can be co pressed down to a few tens of fe to-seconds, and the higher charge of 0 5nC to about one hundred fe to-seconds Also, the linac will be able to provide fe to-second electron bea for electron pulse radiolysis and co pton-scattering e peri ent for fe to-second X-ray

INTRODUCTION

THz radiation source which can provide rich science and une plored technology is beco ing popular And, sub pico-second radiation at that wavelength can provide an unprecedented probe for ultra fast dyna ics like electronic e citations and agnetic e citations 1 Pohang Accelerator Laboratory PAL is constructing a 60-Me electron linac for intense fe to-second THz radiation source, which is the bea line construction project to be co pleted by 2008 The radiation wavenu ber to provide is 10-100 cm^{-1} 0 3 - 3 THz and the radiation pulse duration should be shorter than 200 fs

DESIGN

To achieve this goal, we will ake use of relativistic electron bea with the bunch length of shorter than a few hundred fe to-seconds Relativistic particles e it incoherent radiation at all wavelengths, and additional enhanced coherent radiation at wavelengths of the order of the bunch length and longer The total radiated spectral power fro a ono-energetic bunch of N_e electrons at wavelength λ is

$$P(\lambda) = p(\lambda)N_e[1 + (N_e - 1)f(\lambda)], \qquad 1$$

where $p(\lambda)$ is the spectral radiation power fro a single electron and $f(\lambda)$ is a for factor for an azi uthal sy - etric bunch, which is the Fourier transfor of the actual particle distribution The rst ter in the s uare brackets is the incoherent part of the radiation while the second ter corresponds to the coherent radiation which is N_e ti es the incoherent part assu ing $f(\lambda) \approx 1$ The for factor is de- ned as

$$f(\lambda) = |\int S(x)exp\{i(2\pi x/\lambda)\}dx|^2. \qquad 2$$

where $S(x)$ is the nor alized longitudinal density distribution of electrons in a bunch

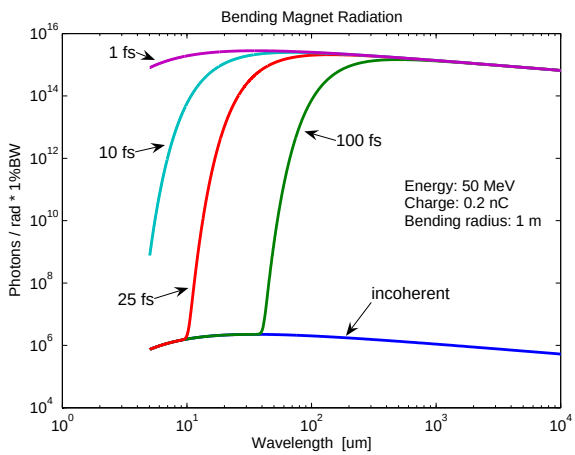

Figure 1 Coherent enhance ent of synchrotron radiation fro a bending agnet at different bunch lengths in r s

Figure 1 shows the coherent enhance ent of synchrotron radiation fro a bending agnet at different bunch lengths in r s The para eters used for the calculation are an electron bea energy of 50 Me , a bending radius for synchrotron radiation of 1 , and the electron bunch charge of 0 2 nC The photon u of coherent radiation is uch higher than that of the incoherent part, si ply N_e ti es

Fro Figure 1, one can nd how s all the bunch length should be to get coherent THz radiation Coherent enhance ent of radiation is deter ined by the bunch for factor in E 2 The re uired bunch length is as short as one tenth of the period of radiation to get the bunch for factor close to 1 For e a ple, to get 10 THz radiation period 100 fs , the bunch length should be s aller than 10 fs, which is obviously i possible to get with 0 2 nC charge bea So, the target bunch length to achieve in this project is about 50 fs with 0 2 nC bea , which can generate coherent THz radiation below 3 THz

Figure 2 depicts the layout of the electron linac The linac will use an S-band photocathode RF-gun as an elec-

* Work supported by orean Ministry of Science and Technology
† hskang postech ac kr

STABILIZATION OF A KLYSTRON VOLTAGE AT 100 PPM LEVEL FOR PAL XFEL

J. S. Oh#, J. H. Suh, Y. G. Son, S. D. Jang, S. J. Kwon, PAL/POSTECH, Pohang 790-784, Korea
E. H. Song, Changwon National University, Changwon 641-773, Korea

Abstract

The PAL XFEL needs a stable electron beam. The stable charging of PFN (pulse forming network) of a klystron-modulator is essential to provide the stable acceleration field for an electron beam. For PAL XFEL, stabilization of klystron voltage pulses at 100-PPM level is required. Short-term stability is determined by a minimum resolution of a charging system. Long-term stability is determined by a thermal stability due to the temperature drift. This paper shows details of hardware R&D and test results to achieve the target stability.

INTRODUCTION

PAL XFEL is proposed as a 4th generation light source that is a coherent X-ray free electron laser by utilizing an existing 2.5-GeV linac [1]. Reasonably stable SASE output requests the RF stability of 0.02% rms for both RF phase and amplitude [2]. This is one of technologically challenging issues for PAL XFEL.

The smart modulator driving a klystron RF source for PAL XFEL will use an inverter charging system. Therefore, the stability of RF sources is directly determined by the one of inverter power supplies. In order to stabilize the charging level, we need an ultra fine inverter power supply and a correct feedback signal of the charging voltage. The proper conditioning of feedback signal with a thermally stable probe is necessary to realize an ultra stable charging performance. This paper shows the hardware development and analysis of the charging stability.

INVERTER CHARGING SYSTEM

A traditional klystron-modulator adopts the resonant charging scheme that uses a constant voltage source. A charging scheme that uses a constant current source such as a inverter power supply provides high reliability: a thyratron switch is safely turned off because next charging schedule is digitally controllable, it is fail-safe system under short-circuit condition due to the current limit feature. In addition, it is naturally compact by using a high frequency inverter [3]. These features are well matched to the next generation modulator for PAL XFEL facility. Figure 1 shows the circuit diagram of a modulator adopting an inverter power supply as a PFN charging power supply. Table 1 summarizes the parameters of a modulator that will provide ultra stable pulses to a klystron (model: Toshiba E3712).

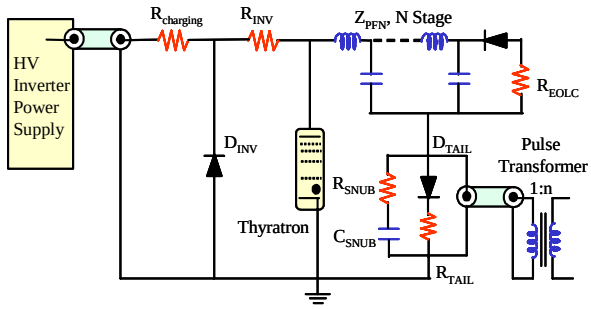

Figure 1: Circuit diagram of a modulator adopting an inverter power as a PFN charging power supply.

Table 1: Modulator specifications

Peak power	160 MW
Peak output voltage	370 kV
Pulse repetition rate	60 Hz
Pulse width	4.7 μs
Pulse energy	750 J
Flat-top width	1.7 μs
Pulse transformer turn ratio	1:17
PFN impedance	2.9 Ω
PFN capacitance	0.8 μF
Main charging inverter	60 kJ/s
Fine charging inverter	2.3 kJ/s
Maximum charging voltage	50 kV

This modulator is to be used for a new facility (fs-THz beamline) of PAL [4], which requires equivalent stability as the one of PAL XFEL. Therefore, this modulator is good test bench for the hardware R&D of the inverter charging system with 100 PPM stability for PAL XFEL.

Figure 2 shows the schematic diagram of the klystron-modulator control including coarse inverters, a fine inverter, a RF driver, a klystron, a thyratron switch of the modulator, a digital inverter controller, a high voltage probe, and a master timing controller (DG535). All the charging inverters are connected to the PFN in parallel. The fine charging inverter has special features that can control the amount of charges per switching cycle to control the regulating ripple of a charging voltage.

Figure 3 shows the timing diagram of a modulator control. The master timing controller provides a charge signal (DG535_A) for inverter power supplies, a thyratron trigger (DG535_B), and a driver trigger for a klystron RF input. The digital inverter controller provides RUN/STOP signals for coarse charging and fine charging.

#jsoh@postech.ac.kr

FOURIER AND NON-FOURIER MODELS FOR PHOTOEMISSION

F. Scarlat, M. Oane, Anca Scarisoreanu, Ecaterina Mitru
National Institute for Laser, Plasma and Radiation Physics - NILPRP, Bucharest, Romania
E-mail of corresponding author: scarlat.f@gmail.com

Abstract

This paper is a theoretical study on the photoemission properties of metallic photocathodes in the high intensity ultrashort laser pulse regime, using Fourier and non Fourier models. First of all the Fourier-model was used. Next an analysis of the electron gas heating phenomenon and how this phenomenon leads to coupled heat equations (two temperature models) was conducted. The authors also tried to show that it is possible to use, in the second approximation, a non-Fourier model instead of two temperature models, using a single temperature hypothesis (the electron gas temperature equals the lattice temperature). The distributions for the thermal fields and photocurrents function of space, time, laser-intensity, incident angle and relaxation time are also represented.

INTRODUCTION

Free electron lasers (FELs) operate over a large portion of the electromagnetic spectrum, i.e.from a μ-wave to the VUV. At the high frequency end of the spectrum, FEL operation is severely limited by a number of factors, among which the transverse beam emittance, which is invers proportional with the square root density current. A high electron density implies not only a high peak current but also a low rms normalized emittance, ε_n. For example, in the case of X-FEL projects, ε_n[mm.mrad] has the values: 1.4 - XFEL [1], 1.2 - LCLS [2] and 0.85 - SCSS [3]. Recent development in the tehnology of photemissive electron sources offer promising advances over the conventional electron injectors [4], [5].

All photo-injector concepts share a drive laser which produces short bunches of photons and a photocathode which converts the photon bunch into short bunches of electrons [6], [7]. Photoemission from photo-cathodes is possible when the work function (or potential barrier, $e\Phi$) of the material is less than the photon energy ($\hbar\omega$) used, by at least: 1 eV if the material is a metal (in this case electrons are extracted from the conduction band) and 2 eV if the material is a semiconductor (electrons are here extracted from the valence band).

A photocathode is characterized by four parameters: quantum efficiency (QE), maximum laser wavelength (λ_m), life time (τ) and its ability to sustain a high electric field (E). For FEL nano-Coulomb pulses in picosecond time are required. The advantages of photoemission are the followings: high peak current density (> 100 A); fast time response (picosecond to femtosecond) and possibility to generate polarized electrons. As drawbaks: the need for very good vacuum, limited lifetime (few month) and very expensive (vacuum systems & laser). Metal cathodes have poor QE but are robust ($\tau \sim$ years).

Alcaline cathodes have good QE but are delicate and they need very good vacuum conditions < 10^{-10} torr. Starting from the above considerations as well as the NUCLEU program [8] for to conduct studies by means of the Nd:YAG laser system with 50 mJ at 1064 nm, 24 mJ at 532 nm, 8 mJ at 355 nm and 4 mJ at 266 nm, this paper represents a start in the metal photocathode studies using Fourier and non Fourier models for photoemission [9].

FOURIER MODELS

Fourier model starting from the basic Fourier heat equation, represented the input of our models [10]

$$\frac{\partial^2 T}{\partial x^2}+\frac{\partial^2 T}{\partial y^2}+\frac{\partial^2 T}{\partial z^2}-\frac{1}{\gamma}\frac{\partial T}{\partial t}=-\frac{Q(x,y,z,t)}{K}, \qquad (1)$$

where K - the thermal conductivity of the sample; γ - the thermal diffusivity of the sample ($\gamma = k/c\cdot\rho$); c -the heat capacity of the sample; ρ - the mass density of the sample. $Q(x, y, z, t)$ represents the heat rate (per volume and time unit) produced by the laser in the solid sample.

Based on Spatial Transform and Laplace Transform, the eigenfunctions from the standard theory and the eigenvalues from the boundary conditions were determined.

So for the proposed device a parallelepiped solid sample with dimensions a, b, and c was considered.
Considering a linear heat transfer (h – heat transfer coefficient) at the sample surface (the "radiation" boundary condition), we have:

$$\left[\frac{\partial K_x}{\partial x}-\frac{h}{K}K_x\right]_{x=-\frac{a}{2}}=0;\left[\frac{\partial K_x}{\partial x}+\frac{h}{K}K_x\right]_{x=\frac{a}{2}}=0, \qquad (2)$$

$$\left[\frac{\partial K_y}{\partial y}+\frac{h}{K}K_y\right]_{y=-\frac{b}{2}}=0;\left[\frac{\partial K_y}{\partial y}+\frac{h}{K}K_y\right]_{y=\frac{b}{2}}=0, \qquad (3)$$

$$\left[\frac{\partial K_z}{\partial z}+\frac{h}{K}K_z\right]_{z=-\frac{c}{2}}=0;\left[\frac{\partial K_z}{\partial z}+\frac{h}{K}K_z\right]_{z=\frac{c}{2}}=0. \qquad (4)$$

The semi-analytical solution to Fourier equation is:

$$\Delta T(x,y,z,t)=\sum_{i=1}^{\infty}\sum_{j=1}^{\infty}\sum_{o=1}^{\infty}a(\alpha_i,\beta_j,\chi_o)\cdot$$
$$\cdot b(\alpha_i,\beta_j,\chi_o,t)K_x(\alpha_i,x)K_y(\beta_j,y)K_z(\chi_o,z), \qquad (5)$$

COHERENCE OF SPACE CHARGE VIBRATION AND PARAMETERS OF ELECTRON GUNS

S. V. Miginsky#, Budker INP, Novosibirsk, Russia

Abstract

Space charge effect always determines the motion of particles in electron guns. Coherence of space charge vibration leads to oscillation of the emittance along a gun or a charge affected beamline. This phenomenon is closely related to a technique known as emittance compensation. It has been considered in the paper. The optimal parameters of guns and the expected emittance of the beam from the optimal ones have been estimated and scaled.

INTRODUCTION

Emittance compensation technique has been mentioned first probably in [1]. It was explained and developed further in [2] and other papers. The two basic effects, caused by the longitudinal nonuniformity of charge density and the transverse one, and their combination in uniform and nonuniform beamlines were considered in [3] - [6], also with accelerating and bunching. The main results of the latter works is that both effects separately or together can be compensated, the charge phase advance through the beamline should be $2n\pi$ (n is integer) and the focusing should be optimal. Then the normalized emittance dilution is well estimated as

$$\varepsilon_n \cong \varepsilon_c x_e \sqrt{\frac{I}{I_0 \beta\gamma}}, \qquad (1)$$

where x_e is the rms size of the beam at the entrance; I is the peak current; $I_0 = 4\pi \cdot mc^2 / Z_0 |e|$, ≈ 17.045 kA for electrons; $\beta = v/c$; $\gamma = 1/\sqrt{1-\beta^2}$; v is the longitudinal velocity; and ε_c is the dimensionless coefficient depended on the type of the beamline.

In this paper we consider electron guns in the same view. We take into account only macroscopic space charge effect and neglect thermal and grid emittance. The main difference between a gun and a beamline is the presence of metallic electrodes near the emitter. Their charge depends on the one of the beam and generates comparable fields, so exclusion of near-cathode electrodes from simulation of beam motion in a gun causes lost of accuracy.

EMITTANCE DILUTION IN GUNS

Phenomena and Basic Scaling

If the emitter is round and the beam is homogeneous and stationary, the gun geometry can be optimized so that the space charge effect doesn't affect the emittance, as in the well known Pierce gun. If the beam is not longitudinally uniform, the transverse phase portraits of its slices differ and their emittances are not zero. Let's consider these phenomena and estimate the total emittance.

Particle motion in the same gun is similar if its voltage and current meet Child-Langmuir law $I \propto U^{3/2}$. In this case the emittance (not normalized!) doesn't depend on the current [5] 4.1. At the same time, the brightness is $I/\varepsilon_n^2 \propto \sqrt{U}$. If all the dimensions of a gun are changed proportionally, its quality factor ε_c preserves while its brightness is $\propto \sqrt{U}/r^2$. Thus, one should find ε_c and the optimal compensation beamline for any gun.

Charge Amplitude and Phase

General equation of small charge vibrations has been derived in [3] (3). It generates a transformation matrix between two arbitrary points of a beamline [5] (2.16). The charge vibration phase is defined in [5] (2.19). Now we can define the differential characteristics of a bunch [5] 4.1, [6]. The local charge phase is

$$\varphi = \arctan\left(\frac{-C'x}{C\sqrt{j}}\right) = \arctan\left(\frac{\dfrac{dx'}{dI} - \dfrac{x'}{x}\dfrac{dx}{dI}}{\left(\dfrac{1}{2I} - \dfrac{1}{x}\dfrac{dx}{dI}\right)\sqrt{j}}\right), \qquad (2)$$

where x is the rms-size of a slice, $j = I/I_0$, C and C' are the transformation matrix elements associated with cos-like trajectories. The quadrant is chosen so that the signs of sinφ and cosφ coincide the ones of the numerator and the denominator respectively. x and x' are considered as functions of the slice current I.

It is also useful to define the relative amplitude of charge vibrations to estimate emittance dilution in a compensation beamline [5] 4.1, [6] (5):

$$a = \sqrt{\left(C'x/\sqrt{j}\right)^2 + C^2}\ . \qquad (3)$$

Then the relative amplitude of a slice is [5] (4.10), [6] (13):

$$A = \sqrt{\left(\frac{2I}{x}\frac{dx}{dI} - 1\right)^2 + \frac{1}{j}\left(2I\left(\frac{dx'}{dI} - \frac{x'}{x}\frac{dx}{dI}\right)\right)^2}\ . \qquad (4)$$

Basic Gun

A simple diode gun has been simulated first. Its geometry is shown in fig. 1. The emitter radius was 5 mm, the distance between the electrodes was 123 mm, while the beam was observed at 200 mm from the cathode. The perveance was very close to the "natural" one, so the optimal current was 2 A at 300 kV. SAM simulation code [7] was used to calculate beam motion in the gun. As usually for emittance compensation, a bunch has been divided by slices, and each slice was considered independently as a steady-state beam. The current density at the cathode was always homogeneous.

#S.V.Miginsky@inp.nsk.su

LOW POWER CONSUMING HYBRID BENDING MAGNET AT THE XFEL BEAM DUMP

F. Hellberg, H. Danared, A. Hedqvist, Manne-Siegbahn Laboratory, 10405 Stockholm, Sweden*
W. Decking, B. Krause, A. Petrov, J. Pflüger, M. Schmitz, DESY, 22603 Hamburg, Germany

Abstract

At the end of the European XFEL the electron beam is separated from the photon beam and directed towards the beam dump with a bending magnet. This dipole magnet is designed to bend 10-25 GeV electrons by 1°/m and is 10 meter long in total. By integrating permanent magnet material into a conventional electromagnet, this so-called hybrid magnet with a 1 T bias magnetic field consumes no power at the nominal energy of the XFEL, 17.5 GeV. The magnetic field can be increased or decreased by magnet coils to obtain 1°/m deflection for all energies between 10 and 25 GeV. Here a proposal for such a hybrid configuration is presented together with its characteristics.

INTRODUCTION

In a free electron laser the electrons are bent away from the laser light with electromagnets and stopped in a beam dump situated away from the experimental hall. At the European XFEL the electrons are bent vertically 10° in a 10 m long double bending achromat magnet [1]. Each beam line ends with such a magnet. It is the largest electromagnet of the XFEL and it consumes a significant amount of power. It is therefore desirable to find a way to lower the power consumption of these magnets. This report presents a feasibility study of the use of a permanent magnet/electromagnet hybrid for this purpose [2, 3]. At the nominal energy of the XFEL, 17.5 GeV, the electrons require a magnetic dipole field of 1 T in order to bend 1°/m. Integrating permanent magnet material (PMM) into an electromagnet to produce a 1 T bias field in the pole gap results in a bending magnet that consumes no power at the nominal energy. Magnet coils can then be used to increase or decrease the magnetic field in the pole gap. The aim has been to design a hybrid magnet that uses less power than a conventional electromagnet between 10 and 25 GeV (0.58 and 1.46 T).

A passive safety system must exist in order to prevent the electron beam from reaching the experimental hall in case of component failure. With conventional electromagnets in the bending unit it is necessary to place an additional permanent magnet further down the photon beam line for safety. The advantage of a hybrid magnet is that the bias magnetic field of the permanent magnet also works as an integrated safety system.

*This project was performed within the framework of the Stockholm-Uppsala Centre for Free Electron Laser Research. For more information, please visit: http://www.frielektronlaser.se

MAGNETIC FIELD CALCULATIONS

In a conventional dipole electromagnet the magnetic field is confined in a steel yoke ($\mu_{\rm rel} \approx 1000$) and a small air gap ($\mu_{\rm rel} \approx 1$). If the air gap is increased more current is needed to maintain the field strength (the slope of the magnetization curve dB/dI becomes smaller). Because the permeability of PMM is similar to the permeability of air, the insertion of PMM in the yoke results in lower dB/dI. Despite this it can be favourable to use a hybrid magnet under certain conditions.

Consider a C-shaped dipole electromagnet and assume that the magnitude of the field in the gap is the same as in the yoke. The Maxwell equation important in this case can be presented in integral form by applying Stokes' theorem:

$$\oint \frac{\vec{B}}{\mu\mu_0} \cdot d\vec{l} = \int_S \vec{J} \cdot d\vec{S} = NI, \qquad (1)$$

where I is the current and N the number of turns. For an electromagnet equation 1 can be written as,

$$NI = \frac{B}{\mu_0} l_g + \frac{B}{\mu_s \mu_0} l_s, \qquad (2)$$

where l_g the size of the gap, l_s the average length of the steel yoke, μ_s permeability of steel, and μ_0 is permeability of air. By replacing part of the steel yoke with PMM a bias magnetic field passes through the yoke and the gap. The relationship between B and H in the direction parallel to the easy axis (the main axis of magnetization) of a PMM is linear in a wide range with slope $\mu_p \approx 1$. The magnetization curve can therefore be written as,

$$B_p = \mu_0 \mu_p H_p + B_r, \qquad (3)$$

where B_p is the magnetic field, H_p is the magnetic field intensity, and B_r is the remanent field of the PMM. The magnetic equation for the hybrid magnet can written, similar to equation (1), as

$$NI = \frac{B}{\mu_0} l_g + \frac{B - B_r}{\mu_0 \mu_p} l_p + \frac{B}{\mu_0 \mu_s} l_s, \qquad (4)$$

where l_p is the length of the permanent magnet material along the easy axis. Equations (2) and (4) show that the more PMM is added to increase the bias field the more current needs to go through the coils for a specific correction of the magnetic field. This is illustrated in figure 1 where the ratio of the power consumption of the two types of magnets is plotted as function of beam energy. It is clear that this simple type of hybrid magnet is not a good option for 10-25 GeV electrons.

INSTALLATION OF THE OPTICAL REPLICA SYNTHESIZER IN FLASH

Angelova, ie ann, Uppsala University, A Meseck, BESS
M Ha berg, P Salen, P van der Meulen, M Larsson, Stockhol University
S han, Bodewadt, A Winter, Universitat Ha burg
E Saldin, H Schlarb, B Sch idt, E Scheid iller, M urkov, ES

Abstract

uring the shutdown in spring 2007 the optical replica synthesizer, a novel device to diagnose ultra-short electron bunches, is asse bled in the FLASH accelerator We report on the status of the construction work with e phasis on the two electro- agnetic undulators needed for icro-bunching and replica-pulse generation

INTRODUCTION

Monitoring and tuning the bunch size are essential for the reliable operation of linac-based SASE free-electron lasers such as the FLASH 1 , XFEL 2 , or LCLS 3 This need has triggered the develop ent of new diagnostic ethods based on a transversely de ecting cavity 4 or electro-optical sa pling 5 The optical replica synthesizer ORS , a co ple entary sche e that was introduced in Ref 6 , is si ilar to an optical klystron FEL seeded by an infrared laser as is shown in Fig 1 In the odulator the interaction of the laser with the transversely oscillating electrons causes an energy odulation A s all chicane turns this energy odulation into a corresponding density odulation at the wavelength of the light In a following radiator undulator the icro-bunched bea radiates coherently and the e itted light pulse has the sa e longitudinal pro le as the electron bea Hence the na e optical replica synthesizer The replica pulse is then e tracted fro the vacuu pipe by an off-a is irror and directed to an optical table with optical diagnostics where it will be analyzed by a co ercially available second-har onic generation FRO fre uency resolved optical gating device, called RENOUILLE 7

uring the spring shutdown 2007 ost co ponents such as the undulators, e ternal laser building, seed laser transport syste , and the optical stations were installed and we report on these activities

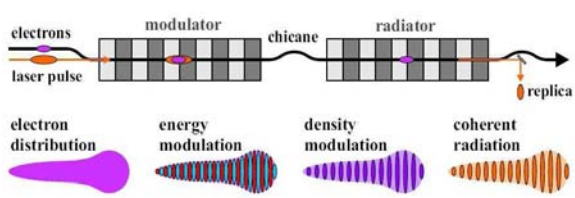

Figure 1 The principle of the optical replica

UNDULATORS AND CHICANE

The undulators were designed, asse bled and tested at Scanditroni Magnet AB, Sweden and were delivered to ES in March They have a length of 1450 , a width of 454 , a height of 817 , and weight 480 kg The gap is 40 in order to acco odate the standard 38 vacuu pipe without having to break vacuu The period length is 200 with 14 poles and 28 coils connected in 4 separate coil circuits This allows adjusting the eld integrals $I_1 = \int_0^L B(z)dz$ and $I_2 = \int_0^L \int_0^z B(z')dz'dz$ by controlling the end coils in the 1 2, -3 4, 1 pattern The rst and last coil with 1 4-e citation have independent supplies and the second and 13th coils are powered in series by another supply Finally, the ten central coils are connected in series to a fourth power supply The a i- u agnetic eld is 0 5 T and no inal eld 0 3 T The undulators can be ounted horizontally or vertically to induce vertical or horizontal bea oscillations, respectively

Upon arrival at ES eld easure ents were perfor ed with a Hall probe and power supply settings were found that zero the eld integrals in order to avoid perturbing the electron bea outside the undulator The individual Hall probe easure ents have an accuracy ε of a few auss, but the calculation of the rst and second eld integrals has an accuracy of $\sigma(I_1) = \varepsilon\sqrt{Ldz}$ and $\sigma(I_2) = \varepsilon L\sqrt{Ldz}/\sqrt{3}$ where dz is the distance between consecutive Hall-probe easure ents 8 This allows us to easure the eld integrals with an accuracy on the order of 10^{-5} T or 10^{-5} T ^{2}, respectively, provided we use a s all step size of $dz = 2$ We then deter ined settings of the power supplies for peak elds of 0 1, 0 2,

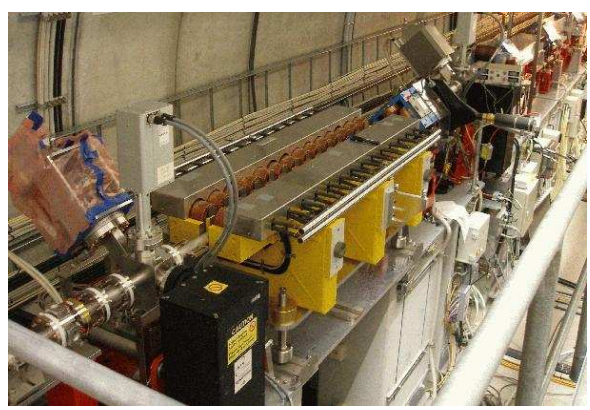

Figure 2 The odulator which causes vertical oscillations

7TH HARMONIC BUNCHER EXPERIMENT AT THE UCLA NEPTUNE LABORATORY

P. Musumeci*, S. Ya. Tochitsky#, R. Tikhoplav*, J. B. Rosenzweig*, C. Joshi#

Abstract

Since typically FEL undulator magnets have period length in the cm range, and the normalized magnetic field strength K is usually close to unity to guarantee a good coupling, a very high energy electron beam is needed to access the UV and x-ray region of the electromagnetic spectrum. One way to reduce the beam energy necessary for short wavelength light sources consists of exploiting the FEL harmonic interaction. An experiment aimed at demonstrating the efficiency of harmonically coupled schemes is proposed for the Neptune Laboratory at UCLA. We plan to inject the 12.4 MeV beam from the split photoinjector in an already available undulator with period = 3.3 cm and K = 1.8. The FEL resonant wavelength with these parameters is 74.2 μm. A copropagating high power 10.6 μm CO2 laser bunches the beam via 7th harmonic FEL/IFEL interaction. Preliminary calculations show that even though the interaction is weakened by the high harmonic number, only 5 -10 MW of laser power are required in order to induce full bunching on the beam in the 10 period long undulator.

INTRODUCTION

Free-electron laser (FEL) amplifiers operating at short wavelengths (<100 nm) are undoubtedly one of the top research fields nowadays because of the new possibilities opened by generation of powerful, short pulses in a range of the electromagnetic spectrum important for material science, biology and chemistry. The lasing wavelength of an FEL depends primarily on the undulator magnet characteristics --period and field amplitude-- and on the electron energy. Since the undulator magnet has typically period lengths in the cm range, and the normalized magnetic field strength *K* is usually close to unity to guarantee an efficient coupling, a very high energy electron beam is needed to access the UV and x-ray region of the electromagnetic spectrum.

One way to reduce the necessary beam energy is to utilize the FEL harmonic interaction[1-5]. The FEL resonance condition, i.e. the condition for efficient energy exchange between the transverse EM wave and the electrons, takes place at electron energies such that the wiggling induced by the laser field has the same frequency as the wiggling induced by the undulator in the electron rest frame. However, a planar undulator resonance can also occur when the laser frequency is a multiple of the undulator wiggling frequency and electrons of a given energy interact with the fundamental radiation frequency and with its higher harmonics[6]. In some cases, when the laser frequency is constrained by the source availability and the energy of the beam is so low that in order to design an FEL at the resonant condition the undulator parameters are unfeasible or the normalized vector potential *K* has to be very small to reduce the magnetic amplitude induced frequency red-shifting, harmonic coupling becomes the only viable solution to ensure a strong interaction.

Even for FEL cascade schemes, one of the factors limiting the frequency multiplication of all cascade schemes is related to the necessity of operating all the stages of the cascade with the same electron beam energy. The change in the resonant wavelength for the different sections must be compensated by variations of the undulator period and *K* parameter. Using the conventional techniques for undulator magnet construction, the span of these variations is limited and harmonic coupling has been considered as a possible solution [7].

Here we propose and discuss an experiment to be carried out at the UCLA Neptune Laboratory to test the efficiency and feasibility of a high order harmonic FEL/IFEL interaction. For this purpose an existing short undulator with a period of 3.3 cm and K = 1.8, for which the resonant wavelength with a 12.4 MeV electron beam is 74.2 μm, will be seeded with a CO2 laser radiation. This will allow to study the microbunching obtained by 7th harmonic FEL/IFEL interaction, since 10.6 x7=74.2μm.

EXPERIMENTAL LAYOUT

Table 1: Parameters for Neptune 7th harmonic interaction experiment

Beam energy	12.4 MeV
Beam energy spread	< 0.2 %
Emittance	5 mm-mrad
Current	100 A
Laser wavelength	10.6 μm
Laser seed Power	10 MW
Laser size (at focus)	650 μm
Undulator period	3.3 cm
Undulator *K*	1.8
Undulator length	33 cm

* UCLA Department of Physics and Astronomy, Los Angeles, CA 90095-1547
# UCLA Department of Electrical Engineering.

The UCSB MM-FEL Injection Locking System *

G. Ramian, S. Takahashi, and M. Sherwin
Dept. of Physics (IQCD and CTST)
University of California, Santa Barbara, CA 93106, USA

Abstract

An Injection locking system has been implemented on the Millimeter Wave Free-Electron Laser (MM-FEL) at the University of California, Santa Barbara (UCSB). It it is based on a commercially available varactor multiplier source and quasi-optical isolator operating at 240 GHz. Lasing on multiple longitudinal modes is shown to collapse to a single repeatable mode by introducing a low power CW signal into the FEL resonator through a silicon-plate coupler. High power and extremely narrow linewidth operation will enable new experimental opportunities such as FEL based pulsed electron paramagnetic resonance spectroscopy.

INTRODUCTION

Injection locking of the UCSB MM-Free-Electron Laser has been demonstrated as shown in Fig. 1. Lasing that normally occurs on a number of longitudinal modes is seen to collapse to a single mode at a single repeatable frequency with less than 1 MHz linewidth. This result is important in demonstrating the suitability of an FEL for applications where extremely narrow linewidth is required.

Linewidth

The UCSB MM-FEL is based on an electrostatic accelerator. As such it does **not** exhibit the picosecond microstructure, characteristic of RF accelerator driven FELs, that Fourier transform limits their linewidth to hundreds of GHz. Instead, a several microsecond quasi-DC macropulse allows sub-MHz width.

The MM-FEL [1, 2] uses a 6.25 meter long resonator which can be described by its Fabry-Perot characteristics. It has a free-spectral range (fsr) of $c/(2L_r)$ = 24 MHz. It has finesse **F** = $\pi/(2\ \mathrm{asin}(1/F))$, where coefficient of finesse $F = 4\sqrt{1-l}\ /(2(1-\sqrt{1-l}\ )-l)$. l is the power loss per pass. Because of its length, the resonator has extremely high $Q = \mathbf{F}N$ where N is the order or simply number of half wavelengths between mirrors. For nominal 25 % loss at 240 GHz, F = 193, **F** = 21.8, Q = 218000. Linewidth is then 240 GHz / Q = 1.1 MHz.

It is important to emphasize that this linewidth is an upper limit, since line-narrowing may take place as in conventional lasers. Line-narrowing can reasonably be expected when lasing is a consequence of stimulated emission and other inhomogeneous broadening effects are correspondingly small.

* Work supported by NSF grants DMR-0321365 and DMR-0520481

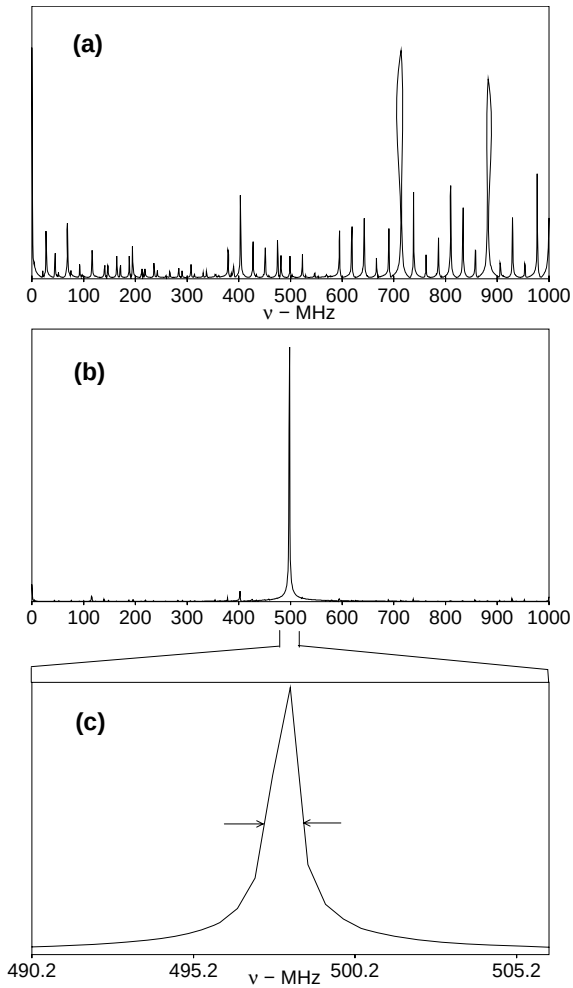

Figure 1: (a) FEL spectrum without injection locking. The spectrum show many longitudinal modes spaced by 25 MHz. (b) FEL spectrum with injection source on. Only single mode lasing with no pulse-to-pulse frequency fluctuation is observed. (c) 1 MHz width is transform limit of sampling window, indicating actual linewidth is much less.

Longitudinal Modes

Another important consequence of the long resonator is the number of longitudinal modes available for lasing. Fig. 2 shows the longitudinal mode structure in relation to the MM-FEL's gain curve. Hundreds of modes would be above threshold and might be expected to lase. However, this doesn't actually happen. Many fewer are seen to lase with only a few growing to dominance. This effect can be understood in terms of the stochastic nature of startup. Startup is from spontaneous emission, essentially noise, so

A SUPERCONDUCTING RF PHOTO-INJECTOR FOR OPERATION AT THE ELBE LINEAR ACCELERATOR*

J. Teichert#, A. Arnold, H. Buettig, D. Janssen, M. Justus, U. Lehnert, P. Michel, K. Moeller, P. Murcek, Ch. Schneider, R. Schurig, F. Staufenbiel, R. Xiang, FZD, Dresden, Germany,
J. Stephan, IKS, Dresden, Germany, W.-D. Lehmann, SGE, Pirna, Germany,
T. Kamps, BESSY, Berlin Germany, G. Klemz, I. Will, MBI, Berlin, Germany,
D. Lipka, A. Matheisen, B. v. d. Horst, DESY, Hamburg, Germany
P. vom Stein, ACCEL Instruments, Bergisch Gladbach, Germany
V. Volkov, BINP, Novosibirsk, Russia

Abstract

For the ELBE superconducting linear accelerator at FZD a radiofrequency photoelectron injector with a superconducting cavity (SRF gun) is under development. The SRF gun combines the excellent beam quality which can be delivered by RF photoinjectors with the possibility of continuous wave operation.

The superconducting niobium cavity of the injector consists of 3½ cells and contains a Cs_2Te photocathode which is normal-conducting and cooled by liquid nitrogen. The RF frequency of the cavity is 1.3 GHz. The final electron energy will be about 9.5 MeV and the average electron current will be 1 mA. In the past years the SRF photo injector has been designed and fabricated. Several critical subsystems have been tested. For the cavity, the results of the RF measurements will be shown. An UV driver laser system has been developed which fulfils the different requirements (77 pC @ 13 MHz, 1 nC @ 500 kHz) for the future operation at ELBE. A photo cathode preparation system was developed and installed. The equipment is now in operation and the first series of Cs_2Te photo cathodes have been produced.

INTRODUCTION

In 2004 a R&D program for the development of a superconducting radiofrequency photoelectron injector (SRF gun) was initiated at Forschungszentrum Dresden-Rossendorf (FZD). This project continues the earlier efforts in SRF gun development [1, 2] with the aim to develop a fully operable SRF photo injector for the ELBE superconducting linear accelerator [3].

Compared to the thermionic injector in use, the new SRF gun will reduce the pulse length and the transverse emittance for the standard FEL operation mode with 77 pC bunch charge and 13 MHz pulse repetition rate. Furthermore a second operation mode is now planned at ELBE with a bunch charge of 1 nC and a repetition rate of 500 kHz. Beside the essential beam quality improvement for ELBE, the project should demonstrate the operation of a SRF gun at an accelerator facility for the first time, and the gun will serve as a test bench for R&D studies in this field (beam parameter measurements and optimize operation, long term studies, investigation of photo cathodes, study of emittance compensation methods). For that reason a sophisticated diagnostics beamline has been designed and constructed [4]. In particular, the operation with 2.5 nC bunch charge will be studied which is essentially important for future application of the SRF gun at the BESSY FEL [5]. The Table 1 gives an overview of the SRF gun parameters and planned operation modes.

Table 1: Gun design parameters and expected beam values for the planned operation modes

	ELBE mode	**high charge mode**	**BESSY-FEL**
RF frequency	1.3 GHz		
beam energy	9.5 MeV		
Operation	CW		
drive laser wave length	262 nm		
Photocathode	Cs_2Te		
quantum efficiency	>1 %		>2.5 %
average current	1 mA	0.5 mA	2.5 µA
pulse length	5 ps	15 ps	40 ps
Repetition rate	13 MHz	500 kHz	1 kHz
bunch charge	77 pC	1 nC	2.5 nC
transverse emittance	1 µm	2.5 µm	3 µm[1)]

[1)] flat top laser

An overview of the ELBE accelerator facility is shown in Fig. 1. The heart of the radiation source is a superconducting linac with a thermionic injector and two cryomodules each containing two TESLA-type RF cavities. The accelerator operates in CW, the maximum electron energy is 40 MeV, and the average current is 1 mA. The electron beam is used in two FELs for the generation of infrared radiation, to conduct nuclear physics and radiation physics experiments, and to produce neutrons and positrons.

* We acknowledge the support of the European Community-Research Infrastructure Activity under the FP6 "Structuring the European Research Area" programme (CARE, contract number RII3-CT-2003-506395) and the support of the German Federal Ministry of Education and Research grant 05 ES4BR1/8.
#j.teichert@fz-rossendorf.de

ELECTRO-OPTIC SPECTRAL DECODING FOR SINGLE-SHOT CHARACTERISATION OF THE COHERENT TRANSITION RADIATION PULSES AT FLASH

V. Arsov, E.-A Knabbe, B. Schmidt, P. Schmüser, B. Steffen, DESY, Hamburg, Germany

Abstract

We report preliminary single-shot electro-optic spectral decoding (EOSD) measurements of coherent transition radiation (CTR) pulses, generated by the electron bunches of the free-electron laser (FLASH) at DESY, Hamburg. The THz radiation is transported through a 20 m long beam-line from the accelerator tunnel to an experimental station outside. The measurements are performed in vacuum with a 0.5 mm ZnTe crystal in crossed-polarizer and near crossed-polarizer detection schemes. Pulses with complex structure and sharp peaks have been detected. The different components have full width at half maximum in the range 400-900 fs.

INTRODUCTION

Intense relativistic electron bunches with a duration less than 100 fs are needed in contemporary light source accelerators, such as the ultraviolet and soft x-ray free-electron laser at Hamburg (FLASH) [1], as well as the future x-ray FELs like the Linac Coherent Light Source at SLAC [2] and the European XFEL [3]. With this there is a growing demand for ultra-fast characterisation of the electron bunches. Some of the leading longitudinal diagnostic techniques with fs abilities are the spectral, the electro-optic (EO), the transverse deflecting cavities and, since recently, the optical replicas [4]. The spectral techniques refer to spectrum measurements of the coherent transition radiation (CTR), diffraction and synchrotron radiation, etc. A Fourier transformation of the measured spectrum has resolved structures with less than 10 fs duration in a single-shot acquisition [5]. In the case of FLASH the single shot CTR spectrometer is situated outside the accelerator tunnel, which is convenient from experimental point of view, but requires knowledge of the transfer function of the beam line. Therefore an independent CTR pulse length measurement, such as an EO technique applied inside the spectrometer can facilitate the interpretation of the CTR spectra.

The EO techniques allow direct characterization of THz fields both in the spectral and in the time-domain. Depending on the analyzer orientation, the measured signal is either linear or quadratic with the THz field [5],[6]. Recently EO signals as short as 55 fs (rms) have been observed, which is a new record in the EO detection of single electron bunches and close to the limit imposed by the properties of the EO material [7].

The temporal profiles of the CTR pulses at FLASH have been measured for the first time by Berden et. al. [8]. Their measurements were carried out in air with ZnTe, using electro-optic spectral decoding (EOSD) in the so called balanced detection scheme. Here we present similar EOSD measurements with ZnTe, but carried out in vacuum, using crossed-polarizer and near crossed-polarizer detection schemes [6].

EXPERIMENTAL SETUP

The CTR electric field temporal profiles are resolved with a spectral decoding electro-optic technique [6], [9]-[11].

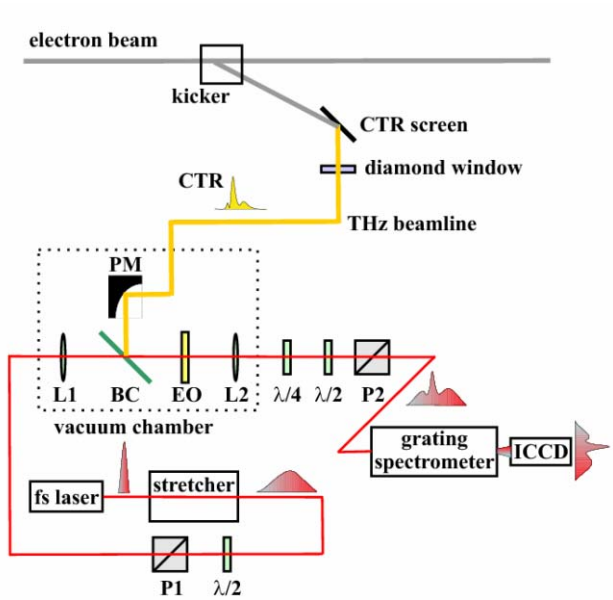

Figure 1: Set-up for electro-optic spectral decoding measurements of coherent transition radiation (CTR). Notations: (l/2), (l/4) – half and quarter wave plates; (P1,2) – polarizers; (L1,2) – lenses; (BC) – indium tin oxide beam combiner; (EO) – 0.5 mm thick ZnTe electro-optic crystal; (PM) – parabolic mirror

A diagram of the experimental setup is shown on Fig. 1. The CTR is generated from single bunches, kicked to an off-axis screen. A diamond window is used to couple the radiation from the ultra high vacuum environment into a 20 m long transfer line, where the pressure is lower than 0.1 mbar. The beam line is equipped with high reflectivity focusing mirrors, designed specially to minimize the diffraction. Special care has been taken to avoid wave guide effects in the pipe by using corrugated bellows. The lowest frequency (ca. 300 GHz) is determined by the diameter of the pipe, which is ca. 200 mm [12]. Outside the accelerator runnel the THz beam line is connected to an evacuated vessel containing several diagnostic experiments, including a single-shot THz grating spectrometer and an EO setup. Alternatively, the radiation

XPS STUDIES OF Cs_2Te PHOTOCATHODES*

S. Lederer†, J.H. Han, and S. Schreiber (DESY, Hamburg, Germany)
A. Vollmer, R. Ovsyannikov, M. Sperling, and H. Duerr (BESSY GmbH, Berlin, Germany)
F. Stephan (DESY, Zeuthen, Germany)
P. Michelato, L. Monaco, C. Pagani, D. Sertore (INFN Milano - LASA, Segrate (MI), Italy)

Abstract

Cesium telluride (Cs_2Te) photocathodes are used as sources for electron beams because of their high quantum efficiency (QE) and their ability to release high peak current electron bunches in a high gradient RF-gun. Starting from a high QE level of about 10 % the quantum efficiency of these cathodes decreases during operation in a photo-injector to below 0.5 %. To understand this behaviour, XPS investigations on the chemical composition were performed at BESSY. In this contribution we compare two fresh cathodes from INFN with one used under normal operation at FLASH and one used at PITZ at a higher than usual RF-gradient of 60 MV/m.

INTRODUCTION

The photocathodes used at FLASH and PITZ are prepared at INFN-LASA (Milano, Italy). The electron emitting film is deposited on polished molybdenum plugs in two steps [1]. First, the plug is coated with 10 nm tellurium. During the following cesium deposition, the quantum efficiency (QE) is monitored, and when maximum QE is reached the Cs evaporation is stopped. During the preparation process the temperature of the plug is kept at 120 °C. The diameter of the Cs_2Te coating is 5 mm. Right after the production of the Cs_2Te cathodes, the QE is about 10 % [2].

During operation in electron guns of accelerators, the QE reduces to below 0.5 %. For a better understanding of the QE degradation, the chemical composition of two new (#90.1 and #42.3) and two used cathodes (#34.6 and #92.1) are investigated by x-ray photoelectron spectroscopy (XPS) at BESSY (Berlin, Germany). In addition, the work function of the cathodes was measured. Cathode #92.1 was used at FLASH under the nominal operation condition for SASE FEL generation for 39 days with a final QE of 0.1 %. Cathode #34.6 was operated at PITZ with accelerating gradients at the cathode of up to 60 MV/m for several days. The QE of this cathode decreased to 2 %.

In this paper first results of the XPS measurements are presented. In the first part an overview in the sense of survey scans is given, followed by a more detailed presentation of precise XPS-studies of the Te 3d levels. In the last part, results of work function determinations are given.

RESULTS AND DISCUSSION

In figure 1, survey scans with photon energies of 900 eV are presented for the two fresh and the two used cathodes. For all spectra, the main peaks correspond to Cs 3d and Te 3d. While for fresh cathodes peaks corresponding to

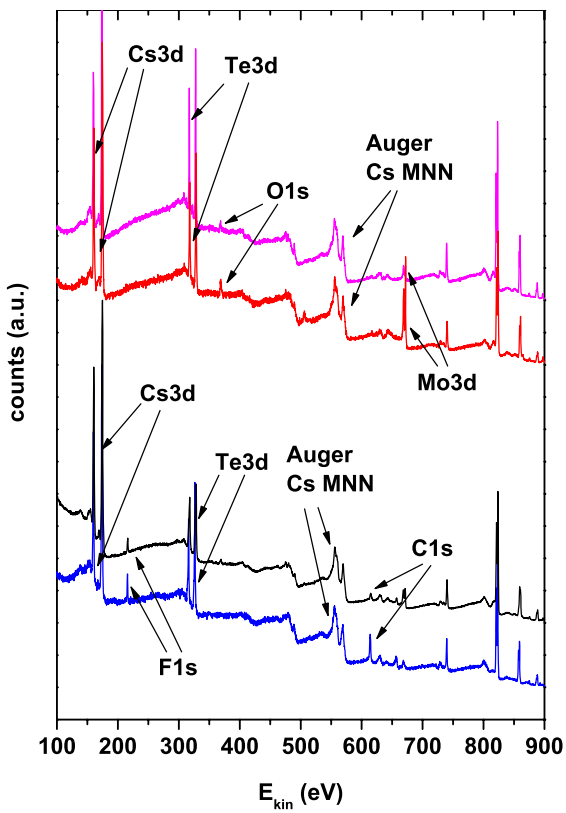

Figure 1: Survey spectra measured at photon energy of 900 eV for fresh cathodes (red: #42.3, magenta: #90.1) and used cathodes (black: #34.6, blue: #92.1)

O 1s are visible, these lines reduce with operation time. We interpret this as a cleaning process during operation caused by the laser pulses (wavelength 262 nm) and the high electrical field at the cathode. Both effects results in

* This work has partly been supported by the European Community, contracts RII3-CT-2004-506008 and 011935, and by the 'Impuls- und Vernetzungsfonds' of the Helmholtz Association, contract VH-FZ-005.

† sven.lederer@desy.de

TEST OF A WIRE SCANNER IN THE DIAGNOSTIC SECTION OF PITZ*

Hans-Juergen Grabosch# , Galina Asova##, Juergen Baehr, , Jang Hui Han§, Sergiy Khodyachykh, Sergey Korepanov, Mikhail Krasilnikov, Velizar Miltchev§§, Anne Oppelt§§§ , Bagrat Petrosyan, Martin Sachwitz#, Lazar Staykov, Frank Stephan, DESY, 15738 Zeuthen , Germany.

Abstract

The Photo Injector Test facility at Zeuthen (PITZ) has been established to produce and optimize electron beams of high brilliance. One wire scanner station, developed and used in the undulator section of the FLASH at DESY [1] [2] , has been installed in the diagnostic section of PITZ. Measurements of beam-profile and beam-position were performed to test the usability of such type of wire scanner at PITZ. The test has shown that wire scanners of this type can be well used as complementary measurement device at PITZ. In the final state of the extension of PITZ, two wire scanners are foreseen as standard diagnostic tools for beam-profile and beam-position measurements.

INTRODUCTION

Wire-scanners are important diagnostic tools for particle accelerators in order to tune the beam-line and to measure the beam-profile. Various types of wire-scanners have been developed for different particle accelerators [3][4][5]. In PITZ the beam-electrons will undergo scattering processes when hitting the wire. Once scattered the electron will hit the beam pipe and create a shower of electrons and photons. The shower signal of electrons and gammas can be observed by means of scintillator counters placed nearby the beam pipe. The measured correlation between the wire position and scintillator signal gives information about the beam-position and the beam-profile.

SETUP AND MEASUREMENT

The configuration of PITZ in the year 2005 (PITZ1.5) with the wire scanner station is shown in Figure 1. A wire scanner station consists of two independent scanners for the vertical- and horizontal-direction, respectively. Each scanner is equipped with two tungsten wires of 30 μm diameter in a distance of 10 mm.The whole set up is combined with a scintillation counter. The counter detects secondary particles which are created when the wire interacts with the electron beam. The light of the scintillation counter is read out by wavelength shifter bars and guided via clear fibers to the photomultiplier H6780-4. The gain of the photomultiplier is steered by a reference voltage $v_{ref.}$ and ranges from $10^2 – 10^6$. For this measurement a gain of ~ 500 is mostly used. The photomultiplier signal is read out and digitized by a Tektronics TDS 5104 oscilloscope. Together with the photomultiplier signal the position of the wire is stored and analyzed afterwards. Vertical and horizontal scans provide vertical resp. horizontal measurements of beam-profile and beam-position with μm resolution. The system allows scanning speeds from 5 μm/sec up to 1 m/sec. Absolute position determination in the range of 50 μm is achieved by calibrating the wires. The wire scanner is integrated in the coordinate system of PITZ.

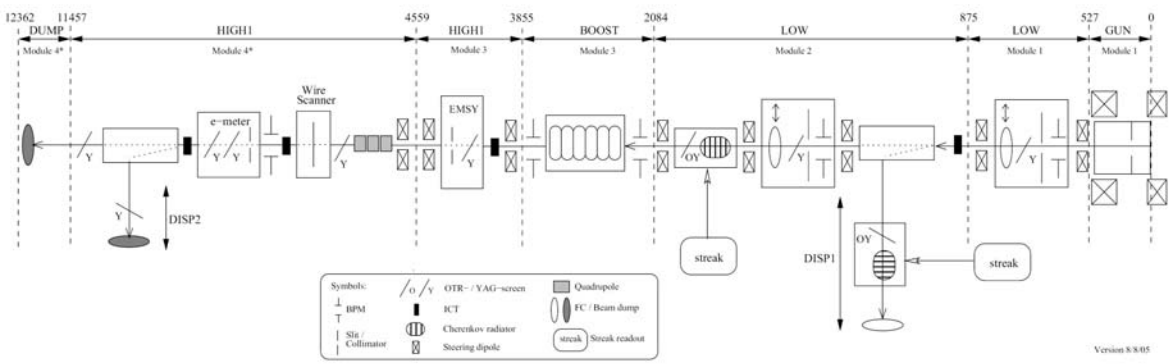

Figure 1: Configuration of PITZ .

* This work has partly been funded by the European Community, contract no.RII3-CT-2004-506008 and 011935 and by the 'Impuls- und Vernetzungsfonds'of the Helmholtz Association, contract no. VH-FZ-005.

hans-juergen.grabosch@desy.de , martin.sachwitz@desy.de

On leave from INRNE, 1784 Sofia, Bulgaria

§ now at DESY , 22603 Hamburg , Germany

§§ now at Hamburg University, 22761 Hamburg, Germany

§§§ now at PSI, 5232 Villingen, Swizerland

DEVELOPMENT OF A BEAM CURRENT TRANSFORMER FOR THE X-FEL PROJECT IN SPRING-8

Atsushi Higashiya #, Hirokazu Maesaka and Yuji Otake
SPring-8 Joint-project for XFEL/RIKEN, 1-1-1,Kouto, Sayo-cho, ayo-gun, Hyogo JAPAN 679-5148.

Abstract

The SCSS prototype accelerator has been constructed at SPring-8. The output signal of a current transformer (CT) for measuring the electron-beam current in the SCSS prototype accelerator had a few megahertz (MHz) noise emitted from the thyratron of a klystron modulator, a ringing signal caused by the weak field of the electron beam. The long-period undulation of an electrical ground level at the CT monitor output also occurred due to a large electric current generated by the klystron modulator, which flows into ground. As a result, it is difficult to correctly measure the beam current. Therefore, we devised a new CT monitor and the differential circuit from CT monitor in order to improve the problem mentioned above.

The improved points are: (I) We think that the thyratron noise and undulation of the ground level comprise common mode noise. Therefore, these noises were reduced by using a differential detection circuit, and contacting between the ground of the CT case and the outer surface of a CT signal cable. (II) The ringing signal was suppressed by intercalating a dumping resistance material into the space between the case and the ferrite core of the CT monitor. By these developments, the environmental influence to the CT monitor could be suppressed in its output circuit. In an experiment to evaluate the CT monitor, the output waveform of the CT monitor was very clean without any noises as mentioned above.

INTRODUCTION

The X-FEL prototype accelerator (SCSS project) was constructed at SPring-8. SASE (self amplification of spontaneous emission) at a wavelength of about 50 nm and was successfully observed during the last year. The X-FEL project, based on SASE, is currently in progress.[1,2]

In generally, it is important to correctly investigate the beam properties such as the current of an electronic beam. For this reason, in the SCSS prototype accelerator, we use CT monitors.

In commissioning of the prototype accelerator, we found that the CT output signal was influenced by the environment such as noise produced by high-voltage switching in the thyratron of a klystron modulator and occurred due to large electric current flow into the ground, which is also generated by the klystron modulator. Figure1 (a) shows the ringing noise in the CT output. The ringing has a period of about 4 ns (500 MHz). Figure 1 (b) also shows a few megahertz noise emitted from the thyratron. First, in order to eliminate the thyratron noise, we made a contact between the ground of the CT case and the outer surface of the CT signal cables as shown in Fig.1 (d) (indicated by a red circle). As a result of the contact, the noise seemed to be suppressed. However, instead of this noise, a long-period undulation of the electrical ground level (about 220ms) appears as shown in Fig.1 (c). Therefore, it was difficult to correctly determine the beam current (electrons charge amount) due to these problems.

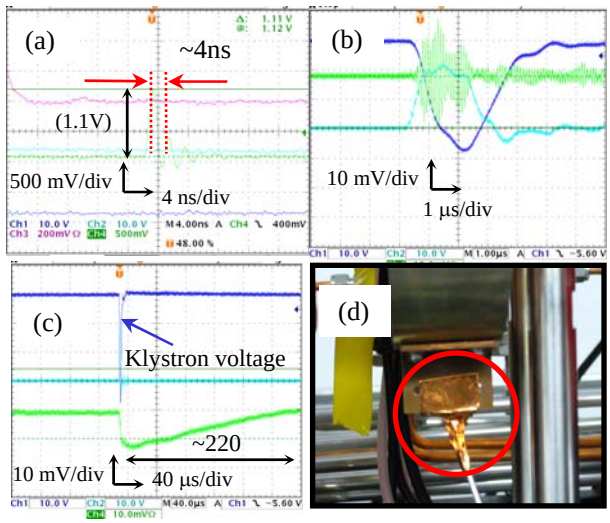

Figure 1: (a) Ringing of the CT output. (b) A few megahertz noise at CT output. (c) Long-period undulation of the electrical ground level at the CT output. (d) Picture of CT at the SCSS prototype accelerator.

In order to improve the problems of the few megahertz noise, the ringing signal and the long-period undulation of the electrical ground level, we devised a differential output-type CT monitor with two output ports and a differential detection circuit to modulate the undulation.

In this paper, we introduce the points of our improvements in the CT used at the prototype accelerator, the detailed configuration of the differential detection circuit, and also demonstrate the clean output waveform without any noises obtained by the differential output-type CT.

codbelo@spring8.or.jp

IN-SITU UNDULATOR FIELD MEASUREMENT WITH THE SAFALI SYSTEM

Takashi Tanaka, R Tsusu, T Nakaji a, T Seike and H ita ura
RI EN SPring-8 Center, oto 1-1-1, Sayo, Hyogo 679-5148, apan

Abstract

A new sche e of undulator eld easure ent has been proposed, which akes it possible to do eld apping inside the vacuu cha ber to verify the nal agnetic perfor ance of in-vacuu undulators I Us after asse bly Optical laser bea s are used in order to easure the positions of the Hall probe during actuation along the longitudinal direction, and dyna ic feedback of the position is carried out to ensure a high stability and accuracy of the easure ent A eld easure ent syste based on this concept has been developed at the SPring-8 in order to easure two different types of I U Principle of the new easure ent sche e and details of the developed syste are described together with the results of the eld easurement

INTRODUCTION

Shortening the undulator period is crucial to reducing the electron energy re uired to get angstro -rays in the SR and XFEL facilities and thus the total cost of construction The in-vacuu undulators I Us have any advantages over out-vacuu devices toward shorter agnetic period and thus have been adopted in a great nu ber of SR facilities all over the world It should be noted, however, that agnetic easure ent after nal asse bly including the vacuu cha ber, i e , nal veri cation of agnetic perfor ance, is not an easy task In addition, re easure ent after installation in the accelerator bea line is not trivial The situation is ore severe for cryogenic per anent agnet undulators CPMUs 1 , an e tension of I Us

We have recently developed a agnetic easure ent syste to easure the eld inside the vacuu cha ber With optical laser bea s introduced into the vacuu cha ber, the align ent of the Hall probe positions is dyna ically carried out, which ensures a high stability and accuracy of the easure ent This syste is called SAFALI for Self-Aligned Field Analyzer with Laser Instru entation The SAFALI syste has been applied to eld easure ent of two different undulators One is an I U installed in Swiss Light Source in 2001 and had been operated for about 3 years The other is a CPMU prototype to de onstrate the principle of CPMU The purpose of the for er easure ent is to investigate the radiation da age during operation, while that of the latter is to check the variation of the agnetic properties according to the te perature change of agnets In this paper, details of the SAFALI syste are given together with the results of the eld easure ents

PRINCIPLE

In the conventional agnetic easure ent syste , a agnetic sensor such as a Hall probe is placed on a cantilever supported by a 2-a is ,y stage ounted on a long actuation table with a high echanical accuracy, which is usually ade of granite ue to pitching, rolling and yawing of the actuation table, the Hall probe position during actuation can uctuate To perfor a agnetic easurement with a high accuracy, the positional uctuation should be kept as low as possible The positional error of a typical easure ent bench is around 30 μ , which corresponds to a eld error of 0 02 for an undulator with a agnetic period of 10 , and thus enough for agnetic easure ent of ost undulators In addition, the easure ent result is uite well reproducible typical deviation of the agnetic easure ent in ter s of the r s phase error is usually lower than 0 3 degree It should be noted, however, that such a Hall-probe scanning ethod cannot be applied to the eld easure ent of I Us as is We have to odify the actuation ethod to be adapted to the eld easurement of I Us after asse bly

The ost straightforward way is to install a huge vacuu cha ber that can acco odate a rigid and robust linear guide with a echanical accuracy co parable to that of the granite bench, which is not only i practical but also inef cient Another way is to onitor the position of the Hall probe during actuation along the longitudinal a is and perfor a dyna ic feedback to ensure that the Hall probe is always in position In this case, the linear guide does not have to be necessarily rigid or robust any ethod of actuation is acceptable unless the positional variation during actuation is too large to be co pensated by feedback

We can consider several ethods to easure the Hall probe position A ong the , we decided to use optical laser bea s co bined with position sensitive detector PS and irises attached to the Hall probe, because they are cost effective co pared to other ethods In order to easure the longitudinal position, we can use a co ercially available laser scale with a resolution better than 0 1mu Hereinafter, let us call the eld easure ent ethod based on this concept SAFALI , for Self-Aligned Field Analyzer with Laser Instru entation We have so far developed two SAFALI syste s for easure ent of two different I Us, the details of which will be discussed in the following sections

SAFALI FOR IVU24

In 2001, an I U with a agnetic period of 24 and agnetic length of 1 5 I U24 has been constructed at the SPring-8 and installed in the storage ring of Swiss

NON-DESTRUCTIVE SINGLE-SHOT 3-D ELECTRON BUNCH MONITOR WITH FEMTOSECOND-TIMING ALL-OPTICAL SYSTEM FOR PUMP & PROBE EXPERIMENTS

H. Tomizawa, H. Hanaki, Accelerator Division, Japan Synchrotron Radiation Research Institute (JASRI/SPring-8), Kouto, Sayo-cho, Sayo-gun, Hyogo 679-5198, Japan
T. Ishikawa, The Institute of Physical and Chemical Research (RIKEN Harima/SPring-8), Kouto, Sayo-cho, Sayo-gun, Hyogo 679-5148, Japan

Abstract

We are developing a non-destructive single-shot 3-D electron bunch monitor based on EO sampling, using the yearlong stable femtosecond laser source developed for the SPring-8 RF gun. The probe laser for spectral decoding EO sampling has been prepared as radial polarized and completely linearly chirped bandwidth (~500nm) supercontinuum generation. The EO-probe element is made of 8 EO-crystals with the assembling of each EO-crystal's optical axes along radial beam axes. The linearly chirped probe laser is longitudinally shifted in 8 transverse sectors for spectral decoding. We are planning to use organic polymer film as a femtosecond resolution EO-probe instead of crystals. This 3-D bunch monitor with spectrograph detects and analyzes the Coulomb field of electron bunches as longitudinally spectral decoding and transversely multi-pole expansion. Our single-shot bunch monitor can characterize the 3-D (both longitudinal (1D) and transverse (2D)) distribution and position of an electron bunch with femtosecond resolution. This non-destructive monitor can be used as an electron energy chirping monitor at a dispersive region for XFEL commissioning. Additionally, the EO-sampled probe laser pulse will be used as a femtosecond-timing signal pulse. This signal pulse is amplified with a NOPA, developing an all-optical timing system.

INTRODUCTION

At the SPring-8 site, construction of the XFEL project [1] has begun under a RIKEN and JASRI joint project. It will enter operation in 2010. For this project, it is necessary to monitor femtosecond electron bunch length for its commissioning. At the moment, the most promising femtosecond electron bunch monitor with an RF deflector, the LOLA cavity [2], is planned to be installed in the 1-GeV energy region of the 8-GeV SPring-8 XFEL linac. However, this monitor requires a few-meters-long cavity structure, and has to measure the bunch length on a fluorescent screen installed a few meters further downstream. The compactness is important in the XFEL project at SPring-8. Therefore, the shorter bunch monitor system is required for bunch length measurement, especially in the 8-GeV region.

In terahertz technology, femtosecond laser pulse duration has been measured utilizing the Pockels effect of ZnTe and so on. This method was the so-called electro-optical sampling (EOS). The variation of the Coulomb field of the electron beam bunch with a duration of less than 1 ps corresponds to terahertz (>10^{12} Hz) in frequency domain. Against this background, this EOS-based bunch monitor has been developed in the accelerator field [3-6]. The advantage of the EOS monitor is that it is non-destructive and has a high resolution of sub-picosecond. To use the laser as a probe allows a timing jitter of femtosecond, and a readout of the monitor head without signal cables. However, the temporal response of inorganic crystals like ZnTe is limited by 110 fs.

There are several types of EOS measurements. One is so-called spectral decoding, that decodes the longitudinal electron bunch structure on the spectrum of the chirped probe laser pulse. One of the others is so-called temporal decoding that is used as conventional pulse measurement with a correlation technique for a femtosecond laser.

The spectral decoding EOS makes possible single-shot measurement with a high repetition rate. Its encoding is simple to perform with a conventional spectrometer. Despite spectral decoding being a convenient method, it is well known that the sensitivity of the signal pulse is reduced because of certain interferences occurring between neighbouring wavelengths. Generally, the temporal resolution R_{res} is given by

$$R_{res} \cong \sqrt{t_0 t_c} \ ,$$

where the Fourier transform limit of the probe laser is t_0, and the probe chirped laser pulse duration is t_c [5-6]. Therefore, it is the tendency for measurement with high precision to use the temporal decoding method, which is superior in resolution. With a broadband (> 400 nm) laser square pulse chirped linearly, for instance, if t_0=2.5 fs, t_c=160 fs, R_{res} is improved around 20 fs.

In our point of view, spectral decoding is simple to encode and useful for measuring more information about the electron bunch. If the three-dimensional charge distribution of the electron bunch is measurable, it is quite useful for many applications. We investigated the bunch-by-bunch measurement possibility of the transverse charge distribution of the electron bunch with spectral decoding. In our strategy, temporal decoding, AO-modulator-based SPIDER [7] (Spectral Phase Interferometry for Direct Electric field Reconstruction) measurement will be used as a precise calibration for our spectral decoding EOS 3-D bunch monitor.

COHERENT THZ LIGHT SOURCE USING VERY SHORT ELECTRON BUNCHES FROM A THERMIONIC RF GUN

Toshiya Muto#, Takumi Tanaka, Fujio Hinode, Masayuki Kawai, Ken-ichi Nanbu, Kittipong Kasamsook, Kazushi Akiyama, Mafuyu Yasuda, Yoshinosuke Mori, Hiroyuki Hama
Laboratory of Nuclear Science, Tohoku University.

Abstract

We have planned to establish intense terahertz light source using coherent radiation from undulator. In order to emit coherent radiation, it is important to generate very short electron beam with a bunch length around 100fs. Now we have developed an injector to generate such short bunch beam. The injector consists of an Independent Tunable Cells thermionic rf gun (ITC rf gun) and a magnetic bunch compressor. Longitudinal and transverse phase space distribution can be controlled by changing input power of each cells and phase difference between cells in this gun. The compressor can change compression rate R_{56} and 2nd order dispersion effect by 2 sets of quadrupoles and a set of sextupoles, respectively. Test model of ITC rf gun was manufactured and basic parameters were measured. From tracking simulation, it has been turned out the bunch compressor can reduce to bunch length less than 100fs. In this paper, we show overview of the coherent terahertz light source and the detail of the ITC rf gun and the bunch compressor.

INTRODUCTION

Intense coherent radiation at the terahertz region ($\lambda \sim 300\mu m$) will be powerful probe for bio-medical science, solid state physics and other many scientific fields. There was not such intense terahertz light source so far. There are two type of terahertz source, or laser based and accelerator based. We have developed accelerator based terahertz light source using intense coherent radiation [1]. Now a coherent terahertz source using undulator radiation has been planed.

In order to get coherent terahertz light, electron beam with very short bunch length $\sigma_t < 100fs$ must be produced. Therefore an injector, which consists of Independent Tunable Cells rf gun (ITC rf gun) and magnetic bunch compressor, has been developed.

In this paper, the project of undulator coherent terahertz light source and the detail of the ultra short bunch injector are presented.

UNDULATOR COHERENT TERAHERTZ LIGHT SOURCE

A light source consists of an injector, an accelerating structure and an undulator. The schematic design is shown in Fig.1. The injector which consists of the ITC rf gun and magnetic bunch compressor generates electron beam with energy E ~2MeV, normalized emittance $\varepsilon_n < 1\pi$mmmrad and bunch length ~100fs. By the accelerating structure, beam energy goes up to 12 MeV. The ultra short bunch beam is passing through the undulator, then coherent terahertz light is emitted.

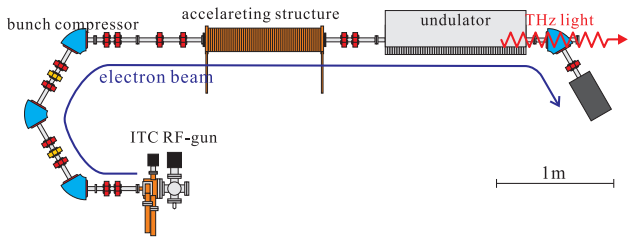

Figure 1: The schematic design of undulator coherent terahertz light source

The parameter of coherent terahertz light source is listed in Table 1.

Table 1: Parameters of coherent terahertz source

Energy ***E***	12MeV
Normalized emittance ε_n	< 1 πmm mrad
Bunch length σ_t	~100fs
Bunch charge I_e	~20pC
Undulator	
period length λ_p	8 cm
# of periods	15
Peak magnetic field B_{ymax}	0.3 T

Calculated terahertz spectrum from the undulator was shown in Fig.2 and Fig.3, where bunch length σ_t=100fs, number of electrons N_e = 1.25 x10^8 electrons /bunch (bunch charge is 20pC).

The fundamental wavelength λ_1 and its harmonics λ_i is

$$\lambda_i = \frac{\lambda_p}{2\gamma^2 i}\left(1+\frac{K^2}{2}+\gamma^2\theta^2\right), \quad (1)$$

where i is harmonic number, K=93.4 B_{ymax}[T] λ_p[m] is the strength parameter, γ is Lorentz factor, θ is the observation angle with respect to the axis[2]. In this case, the fundamental wavelength λ_1 is 257μm. Since bunch length σ_t=100fs ~ 30μm, only the radiation with fundamental wavelength is coherent, so proportional to N^2 ~ 10^{16}. Therefore, compared with the fundamental radiation, higherharmonics is suppressed (See Fig.2 and 3).

#muto@lns.tohoku.ac.jp

CHARACTERISTICS OF SMITH-PURCELL RADIATION FROM DIFFERENT PROFILE GRATINGS*

G. Naumenko#, B. Kalinin, G. Saruev, NPI, Tomsk, Russia
D. Karlovets, Yu. Popov, A. Potylitsyn, L. Sukhikh, V. Cha, TPU, Tomsk, Russia

Abstract

To choose the most effective grating the absolute coherent SPR characteristics were measured on the 6.2 MeV electron beam. Gratings with lamellar, triangular and so-called "flat" gratings were studied. It was shown the grating consisted of the conductive strips is more preferable target for SPR generation.

INTRODUCTION

Smith-Purcell radiation (SPR) is widely considered as the spontaneous mechanism for FEL (for example[7]). In recent experiments [1,2], the possibility of creating a monochromatic radiation source of the THz range on the basis of the Smith-Purcell radiation (SPR) has been demonstrated. The SPR from low relativistic electrons is also used in orotrons. For the nonrelativistic electron energies ($E_e \le 100$kev), the approach developed by van den Berg [3,4] ensures a reasonable agreement with experiment [5,6]. In [8] the different models for SPR characteristics calculation were compared for high relativistic electrons. There was shown that the predictions of most models differ by approximately 2 orders of magnitude for the electrons with energy ~20 MeV [9] and by several orders for the electron energies Ee=855 MeV [10]. The available experimental results do not provide an ultimate conclusion on the validity of one of these models.

We distinguish two types of periodic targets, which can be used to generate the SPR: "Volume" gratings (a lamellar grating (Fig. 1) and a grating which consist of a periodic set of conducting strips separated by vacuum gaps) and "Flat" gratings (consisting of separate conducting strips having the thickness essentially smaller than a wavelength).

The coherent Smith-Purcell radiation (CSPR) emitted from the first-type targets with different profile was studied experimentally by several experimental groups ([11, 12]). However, all these works differ in the applied methods. On the other hand, it was shown in works [13, 1] that flat targets are more effective in order to obtain an intensive monochromatic radiation. Therefore, the direct comparison of the measured characteristics of radiation from these targets is difficult. That is why the research of the CSPR characteristics from the targets of different types but under similar conditions is desirable.

* The work was supported by the Ministry of Education and Science of Russian Federation [project no. 2.1.1.889 "Development of Scientific Potential of Higher School (2006-2008)"].
# Naumenko@npi.tpu.ru

MODELS

There are few theoretical models to calculate the SPR characteristics for the different grating profiles. We consider here three models: van den Berg's (vdB) model [3] (applicable for volume gratings), surface current (SC) model [14,15] (the SPR is considered as a radiation generated by the current induced by the field of a particle moving in vacuum close to a perfect conducting periodic surface), and resonant diffraction radiation (RDR) model [16] (for gratings consisting of infinitely thin perfect conducting strips separated by vacuum gaps).

Comparison of models for thin strips grating

We use for calculations the formulas from [8] for the case $\Phi = 0$ (see Fig. 1)

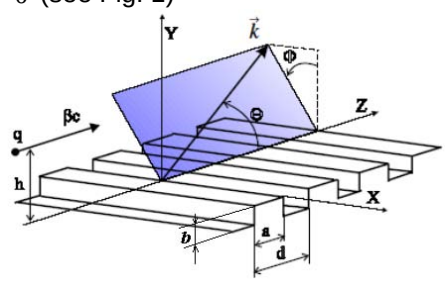

Fig. 1. Scheme of the Smith-Purcell radiation generation

The calculations (Fig. 2) were made for the Lorenz-factor γ = 12 and the grating period d = 8 mm.

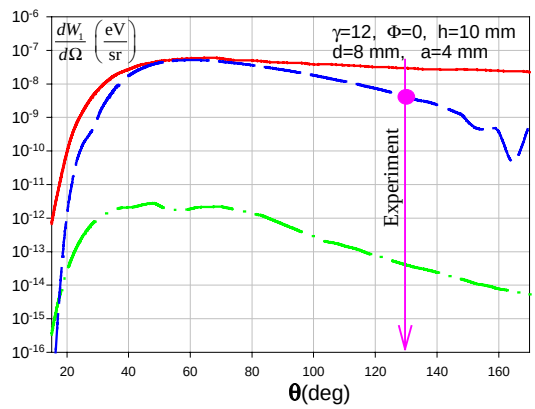

Fig. 2. Angular distribution of the SPR intensity for a flat grating according to the RDR model (red solid line), surface current model (blue a dashed curve) and for van den Berg's model (green dash-dotted line, b/d = 0.001).

We can see from the Fig. 2 a large discrepancy between radiation yields obtained using these three models.

GAIN AND COHERENCE ENHANCEMENT OF SASE FEL USING LASER-PREBUNCHED ELECTRONS

Yen-Chieh Huang and Chia-Hsian Chen, Institute of Photonics Technologies, National Tsinghua University, Hsinch 30013, Taiwan
Wai-Keung Lau and Gwo-Huei Luo, National Synchrotron Radiation Research Centre, Hsinchu 30076, Taiwan

Abstract

We conduct a simulation study on the acceleration of periodically loaded electrons in a 6-MeV photocathode electron gun driven by a laser beat wave with a beat frequency of 4.35 THz. The density modulation of the electrons is well preserved during particle acceleration. The periodically bunched electrons are then injected into a single-pass free-electron laser to quickly generate a few tens of kW electron superradiance at 63.5 μm.

INTRODUCTION

It is well known that, if the electron bunch length is significantly shorter than the radiation wavelength, the spectral power of the electron radiation is proportional to the square of the electron current or to the square of the total number of electrons participating in the radiation process. This coherent radiation is dubbed as electron superradiance.

To facilitate the discussion, we briefly describe in the following the theory of electron superradiance based on Gover's formulation [1]. In general, the spectral energy of the radiation from an electron bunch with a bunch length τ_b and an electron number N_b is expressed by the equation

$$(dW/d\omega)_{SR} = N_b^2 (dW/d\omega)_1 M_b^2(\omega), \qquad (1)$$

where $(dW/d\omega)_1$ denotes the spectral energy emitted from a single electron with W being the radiation energy and ω being the angular frequency of the radiation, $M_b(\omega)$ is the Fourier transform of the electron pulse-shape function with a unitary peak amplitude. If the radiating electron beam contains N_{pb} such electron bunches repeating at a rate $\omega_{pb}/2\pi$, the total radiated spectral energy becomes

$$(dW/d\omega)_{SR,pb} = N_b^2 N_{pb}^2 (dW/d\omega)_1 M_b^2(\omega) M_{pb}^2(\omega), \qquad (2)$$

where

$$M_{pb}^2(\omega) = \frac{\sin^2(N_{pb}\pi\omega/\omega_{pb})}{N_{pb}^2 \sin^2(\pi\omega/\omega_{pb})}, \qquad (3)$$

is the coherent sum of the radiation fields from all the micro-bunches and has a unitary peak amplitude at the frequencies $\omega = m\omega_{pb}$ (m = 1, 2, 3…). For a short electron bunch, $M_b^2(\omega)$ is usually a broad-band function. The spectral linewidth of $M_{pb}^2(\omega)$ at $\omega = m\omega_{pb}$ is given by $\sim \omega_{pb}/N_{pb}$, which, for a large number of periodic electron bunches, could be much narrower than the intrinsic spectral linewidth of a radiation device governed by $(dW/d\omega)_1$. Therefore, a self-amplified spontaneous emission (SASE) free-electron laser (FEL) is expected to have enhanced gain and coherence when driven by a periodically bunched electron beam. Since electrons are discrete particles, the term $M_b(\omega)M_{pb}(\omega)$, describing the degree of electron bunching at the frequency ω, is sometimes called the electron bunching factor.

Previously we have proposed the use of a laser beat wave to excite periodic emissions of electrons from the photocathode of an electron accelerator [2]. In this paper, we study a THz single-pass FEL driven by such a laser-beat-wave (Labew) photocathode accelerator. The system configuration of this study is depicted in Fig. 1, consisting of two major components, a RF photocathode gun and a solenoid-derived wiggler. The periodically bunched electrons are excited by a laser beat wave at the cathode, accelerated by a 1.6-cell S-band accelerator, and directly injected into a solenoid-derived wiggler to generate the electron superradiance.

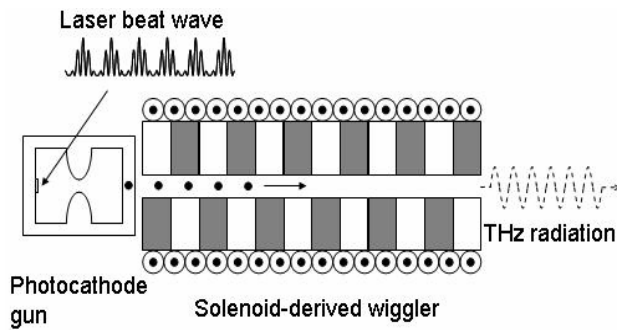

Figure 1: The system configuration for studying a THz superradiance FEL driven by a Labew photocathode gun.

Labew PHOTOCATHODE GUN

In this section, we study the acceleration of periodically bunched electrons in the BNL/UCLA/SLAC 1.6-cell S-band photocathode electron gun [3] by using the space charge tracking code ASTRA [4]. We operate the gun at a peak acceleration gradient of 140 MV/m. The electrons are emitted from the photocathode with a radial distribution within a 0.75-mm rms radius. For the first case in our simulation, we emitted a total of 1-nC electrons uniformly distributed over 10-ps duration. For the second case in our simulation, we equally divided the

APPROACHES IN MODELLING A WAVEGUIDE RF-LINAC THz-FEL

Yu. Lurie*, Y. Pinhasi, Ariel University Center of Samaria, Ariel, Israel
M. Tecimer, NHMFL / Florida State University, Tallahassee, FL 32310, USA

Abstract

A widely used approach in describing radiation fields generated by short pulse rf linac FEL oscillators is based on modal expansion of the intracavity fields and solving the wave equation for the amplitudes of the excited transverse cavity eigenmodes, in time and axial dimension. In this time domain approach, mode amplitudes are calculated by adopting the slowly varying envelope approximation (SVEA). The longitudinal propagation number k_z of the carrier wave is usually assumed to represent a group velocity and a wave impedance of the frequencies encompassed within the spectral bandwidth of the optical pulse envelope as it evolves within the interaction region. However, in cases where dispersive effects arising from a waveguided cavity become influential, the space-frequency approach is a straightforward method to tackle the problem without introducing further approximations. One such case is being studied based on a highly slippage dominated short pulse rf-linac FEL operating at long wavelengths.

INTRODUCTION

The aim of this paper is to present numerical design tools for investigating the temporal and spectral characteristics of THz pulses generated by short pulse rf-linac based waveguided FEL oscillators. We demonstrate application of these numerical tools on the design study and parameter optimization of a THz FEL system that is expected to operate over a frequency range between 100-1100 microns [1]. Combination of effects resulting from the use of picoseconds short electron pulses and long radiation wavelengths spread over such a wide spectral range on the one hand and propagation of short radiation pulses in lengthy waveguide resonators (as required in most of the rf-linac driven FELs) on the other hand, necessitate a careful analysis of the interplay between enhanced coherent spontaneous emission (CSE), waveguide dispersion (group velocity dispersion), slippage and cavity desynchronisation effects. In devising the numerical design tool, we adopt space-frequency approach [2, 3] which enables a correct description of these effects but it is time consuming when simulating an oscillator FEL configuration. On the other hand, employing an additional formalism to model the relevant aspects of the problem in an approximated way while creating practical means in terms of cpu usage. The former rigorous formalism is used to validate the application range of the latter in tackling the design problem with a reasonable accuracy and replace it in cases of shortcomings in modelling properly the physics of the above mentioned THz FEL system. The two methods presented in the paper are contemplated for the design study of the planed wide spectral range, long wavelength, short pulse waveguide THz-FEL oscillator.

Sample results are given applying the developed formalisms on a highly slippage dominated FEL regime where submillimeter to millimeter wavelength radiation is generated by a few picoseconds long high peak current electron bunches.

* ylurie@yosh.ac.il

DESCRIPTION OF THE MODELS

Time domain model

The time domain approach presented here and the implemented numerical algorithm is described in details in [4, 5]. Several assumptions are adopted in the model that reduce greatly the computational effort in order to enable an optimization of the system parameters. The longitudinal motion of each macroparticle is tracked whereas the transverse motion is accounted for by the beam envelope equations [4]. The latter includes the influence of 3D beam effects in an averaged manner. The profile of the optical field is defined by the transverse modes that are excited in a parallel plate (PP) waveguide resonator [5, 6]. The evolution of the mode amplitudes is governed by Eq. (1) where, by adopting SVEA and introducing the transformations $z' = z - v_g t$ and $\overline{z} = z - v_z t$, the inhomogeneous wave equation simplifies into:

$$\frac{\partial}{\partial z}u_q(z,z') = j\frac{f_b \mathbf{F} A_{u0}}{2k_{zq}} \cdot \frac{\omega_p^2}{c^2} \times \zeta_q(z,\overline{z})\frac{\chi(z,\overline{z})}{N_{\overline{z}}(z,\overline{z})} \sum_i^{N_{\overline{z}}(z,\overline{z})} e^{-j\theta_{iq}(z,\overline{z})} \quad (1)$$

In (1) $u_q(z,z')$ is the complex envelope of a modulated wave train with carrier frequency ω and axial wavenumber k_{zq} of the excited q'th mode, which satisfy the waveguide dispersion relation. $\theta_{iq}(z,\overline{z})$ is the ponderomotive phase. The longitudinal distribution of the particles is represented by the term $\chi(z,\overline{z}) = N_{\overline{z}}(z,\overline{z})/n_0\pi r_b^2\Lambda$, where $N_{\overline{z}}(z,\overline{z})$ denotes the number of particles within a fraction of the radiation period allowing for a more accurate description of CSE effects when the current profile of the electron bunch varies significantly at the scale of the radiation period [5]. The source term is averaged over the associated subwavelength long beam segment Λ. $\mathbf{F}$ is the filling factor. $\zeta_q(z,\overline{z})$ results from averaging the source term over the transverse gaussian density profile of the electron beam. For the case of a parallel plates (PP) waveguide it can be expressed by

EXPERIENCE AND PLANS OF THE JLAB FEL FACILITY AS A USER FACILITY*

Michelle D. Shinn#, Thomas Jefferson National Accelerator Facility, 1200 Jefferson ave., Newport News, VA 23606, USA

Abstract

Jefferson Lab's IR Upgrade FEL building was planned from the beginning to be a user facility, and includes an associated 600 m^2 area containing seven laboratories. The high average power capability (multikilowatt-level) in the near-infrared (1-3 microns), and many hundreds of watts at longer wavelengths, along with an ultrafast (~ 1 ps) high PRF (10's MHz) temporal structure makes this laser a unique source for both applied and basic research. In addition to the FEL, we have a dedicated laboratory capable of delivering high power (many tens of watts) of broadband THz light. After commissioning the IR Upgrade, we once again began delivering beam to users in 2005. In this presentation, I will give an overview of the FEL facility and its current performance, lessons learned over the last two years, and a synopsis of current and future experiments.

INTRODUCTION

The Free-electron laser (FEL) User Facility at Jefferson Lab (JLab) saw first light in 1998, and ran as a User Facility from 1999-2001. We then decommissioned our first FEL, the IR Demo, so we could install the IR Upgrade, which had almost an order of magnitude higher output and a larger tuning range. We once again began providing light to users in 2005. Previous reports [1,2] provide details of the uniqueness of the FEL driver accelerator, so this will be touched on only briefly. Along with the capability of the IR Demo to produce high average power, are other unique properties for a laser source (even compared to other FELs) in the mid-IR. To exploit the IR Demo the building that houses it was designed to be a user facility. An earlier report [3] gave some of the details of the facility while it was being built. This paper updates the current status of the facility, including measured values of the laser output, and discusses some of the infrastructure needed to run a user facility efficiently and safely. We then consider some of the interesting applied and basic research which is being done, and conclude with future plans for the facility.

*Work supported by the Commonwealth of Virginia and DOE Contract DE-AC05-06OR23177

#shinn@jlab.org

THE IR UPGRADE FEL

The Electron Accelerator

The driver accelerator of the IR Upgrade FEL uses SRF accelerator technology consisting of a 10 MeV injector (containing a DC photocathode gun driven by a Nd:YLF laser) and a SRF linac (whose total accelerating voltage may be as high as ~ 150 MeV) to produce an electron beam with an average current of ~ 10 mA at a PRF of 74.85 MHz. More than one percent of the electron beam power is converted to outcoupled laser radiation. The beam is then transported back through the linac where it is decelerated and most of the kinetic energy increase due to the linac is converted back into RF power. The use of an energy-recovering linac (ERL) greatly reduces the utility demands and installed RF power and has an added benefit that the waste beam is dumped at an energy below the giant photonuclear resonance threshold, eliminating activation of the beam dump.

This type of FEL was first demonstrated at the Jefferson Lab in the spring of 1999 and, its design and performance has been the subject of a number of papers. [4,5] The FEL is housed in the vault of the user facility [3] and has delivered several thousand hours of laser beam time to users. Given our desire to develop the FEL as an industrial tool, a generous amount of this beam time was delivered to users working on potential industrial applications. [6,7]

The advantage of ERL FELs is the ability to scale the output power to very high levels, many 10's of kW in the IR, without greatly increasing the space required to house it. This is because the FEL output power scales with electron beam power, which can be varied either with electron beam current or energy. Another advantage is the ability to lase at wavelengths that aren't accessible with conventional laser sources and at higher output powers. A disadvantage is that FELs are larger and more complex than conventional laser sources, however, an industrial version could be built which is more compact, and we have already demonstrated high availability (approaching 95% over 80 hours).

EXPERIMENTAL STUDY OF VOLUME FREE ELECTRON LASER USING A "GRID" PHOTONIC CRYSTAL WITH VARIABLE PERIOD

Baryshevsky, N A Belous, A A urinovich, A Evdoki ov,
P Molchanov *, A Oskin, P F Safronov
Research Institute for Nuclear Proble s, 11 Bobryiskaya str , 220050, Minsk, Belarus

Abstract

E peri ental Study of olu e Free Electron Laser with a grid resonator grid photonic crystal with changing in space para eters are reported

INTRODUCTION

enerators using radiation fro an electron bea in a periodic circuit traveling wave tubes 1,2 , backward wave oscillators, free electron lasers are now widespread 3

All the above devices use one-di ensional feedback, which is for ed by either two parallel irrors placed on the both sides of working area or a diffraction grating

But there are so e challenges that restrict applications of such devices electrical endurance of resonator li its radiation power and current of acceptable electron bea Conventional waveguide syste s are essentially restricted by the re uire ent for transverse di ensions of resonator, which should not signi cantly e ceed radiation wavelength

The indicated proble s can be overco e by the aid of volu e non-one-di ensional ulti-wave distributed feedback 4 10 New type of radiation generators using volu e ulti-wave distributed feedback was called olu e Free Electron Laser FEL Transverse di ensions of FEL resonator could signi cantly e ceed radiation wavelength The electron bea and radiation power are distributed over the large volu e that is bene cial for electrical endurance of the syste

One of the FEL types uses a grid photonic crystal that is for ed by a periodically strained either dielectric or etallic threads, which provides to weaken re uire ents for bea guiding

The grid structure of dielectric threads was e peri ental studied in 11 , where it was shown that such grid photonic crystals have suf ciently high Q-factor $10^4 - 10^6$

Theoretical analysis 12, 13 showed that periodic etal grid does not absorb electro agnetic radiation and the grid photonic crystal, ade of etal threads, is al ost transparent for the electro agnetic waves in the fre uency range fro Hz to THz In this range the skin depth δ is about 1 icron or less for the ost of etals for e a ple, for 10 Hz $\delta_{Cu} = 0.66\ \mu$, $\delta_{Al} = 0.8\ \mu$, $\delta_W = 1.16\ \mu$ and so on Thus, in this fre uency range the etallic threads can be considered as perfect conducting

Theory of FEL with spatially variable period was developed in 16, 17 There it was shown that use of photonic crystal with variable period could provide signi cant increase in radiation output It was entioned that diffraction gratings photonic crystal can be used for creation the dyna ical wiggler with variable period in the syste This akes possible to develop double-cascaded FEL with variable para eters changing, which ef ciency can be signi cantly higher that of conventional syste

In the present paper e peri ental study of olu e Free Electron Laser with a grid resonator grid photonic crystal with changing in space para eters are considered

EXPERIMENTAL SETUP

The grid photonic crystal is built fro tungsten threads with the dia eter 0 1 strained inside the rectangular waveguide with the transversal di ensions $a = 35$, $b = 35$ and length 300 see Fig 1 A pencil-like electron bea with the dia eter 32 , energy up to 200 ke and current about 2kA passes through the above structure The agnetic eld guiding the electron bea is $\sim 1.55 - 1.6$ tesla Period of grid photonic crystal is chosen to provide radiation fre uency ~ 8.4 Hz The grid

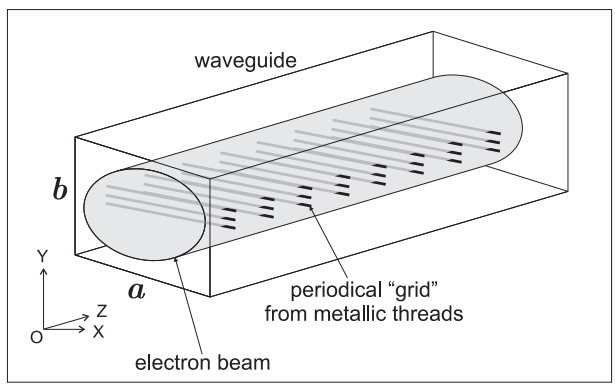

Figure 1 The grid diffraction grating placed inside the waveguide

structure is ade of separate fra es each containing the layer of 1, 3 or 5 parallel threads with the distance between the ne t threads $d_y = 6$ Fra es are joined to get the grid structure with the distance d_z between layers

Fre uency range is evaluated by eans of tunable waveguide lters, which were tuned in the band 7 8 - 12 4 Hz with passbands 0 25 Hz, 0 5 Hz and 1 Hz Attenuation of radiation in the suppressed band of this lter

* olchanov inp insk by

RESEARCH HIGHLIGHTS FROM FLASH

R. Treusch and J. Feldhaus, DESY, Hamburg, Germany

Abstract

The Free electron LASer in Hamburg (FLASH) has started regular user operation in summer 2005, providing XUV radiation pulses with pulse energies in the 10–100 μJ range and pulse durations of 10–50 fs. The science programme at FLASH covers a broad range of novel applications including fundamental studies on atoms, ions, molecules and clusters, creation and characterisation of warm dense matter, diffraction imaging of nanoparticles, spectroscopy of bulk solids and surfaces, investigation of surface reactions and spin dynamics, and the development of advanced photon diagnostics and experimental techniques. So far, 16 science projects have been pursued involving approximately 200 scientists from 11 countries. Some of the research highlights were presented in the talk.

Most of the presented results are presently in the publishing process. Hence the reader is kindly referred to the selection of already published research at FLASH as listed below.

SELECTED PUBLICATIONS ON RESEARCH AT FLASH

1. V. Ayvazyan et al.,
First operation of a Free-Electron Laser generating GW power radiation at 32 nm wavelength,
Eur. Phys. J. D, **37**, 297-303 (2006)

2. S. Düsterer et al.,
Spectroscopic characterization of vacuum ultraviolet free electron laser pulses,
Opt. Lett. **31**, 1750-1752 (2006)

3. A.A. Sorokin et al.,
Multi-photon ionization of molecular nitrogen by femtosecond soft x-ray FEL pulses,
J. Phys. B: At. Mol. Opt. Phys. **39**,L299-L304 (2006)

4. H.N. Chapman et al.,
Femtosecond diffractive imaging with a soft-X-ray free-electron laser,
Nature Physics **2**, 839-843 (2006)

5. M. Meyer et al.,
Two-color photoionization in xuv free-electron and visible laser fields,
Phys. Rev. A **74**, 011401(R) (2006)

6. A.A. Sorokin et al.,
Method based on atomic photoionization for spot-size measurement on focused soft x-ray free-electron laser beams,
Appl. Phys. Lett. **89**, 221114 (2006)

7. N. Stojanovic et al.,
Ablation of solids using a femtosecond extreme ultraviolet free electron laser,
Appl. Phys. Lett. **89**, 241909 (2006)

8. A.R.B. de Castro et al.,
Spectroscopy of rare gas clusters using VUV light from a free-electron-laser,
J. Electron Spectrosc. Relat. Phenom. **156158**, 25-29 (2007)

9. M. Kirm et al.,
Time resolved luminescence of solids excited by femtosecond VUV pulses and synchrotron radiation,
phys. stat. sol. (c) **4**, No. 3, 870876 (2007)

10. S. Cunovic et al.,
Time-to-space mapping in a gas medium for the temporal characterization of vacuum-ultraviolet pulses,
Appl. Phys. Lett. **90**, 121112 (2007)

11. P. Radcliffe et al.,
Single-shot characterization of independent femtosecond extreme ultraviolet free electron and infrared laser pulses,
Appl. Phys. Lett. **90**, 131108 (2007)

12. S.P. Hau-Riege et al.,
Damage threshold of inorganic solids under free-electron laser irradiation at 32.5 nm wavelength,
Appl. Phys. Lett. **90**, 173128 (2007)

13. S.P. Hau-Riege et al.,
Subnanometer-Scale Measurements of the Interaction of Ultrafast Soft X-Ray Free-Electron-Laser Pulses with Matter,
Phys. Rev. Lett. **98**, 145502 (2007)

14. S.W. Epp et al.,
Soft x-ray laser spectroscopy on trapped highly charged ions at FLASH,
Phys. Rev. Lett. **98**, 183001 (2007)

15. J. Chalupský et al.,
Characteristics of focused soft X-ray free-electron laser beam determined by ablation of organic molecular solids,
Optics Express **15**, 6036-6043 (2007)

16. A.A. Sorokin et al.,
X-ray-laser interaction with matter and the role of multiphoton ionization: Free-electron-laser studies on neon and helium,
Phys. Rev. A **75**, 051402(R) (2007)

MILLIMETER WAVES SENSING BEHIND WALLS - FESEABILITY STUDY WITH FEL RADIATION*

B.Kapilevich, M.Einat, A.Yahalom, M.Kanter, B.Litvak, The Israeli FEL Knowledge Center, the Ariel University Center of Samaria, Ariel, 44837, Israel
A.Gover, Tel Aviv University, Israel

Abstract

Design of through-wall imaging (TWI) system needs the knowledge of constitutive parameters of different building materials. The paper describes the results of measurements of the effective attenuation constant of typical building materials such as concrete bricks, wood, tiles, sand, gypsum, etc. on mm-waves using powerful pulse FEL radiation. Since the Rayleigh criterion for surface roughness cannot be satisfied for majority of measured building materials on mm waves, the increased measured attenuation in comparison with bulky material is taken place. Additional experiments were performed to estimate a role of these effects using quasi-noise mm-wave source and wide-band mm-wave receiver.

INTRODUCTION

The through-wall imaging (TWI) systems provide unique possibility to detect and image objects behind the walls, door and other opaque medium [1, 2]. Basically, through-wall imaging (TWI) systems operate in 1.99 – 10.6 GHz or below 960 MHz [3]. The penetration capability at these frequencies is characterized by rather small attenuation caused by building material as shown in Fig.1 [4]. However, the spatial resolution of TWI systems is degraded when the operating frequency is relatively low. On the other hand, a majority of building materials demonstrate increased losses as the frequency increases. As a result, higher RF power from the source is required for quality TWI process.

The Israeli mm-wave FEL provides unique opportunity to solve the above TWI problem delivering an output power of 100-1000W at 85-105 GHz. But design of TWI system operating on mm-waves needs comprehensive study of constitutive parameters of different building materials that must be measured in real pulse operation FEL conditions. The paper describes the experimental setup assembled for measurements of the effective attenuation constant of typical building materials such as concrete bricks, wood, tiles, sand, gypsum, etc. on mm-waves using powerful FEL radiation. Since the Rayleigh criterion for surface roughness at mm-waves cannot be satisfied for majority of measured materials, the measured attenuation is different in comparison with bulky material.

Additional experiments were performed to estimate a contribution of this effect into the measured attenuation. The special W-band quasi-noise sensor has been designed and assembled to carry out such experiments.

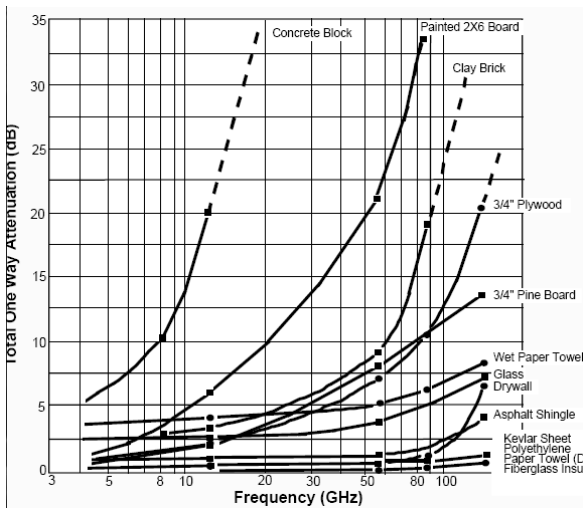

Figure 1: Illustration of penetration capabilities of different building materials as a function of frequency [4].

EXPERIMENTAL SETUP AND CALIBRATION PROCEDURE

The block-diagram of the experimental setup used for measurement of effective attenuation constant is shown in Fig.2. The pulse mm-wave FEL radiation (5-10 μs) propagating in the corrugated wave guide line excites the Tx standard rectangular horn antenna that transforms it to plane wave. This wave partially penetrates though the sample of the tested material and is captured by a similar Rx antenna coupled with the W-band programmable attenuator and DXP-10 detector (Millitech). A similar detector is coupled with the directional couplers providing a total coupling level of -64dB. Both detected signals are independently recorded by the Tektronix digital scope.

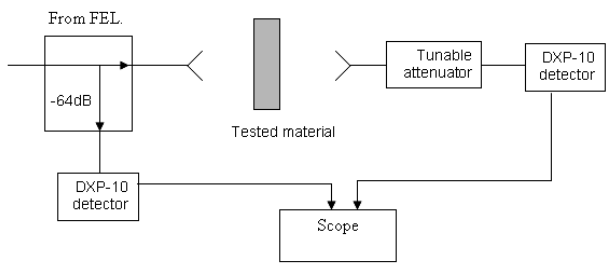

Figure 2: The block-diagram of the experimental setup.

*Work was partly supported by the Israeli Ministry of Science.

SOURCES OF RADIATION ON ARC-EN-CIEL PROPOSAL

M. E. Couprie, C. Benabderrhamane, C. Bruni, O.Chubar, M. Labat, G. Lambert, A. Loulergue, O. Marcouillé, Synchrotron-SOLEIL, Saint-Aubin, France
L. Giannessi, ENEA, Frascati, Italy.

Abstract

The ARC-EN-CIEL project [1] proposes a panoply of light sources for the scientific community. The choice to base the FEL sources on HGHG (High Gain Harmonic Generation) radiation and their Non Linear Harmonics seeded with the High order Harmonics generated in Gas (HHG) is further confirmed with the successful demonstration experiment of such a scheme at SCSS Prototype Accelerator in Japan [2]. In phase 1 (220 MeV), the radiation extends down to 30 nm, phase 1' (800 MeV) and phase 2 (1 GeV), the radiation reaches 1 nm, with 30-100 fs pulses. The first FEL "LEL1" utilizes in-vacuum undulators of period 26 mm for the modulator, and APPLE-type radiators of period 30 mm, close to the standard SOLEIL insertion devices. The second FEL branch "LEL2" uses in-vacuum planar U18 undulators as radiator. In addition, THz radiation from the magnets of the compression chicanes will be provided and has been calculated using SRW. ARC-EN-CIEL Phase 3 adds ERL loops at 1 GeV and 2 GeV where undulators emit conventional synchrotron radiation above 10 keV from short period in-vacuum undulators and soft X ray using a variable polarisation undulator. An FEL oscillator in the 40-8 nm spectral range is installed in the 1 GeV loop. The HHG seeded "LEL4" uses the electron beam from the 2 GeV loop and further accelerated to 3 GeV for producing coherent light production below 1 nm. Recent calculations and optimisations are presented.

INTRODUCTION

ARC-EN-CIEL (Accelerator-Radiation for Enhanced Coherent Intense Extended Light) aims at providing the user community with coherent femtosecond light pulses covering from UV to soft X ray spectral range in France [2]. It is based on a CW 1.3 GHz superconducting linear accelerator delivering high charge, subpicosecond, low emittance electron bunches at high repetition rate. The completion of ARC-EN-CIEL relies on different phases, according to the electron beam energy, the average current and the light sources available for the users. Phase 1 uses a 1 kHz high charge, short bunch electron beam, reaching an energy of 220 MeV with 3 cryomodules, and a first bunch compressor delivered by a modified Zeuthen RF gun [3], illuminated by a Ti:Sa laser. LEL1 is based on a FEL seeded with HHG with an APPLE-II type undulator as a radiator for adjustable polarisation radiation. Phase 1 (220 MeV, 30 nm) is now extended to 800 MeV (Phase1') with an additional bunch compressor and five cryomodules, and fits in the tunnel of the ALS (Accelerateur Linéaire de Saclay) allowing LEL1 radiation to be extended to shorter wavelengths for users applications. With two additional cryomodules on the Linac leading to 1 GeV (Phase 2), the FEL source "LEL2" will be installed, allowing stronger radiation to be achieved in the 1 nm range. Then, with the installation of an additional high average current gun (AES/JLab type [4]) illuminated by a Ytterbium diode pump fiber laser, two ERL loops at 1 and 2 GeV will be added. On the 1 GeV loop is planned LEL3 and FEL oscillator taking advantage of the mirror development for lithography, and an APPLE-II for subpicosecond radiation synchrotron radiation. On the 2 GeV loop, 6 in vacuum U20 (period of 20 mm) will be installed for hard X ray spontaneous emission. When the 2 GeV beams is not energy recovered but once again accelerated up to 3 GeV, it is sent to "LEL4", an FEL seeded with HHG and using cryogenic undulators. THz radiation is also produced in the bending magnets of the compression chicanes and of the arcs. The general scheme of ARC-EN-CIEL is shown in fig. 1.

Table 1: List of radiation sources on ARC-EN-CIEL. Phase: P. M for Modulator and R for Radiator. SR: Synchrotron Radiation. CSR: Coherent Synchrotron Radiation. BC Bunch Compressor. E: Energy. N: number of periods. Conf: configuration. BL: beam line.

	P	E GeV	Type	M/R, N	Spectral range
FEL radiation					
LEL1 Planar helical branch	1, 1', 2	0.22 - 1	HGHG conf 1-1 1-3 HHG seed	M :U26 200 R : HU30, N2=700	200-1.5 nm
LEL2 Planar branch	2	0.8-1.2	HGHG, conf 1-1 et 1-3 HHG seed	M : U26, N1=500 R : U18 N2=500	10-0.5 nm
LEL4 planar branch	3	3	HGHG conf 1-3and 1-5 HHG seed	M :U35, N1=700 R :U18, N2=1000	2-0.2 nm
LEL3	3	1	FEL oscillator	HU30, N=350	40-8 nm
Spontaneous emission					
VUV BL	3	1	SR	HU30	0.2-4 keV
X BL	3	2	SR	U 20, 100	1-20 keV
THz Radiation					
	1-1' 2, 3		CSR	BC1, 2, arc	0.1-10 THz

STATUS OF THE FEL TEST FACILITY AT MAX-LAB *

Mathias Brandin, Filip Lindau, Nino Cutic, Sara Thorin, Sverker Werin#, MAX-lab, Lund, Sweden
Johannes Bahrdt, Kathrin Goldammer, Michael Abo-Bakr, Dmytro Pugachov, BESSY GmbH, Berlin, Germany
Anne L'Huillier, Lund University, Lund, Sweden

Abstract

An FEL test facility is built on the existing MAX-lab linac system in collaboration between MAX-lab and BESSY. The goal is to study and analyse seeding, harmonic generation, beam compression and diagnostic techniques with the focus of gaining knowledge and experience for the MAX IV FEL and the BESSY FEL projects. The test facility will in the first stage be using the 400 MeV linac beam to generate the third harmonic at 88 nm from a 266 nm Ti:Sapphire seed laser.

The optical klystron is installed and magnetic system, gun and seed laser systems are currently being finalised. Start-to-end simulations have been performed and operation modes for bunch compression defined. The linac and beam transport system is already in operation.

INTRODUCTION

The BESSY FEL project [1] and the MAX IV proposal [2] are both focused on seeded FEL sources as part of the facilities. In the aim of improving the designs a decision was made to build a test facility for harmonic generation at MAX-lab.

By utilising the gun, injector and linac system already available at MAX-lab a test facility for seeded FEL/Harmonic generation could be accomplished by relative low additional funding. Contacts had been taken with BESSY and with the application for the EUROFEL collaboration the project was started. The focus of the activities is to explore ideas of harmonic generation and gain experience with the FEL technology, test diagnostics and working with short pulses.

OVERVIEW OF THE PROJECT

The project is built in one major phase (I) with two improvement phases (phase II: an improved gun system and phase III: HHG seeding). The starting point is the injector built at MAX-lab in the first years of this millennium which was designed to be flexible and also allow accelerator development. A linac system was chosen together with a flexible gun mounting system equipped with a thermionic RF-gun. The source is used for injection into the storage rings (MAX I, II, III) and in the intermediate time this source is one of few available sites for tests of FEL operation at these energies.

An optical klystron system and a seed laser at 266 nm will produce the 3rd and 5th harmonic at 88 and 53 nm respectively using the 400-450 MeV electron beam. The radiator undulator in the optical klystron is not enough for amplification, and thus the activities are focused on harmonic generation. BESSY is providing the undulator and chicane system while MAX-lab is providing the electron beam and the laser system.

The aim is to study several features in the design and operation of this kind of facility. On the electron beam side: bunch compression, electron beam transport (especially with low emittance), beam stability, synchronisation and stability. On the FEL side: Harmonic

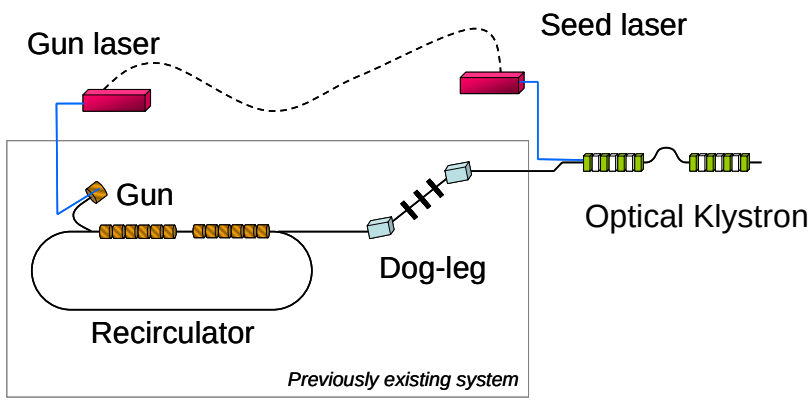

Fig 1. Overview of the accelerator systems and test FEL.

* This work has been partially supported by the EU Commission in the Sixth Framework Program, Contract No. 011935 – EUROFEL and the Swedish Research Council
# sverker.werin@maxlab.lu.se

COMPACT RING FEL AS A SOURCE OF HIGH POWER INFRARED RADIATION

O.A. Shevchenko[#], A.N. Matveenko, N.A. Vinokurov,
Budker Institute of Nuclear Physics, 11 Acad. Lavrentyev Prosp., 630090, Novosibirsk, Russia

Abstract

Ring FELs [1] were proposed mainly to improve the quality of radiation of x-ray FELs. Their main advantage is the absence of mirrors. It appears that this advantage is also useful for high power FELs. Another reason to build infrared ring FEL is the proof-of-principle for shorter wavelength FELs. Therefore we considered the scheme of infrared ring FEL which requires ERL with beam energy 50 MeV. Using extensive simulations we developed requirements for electron beam parameters and magnetic system of ring FEL. In spite of rather compact design such FEL may provide more than 10 kW average power.

INTRODUCTION

The further development of FELs towards the region of short wavelengths and high powers is limited by the absence of mirrors with appropriate parameters. There exist different approaches to the solution of this problem. One of them is based on the fact that the beam microbunching which appears in undulator can be partly conserved in the specially designed isochronous bend. Electron outcoupling may be considered as the simplest scheme which utilizes this idea [2-3].

The further evolution of this approach leads to the scheme of the ring FEL which has been proposed in [1]. The lattice of the ring FEL consists of straight undulator sections and isochronous bends which compose a ring. At the bends radiation is lost. The signal between adjacent undulator sections is transferred trough microbunching. Radiation from the last undulator produces energy modulation of the new coming beam inside the first undulator and amplification goes on till saturation. The basic advantage of this scheme is that it has a feedback which is realized without any mirrors.

High power ring FEL implies CW operation mode. Therefore one has to use energy recovery linac (ERL) as a source of electron beams for such FEL. The present state of the art of ERLs allows for producing the beams with required parameters which makes the ring FEL project feasible.

The main problem of the ring FEL which becomes very essential for the short wavelength is that it requires isochronous bends to conserve microbunching. The problem of creating of such bend is discussed in detail in [4]. To demonstrate the feasibility of the ring FEL concept it is desirable to build first the small-scale model for longer wavelength which may be interesting itself as a source of high power infrared radiation.

In this paper we consider the possible design of compact high power infrared ring FEL. We present the possible lattice of the bends, required electron beam parameters and results of simulation of FEL operation.

RING FEL SCHEME AND ELECTRON BEAM PARAMETERS

The schematic layout of the ring FEL is presented in Fig. 1. It includes two undulator sections. One of them plays the role of "modulator" where the energy modulation takes place. The other one may be called "radiator", here the FEL radiation is generated. In the long wavelength case the debunching of the beam is not very severe problem. Therefore one can use 360 degrees bend and additional undulator sections are not required.

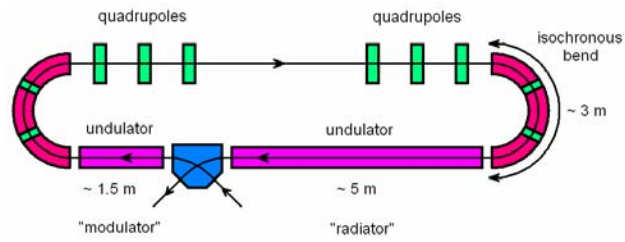

Figure 1. Schematic layout of the ring FEL.

The total 360 degrees bend in the proposed layout is comprised of two 180 degrees isochronous bend sections and a straight section with matching quadrupoles. The lattice of the isochronous bend is presented in Fig 2. It includes three bending magnets with different curvature sign, quadrupoles which are required to focus transversal dispersion and sextupoles which correct the second order aberrations.

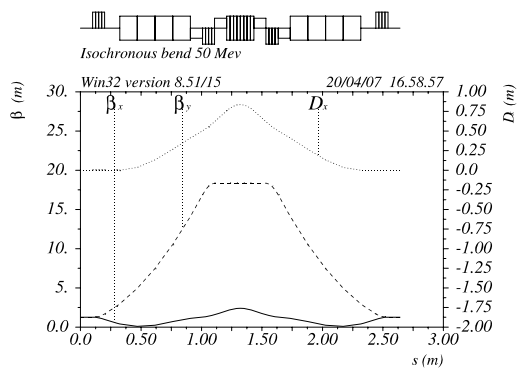

Figure 2. Magnetic lattice of the isochronous bend.

The beam and undulator parameters used in simulations are listed in Table 1.

[#]O.A.Shevchenko@inp.nsk.su

RE-COMMISSIONING OF THE FAR-INFRARED FREE ELECTRON LASER FOR STABLE AND HIGH POWER OPERATION AFTER THE RENEWAL OF THE L-BAND LINAC AT ISIR, OSAKA UNIVERSITY

R. Kato, S. Kashiwagi,T. Igo, Y. Morio, G. Isoyama#
Institute of Scientific and Industrial Research, Osaka University, Osaka, Japan

Abstract

The far-infrared FEL at the Institute of Scientific and Industrial Research (ISIR), Osaka University, which was operated in the wavelength region from 32 to 150 μm and was suspended since 1998, is being commissioned for stable and high power operation. The FEL is based on the L-band electron linac constructed in 1978, but it was largely remodelled for higher stability and reproducibility of operation as well as for long pulse operation for FEL. The long pulse mode has been successfully commissioned using a feed forward control system, which can stabilize the amplitude and the phase of the 1.3 GHz RF power in the macropulse within 0.5 % in amplitude and 0.3º in phase. The FEL system is the same as before except for the strong focusing wiggler based on the edge-focussing scheme, which was recently introduced. The FEL experiment is all set up and we are waiting for the next machine time and lasing.

INTRODUCTION

We have been developing a far-infrared FEL since late 1980s based on the 40 MeV, L-band electron linac at the Institute of Scientific and Industrial Research (ISIR), Osaka University. The first lasing was obtained at 32~40 μm in 1994 [1] and since then we progressively modified the FEL system and continued experiment in between to expand the wavelength region toward the longer wavelength side beyond 100 μm. We finally obtained lasing at 150 μm in 1998 [2], which was, at that time, the longest wavelength obtained with FELs based on RF linacs. We could not obtain power saturation because the macropulse duration is 2 μs, though the RF pulse is 4 μs long, due to a long filling time of the acceleration tube of the L-band linac and the number of amplification times is limited to 50 only. The linac was constructed approximately 30 years ago and it was not suitable for stable and high power operation of FEL, so that we suspended the development of the FEL.

In 2002, we had an opportunity to remodel the linac largely for higher stability and reproducibility of operation. We also added a new operation mode for FEL in which the macropulse duration can be extended to 8 μs. I took time to remodel the linac and commission it, but finally the operation mode for FEL is being commissioned and we are resuming the FEL again after the long suspension. We will report the progress and the current status of the re-commissioning of the FEL.

#isoyama@sanken.osaka-u.ac.jp

RENEWED LINAC

The linac is comprised of a thermionic electron gun, a three-stage sub-harmonic buncher system with two 108 MHz RF cavities and a 216 MHz cavity, a pre-buncher, a buncher, and a 3 m long accelerating tube. The last three components are excited by a single klystron of the 1.3 GHz frequency, the maximum peak output power of 30 MW, the pulse duration of up to 8 μs, and the repetition frequency of 60 Hz. The main parameters of the linac are listed in Table 1. A klystron modulator, which provides high voltage pulses to the klystron, has two operation modes; one is the normal mode with the pulse duration of 4 μs and the repetition rate of 60 pps and the other is the long-pulse mode with 8 μs and 30 pps. The operation modes can be changed manually but easily in a short time.

The maximum output power of the klystron is limited to 25 MW in the long pulse mode, so that the maximum beam energy in the multi-bunch mode used for FEL is slightly lower than 40 MeV.

Stability and reproducibility of linac operation are essential for advanced studies with the linac, including FEL and all the possible measures have been taken in the remodelling to reduce fast fluctuations and long-term drifts. Most influential power supply for the stability is the klystron modulator and it is designed and fabricated to reduce pulse-to-pulse fluctuations less than 0.1 %. Voltage ripples on the flat top of the square pulse applied to the klystron should be less than 0.1 % in order to make the amplitude and the phase of the output power from the

Table 1: Main Parameters of the L-Band Linac

Acceleration frequency	1.3 GHz
Sub-harmonic buncher	108 MHz×2, 216MHz×1 λ/4 coaxial resonators
Accelerating structures	Prebuncher×1, Buncher×1, Accelerating tube×1 Travelling wave, 2π/3 mode
Electron gun	Thermionic cathode (EIMAC YU-156), DC 100 kV
Operation modes, peak currents or maximum charge, and pulse durations	Transient: 1.9 A, 8 ns Single bunch: 91 nC, 20 ps Steady: 1.9 A, 4 μs Multi-bunch: 1.9 A, 8 μs
Repetition rate	≤ 60 pps
Klystron	30 MW×1
Total length	10.5 m